Post-transcriptional Regulation of Gene Expression in Innate Immunity

Author:
Lai, Hui-Chi

Publication Date:
2021

DOI:
https://doi.org/10.26190/unsworks/2048

License:
https://creativecommons.org/licenses/by/4.0/
Link to license to see what you are allowed to do with this resource.

Post-transcriptional Regulation of Gene Expression in Innate Immunity

Tess Hui-Chi Lai

A thesis in fulfilment of the requirements for the degree of

Doctor of Philosophy

SWS Clinical School

Faculty of Medicine

August 2021

Abstract

Surname/Family Name	:	LAI
Given Name/s	:	HUI-CHI
Abbreviation for degree as give in the University calendar	:	PhD degree
Faculty	:	Medicine
School	:	SWS Clinical School
Thesis Title	:	Post-transcriptional Regulation of Gene Expression in Innate Immunity

Abstract 350 words maximum: (PLEASE TYPE)

Gene expression can be regulated from transcriptional initiation to RNA processing and turnover time and post-translational modification of a protein. The majority of studies of gene expression have focussed on transcription. However, it is also important to understand how post-transcriptional pathways are regulated in response to inflammatory stimuli. Chapter 1 introduces background to gene expression during post-transcriptional regulation and its regulation related to inflammatory diseases. The innate immune response to LPS is highly dynamic yet tightly regulated. RNA decay pathways include nonsense-mediated decay, the RNA decay exosome, P-body localised deadenylation, decapping and degradation and AU-rich element targeted decay mediated by tristetraprolin. Chapter 2, we examined theregulation of RNA degradation pathways during the lipopolysaccharide response in macrophages and these results have been published.

Alternative splicing has been identified as a key process in post-transcriptional regulation of gene expression in higher eukaryotes. In the immune system, alternative splicing provides a major role in regulating gene expression and generating the diverse mRNA transcripts and protein isoforms, therefore giving rise to protein diversity. Intron retention (IR) is a form of alternative splicing where an intron is not removed during transcription coupled splicing and is considered a widely regulated process during gene expression. Chapter 3 we examined its regulation during inflammation. Also, gene expression can be regulated via nonsense-mediated decay, which can precisely control the timing and level of gene expression as well as eliminating unstable or toxic protein production. SMG1 is a member of the PIKK (phosphoinisitide 3-kinase related kinases) family and plays an important role in NMD. For Chapter 4 we investigated the role of SMG1 in the regulating in response to inflammatory stimuli. We generated a novel animal model of total SMG1 loss in macrophages to address this question. For Chapter 5, we showed how to analyse RNA-seq. of BMM from *LysM+/CreSmg1fl/fl* (Cre) and *Smg1fl/fl* (wild-type) mice treated with LPS treatment at dedicated time points by gene ontology tools to discover gene enriched clusters during an LPS treatment between *LysM+/CreSmg1fl/fl* (Cre) and *Smg1fl/fl* (wild-type) mice. A final discussion and future directions for this field of study are provided in Chapter 6.

Originality statement

Copyright and Authenticity statements

Inclusion of Publications Statement

UNSW is supportive of candidates publishing their research results during their candidature as detailed in the UNSW Thesis Examination Procedure.

Publications can be used in their thesis in lieu of a Chapter if:

- The candidate contributed greater than 50% of the content in the publication and is the "primary author", ie. the candidate was responsible primarily for the planning, execution and preparation of the work for publication
- The candidate has approval to include the publication in their thesis in lieu of a Chapter from their supervisor and Postgraduate Coordinator.
- The publication is not subject to any obligations or contractual agreements with a third party that would constrain its inclusion in the thesis

Please indicate whether this thesis contains published material or not:

☐ This thesis contains no publications, either published or submitted for publication
(if this box is checked, you may delete all the material on page 2)

☒ Some of the work described in this thesis has been published and it has been documented in the relevant Chapters with acknowledgement
(if this box is checked, you may delete all the material on page 2)

☐ This thesis has publications (either published or submitted for publication) incorporated into it in lieu of a chapter and the details are presented below

Acknowledgments

First of all, I have to thanks my primary supervisor Tara Roberts for endless supporting and many thesis drafts as well as teaching me lots of knowledge in innate immunity. Thanks for give me this opportunity to join your group and being your student in Australia. Also, I have to thanks my other supervisors Alex who gave me enough technical supporting and suggestions when I was struggling with experiments.

I would like to thanks Paul De Souza and other members of the lab, past and present, for listening my complaints and get coffee time together.

Also I have to thanks my best friends Ginger and Uda – thanks you for helping me everything whatever I need and went through so far of my research life.

Last but not least, I have to thanks my husband of endless supply of love, without him I could never have completed this study. Thanks for being with me always and you are the only one who support and believe I can complete my study. I did it!!!

Contributions by others to the thesis

Dr. Tara L. Roberts was the Primary supervisor and contributed to discussion on conception and study design, data analysis and interpretation, and provided comment on the thesis and manuscript (60%).

Dr. Paul De Souza was the head of Medical Oncology group of Liverpool hospital (where is located at Ingham Institute) and provided the research finding to this thesis and contributed to discussion in conception and provided comments on the thesis (20%).

Dr. Alexander James is the senior researcher of Tara's group and my secondary supervisor as well. He contributed technical supporting and comments to this thesis and participated in discussion as well as study design, data interpretation and provided comments on the thesis (20%).

Miss Alison Richards assisted in breeding, mating of mice colony, and genotyping of mice.

Professor Christine Wells, Rowland Mosbergen, Jarny Choi and **Issac Virshup** performed quality control, normalisation and initial fold change analysis for RNA sequencing data and uploaded the data into the stemformatics platform.

Dr. Justin J-L Wong and **Dr. Ulf Schmitz** performed the intron retention analysis using IRFinder. **Dr. Schmitz** generated the raw figures presented as Figure 3-1, 3-2, 3-4B in Chapter 3.

Dr. Uda Ho, John Luff and **Dr. Tara Roberts** generated data in Figure 4-2A in Chapter 4.

Table of Contents

List of Figures

Figure S2: Validation of regulation of expected proinflammatory cytokines in response to LPS.

Figure S3: Regulation of components of the exosome (Exosc5 and 7) and a member of the deadenylation complex (Cnot7) did not validate by qPCR.

Figure S4: Tristetraprolin (TTP encoded by Zfp36) and Regnase 1 (encoded by Zc3h12a) are regulated during the LPS response.

Figure S5: Analysis of RNA decay genes in human samples.

List of Tables

List of Abbreviations

ALKBH3: Alpha-Ketoglutarate Dependent Dioxygenase

ATCC: American Type Culture Collection

ATF4: Activating transcription factor 4

Bp: base pair

BSA: Bovine serum albumin

BMM: Bone marrow derived macrophage

C57BL/6: C57 black 6 mouse strain

cDNA: complementary deoxyribonucleic acid

CO_2: Carbon dioxide

Cre: Cre recombinase

CNOT7: CCR4-NOT Transcription Complex Subunit 7

CSF1: colony stimulating factor 1

DCP1A: mRNA-decapping enzyme 1A

DCP2: Decapping mRNA 2

DIS3: Exosome complex exonuclease RRP44

DMSO: Dimethyl sulfoxide

DNA: Deoxyribonucleic acid

DNA-PK: DNA-dependent protein kinase

dNTPs: Deoxy nucleotide

DTT: Dithiothreitol

ds: double-stranded

EST1A: Telomerase-binding protein

E.coli: Escherichia coli

EDTA: Ethylene diamine tetra acetate

ERK: extracellular signal related kinase

GAS1: Growth arrest specific 1

GAPDH: Glyceraldehyde 3-phosphate dehydrogenase

GAS5: Growth arrest specific 5

GTPase: Guanine triphosphatase

HCl: Hydrochloric acid

Hr: hour

IF: Immunofluorescence

IFN: interferon

Ig: immunoglobulin

IRF3: Interferon regulatory factor 3

IKKα/IKKβ: IKB Kinase α/ IKB Kinase β

IL: interleukin

iNOS: inducible nitric oxide synthase

IP: immunoprecitation

IRAK: IL-1 receptor associated kinase

IL-6: Interleukin 6

IL-1β: Interleukin 1 beta

IRF: interferon regulatory factor

JNK: c-Jun N-terminal kinase

KDa: kilo Dalton

L: Litre

LPS: Lipopolysaccharide

Luc7l: Putative RNA-binding protein luc7-like 1

M: Molar

MAPK: mitogen activated protein kinase

MEF: Mouse embryonic fibroblast

MET: Mesenchymal epithelial transition

$MgCl_2$: Magnesium chloride

μM: micro Molar

μg: micro gram

mL: milli litre

mM: milli Molar

min: minute

mRNA: messenger ribonucleic acid

MW: Molecular weight

MyD88: Myeloid differentiation primary response 88

M-CSF: Macrophage colony-stimulating factor

NF-κB: Nuclear Factor kappa-light-chain-enhancer of activated B cells

NaCl: Sodium chloride

NMD: Nonsense mediated decay

NO: nitric oxide

nt: nucleotide

PAMP: pathogen associated molecular pattern

PBS: Phosphate buffer saline

PCR: Polymerase chain reaction

qPCR: Quantitative reverse transcriptase polymerase chain reaction

PTC: Premature termination codon

PPP: Pathogen recognition receptor

RNA: Ribonucleic acid

rpm: round per minute

RT-PCR: reverse transcriptase PCR

SDS: sodium dodecyl sulphate

SMG1: SMG1 Phosphatidylinositol 3-Kinase-Related Kinase

SMG5: SMG5 Nonsense Mediated MRNA Decay Factor

SMG6: SMG6 Nonsense Mediated MRNA Decay Factor

SMG7: SMG7 Nonsense Mediated MRNA Decay Factor

STAUFEN1: STAU1-mediated mRNA decay protein

ss: single-stranded

TBK1: TANK-binding kinase 1

TRIF: TIR-domain-containing adapter-inducing interferon-β

TRAF: TNF receptor associated factor

TIR: toll/IL-like receptor

TNFα: Tumour necrosis factor alpha

UPF1: RNA helicase and ATPase

TBL2: Transducin beta like 2

TGM2: Transglutaminase 2

TTP: Tristetraprolin

UPF3B: Up-frameshift suppressor 3 homolog on chromosome X

WT: Wild-type

XRN1: 5'-3' Exoribonuclease

List of Publications and Presentations

Papers:

Hui-Chi Lai, Uda Y. Ho, Alexander James, Paul De Souza and Tara L. Roberts. (2021) RNA metabolism and links to inflammatory regulation and disease. Submitted to *Journal of Cellular and Molecular Life Sciences*.

Lai, H., James, A., Luff, J., Souza, P., Quek, H., Ho, U., Lavin, M. and Roberts, T. (2020), 'Regulation of RNA degradation pathways during the lipopolysaccharide response in macrophages', JLB. https://doi.org/10.1002/JLB.2AB0420-151RR.
(Draft of this manuscript is in Chapter 2 of this thesis and additional experiment results can be found on line.)

Ho, U., Luff, J., James, A., Lee, C., Quek, H., **Lai, H**., Apte, S., Lim, Y., Lavin, M. and Roberts,T. (2019), 'SMG1 heterozygosity exacerbates haematopoietic cancer development in Atm null mice by increasing persistent DNA damage and oxidative stress', Journal of Cellular and Molecular Medicine, vol 23, no 12 , pp 8151 - 8160.

Conference Presentations

Lorne Infection and Immunity 2021(virtual conference), 17-19 Feb, Australia-Oral Presentation

Transcription and RNA Regulation in Inflammation and Immunity 2019 at Tahoe City ,2-5 Feb USA-Post Presentation

Health Beyond Research and Innovation Showcase 2019 at Willian Inglis Hotel, Australia, 12-13 June -Post Presentation.

Australasian Society of Immunology 2018 at Pan Pacific Hotel of Perth,2-6 December, Australia -Post Presentation

Health Beyond Research and Innovation Showcase 2018 at Willian Inglis Hotel, Australia, 6-7 June -Post Presentation.

Australasian society of immunology 2017 at Convention Centre in Brisbane from 27th November-1th December -Post Presentation

Health Beyond Research and Innovation Showcase 2017 at the Campbelltown Catholic Club, Australia, 7-8 June 2017-Oral Presentation.

Health Beyond Research and Innovation Showcase 2016 at the Liverpool Catholic Club, Australia, 18-19 October-Oral Presentation.

Chapter 1- Literature Review

In this chapter I will review the literature related to major focusses of this thesis. Firstly I will describe RNA metabolism in the context of post-transcriptional regulation during RNA splicing, alternative splicing, nonsense-mediated decay pathway, RNA degradation as well as m6A modification. Subsequently, I will introduce post-transcriptional regulation in inflammation and TLR4 signalling. In the end of this chapter, I will give outline and summary of the thesis.

1.1 RNA splicing discovery: Intron, Exon and Spliceosome

Most genes in higher eukaryotes are transcribed as pre-mRNAs that contain intervening sequences (introns), as well as expressed sequences (exons). Discovered in the late 1970s, introns are removed during the process of pre-mRNA splicing, which joins exons together to produce mature mRNAs [1, 2]. The mechanism of pre-mRNA splicing is a complex process and requires the small nuclear ribonucleoproteins, splicing factors and RNA-processing factors [3]. The spliceosome is primarily responsible for recognising the intron/exon boundaries and also performing cut-and-paste reactions in order to excise the introns and join the exons. The spliceosome is made up of five small nuclear ribonucleoproteins (snRNPs): U1, U2, U4, U5,and U6. These proteins form a complex during splicing. Each snRNP is composed of a single uridine-rich small nuclear RNA (snRNA) and multiple proteins. The splicing reaction itself is mediated via a sequence of carefully controlled interactions between the snRNPs, proteins and the pre-mRNA transcript [2, 4]. Firstly, U1 snRNP is recruited to the the 5'-splice site, while U2 binds to the intron's branch point. A triple snRNP complex consisting of U4, U5 and U6 is then recruited to form the spliceosome. Then U4 leaves the complex which allows U6 to

replace U1 at the 5'-splice site. U6 then interacts with U2 to bring the branch point into close proximity with the 5'-splice site. At this point a transesterification reaction cleaves the 5'-end of the intron from the upstream exon and attaches it to the branch point, thus forming a lariat structure. Further interactions mediated by U5 then bring the 3'-end of the upstream exon and the 5'-end of the downstream exon into close proximity with each other. This allows a second transesterification reaction to cleave the remaining 3'-end of the intron and join the two exons together (Figure 1-1).
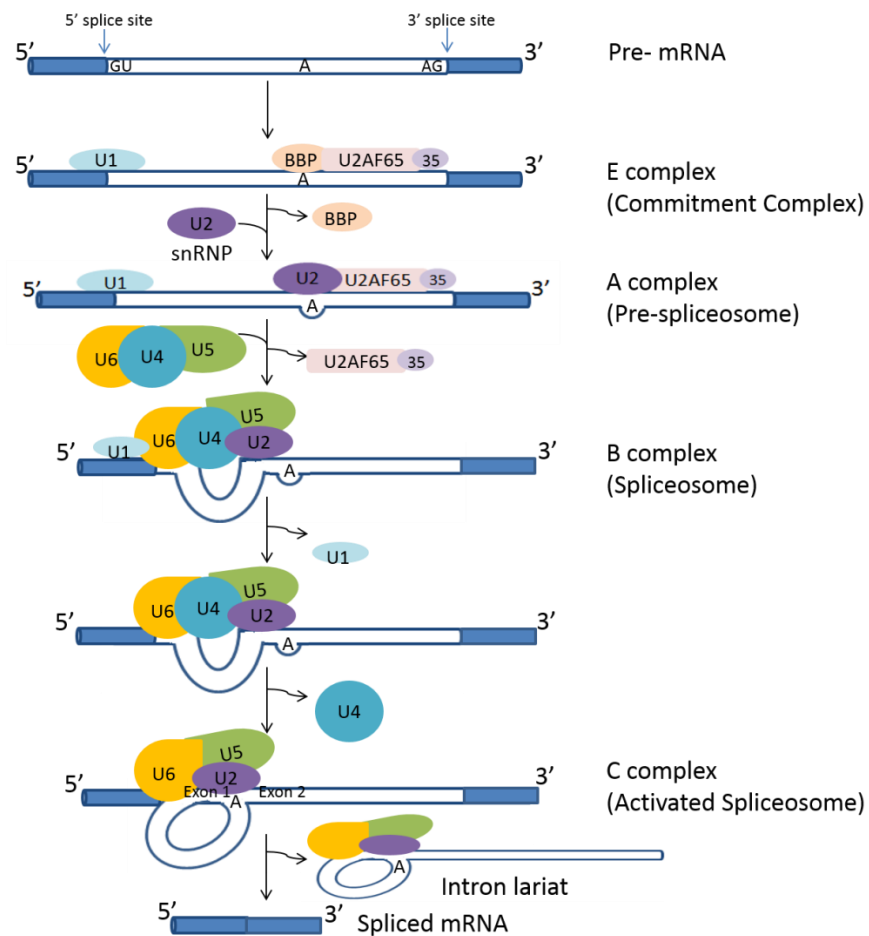
Figure 1-1: Spliceosome function in RNA splicing.

Splicing is carried out by the spliceosome, which contains five small nuclear ribonucleoproteins that are assembled onto the intron. The Early (E) complex contains the U1 snRNP bound to the 5' splice site. Each element of the 3' splice site is bound by a specific protein: the branch point by SF1, the polypyrimidine tract by U2AF 65, and the AG dinucleotide by U2AF 35. The A complex forms when U2 engages the branch point via RNA/RNA base–pairing. This complex is joined by the U4/5/6 Tri-snRNPs to form the B complex. The B complex is then extensively rearranged to form the catalytic C complex. During this rearrangement the interaction of the U1 and U4 snRNPs are lost and the U6 snRNP is brought into contact with the 5' splice site. The C complex catalyses excision of intron as lariat and ligation of the exon sequences.

Splicing defects and dysregulation of pre-mRNA processing can lead to inflammatory related disorders and cancer. Dysregulation of splicing or spliceosomal mutations are a common feature of many human diseases including chronic lymphocytic leukaemia (CLL) and myelodysplasia (MDS) [5]. The core components of the U2 snRNP, such as the splicing factors 3B subunit 1 (SF3B1) and U2 auxiliary factor 35 (U2AF35), are commonly mutated in these diseases [6, 7], with U2AF1 mutations detected in 9% of MDS patients and SF3B1 mutations in 10% of CLL cases [8]. Further, the most frequent aberrant splicing event was a mutation in the 3' promoter region of *NOTCH1* that led to mRNA splicing errors and was associated with more aggressive CLL [9]. Aberrant splicing is common in genes associated with susceptibility and progression of cancer [10]. Moreover, heritable mutations in splicing genes may cause several rare diseases including spinal muscular atrophy, retinitis pigmentosa, Nager syndrome, mandibulofacial dysostosis and oesophageal atresia [11-23].

1.2 RNA splicing regulation: Intron, Exon and Spliceosome

Regulation of the splicing process is carried out by the serine/arginine rich (SR) protein family together with the heterogeneous nuclear ribonucleoparticle (hnRNP) proteins. The SR proteins are a large superfamily of RNA binding proteins and they share common RNA binding motifs with the hnRNP proteins [24-26]. Heterogeneous nuclear ribonucleoproteins (hnRNPs) belong to an RNA-binding protein (RBP) family and have multiple functions in regulating alternative splicing, mRNA stabilisation, and transcriptional and translational regulation. The SR proteins recognise the enhancer elements: exonic splicing enhancers (ESEs) and intronic splicing enhancers (ISEs) thereby acting as splicing activators. On the other hand, the hnRNP protein family recognises the silencer elements: exonic splicing silencers (ESSs) and intronic splicing

silencers (ISSs) and thus repress splicing. As a result, the SR proteins can bind to the splicing enhancer spliceosome assembly at weak splice site while the hnRNPs bind to the silencer during the regulation of alternative splicing [27].

Moreover, the kinetics of pre-mRNA splicing may regulate gene expression during innate immune responses. Transcriptome analysis of pro-inflammatory gene regulation in activated macrophages showed an accumulation of full-length transcripts but these were incompletely spliced in the chromatin fraction, suggesting that splicing often occurs after transcription has been completed, with transcripts retained on the chromatin until fully spliced [28]. PCR-based methodology also indicated the splicing rate was different in tumour necrosis factor alpha (TNFα) activated mouse fibroblasts and primary macrophages. Intermediate and late transcripts showed longer half-life compared to early gene pre-mRNAs for splicing [28, 29].

1.3 Models of alternative splicing (AS) events

Alternative splicing (AS) is involved in regulating the normal function and responses of the immune system. Alternative splicing alterations in non-coding regions of the mature mRNA transcript can impact on translational enhancers and mRNA stability. Several types of alternative splicing events have been reported, ranging from common events such as exon skipping, intron retention and alternative use of 5' and 3' splice sites, to more rare events including the use of mutually exclusive exons (Figure 1-2).
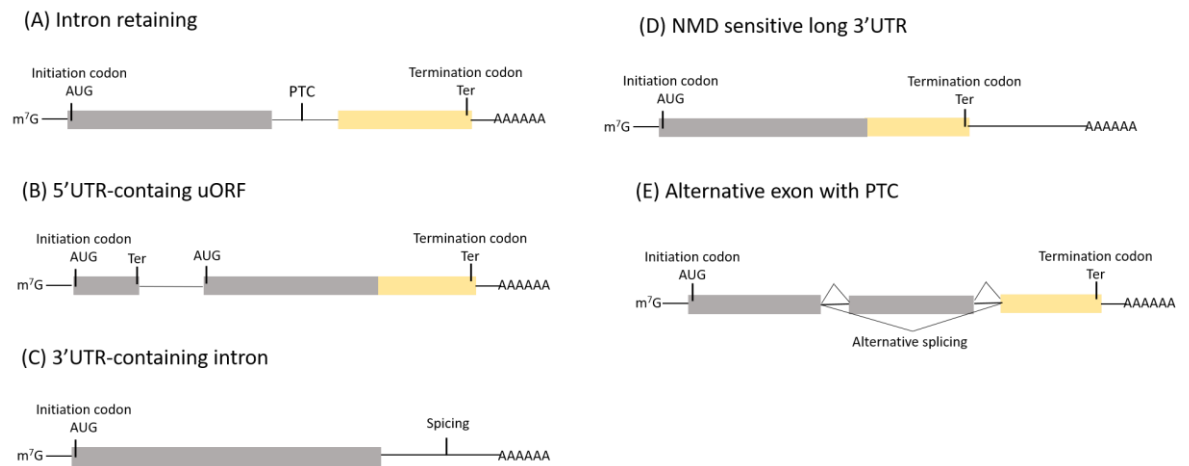
Figure 1-2: Examples of patterns of alternative splicing in NMD.

(A) Intron retaining (B) 5'UTR-containg uORF (C) 3'UTR-containing intron (D) NMD sensitive long 3'UTR (E) Alternative exon with PTC. Exons are represented grey and yellow blocks and introns as line in between.

1.4 Alternative splicing regulates gene expression in immune system

The first example of alternative splicing in eukaryotes was identified in the mRNA of IgM, a member of the immunoglobulin superfamily [30]. Following this, several alternatively spliced genes with functional roles in the immune system have been identified (Table 1-1). For example, alternative splicing can regulate T cell activation and function [31]. CD44 is crucial for T cell homing and function, and alternative splicing of CD44 can generate ten variable exons and six distinct protein isoforms. Naïve T cells mainly express the smallest CD44 isoform that lacks all variable exons, whereas activated T cells express multiple CD44 isoforms [32]. Quantitative microarray analysis has also been used to analyse changes in alternative splicing events during activation of the Jurkat T cell line, which showed 10-15% of alternative exons undergo a >10% change in inclusion level during activation. Furthermore, results from quantitative PCR showed that

over half of the microarray-predicted alternative spliced events saw a significant change when primary $CD4^+$ or $CD8^+$ human T cells were stimulated [33]. In human dendritic cells, around 20% of the genes undergo alternative splicing events and most of these genes have been reported to be involved in regulating cellular functions and defence against antimicrobial invasion [34]. In summary, alternative splicing can regulate and fine tune gene expression in different cell types during development; intruigingly these can also differ between species and may explain nuances in immune regulation that are not conserved across species barriers [35-37].

Table 1-1: Known alternatively spliced genes with changed function in immune responses.

Gene	Description in immune system	Functional change	Refs
SLAT	SLAT functions to regulate CD4$^+$ T cell inflammatory responses by controlling Ca^{2+}/NFAT signalling.	A spliced isoform of SLAT(SWAP-70-like adapter of T cells), called SLAT2, which lacks the region encoded by exons 2 to 7 of the *Def6* gene and was selectively expressed in differentiated Th2 cells after in vitro stimulation, but not in differentiated Th1, Th17, or regulatory T (Treg) cells.	[38]
AKT	AKT is a serine threonine kinase that is required for T cell development.	Akt2 can regulate CD4 T cell responses. Akt2 knockout Th17 cells suppress cholesterol biosynthesis and IL-6 production by microarray analysis.	[39]
IL-6	IL-6 promotes differentiation of CD4+ T to Th2 cells.	IL-6Δexon has been identified as a competitor with native IL-6 for binding to IL-6R, but it is unlikely to mediate IL-6Rβ signalling pathway in primary human lung specimens and cultured fibroblasts.	[40]
IL-32	IL-32 can induce several cytokines such as TNFα and Interleukins. It is activated via NF-κβ and p38 MAPK pathways.	IL-32γ and IL-32β can induce caspase-8-dependent cell death. Overexpression of IL-32β or IL-32γ isoforms enhance the expression of the survival cytokine IL-8.	[41]

IL-15	IL-15 is a cytokine.	IL-15ΔE7 is an alternatively spliced IL-15 mRNA isoform that dampens an inflammatory response to external stimulation in memory deficient keratinocytes.	[42]
IL-4	IL-4 is a cytokine and can be detected in purified CD3+ T cells.	Human IL-4Δexon2 isoform enhances pulmonary cytokine production and reduces eosinophil counts/activities in mouse, with similar pulmonary infiltration of T and B cells as IL-4 stimulated.	[43]
γ-chain (γc)	γc is a cytokine receptor subunit and it is required for development of T cells.	One γc spliced isoform, called sγc, is an immunomodulator and can inhibit the regulation of cytokine pathway by directly binding to IL-2Rβ and IL-7Rα on T cells. Additionally, sγc suppressed IL-7 signalling to impair naive T cell survival during homeostasis and exacerbated Th17-cell-mediated inflammation by inhibiting IL-2 signalling upon T cell activation.	[44]

1.5 Post-translational gene expression regulation by Nonsense Mediated Decay

Nonsense-mediated decay (NMD) is the major RNA decay pathway which recognises and degrades mRNA with premature termination codon (PTCs), to prevent the production of non-functional or truncated proteins. Generally, there are two well-established pathways that can trigger NMD activation – 1) PTC recognition which depends on the exon-junction complex (EJC) and 2) a mechanism based on the distance between a PTC and the poly (A) tail of an mRNA (Figure 1-3).
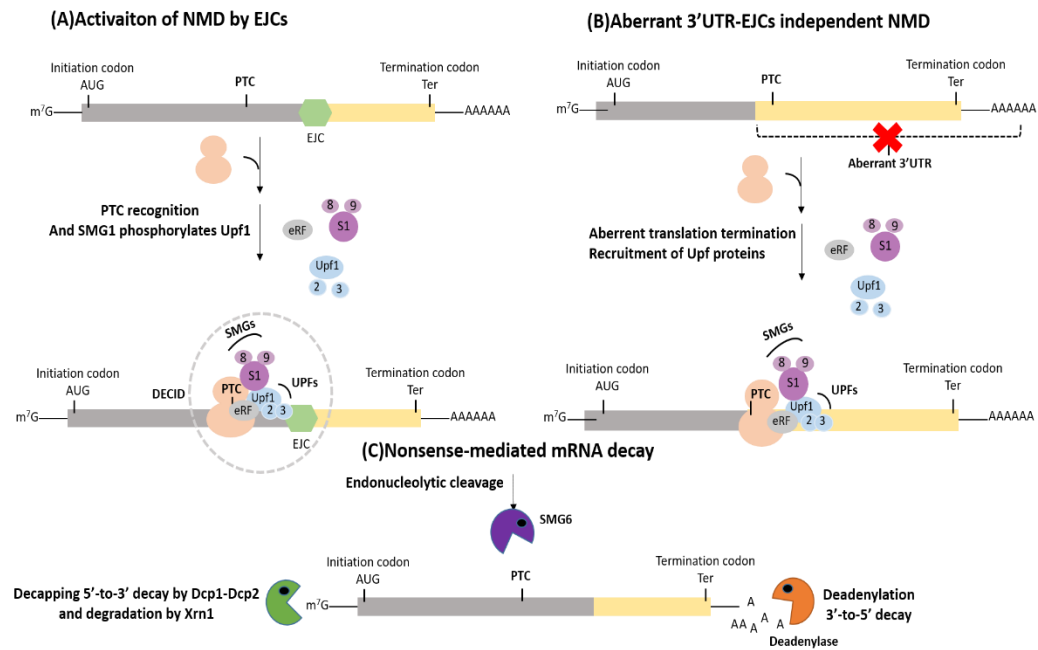
Figure 1-3: NMD mechanism in eukaryotic cells. (A) Activation of NMD by EJCs. Premature termination codon (PTC) recognition relies on the protein complex called the exon-junction complex (EJCs) during the initial round of translation. During translation termination, the mRNA surveillance complex-SURF, composed of SMGs (SMG-1/SMG-8/SMG-9 complex), UPF1 and eRF, detects the downstream EJC and forms the decay-inducing complex (DECID), which induces SMG1-mediated UPF1 phosphorylation. The SMG-5/SMG-7 complex binds to phospho-S1096 of UPF1 to dissociate the ribosome and release factor from UPF1. SMG-6 binds to phospho-T28 of UPF1 to induce UPF1 dissociation from the mRNA. (B) Aberrant 3'UTR-EJC independent NMD. EJCs are not always required for NMD. In the presence of aberrant 3'UTR, translation termination is induced by UPF1 dissociation from the mRNA. This allows for assembly of UPF proteins and recruitment of SMGs independently of an EJC. (C) mRNA decay by NMD mRNA degradation is initiated by deadenylation and SMG-6 mediated endonucleolytic cleavage, cap hydrolysis and finally XRN1 (5' to 3') and exosome (3' to 5') degradation from both ends of the mRNA fragment.

1.5.1 Activation of NMD by EJCs

The EJC is a multiprotein complex that can link splicing and NMD [45, 46]. During splicing the EJC is deposited at each splice junction. In the initial round of translation, an EJC downstream of a stop codon marks the stop codon as premature and can trigger NMD by recruiting and activating UPF1 on the mRNA. If the stop codon is downstream or within 50 nucleotides (nt) of the final EJC, then the transcript is translated normally. However when a PTC is located greater than 50-55nt from the EJCs, it is recognised by the mRNA surveillance complex called "SURF" (SMG1/Upf1/eRF1/eRF3) on the transcript [47-49] and the transcript is targeted to nonsense mediated decay.

SMG1 is a member of the PIKK (phosphoinisitide 3-kinase related kinases) family and plays an important role in NMD. Its kinase activity is suppressed by SMG8 in the absence of PTC. UPF1 is an ATP-dependent RNA helicase crucial for mRNA degradation. UPF1 is recuited to the PTC by binding to the translation release factors, eRF1 and eRF3, via its N-terminal cysteine-histidine rich domain. Upon PTC recognition and association, the SURF complex interacts with the downstream EJC via UPF2 and UPF3 to form the decay-inducing complex (DECID). This triggers SMG1-mediated UPF1 phosphorylation at multiple sites [57-60] and this process is the rate limiting step in NMD [46-49]. Additionally, SMG1 can activate p53 in response to DNA double-strand breaks independently only under oxidative stress [50].

In particular, SMG1-mediated phosphorylation of UPF1 at threonine 28 triggers downstream phosphorylation and specific recruitment of SMG6 to the N-terminal conserved region of UPF1 [47] resulting in UPF1 dissociation from the mRNA. The

SMG6 PIN domain (homologues of the pilT N-terminal domain) contains ribonuclease properties for endonucleolytic mRNA degradation [51, 52]. In addition, SMG1 phosphorylates UPF1 at serine 1096, which recruits the SMG5/SMG7 heterodimer complex to the C-terminal SQ-rich region of UPF1 [47], leading to dissociation of eRF1 and eRF3 from the DECID complex [61] as well as ribosome dissociation from the mRNA transcript. Furthermore, SMG5/7 recruits decapping and deadenylation machinery leading to exonucleolytic decay of mRNA (see Section on mRNA decay machinery below 1.11) (Figure 1-3) [62, 63]. Subsequently, SMG5, SMG6 and SMG7 bind to phosphorylated UPF1 via 14-3-3 domains and recruit protein phosphatase 2A (PP2A) to promote UPF1 degradation [53-57]. Although SMG5 and SMG6 both have the broad C-terminal PIN domain [58], only SMG6 has the key catalytic residues, which means SMG6 can mediate endonucleolytic cleavage in human NMD [59].

1.5.2 3'UTR EJC-independent NMD

EJCs are not always required for NMD. EJC-independent NMD is triggered by the distance of 3'UTR from the termination codon and the efficiency of ribosome release from the termination codon. The poly (A) tail is coated by PABPs (PABPC1, PABPC4 and PABPN1) that recruit release factors, eRF1 and eRF3, to the ribosome for efficient translation termination. UPF1 preferentially associates with transcripts containing 3'UTRs and allows for the assembly of UPF proteins and recruitment of SMG1/8/9 independent of an EJC. Phosphorylated UPF1 can recruit SMG5/6/7 for mRNA degradation. Cytoplasmic poly (A)-binding protein 1 (PABPC1) has been identified as a human NMD antagonising factor, which inhibits the binding of UPF1 to the translation release factors eRF1 and eRF3 [60, 61]. PABPC1 can inhibit NMD when it is brought

into close proximity to the PTC, regardless of cleavage or polyadenylation. The role of PABPC1 in NMD must go beyond that of providing positional information for PTC definition, because its depletion suppresses NMD under conditions in which translation efficiency is not affected [62]. These findings highlight that the length of 3'UTR can also can contribute to mRNA quality control. Longer 3'UTRs can result from a PTR, but may also exist to regulate gene expression

Smg1 deficient mouse models have highlighted the importance of NMD in development and cancer. Smg1 deficient mice are embryonic lethal by E8.5 and murine embryonic fibroblasts derived from the homozygous knocked out embryos did not have an intact NMD pathway, indicating that Smg1 is vital for NMD and mouse development [63, 64]. Furthermore, Smg1 heterozygous mice showed enhanced pro-inflammatory cytokine production and tumour formation, though these animals did not have significant defects in basal NMD [64]. Therefore, SMG1 may have other roles apart from NMD in regulating gene expression and inflammation.

1.6 Premature termination codon (PTC)-associated NMD in genetic diseases

PTC can arise from mutations including nonsense, frameshift and splice site mutations. Approximately one-third of genetic disorders [65] and cancer-associated mutations produce PTCs. These PTC-mRNAs can encode aberrant truncated proteins that can display loss-of-function, gain-of-function or dominant-negative effects [65, 66]. In some cases, NMD limits the severity of the diseases by degrading truncated proteins with dominant-negative effect such as in β-thalassemia and osteogenesis imperfecta. In other cases where patients have truncated proteins that still retain normal or partial function,

NMD may cause more severe phenotypes by degrading the partially functional transcript thus resulting in no functional protein expression. This occurs in diseases including Duchenne muscular dystrophy (DMD) and Ullrich's disease [67] (Table 1-2). Additionally, mutations in the SRY-related HMG-box 10 (SOX10) can cause distinct neurological phenotypes depending where the truncating mutation occurs. SOX10 is a transcription factor that is required for the development of neural crest including the maintenance of Schwann cells and melanocytes. Interestingly when the mutation is located in the first half of the SOX10 gene, it causes a milder phenotype called Waardenburg–Shahsyndrome due to haploinsufficiency as the mutated transcript is degraded; whereas truncating mutations in the last half of the gene give rise to transcripts resistant to NMD and leads to a more severe neurological mechanism because of a dominant negative effect of the truncated protein [68]. Therefore, NMD can prevent or exacerbate nonsense mutation/PTC-mediated congenital and spontaneous diseases.

Several studies have also demonstrated the importance of NMD during viral infection [69-72]. Garcia *et al.* showed NMD-mediated control of gene expression from *turnip crinkle virus* and *potato virus X* via NMD recognition of transcripts with long 3'UTRs [72]. Interestingly both viruses displayed mechanisms aiming to counteract NMD during infection. Further, Gloggnitzer *et al.* demonstrated reduced NMD efficacy during bacterial infection [70]. TIR-domain containing, nucleotide binding, leucine-rich repeat (TNL) proteins (plant pathogen recognition receptors related to the TLR family) are targets of NMD. Knockdown of NMD components in HeLa cells also affected viral infection allowing for increased Semliki Forest virus replication [71] and depletion of Upf1 resulted in increased presence of viral derived dsRNA.

Table 1-2: The relationship between PTC-caused diseases and Nonsense-mediated decay.

Disease or Syndrome	Gene affected	PTC-mutation	NMD role	Refs
Ullrich disease	Collagen type V1α2 gene	Frameshift mutation	Suppressing SMG-8 effectively ameliorates NMD-exacerbated mutant types.	[67, 73]
Leukoence phalopathy	HtrA serine peptidase	PTC-containing mutation	Knockdown of SMG-8 produces an effect for restoring defective mRNA and protein levels without affecting cell growth, cell-cycle progression or endoplasmic reticulum stress.	[67]
Townes–Brocks syndrome	*SALL1*	Frame-shift mutation	This mutation caused a much milder phenotype including a higher susceptibility to NMD.	[74]
Limb Malformati on syndromes	*GLI3*	Frame-shift mutation	In patients' derived fibroblast found that all three mutant alleles were susceptible to NMD.	[74]
β-thalassemi a	β-globin gene	nonsense mutation	Patients with mutation in exon III β12l (G-T) and β127 (C-T) with the clinical phenotype of thalassemia and be related to the lack of mRNA instability.	[75]
Spinal Muscular Atrophy (SMA)	*SMN1*	point mutation	*In-vivo* splicing assays demonstrated that *SMN1* mutations in exon 3 (c.469C>T) and a substitution in intron 4 (c.628-140A>G) render SMN1 transcripts susceptible to NMD.	[76]
Hereditary Diffuse Gastric Cancer (HDGC)	*CDH1*	Germline mutations	Results from mutant and wild-type CDH1 alleles by allele-specific expression (ASE) indicate that NMD may be detrimental for patients harbouring CDH1 alleles with PTCs.	[77]

Ataxia-Telangiectasia (A-T) syndrome	Ataxia-Telangiectasia mutations gene (*ATM*)	Frameshift and nonsense mutations	A-T patients with truncating mutation near the 3'PTC showed a shorter survival, however 5'PTC saw a mild form of ataxia syndrome.	[78]

1.7 AU-rich elements regulate RNA stability in inflammation

Post-transcriptional gene expression regulation involves RNA stability, translation, modification, localisation as well as already discussed alternative splicing of the mRNA [79]. These systems are regulated by various RNA binding proteins that control gene expression by binding to RNA sequences or secondary structures via different RNA binding motifs. Among these, the most common motifs are AU-rich elements (AREs). AREs are conserved sequences with frequent adenine and uridine bases in the mRNA the 3'UTR which target the mRNA for rapid degradation [80-82]. The first evidence came in 1986, conserved AU-rich sequences were found in the 3'UTR of the genes that encode TNFα and granulocyte–macrophage colony-stimulating factor (GM-CSF; which is encoded by *CSF2*) [83]. Insertion of the *CSF2* AU-rich sequence into the 3'UTR of a β-globin mRNA reporter construct induced β-globin mRNA transcript degradation. Conserved AREs are found in the 3'UTRs of inflammatory mRNAs that encode for IL-6, IL-8, TNF, IL-2, IL-1β, cyclooxygenase 2 (COX2), IFN-γ, GM-CSF, inducible nitric oxide synthase (iNOS; also known as NOS2), transforming growth factor-β (TGFβ) and IL-10 [79, 84, 85].

AREs are recognised by ARE-binding proteins. Among them, tristetraprolin (TTP), ZFP36L1 (also known as BRF1), ZFP36L2 (also known as BRF2), and AUF1 (AU-rich element RNA-binding protein 1; also known as HNRNPD) and KHSRP (KH-type

16

splicing regulatory protein) promote deadenylation and degradation of target mRNAs [84, 85], while HuR (human antigen R) stabilises target mRNAs by competing with destabilising factors to inhibit ARE-mediated RNA degradation [86]. In the last decade, increasing numbers of studies have focussed on ARE-mediated post-transcriptional control of inflammation. Pro-inflammatory mRNA transcripts such as TNFα, IL-1β and IL-6 are relatively short-lived and unstable due to the presence of AREs in their 3' UTRs that cause rapid transcript degradation [87]. HuR stabilises short-lived ARE-containing mRNAs in mammalian cells [88] and mediates TNFα and IL-1β mRNA stability upon LPS stimulation. However, ARE-mediated mRNA regulation can differ between genes. This is presumably due to different ARE-binding proteins interacting with the ARE-containing mRNA. When TTP is dephosphorylated by protein phosphatase 2A, TTP displaces HuR binding to the TNFα ARE with high affinity but not IL-1β bound HuR. Therefore, upon LPS stimulation, TNFα has rapid response because its mRNA is degraded at a faster rate compared to IL-1β [89]. TTP-deficient mice develop inflammatory syndromes such as arthritis, dermatitis and cachexia [90, 91], as well as severe inflammatory diseases [92] such as LPS-induced shock [93, 94] which results from excessive TNFα and IL-1β production. These findings support the concept that ARE-mediated mRNA regulation controls inflammatory responses.

Moreover, ARE-binding protein association with ARE-containing transcripts can also be modified by intracellular signalling molecules during an immune response. For example, p38-MAPK/MK2 kinase can stabilise ARE-containing TNFα mRNA transcript by inhibiting TTP-mediated mRNA degradation, which leads to rapid TNFα expression upon LPS stimulation in macrophages [95]. Therefore, AREs can regulate pro-inflammatory mRNA transcripts after LPS stimulation. The regulation of ARE-containing transcripts is

a dynamic process after the coordination among ARE-binding proteins during immune cellular activation.

1.8 m6A is the most common mRNA modification

N6-methyladenosine (m6A) is the most abundant mRNA modification which influences almost every step of RNA metabolism including mRNA export from nucleus to the cytoplasm, mRNA translation, mRNA decay, the biogenesis of long-non-coding RNA (lncRNA) and microRNA (miRNA). Previous studies have found that the abundance of m6A is 0.1-0.4% of adenosine residues in total isolated RNA, suggesting that m6A is a widespread modification throughout the transcriptome [96-98]. The distribution of m6A has been demonstrated to be highly enriched near the stop codons and in the 3'UTRs, particularly in precursor mRNAs [99]. Additionally, around 30% of genes containing microRNA binding sites in their 3'UTRs have m6A residues indicating a relationship between microRNA-binding sites and m6A modification [99, 100]. The mechanism of m6A modification includes three important regulators which are called "writers", "erasers" and "readers" that can add, remove or preferentially bind to the m6A site. Several proteins have been identified as 'm6A writers';'m6A erasers';'m6A readers'. These include the catalytic subunit METTL3 and cofactors: METTL14 and WTAP [101-103]; ALKBH5 and FTO [104-106]; and the cytoplasmic YTH-domain family 1 (YTHDF1), YTHDF2 and YTHDF3 [107].

The m6A RNA modification is catalysed by the RNA methyltransferase complex or 'm6A writers'. Methyltransferase-like 3 (METTL3) was identified as the first S-adenosylmethionine (SAM)-binding subunit of the RNA methyltransferase complex which drives m6A RNA methylation [108]. High levels of SAM enzyme activity can

drive methylation while low levels of SAM can stimulate demethylation [109]. METTL3 and methyltransferase-like 14 (METTL14) [102] co-localise in nuclear speckles and form a stable complex. METTL3 binds to SAM while METTL14 plays a structural role critical for substrate recognition. Wilms tumour 1-associated protein (WTAP) [110] and KIAA1429 (also known as VIRMA) [111] are adaptor proteins which interact with the METTL3-METTL14 heterodimer and recruit other factors to the methyltransferase complex. Other adaptor proteins such as RNA-binding motif protein 15 (RBM15) and its paralogue RBM15B can also interact with METTL3 complex and depletion of these adaptors decreased intracellular m6A level [112]. A newly discovered m6A methyltransferase, METTL16, has a major function in 3'UTR methylation as METTL16 deletion leads to ~20% decrease in 3'UTR methylation [113]. The two m6A erasers, AlkB homolog 5 (ALKBH5) and Fat mass and obesity-associated (FTO), can remove m6A modification from the mRNA transcripts by catalysing the oxidative demethylation of thymidine and uracil as well as using ferrous iron and α-ketoglutarate as substrates to demethylate the m6A site [104, 106].

The m6A effect is mediated through the recognition of the m6A site by "readers" directly or indirectly. Direct reader refers to selective binding of m6A "readers" to the m6A site of RNAs. The YTH (YT521-B homology) family proteins YTHDF1-3 and nuclear member YTHDC1 are direct readers that bind to m6A sites on the RNA [107, 114]. Indirect reading means that the m6A modification alters the RNA secondary structures and thereby renders accessibility of the RNAs to RNA-binding proteins. Heterogeneous nuclear ribonucleoprotein A1/B1 (HNRNPA2B1) and heterogeneous nuclear ribonucleoprotein C (HNRNPC) are two abundant nuclear RNA-binding proteins responsible for pre-mRNA processing [115]. The m6A site of pre-mRNA indirectly alters

the binding of HNRNPC to its U-tract motifs. HNRNPA2B1 directly binds to m6A site of RNA and was identified to be a regulator in microRNA processing [115]. Eukaryotic initiation factor 3 (ELF3) was identified as a direct m6A-binding protein to promote cap-independent translation [114]. Therefore, m6A modification is a complex yet tightly regulated process for fine-tuning post-transcriptional mRNA levels.

1.9 m6A modification machinery affects viral infection and host immune responses

Regulation of inflammation includes controlling cytokine and chemokine production as well as recruitment and activation of innate and adaptive immune cells [116]. Recent studies have indicated that the depletion of m6A modification machinery leads to dysregulated methylation of diverse viruses, therefore impacting virus reproduction and host immune responses [117, 118]. Deletion of the m6A 'writer' METTL3 or 'reader' YTHDF2 following viral infection led to an increase in the induction of IFNβ and downstream interferon-stimulated genes (ISGs). The IFNβ mRNA was modified by m6A and was stabilised following viral infection and depletion of METTL3 or YTHDF2 [117]. In a separate study, the host m6A modification machinery regulated IFNβ production in response to human cytomegalovirus (HCMV) infection or dsDNA transfection to activate the cytosolic DNA detection pathway via cGAS/STING pathway, leading to trigger of inflammatory genes expression [119, 120]. The depletion of METTL14 led to reduced viral protein reproduction and IFNβ mRNA accumulation following the dsDNA treatment or HMCV infection. However, deletion of the m6A eraser ALKBH5 showed the opposite effect [118]. Moreover, IFNβ1 mRNA was m6A-modified in both the coding sequence and the 3′UTR, suggesting that m6A modification enzymes can regulate cellular responses to dsDNA sensing thus shaping host immunity [118]. These findings have

highlighted that m6A can act as a negative regulator of the interferon response by dictating the fast turnover of interferon mRNAs and facilitating viral propagation. Therefore, m6A RNA modification machinery affects both viral infection and the host immune response.

1.10 mRNA decay machinery

Pathways controlling RNA decay include the RNA decay exosome, deadenylation, decapping and degradation, NMD, and AU-rich element targeted decay mediated by tristetraprolin (TTP). In eukaryotes, most mRNAs undergo decay by the deadenylation-dependent pathway. The majority of mammalian cytoplasmic mRNA decay starts with shortening of the poly(A) tail followed by 5'-cap hydrolysis and degradation of the remaining mRNA by XRN1-mediated 5'>3' or exosome-mediated 3'>5'degradation and cap hydrolysis. The 5'-cap and 3'-poly(A) tail protect the mRNA transcript from the attack of exonucleases and interact with eIF4E and the poly(A)-binding protein (PABP) to enhance translation initiation. Initially, poly(A) tail shortening occurs via the PAN2/PAN3 complex and subsequently degradation occurs via the CCR4/NOT complex [121]. The CCR4/NOT complex consists of 10 subunits (CNOT1, CNOT2, CNO3, CNOT4, CNOT6, CNOT6L, CNOT7, CNOT8, CONT9/Caf40/Rcd1, CNOT10/Caf130) and CCR4 is mainly responsible for deadenylation [122]. Next, the 5'-cap is removed by decapping via the DCP1-DCP2 complex [123, 124]. Then the RNA is degraded by the XRN1 exonuclease. Alternatively, the exosome complex degrades mRNA in the 3'>5' direction. RNA decay can occur co-translationally or in cytoplasmic foci called processing bodies (P-bodies). P-bodies are sites where mRNAs are targeted to decay factors and are either degraded or shuttled to other cytoplasmic foci called stress granules where some transcripts are stored for later translation [125].

Decapping is a critical step in mRNA decay and occurs by poly(A) shortening, and oligoadenylated mRNAs (but not polyadenylated mRNAs) in the 5'>3' decay pathway. There are several factors involving in controlling this step, including the poly(A) binding protein and decapping activators: LSM1-7/Pat1. Evidence in the yeast system indicates that PABP can inhibit the decapping of polyadenylated mRNAs *in vivo* [123, 126-128]. On the other side, the LSM1-7/Pat1 complexes activate the decapping to the P-bodies in the cytoplasm and followed by 5'>3'degradation [124, 129]. Also, LSM1-7/Pat1 complexes can inhibit exosome attachment by preferentially binding the 3'-end of oligoadenylated mRNA [130].

1.11 Overview of post-transcriptional gene regulation in innate immunity

Gene expression can be regulated from transcriptional initiation to RNA processing and post-translational modification of proteins. Alternative splicing has been identified as a key process in post-transcriptional regulation of gene expression in higher eukaryotes, thus allowing a single gene to code for multiple mRNA transcripts and protein isoforms, therefore giving rise to protein diversity. More than 90% of the human genes undergo alternative splicing and around 50% of disease-causing genetic mutations can lead to splicing defects, thereby affecting cellular functions or contributing to pathological effects [131, 132].

Alternative splicing modulates the transcriptomic variability in different tissues. There is an increasing number of studies investigating aberrant alternative splicing events in inflammation related diseases such as osteoarthritis [133], atherosclerotic plaque progression [134], multiple sclerosis [135], systemic lupus erythematosus [136],

Crohn's disease [137], and type 1 diabetes [138]. In the immune system, alternative splicing provides a major role in regulating gene expression and generating the diverse repertoire of antigen receptors expressed by B and T cells [139, 140]. Also, gene expression can be regulated via nonsense-mediated decay (detailed above section 1.5), which can precisely control the timing and level of gene expression as well as eliminating unstable or toxic truncated protein production. Understanding the regulation of gene expression, at the level of RNA biology, will be helpful in the development of a new generation of drugs to treat inflammation associated diseases including cancer, autoimmune disorders and infectious diseases.

1.12 Interactions of innate and adaptive immunity

The mammalian immune system can be broadly divided into innate immunity and adaptive immunity. The innate and adaptive immune systems have to cooperate to recognise and respond to infective microorganisms. During the first few hours after infection, innate immunity is essential to provide a first line of defence against pathogens. It consists of complement proteins and intracellular effectors including granulocytes, mast cells, macrophages, dendritic cells (DCs) and natural killer (NK) cells. When pathogens invade the body, the innate immune system is activated first and participates in the initial attack against the pathogens. Among the cells involved in innate immunity, dendritic cells act as antigen-presenting cells and migrate from the infected tissue to the regional lymph nodes where they present the antigens to T cells. Subsequently, the adaptive immune system is activated, and antibody production and cytotoxic T cells are induced. The resulting antibodies and cytotoxic T cells specifically attack the pathogens. The adaptive immune response does not immediately react but requires signals from the host exposure to pathogens. Natural killer T cells and γδ T cells are additional cytotoxic

lymphocytes which function at the interface of innate and adaptive immunity [141]. Innate immune responses make crucial contributions to the activation of adaptive immunity. For example, macrophages of the innate immune system are required for the control of defence against bacterial and viral infections and sculpt the adaptive immune response via production of M1 vs M2 cytokine profiles (please find more details as below 1.12.1). The initial innate immune response is essential to control the first phase of infection while the adaptive immune response takes at least 5-7 days after antigen exposure to develop [142, 143].

1.12.1 Macrophage polarisation and its role in inflammation

Macrophages are members of the mononuclear phagocyte system (MPS). This includes bone marrow progenitors, circulating monocytes, tissue macrophages and DCs [144, 145]. Precursors in the bone marrow give rise to monoblasts, which then differentiate into blood monocytes. Monocytes circulate in the blood before migrating via the blood vessel walls to become tissue macrophages. Alternatively, some populations of tissue macrophages are established early in development and undergo self-renewal. Terminal differentiation of monocytes gives rise to a wide range of cells that are all members of the MPS. These cells include osteoclasts in the bone, microglia in the brain and Kupffer cells in the liver [145]. Elie Metchnikoff [146] first identified macrophages as large phagocytic mononuclear cells which play a major role in immunity. Macrophage polarisation into different phenotypes seems to shape macrophage responses depending on stimulants such as microenvironmental stimuli and the amounts of cytokines produced. This polarisation has been at its simplest separated into two programs, M1 (classically activated macrophages) and M2 (alternatively activated macrophages) [147]. M1 macrophages

show a proinflammatory phenotype [148], whereas M2 are considered anti-inflammatory for macrophages [149].

M1 macrophages emerge as the first line of defence against pathogen invasion and promote the Th1 polarisation of CD4$^+$ T cells [150]. In vitro M1 macrophages can be differentiated by IFNγ treatment that results in release of pro-inflammatory cytokines including IL-1, IL-12 and TNF-α [151]. However, the main role of M2 macrophages is to inhibit inflammation and they can be induced by Th2 cells with IL-4. The main M2 macrophage products are arginase-I, IL-10 and TGF-β and other anti-inflammatory cytokines which lead to decreasing inflammation and contribute to tumour growth and immunosuppressive functions [152, 153]. Interleukin 10 (IL-10) has been reported as potential inhibitory effect on the production of several inflammatory cytokines including TNF-alpha in alveolar macrophages and peripheral blood monocyte [154]. Both of M1 and M2 participate in the arginine metabolic pathway [155-157]. M1 macrophages induce inducible NO synthase (iNOS) via arginine metabolism, which leads to the production of large amounts of NO and citrulline. This can help downstream toxic metabolites that work together for M1 mediated killing. Rapid killing is important during the first phase of immune responses [158] to prevent rapid pathogen proliferation prior to development of adaptive responses [159].

Table 1-3: List of functions and relative cytokine productions of M1 and M2 macrophages.

Types	Functions	cytokines	Refs.
M1	-Produces proinflammatory cytokines and chemokines - Induces Th1 response activation -Mediated phagocytosis -Participates in type I inflammation	IL-1β, IL-6, IL-12, IL-18 IL-23, TNF-α, and type I IFN, CXCL1, CXCL3, CXCL5, CXCL8, CXCL9, CXCL10, CXCL11, CXCL13, CXCL16; CCL2, CCL3, CCL4, CCL5, CCL8, CCL15, CCL11, CCL19, CCL20, CX3CL1	[160-165]
M2	-Regulates cell functions during parasitic, helminthic, and fungal infections -Participates in anti-inflammatory cytokine production	IL-13, CCL1, CCL2, CCL13, CCL14, CCL17, CCL18, CCL22, CCL23, CCL24, CCL26, IL-1R, IL-8, MCP-1(monocyte chemo-attractant protein-1), IP-10, MIP-1β (macrophages inflammatory protein-1β)	[163, 166-168]

1.13 Pathogen associated molecular patterns and their receptors

The innate immune system relies on families of germ line-encoded receptors to recognise conserved microbial components that are absent in the host. These molecules are called pathogen-associated molecular patterns (PAMPs). PAMPs are essential structures for pathogen survival and therefore cannot be easily mutated to avoid the immune response. Various types of PAMPs are able to induce inflammatory responses and phagocytosis by cells such as macrophages and dendritic cells. Examples of PAMPs include bacterial cell wall components such as lipopolysaccharide (LPS), lipopeptide, and peptidoglycan, as well as other structural components including flagellin and nucleic acids such as double-stranded RNA. PAMPs are detected by pattern recognition receptors (PRRs) [169]. Examples of PRRs in mammals include Toll-like receptors (TLRs), RIG-I-like receptors

(RLRs), Nod-like receptors (NLRs), AIM2-like receptors (ALRs), C-type lectin receptors (CLRs), as well as intracellular DNA sensors such as cGAS [170, 171]. The recognition of PAMPs by PRRs leads to production of inflammatory cytokines, including type I interferon (IFN) and chemokines and later these processes can trigger activation of antigen-presenting cells and adaptive immune responses.

1.14 Toll-like receptor induced signalling pathways

The toll-like receptor family includes 10 members (TLR1-TLR10) in human and 12 (TLR1-TLR9, TLR11-TLR13) in mouse [169]. TLRs are type I integral transmembrane proteins with 19-25 leucine rich repeat (LRR) domains in their N-terminus which mediate PAMP recognition [172], and a conserved Toll/IL-1 receptor (TIR) domain in the C-terminus that is required for downstream signalling initiation [173]. TLRs localised to the cell surface include TLR1, TLR2, TLR4, TLR5, TLR6 and TLR10. Other TLRs are localised to the endosome such as TLR3, TLR7, TLR8, TLR9, TLR11, TLR12 and TLR13 [174, 175]. Cell surface TLRs mainly recognise microbial surface PAMPs such as lipids, lipoproteins, and proteins. TLR4 recognises bacterial lipopolysaccharide (LPS) on the cell surface. TLR2 recognises lipoproteins derived from bacteria, viruses, fungi and parasites by forming a heterodimer either TLR1 or TLR6 [176]. TLR5 recognises bacterial flagellin [177]. Intracellular TLRs recognise nucleic acids derived from bacteria and viruses, and also recognise endogenous nucleic acid in pathogenic progress such as autoimmunity [178]. TLR3 recognises viral double-stranded RNA (dsRNA) [179], TLR7/TLR8 heterodimeric complex detects single-stranded RNA (ssRNA) [180, 181], TLR9 recognises unmethylated DNA with CpG motifs[182], TLR11 recognises the parasite protein profiling [183], TLR12 recognises *T.gondii* profiling (TgPRF) [184], TLR13 recognises bacterial 23S rRNA [185].

TLRs are expressed by hematopoietic cells include dendritic cells, macrophages, and granulocytes and non-hematopoietic cells such as endothelial cells [186] and cardiac myocytes [187]. Upon binding of a pathogen ligand, TLRs trigger a cascade of signalling pathways. In mammalian cells, this recognition not only can lead to the induction of pro-inflammatory cytokines, but also promote antigen presentation capacity in dendritic cells and macrophages. Therefore, TLRs stimulation can act as bridge between innate and adaptive immune responses.

TLR adaptors play an important role to TLRs by binding directly to the TIR domains of the receptor and triggering downstream signalling cascades [188]. The canonical adaptors are myeloid differentiation primary response 88 (MyD88), TIR-domain containing adaptor-inducing interferon-β (TRIF, also known as TICAM1), TRIF-related adaptor molecule (TRAM, also known as TICAM2) and MyD88 adaptor-like (MAL or TIRAP). Another group of TLR adaptors are called 'regulatory adaptors', which are recruited to provide a scaffold downstream kinase or act as negative regulators of TLR signalling. These include sterile α- and armadillo motif (SARM, also known as SARM1), B-cell adaptor for phosphoinositide 3-kinase (PI3K) (BCAP, also known as PIK3AP1) and SLP65/76 and Csk-interacting membrane protein (SCIMP) [189].

1.15 TLR4 signalling pathway

We will focus on TLR4 signalling and stimulation. TLR4 is activated by LPS, which in turn triggers both MyD88-dependent and MyD88-independent (TRIF-dependent) pathways (Figure 1-4). Signalling through the MyD88-dependent pathway is responsible for early phase nuclear factor (NF)-κB and mitogen-activated protein kinase (MAPK) activation that facilitates the induction of pro-inflammatory cytokines. The TRIF-

dependent pathway activates IRF3, which culminates in the induction of IFN-β and IFN-inducible genes.

TLR4 requires MD2 (myeloid differentiation 2), LPS-binding protein (LBP) and CD14 for LPS recognition and ligand-induced activation [190, 191]. After LPS binding, two TLR4/MD2 complexes homodimerise and induce the recruitment of adaptor proteins and trigger downstream signalling cascades and cytokine production [192]. MyD88-dependent signalling [169, 193, 194] occurs mainly at the plasma membrane and recruits MyD88 and MAL proteins followed by the recruitment and activation of IRAKs: IRAK-1, IRAK-2, and IRAK-4 (phosphorylation of IL-1R-associated kinases), and TRAF-6 (TNF-receptor-associated factor 6) which induce TAK-1 (transforming growth factor β-activated kinase 1) activation. TAK-1 activity is mediated by two adaptor proteins: TAB-2 (TAK-1-binding protein 2) and TAB-3 (TAK1-binding protein 3). TAK-1, in turn, leads to the activation of the MAPKs (mitogen-activated protein kinases): JNK (JUN N-terminal kinase), p38 (extracellular signal-regulated kinases (ERK1/2)), and the IκB kinase complex (IKK). As a result, these interactions activate NF-κB (nuclear factor-κB) and AP-1 (activator protein-1) and lead to production of proinflammatory cytokines [192].

Instigation of the MyD88-independent pathway signalling [195-197] occurs in the endosomal compartment after internalisation of the TLR4-MD2 complex and involves the recruitment of adaptor proteins TRIF and TRAM. Engagement of these adaptor proteins activate TNF receptor-associated factor 3 (TRAF-3) and leads to the induction of IFN regulatory factor 3 nuclear transcription factor (IRF-3) which is mediated by TBK-1 (Tank-binding kinase 1) and IKKε. The IRF-3 transcription factor induces the

production of type I IFNs and IFN-responsive genes. MyD88-deficient mice lack the ability to produce cytokines but still partially respond to LPS, including the induction of interferon-inducible genes and the maturation of dendritic cells [198, 199]. MAL (also called TIRAP) is another adaptor protein which is recruited to TLR4 and participates in LPS signalling [200]. MAL-deficient mice lack cytokine production and activation of nuclear factor NF-κB as well as MAP kinases in response to LPS treatment [199].
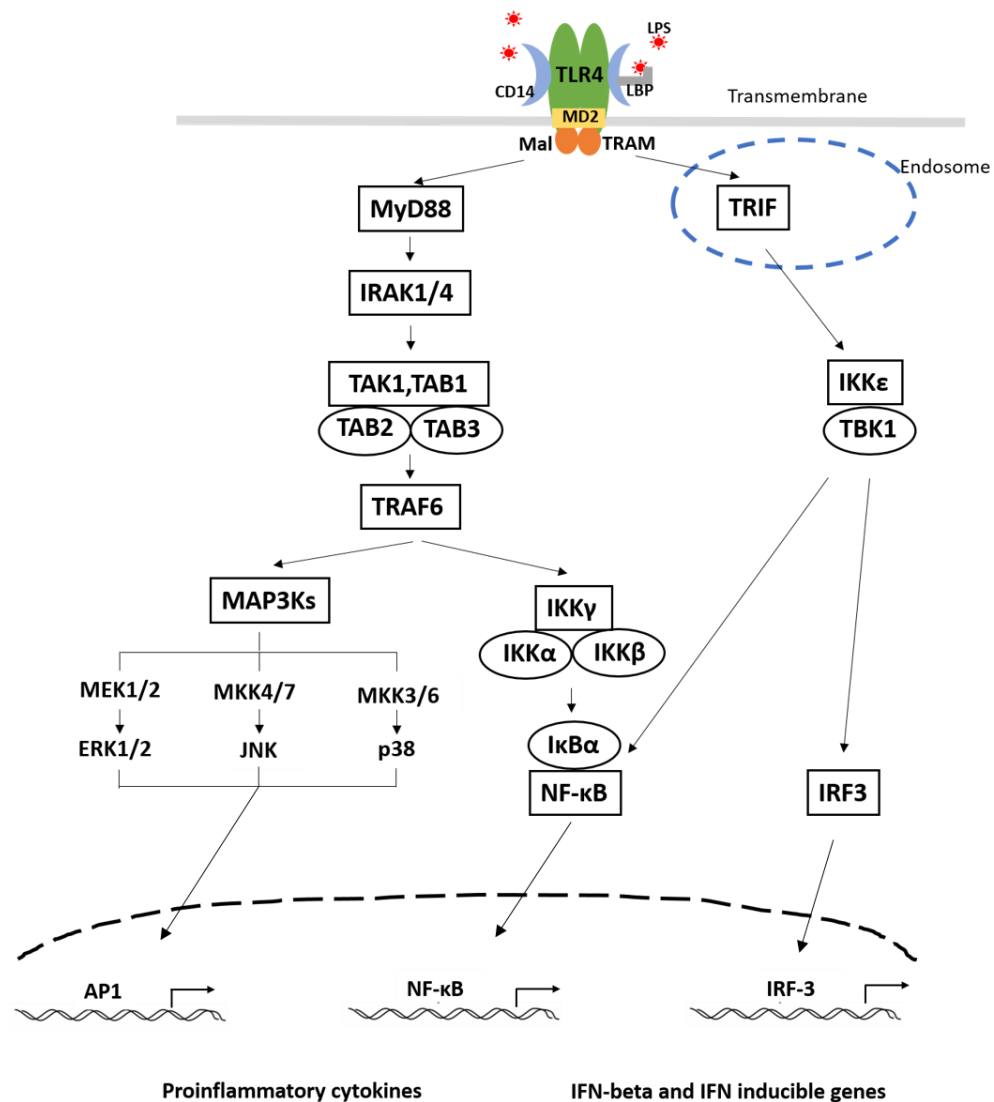
Figure 1-4: The Toll-like receptor 4 signalling pathway. Both of MyD88-dependent and MyD88-independent pathways are induced by stimulation of lipopolysaccharides (LPS) and binds to TLR4 on the cell membrane with CD14 and MD-2. The MyD88-dependent pathway signals through activation of IKK complex kinase and mitogen activated protein kinase (MAPK) pathways, which in turn leads to activation of NF-κB and activator protein 1 (AP1), respectively. The MyD88-independent pathway is mediated by the TIR domain-containing adaptor inducing interferon β (TRIF), which activates interferon regulatory 3 (IRF3) and induces the expression of IFNβ and IFN-responsive genes.

1.16 Molecular and cellular regulation of TLR4 signalling activated by LPS

TLR4 induces strong pro-inflammatory responses that are tempered by many negative feedback loops. Loss of balance in this system may lead to severe inflammatory responses e.g. sepsis, autoinflammatory and autoimmune disorders. TLR4 can regulate cellular control mechanisms from biosynthesis and trafficking to signal transduction and degradation[201] as well as mediate inflammation activated by exogenous or endogenous ligands. Animal models lacking TLR4 (naturally mutated in C3H/HeJ mice [202] or TLR4 knockout mice [202, 203]) showed an increased susceptibility to sepsis from gram-negative bacterial infections such as *Salmonella typhimurium* and *Neisseria meningitides* [202, 204, 205]. These findings support that TLR4 may be a possible drug target to protect from endotoxin shock induced by *E. coli* infection [206, 207].

1.17 Alternative splicing regulation in TLRs signalling

Alternative splicing events not only affect immune cells upon stimulation, but regulate signalling pathways during immune responses. Uncontrolled TLR activation may induce potentially harmful inflammatory responses, or even contribute to diseases such as septic shock. Members of the TLR family are highly alternatively spliced, with 256 variant transcripts identified in mouse primary macrophages [208]. These different transcripts result in numerous novel proteins with potential to functionally alter the inflammatory outcomes in response to TLR ligands.

Each TLR gene has alternatively spliced variants that can inhibit or induce regulation of downstream signalling pathways. A TLR4 splice variant that contains an additional exon with a premature stop codon can upregulate the total TLR4 transcript pool in human

monocytes in the presence of LPS stimulation. Induction of this variant following LPS stimulation correlated with significantly more tumour TNFα in monocytes from cystic fibrosis patients compared to healthy controls [209]. In another example, an isoform of mouse TLR4 mRNA contains an additional exon with an in-frame stop codon that generates a protein known as soluble mTLR4 (smTLR4), which lacks the transmembrane and intracellular domains. This smTLR4 significantly inhibited LPS-mediated TLR signalling, NF-κB activation and the production of TNFα [210]. Similarly, a soluble isoform of TLR2 inhibits IL-8 and TNF production upon TLR2 ligand stimulation [211]. These findings suggest that alternatively spliced TLR transcripts can provide negative feedback to limit transcript expression and excessive inflammation.

MyD88 is the most ubiquitously utilised adaptor protein (all TLRs except TLR3 require the presence of MyD88 as well as interleukin 1 receptor (IL-1R)) [174, 212]. MyD88 is encoded by an mRNA with five exons (long form or MyD88L) that activates innate immunity by transducing Toll-like receptor (TLR) signals; However, a short form (MyD88s), whose mRNA is missing the 135 base pair second exon, inhibits downstream responses [213]. MyD88s levels are regulated by the SF3A and SF3B mRNA splicing complexes in the response to inflammatory cytokine production in murine macrophages [214]. During TLR or IL-1R activation, MyD88 is required for IRAK-4–induced IRAK-1 phosphorylation. However, in the presence of MyD88s, IRAK-1 is not phosphorylated and recruitment of IRAK-4 is blocked [213, 215]. These results implicated that an alternatively spliced form can act as a negative regulator of downstream trigger signals.

1.18 Negative regulation of TLR signalling

Given the strong inflammatory response elicited by TLR4 there are tight regulatory controls to ensure that the response to proportional to the challenge [216-218]. As one regulatory mechanism TLR4 can be transported from the plasma membrane to the endosome for ubiquitination and subsequent degradation. Ligand recognition leads to internalisation of the surface receptor complex into lysosomes, and causes termination of the LPS response. Further, Ras related in brain (Rab) proteins are small guanosine triphosphatases (GTPases) which function in the regulating of vesicular formation, movement, and fusion process [219, 220] as well as in the regulation of membrane trafficking [221]. Ras7b negatively regulates TLR4 signalling in macrophages by promoting the translocation of TLR4 into lysosomes for degradation [222]. Rab10, another small GTPase can regulate the TLR4 pathway by continually replenishing TLR4 onto the plasma membrane. Consequently, altered Rab10 expression increased disease severity in a LPS-induced acute lung injury animal model [223].

In summary, a better understanding of the regulation of TLR4 expression, homeostasis of the surface levels of the TLR4 receptor complex and the promotion of TLR4 degradation is essential for the development of new possible therapeutic treatments of inflammatory diseases. Therefore, it is imperative for researchers to find out new regulators and understand currently identified regulators (Table 1-4) of TLR4 signalling pathways.

Table 1-4: Intracellular negative regulators of Toll-like receptor 4 induced signalling.

Regulator	Full-name	Possible mechanism	Refs.
MyD88s	Myeloid differentiation primary response protein	Suppresses the ability of IRAK4 to phosphorylate IRAK1	[224]
ST2825	ST2825	Inhibits MyD88 dimerisation	[225]
NRDP-1	Neuregulin Receptor Degradation Protein-1	Promotes Myd88 degradation by polyubiquitinating MyD88 and TBK1	[226]
SARM	Sterile alpha- and Armadillo-motif-containing protein	Inhibits MAPK activation	[227]
sTLR4	Soluble decoy TLR4	Blocks interaction of TLR4 and MD2	[210]
IRAKM	Interleukin-1 receptor-associated kinase	Inhibits formation of IRAK1-TRAF6 complex	[228]
SOCS1	Suppressor of cytokine signalling 1	Suppresses IRAK1 and directly inhibits the LPS signalling cascade	[229, 230]
TAG	TRAM adaptor with GOLD domain	Inhibits IFR3 activation	[231]
PIN1	Peptidyl-prolyl isomerase	Inhibits IRF3 activation	[232].
ATF3	Activating transcription factor 3	Suppresses NF-κB activation	[233]
PI3K	Phosphatidylinositol 3 kinase	Inhibits p38, JNK, and NF-κB function	[234]
DUBA	Deubiquitinating enzyme A	Deubiquitinates TRAF3	[235]
TOLLIP	Toll-interacting protein	Autophosphorylates IRAK1	[236-238]
PDLIM2	PDZ And LIM Domain Protein 2	Promotes p65 polyubiquitination	[239]
RAUL	Ubiquitin Protein Ligase E3C	Inhibits IRF3 activation	[240]

A20	TNF-induced zinc finger protein	Suppresses TNF-mediated NF-κB activation by de-ubiquitylation TRAF6	[241]
USP4	Ubiquitin-specific protease 4	Deubiquitinates TRAF6	[242]
TRIAD3A	Ring finger E3 ligase protein	Promotes ubiquitylation and degradation of TLR4	[243]
CYLD	Cylindromatosis	Deubiquitinates TRAF6	[244]
ST2L	Fill in	Sequesters MyD88 and MAL	[245]
SIGIRR	Single immunoglobulin interleukin-1 related receptor	Interacts with TLR4,TRAF6 and IRAK	[246, 247]
TRAILR	Tumour-necrosis factor-related apoptosis-inducing ligand receptor	Inhibits TLR effects by Stabilizing IκBα	[248]
TANK	TRAF Family Member-associated NF-κB Activator	Inhibits TRAF6 ubiquitination	[249]
TRIM38	tripartite motif (TRIM) 38	Promotes proteasomal degradation of TRAF6	[250]
SHP	Small heterodimer partner	Suppresses NF-κB activation	[251]
Nurr1	Nuclear receptor related 1	Suppresses NF-κB activation	[252]

1.19 Thesis Outline

Inflammation is vital to protect the host against foreign organism invasion and cellular damage. It requires tight and concise gene expression for regulation of pro- and anti-inflammatory genes in the immune cells. The mechanisms underlying post-transcriptional gene expression regulation include mRNA splicing, mRNA export, mRNA localisation, mRNA stability, RNA/Protein interaction and post-translational events such as protein stability and modification. The majority of studies to date have focused on transcriptional control pathways. However post-transcriptional regulation of mRNA in eukaryotes is

equally important and related information is lacking. This is the area investigated in this thesis.

Aims and hypotheses:

Hypothesis 1: That RNA degradation pathways will be regulated during the response to LPS (chapter 2).

Aim: To characterise the regulation of RNA decay pathways during the lipopolysaccharide response in macrophages.

Hypothesis 2: That intron retention may play a role in regulation of toll-like receptor responses (chapter 3).

Aim 1: To analyse patterns of intron retention during LPS responses.

Hypothesis 3: SMG1 regulates toll-like receptor induced signalling pathways (chapters 4 and 5).

Aim: To identify mechanisms by which SMG1 regulates TLR-induced signalling.

Summary of each chapter's findings:

For chapter 2, we treated bone marrow derived macrophages (BMMs) with LPS over a time course of 0, 2, 6 and 24 hours and analysed the transcriptional profiles by RNA sequencing. Our data shows that components of RNA degradation pathways are regulated during an LPS response. We examined components of RNA degradation pathways, including the RNA decay exosome, P-body localised deadenylation, decapping and degradation, and AU-rich element targeted decay mediated by tristetraprolin (TTP). This chapter provides a clear overview the regulation of RNA degradation pathways during the lipopolysaccharide response in macrophages. This work has been published in Journal of Leukocyte Biology [130].

Intron retention (IR) is considered a widely regulated process during gene expression, however its regulation during innate immune responses had not been examined. Intron retention (IR) is a form of alternative splicing where an intron is not removed during transcription coupled splicing. This can occur in a co-ordinated manner to control broad cellular processes such as differentiation or response to external stimuli either leading to NMD or detained introns may be blocked in the nuclei. For chapter 3, we further analysed RNA sequencing data from chapter 2 for the presence of IR events by using 'IRFinder' software. Our data shows that at 2h there is a significant increase in intron-retention over the other timepoints. Genes identified as having significantly increased intron retention were enriched for interferon inducible genes and those involved in pattern recognition pathways for example caspase-1 and IRF8. We validated intron retention in a subset of these genes by quantitative PCR. These experiments confirmed that introns being retained included those that were not incorporated into known protein isoforms suggesting that they are playing a regulatory role in this context. In summary, this chapter highlights that intron retention is an additional layer of regulation in innate immune responses.

In chapter 4, we focus on the role of the NMD key kinase SMG1 in response to inflammatory stimuli. NMD is the major RNA decay pathway which recognises and degrades mRNA with premature termination codon (PTCs), to prevent the production of non-functional or truncated proteins. Previously, Smg1-mice were demonstrated to have increased basal inflammation. To understand the role of SMG1 in TLR mediated responses, we generated a novel model of SMG1 loss in macrophages to address this question. Results showed that BMMs from $LysM^{+/Cre}Smg1^{fl/fl}$ (Cre) male mice showed less induction of the pro-inflammatory cytokines IL-1β, IFNβ, and TNFα, while increased pro-inflammatory cytokines production can be observed in BMMs from

LysM$^{+/Cre}$Smg1$^{fl/fl}$ (Cre) female mice compared with BMM from wildtype littermates. This data suggests that SMG1 can regulate TLR4 induced inflammatory responses in a sex dependent manner. Interestingly, loss of SMG1 may be implicated X chromosome inactivation. In summary, loss of SMG1 may involve in the regulation of innate immunity with potential sex differences affecting pro-inflammatory cytokine production in response to LPS treatment.

For chapter 5, we report RNA-sequencing data from BMM from *LysM$^{+/Cre}$Smg1$^{fl/fl}$* (Cre) and *Smg1$^{fl/fl}$* mice (wild-type) treated with LPS by using initial expression analysis, gene ontology analysis aimed at identifying differences between *LysM$^{+/Cre}$Smg1$^{fl/fl}$* (Cre) and *Smg1$^{fl/fl}$* mice(wild-type). However, our *LysM$^{+/Cre}$Smg1$^{fl/fl}$* (Cre) mice showed an altered phenotype in different housing environments therefore, we have concluded that the results from this experiment are flawed and could not be validated in independent cohorts in new housing conditions.

Finally I discuss my conclusions and future directions for the field in chapter 6.

Chapter 2- Regulation of RNA degradation pathways during the lipopolysaccharide response in macrophages

2.1 Link to thesis

For this Chapter, we investigated the regulation in the innate immune response to LPS. This chapter provides a clear overview the regulation of RNA degradation pathways during the lipopolysaccharide response in macrophages. This work has been published in Journal of Leukocyte Biology [130] and supplementary data and other figures is available on-line and also can find as an appendix in the end of thesis.

2.2 Introduction

Signalling through the toll-like receptors (TLRs) is a well-known pathway in the recognition of pathogen associated molecular patterns (PAMPs); specific molecular patterns that are present in microbial components. The TLR family consists of 11 members [216] which respond to a range of PAMPs to induce pro-inflammatory cytokine production, up-regulation of co-stimulatory molecules and sculpting of the adaptive immune response [216, 253].

In this study, we focused on TLR4 signalling. TLR4 is activated by lipopolysaccharide (LPS) and can recruit adaptor proteins MyD88 and TRIF. MyD88 binds to the cytoplasmic portion of TLRs through interaction between individual toll-interleukin 1 receptor (TIR) domains. Upon stimulation, MyD88 downstream signalling leads to activation of Mitogen activated protein (MAP) kinases and NF-κB, and induction of the transcription of cytokines and immune regulatory genes [216]. In addition to MyD88-

dependent signalling, TLR4 also activates the MyD88–independent pathway (TRIF-dependent) that leads to activation of IRF3 via TBK1 and IKKα/IKKβ and induces IFN-β and IFN-inducible genes [253].

Gene expression is controlled at multiple steps including transcription, splicing, mRNA export, RNA stability and rate of translation [254]. Compared to induction of gene expression [255], there is less known about how post-transcriptional pathways are regulated in response to inflammatory stimuli. Alternative splicing results in the generation of alternative protein isoforms and incorporation of additional regulatory elements and is important for innate immune regulation [35, 208]. Regulatory elements can control the stability of the mRNA transcript, in innate immunity particularly adenylate/uridylate-rich (AU-rich) elements that control mRNA stability of many cytokines including TNFα, IL-6 and IL-1β [256]. Other elements such as the constitutive decay element in TNFα have also been described [257]. miRNA can also regulate RNA degradation and translation rates in inflammatory responses in macrophages [258]. Regulation of RNA decay pathways more broadly has not been described in response to TLR signalling with most studies describing how these pathways may target viral transcripts. RNA decay also plays an essential role in post-transcriptional regulation of gene expression. The rate of RNA degradation of specific transcripts compared to new transcription is important for overall expression. Pathways controlling RNA decay include the RNA decay exosome, P-body localised deadenylation, decapping and degradation, quality control systems including nonsense-mediated decay, and AU-rich element targeted decay mediated by tristetraprolin (TTP) (Table 2-1). In eukaryotes, 5'-cap and 3'-poly (A) tails are considered features which protect from the attack of exonucleases and these two structures can interact with the cytoplasmic proteins eIF4E

and the poly (A)-binding protein (PABP), respectively. As a result, mRNA transcripts are protected from exonucleases leading to enhanced translation. The process of RNA decay frequently starts with deprotection of the mRNA transcript i.e. – decapping and deadenylation. mRNA may subsequently be degraded by the XRN1 exonuclease or alternatively, the exosome complex degrades mRNA in the 3' to 5' direction. RNA decay can occur co-translationally or in cytoplasmic foci called P-bodies which are sites where mRNAs are targeted to decay factors and are either degraded or shuttled to other cytoplasmic foci called stress granules where some transcripts are stored for later translation [125]. Sequence-specific RNA decay pathways or quality control pathways direct mRNAs to these sites of degradation. Here we have examined the regulation of key RNA decay pathways during the timecourse of the LPS response in macrophages. These results highlight targeted regulation of these pathways during innate immunity as an additional layer of control on inflammatory processes.

2.3 Results

2.3.1 RNA degradation pathways are regulated during an LPS response.

We performed RNA sequencing to analyse gene expression changes during the LPS response [259]. Quadruplicate samples from BMM treated with LPS for 0, 2, 6 and 24h were analysed (schematic of the experimental process is shown in Figure 2-1A). We examined differentially expressed genes across the timecourse including performing gene ontology analysis via the GOrilla platform [260, 261], example output for the 2h timepoint is shown in Figure S1. This demonstrated the expected increase in pathways associated with innate immune responses and regulation of cytokine production (among multiple immune related pathways). We also validated the regulation of key cytokines involved in LPS responses, as seen in RNA sequencing data (Figure S2A), by realtime

PCR (Figure S2AB) which indicated that macrophages were responding to LPS as expected within this dataset. In addition to immune related genes we were interested to note that the RNA metabolism gene ontology classes were also significantly regulated (Figure S1 and S2C). Within these gene lists we noticed a large number of RNA decay genes. To examine this further we utilised the stemformatics platform to examine specifically genes annotated as associated with RNA decay. A heat map showing changes in expression of RNA decay related genes was generated from this data (Figure 2-1B). This demonstrated that there were significant alterations of the expression of genes related to RNA decay during an LPS response with 56/60 of the annotated RNA decay genes either up- or down-regulated. The number of genes significantly regulated for each of the RNA decay related pathways is shown in Figure 2-1C. These pathways include multiple stages of the RNA decay process deadenylation, core exosome, exosome-associated factors, decapping, P-bodies and stress granules, RNA degradosome and nonsense mediated decay (NMD). Specific genes shown to be regulated in the heat map (Figure 2-1B) have been consolidated in Table 2-1. Figure S2D shows how these genes are regulated on volcano plots. Similar to the single gene profiles at 2h there is less regulation with some significantly up and down regulated genes, this is more dramatic at 6h, with a broader trend towards decreased expression than at 2h.
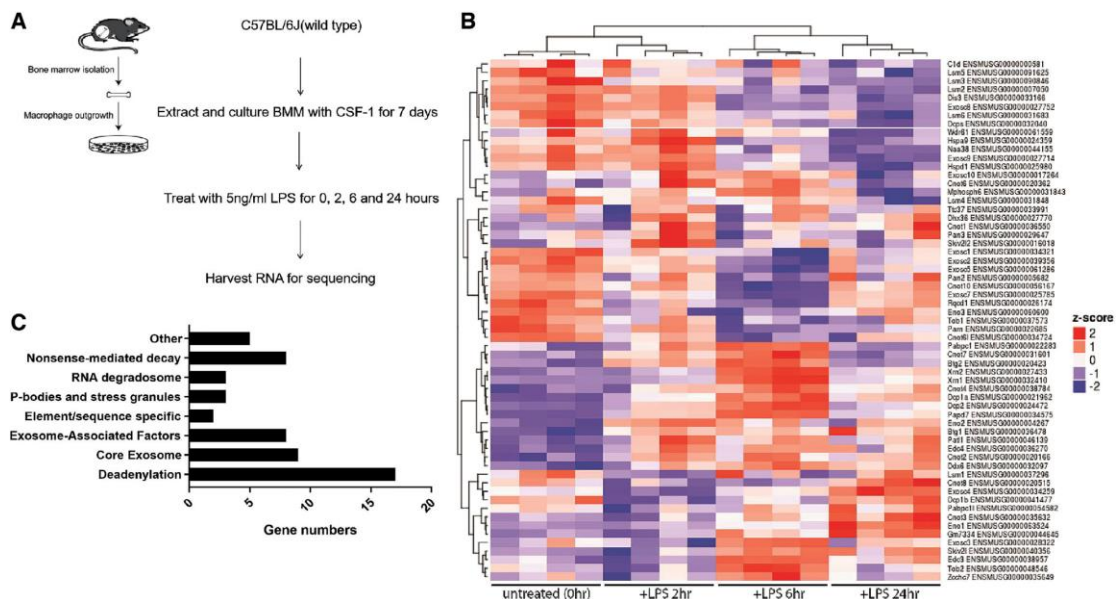
Figure 2-1: RNA sequencing analysis of the LPS response in macrophages. **A:** Schematic of the sample production for RNA sequencing. **B:** Heat-map was generated from RNA sequencing data and shows RNA decay related genes with regulated over the time-course of the LPS treatment (0, 2, 6, 24 hours). Colours indicate the range of each gene's expression in response to LPS treatment, see key on right hand side. **C:** Graph indicating the number of genes regulated for each of the major RNA decay pathways.

Table 2-1 Genes regulated by LPS and related to RNA decay pathways

Regulation by RNA decay pathways	Genes
Deadenylation (Ccr4-NOT Complex)(17)	Cnot1, Cnot2, Cnot3, Cnot4, Cnot6, Cnot7, Cnot8, Rqcd1(Cnot9), Cnot10, *Pam*, Cnot6l, *Pan2 (Ampd3)*, Pan3, Tob1, *Tob2*, **Btg1**, Btg2
Core Exosome (9)	Dis3, *Exosc1*, Exosc2, Exosc3, Exosc4, Exosc5, Exosc7, Exosc8, Exosc9
Exosome-Associated Factors(8)	C1d, Mphosph6, *Exosc10*, *Pabpc1*, Skiv2l2, **Papd7**, Skiv2l, Zcchc7
Element/sequence specific(2)	Dhx36, Pabpc1
Decapping (16)	**Xrn1**, **Xrn2**, Dcp1a, **Dcp2**, Edc3, Dcp1b, Dcps, Wdr61(Ski8), Ttc37, *Lsm1*, Lsm2, Lsm3, Lsm4, Lsm5, Lsm6, Edc4
P-bodies and stress granules(3)	**Xrn1**, Ddx6, *Pat1*
RNA degradosome (3)	Eno1, *Eno2*, Eno3
Nonsense-mediated decay(8)	Upf1, Upf2, Upf3a, Upf3b, Smg1, Smg5, Smg6, Smg7
Other(4)	Hspd1, Naa38, Hspa9, Wdr61

Bold, up-regulated > 1.5-fold by IFN. Italics, down-regulated > 1.5-fold by IFN (according to interferome database, www.interferome.org).

2.3.2 Validation of gene expression changes by quantitative PCR.

A subset of regulated core RNA decay genes were chosen for validation by quantitative PCR. The single gene profiles were generated using the stemformatics platform [259, 262] and compared to data from qPCR (Figure 2-2 and supplementary Figure 3). The qPCR results confirmed that mRNA for the key catalytic subunit of the nuclear exosome (Dis3) was downregulated but rate limiting components of the decapping pathway Dcp1 and Dcp2a, and 5' exonuclease XRN1 are induced (Figure 2-2A (RNA sequencing data) and 2B (validation data)). In contrast, components of the exosome (Exosc5 and 7) and a member of the deadenylation complex (Cnot7) did not show significant regulation in validation samples (Figure S3A (RNA seq data) and S3B (validation data)). As a positive control we also validated two RNA regulatory proteins known to play an important role in innate immune responses with well-established induction in response to LPS. Tristetraprolin (TTP encoded by Zfp36) is key in regulation via AU-rich elements [263] and Regnase 1 (encoded by Zc3h12a) is a ribonuclease and key negative regulator of TLR responses [264]. The mRNA for both of these was strongly induced in response to LPS (Figure S4A (RNA sequencing data) and S4B (validation data)).

We also examined whether the changes seen at the mRNA level led to protein level changes for a subset of regulated genes. Western blotting was performed on protein extracts from BMM over a timecourse in response to LPS treatment (0, 2, 6, 16, 24, 48h). These results indicated that 5'exonuclease XRN1 and major decapping enzyme DCP1A are induced during an LPS treatment from 6h onwards. This was expected as mRNA was strongly induced by this timepoint. In contrast to the mRNA data, there were no major changes in Dis3 protein expression during LPS treatment 0-48h (Figure 2-3). This was

surprising as the mRNA level was clearly decreased at 6 and 24h. This indicates that there may be additional layers of regulation of Dis3 expression during the LPS response or that the Dis3 protein is quite stable.

We also compared our validated genes to data available in the online Macrophage Comparative Expression Gateway (http://macgate.qfab.org/index.htm and [265]) as this data was performed at the same timepoints as our analysis but by microarray. Where available the online BMM data matched with our data and the profiles across the timecourse in BMM did not differ significantly from human macrophages (example data and p-values for timecourse where available in Figure S5A-B). It should be noted that for individual timepoints for some genes showed a significant difference between mouse and human macrophages but the overall profile was similar. This data indicates that the regulation of RNA decay genes is largely conserved between mouse and human macrophages.
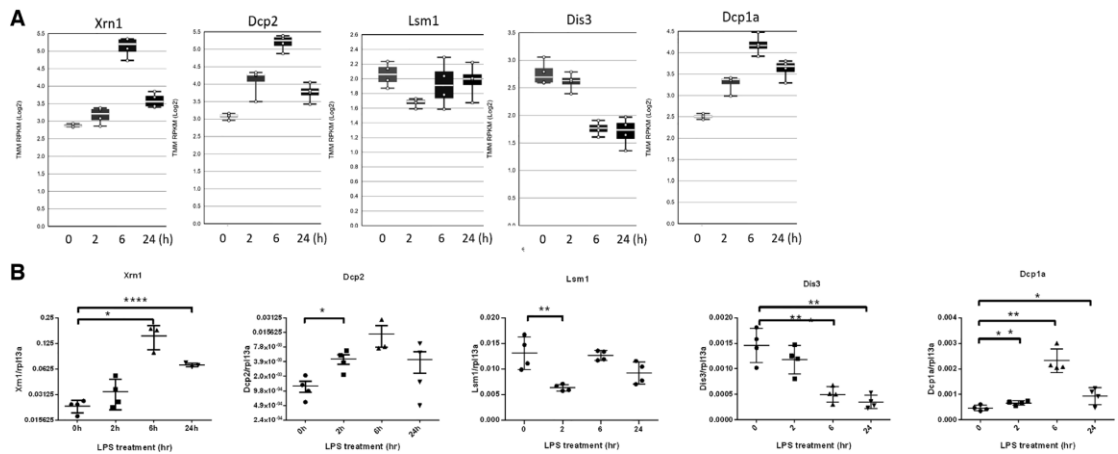
Figure 2-2: Validation of regulation of core RNA decay pathway components in response to LPS. **A:** Single gene profiles were generated with the stemformatics platform for genes to be validated. Each graph shows the level of gene expression in a log scale on the y-axis the timecourse of LPS treatment at 0, 2, 6 and 24 hours across the x-axis. For each data group the white line shows the average expression, the white dots the individual data points for each replicate sample and the error bars the full range of the independent samples. **B:** The expression pattern of a subset of genes was validated by quantitative PCR. The level of each gene was compared to the control gene (rpl13a) in 3-4 samples from independent mice at 0, 2, 6, 24 hours after LPS treatment. Graphs show the individual values as the symbols and the error bar show the standard deviation. *$p < 0.05$, **$p < 0.01$, ***$p < 0.001$.

Figure 2-3: Members of the RNA decay pathways are also regulated at the protein level. **A:** Representative images of western blots for Xrn1, Dcp1A, Dis3 and β-actin as a loading control. **B:** Protein levels were quantified using a Licor Odyssey. The protein level was normalised to β-actin and graphs show data combined from 3 independent animals. Statistical significance was assessed using a t-test in GraphPad Prism. Bars indicate the mean and error bars the standard error of the mean. $*p<0.05$, $**p<0.01$, $***p<0.001$.

2.3.3 Regulation of nonsense-mediated decay pathways following LPS treatment

We next went on to validate regulation of one of the targeted RNA decay pathways. Nonsense-mediated decay (NMD) is a mechanism that protects cells from the accumulation of aberrant mRNAs with premature termination codons (PTCs) which may encode for truncated proteins. NMD has also been implicated in regulation of non-PTC containing transcripts (up to 10% of the transcriptome) [266]. We chose to examine this pathway as it has been implicated in anti-viral responses and is essential for

haematopoiesis [70-72,267, 268] but regulation of NMD during innate immune responses is poorly understood. Briefly, SMG1 phosphorylates UPF1 and phosphorylated-UPF1 recruits SMG-5/SMG-7 and the SMG-6 endonuclease to initiate RNA decay [269]. Single gene Stemformatics profiles (Figure 2-4A) were compared to the qPCR validation data (Figure 2-4B). We validated the changes in expression for key NMD members. The qPCR data confirmed that Upf1 and Smg7 mRNA were strongly induced at 24h and 6h post-LPS respectively. While Smg1 mRNA trended towards an increase at 6 and 24h post-LPS it did not reach statistical significance (Figure 2-4B). Upf3b appeared to be strongly downregulated at 2 and 6h post-LPS in the RNA sequencing data. The qPCR results indicate that this down-regulation, while statistically significant, is of a smaller magnitude than in the sequencing analysis (Figure 2-4B). We also examined the protein levels of SMG1, UPF1 and SMG6. We found that SMG1 is induced at 16 hours after LPS treatment along with strongly increased UPF1 protein level expression at 16h onwards (Figure 2-5A and 2-5B). Interestingly UPF1 protein levels appeared to be decreased at 2h post-LPS. Smg6 levels were increased from 6-48h post-LPS. This indicates that NMD components are strongly regulated during an LPS response.
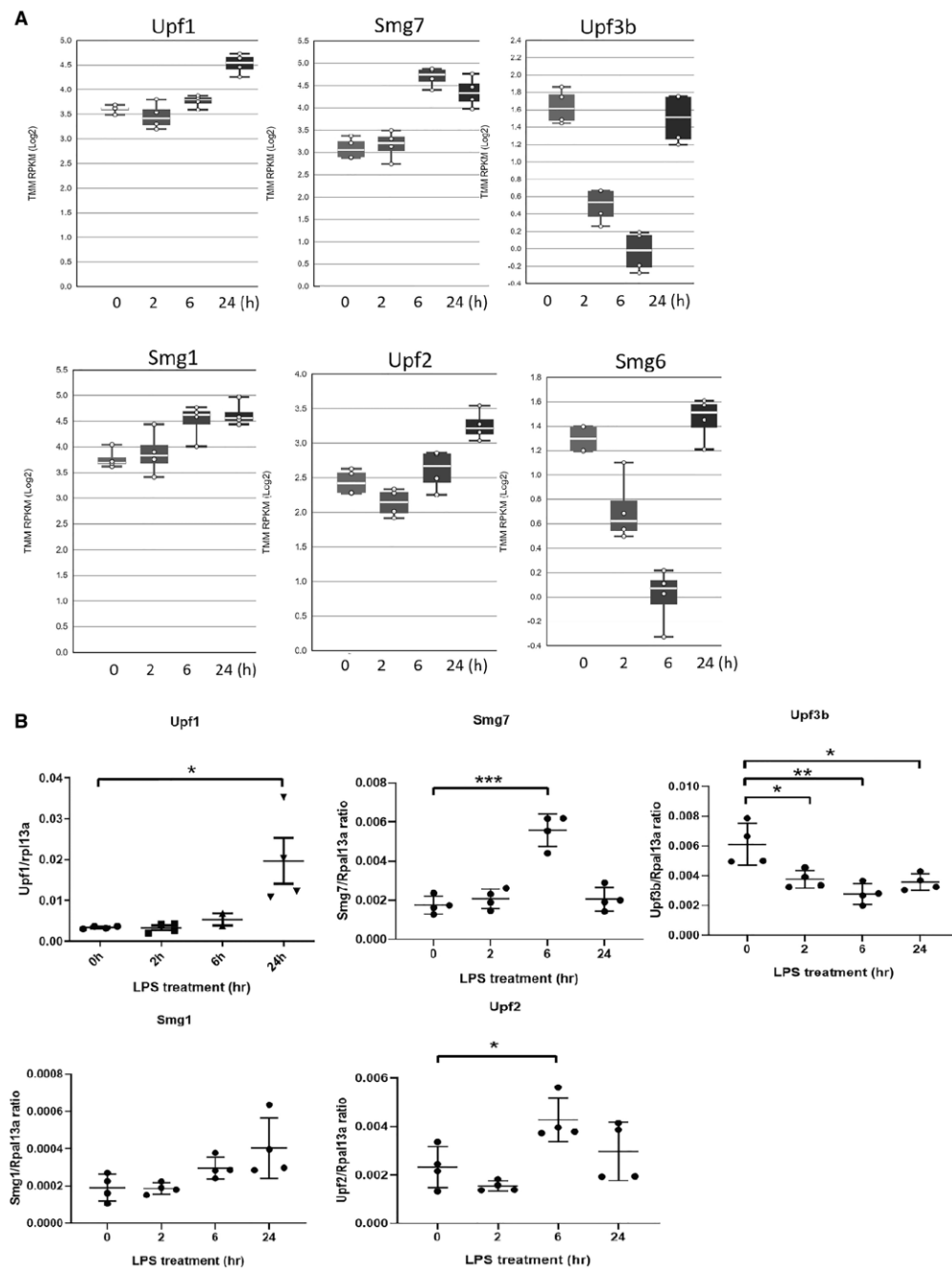
Figure 2-4: The regulation in the mediated by Nonsense-mediated decay (NMD) pathway during

an LPS treatment. **A:** Single gene profiles were generated with the stemformatics platform for

genes to be validated. Each graph shows the level of gene expression in a log scale on the y-axis

the timecourse of LPS treatment at 0, 2, 6 and 24 hours across the x-axis. For each data group the

white line shows the average expression, the white dots the individual data points for each

replicate sample and the error bars the full range of the independent samples. **B:** The expression

pattern of a subset of genes was validated by quantitative PCR. The level of each gene was compared to the control gene (rpl13a) in 3-4 samples from independent mice at 0, 2, 6, 24 hours after LPS treatment. Graphs show the individual values as the symbols and the error bar show the standard deviation. *$p<0.05$, **$p<0.01$, ***$p<0.001$.

Figure 2-5: Protein level analysis by western blotting for key components of the NMD pathway and quantification. **A**: Representative images of western blots for SMG1, UPF1, SMG6 and β-actin as a loading control. **B**: Protein levels were quantified using a licor odyssey. The protein level was normalised to β-actin and graphs show data combined from 3 independent animals. Statistical significance was assessed using a t-test in GraphPad Prism. Bars indicate the mean and error bars the standard error of the mean. *$p<0.05$, **$p<0.01$, ***$p<0.001$.

SMG1 is a member of the phosphoinositide 3 kinase-like kinase (PIKK) family of proteins [64], which, unlike classical PI3 kinases, phosphorylates proteins at serine/threonine followed by glutamine [(S/T)Q sites]. PIKKs are very large (250-480kDa)

and as such short-term regulation is often by control of their kinase activity rather than control of protein level (as based on average rates transcription and translation of new protein would take over 1 hour) [270, 271]. UPF1 is the key substrate for SMG1 in NMD and SMG1 kinase activity can be measured by the levels of UPF1 phosphorylation [125]. Therefore, we immunopreciptated UPF1 from the human monocyte cell line THP-1 at 0, 2 and 6h post-LPS treatment, samples were then analysed by western blotting for phosphorylated (S/T)Q sites indicating SMG1 mediated phosphorylation of UPF1. Human cells were used here as the available antibodies for UPF1 are substantially more effective on the human proteins. Figure 2-6A (representative image) and B (quantification) shows that UPF1 phosphorylation was increased at 2h post-LPS but returned to approximate baseline levels by 6h post-LPS. This suggests that during the early response to LPS SMG1 kinase activity is increased and consequently NMD efficiency is likely also increased. We therefore measured NMD efficiency in response to LPS. GAS5 is a well-established NMD target and as such its levels decrease when NMD activity increases [64]. GAS5 levels were decreased at all timpoints post-LPS (2-24h, Figure 2-6C) which fits with increased activity of SMG1 and consequent increased UPF1 phosphorylation at early timepoints and increased expression of both SMG1 and UPF1 at later timepoints. This was also the case for the splice variants of ALKBH3 and LUC7l that are NMD targets in BMMs [64] (Figure 2-6D). We also examined Gas5 levels in SMG1 heterozygous mice. Complete loss of SMG1 causes early embryonic lethality but SMG1 heterozygous mice are viable with a 50-80% reduction in SMG1 protein level [64]. Basal NMD levels are normal in these animals as described previously [64], and at the 0h timepoint, there is no difference in gas5 levels (Figure 2-6C). However, the decrease in gas5 in response to LPS was not observed in BMM from SMG1 heterozygous animals (Figure 2-6C) indicating that SMG1 levels are limiting when there is increased NMD occurring during the LPS

response. In THP-1 cells we saw a decrease in GAS5 expression post-LPS treatment as well but for other known targets of NMD in THP-1 (ATF4, TBL2 and TGM2) we saw an initial increase at 2h post-LPS followed by decreased levels (Figure S5C-E). In response to siRNA knockdown of SMG1, rather than the decrease in GAS5 observed levels were increased (Figure S5D). We next treated THP-1 cells with an inhibitor of NMD which acts to disrupt the interaction between UPF1 and SMG7 [272] as an independent mechanism of blocking NMD. THP-1 were treated overnight with inhibitor or DMSO alone prior to treatment with LPS. In DMSO treated samples GAS5 levels decreased compared to and this was blunted by the addition of NMD inhibitor but did not reach statisitical significance (Figure S5E). Combined these experiments indicate that targets of NMD are decreased in both mouse and human macrophages and that this effect is limited by blocking NMD either by decreasing SMG1 expression or to a lesser degree by chemical inhibition of NMD.
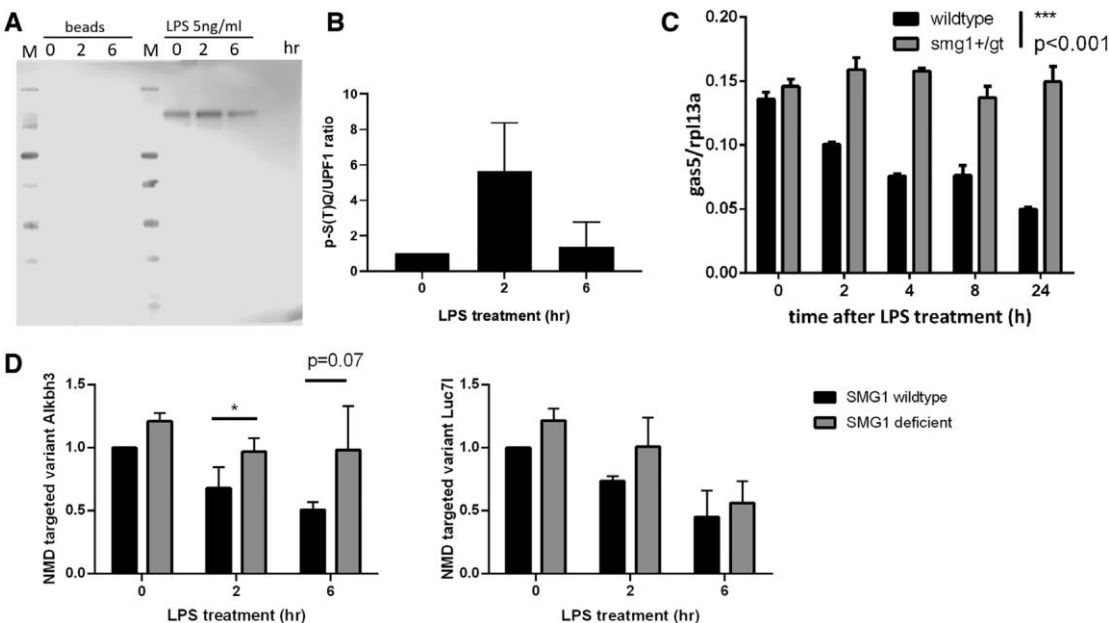
Figure 2-6: Nonsense medicated decay is regulated during an LPS response. **A:** UPF1 was immunoprecipitated from THP1 lysates at the indicated time and westerns probed with anti-

(S/T)Q antibody to detect SMG1 mediated phosphorylation. UPF1 phosphorylation was increased at 2h post-LPS but returned to baseline at 6h post-LPS. **B:** Quantification of the ratio of phosphorylated UPF1 to total UPF1 in two independent samples. **C:** The level of NMD target mRNA, GAS5, was measured by qPCR in BMM from wildtype and SMG1 deficient mice at indicated times after LPS treatment (n=3) ***$p<0.0001$. **D:** The level of splice variants of ALKBH3 and LUC7l which are known NMD targets. Splice variants were amplified by qPCR, separated by polyacrylamide electrophoresis and quantified using a Licor Odyssey system (n=3). Data shown as mean ± SEM. *$p<0.05$.

2.4 Discussion

Our data shows that components of multiple RNA degradation pathways are regulated during the LPS response at indicated timepoints (summarised in Figure S3). General RNA decay requires deadenylation and decapping. From RNA sequencing data, multiple members of the deadenylation pathway and the exosome were up- or down-regulated at the mRNA level in macrophages after LPS treatment (Figure 2-1B and Table 2-1) though this regulation was not confirmed in independent samples (Figure S3). However, two key proteins in the decapping complex, the enzyme Dcp2 and its regulatory subunit Dcp1a were significantly up-regulated in response to LPS as was the endonuclease Xrn1. Regulation of these factors was validated in independent animals and at the protein level for Dcp1a and Xrn1 (Figure 2-2 and 2-3). These are rate limiting factors in RNA decay. Regulation of Dcp1a in response to interleukin-1α (IL-1α) has been described previously [273]. In response to IL-1α Dcp1a is post-translationally modified (phosphorylation and ubiquitylation), and this alters P-body formation and composition, and the stability of a set of pro-inflammatory mRNAs. This post-translational modification occurs early during the IL-1α response (1h post-treatment) [273]. Here we show that Dcp1a and Dcp2 are

also induced in response to LPS with mRNA and protein induced from 2h post-LPS (Figure 2-3) but most dramatically from 6h post-LPS. Therefore, this later induction may result in reassembly of P-bodies and increased decapping at later timepoints.

Multiple RNA decay pathways will feed transcripts to P-bodies and the associated decapping complex. AU-rich elements and their role in regulating inflammatory mRNA have been well studied and reviewed [1, 254]. Tristetraprolin (TTP) is induced by LPS ([263]and Figure S4) and it controls multiple feedback pathways in response to LPS. In general TTP binds to AU-rich elements and targets these mRNAs for decay. However, this function of TTP is also temporally controlled by transient phosphorylation post-LPS. Early in the LPS response TTP is phosphorylated downstream of p38 MAPK and degradation of targeted transcripts is limited. At later timepoints the phosphorylation is removed and transcripts are targeted to P-bodies. The known increase in TTP expression in response to LPS was also observed in our data (Figure S4). The timing of TTP induction is similar to that for Dcp1a and Dcp2 suggesting this may be a co-ordinated response to re-induce RNA decay after initial limiting of decay pathways during early inflammatory responses.

Nonsense mediated decay (NMD) is a quality control pathway; as originally described it recognises the presence of premature termination codons (PTC) in the mRNA and directs these transcripts to be degraded thus preventing the production of truncated proteins. A PTC is recognised as premature if it is located at least 55 nucleotides upstream of an exon-exon junction complex EJC [274]. Detection of a PTC causes the EJC to recruit UPF2 associated with the SURF surveillance complex (SMG-1/Upf1/eRF1/3RF3) leading to SMG1 induced phosphorylation of UPF1. This in turn recruits SMG-5/7, leads to UPF1

dephosphorylation and finally mRNA degradation including endonucleolytic cleavage by SMG6. NMD also regulates transcripts without PTCs; transcriptomics studies suggest that greater than 10% of all transcripts are regulated by NMD [275, 276] and that NMD is particularly important for regulating selenoprotein mRNA and alternative splicing [275]. How NMD regulates non-PTC transcripts is not fully understood.

A recent set of articles has implicated NMD in controlling infection [69-72]. NMD controlled the expression of genes from *potato virus X* and *turnip crinkle virus* [72]. Further *turnip mosaic virus* and *potato virus X* have developed strategies to evade NMD targeting during infection suggesting the NMD targeting adversely affects viral replication and transmission. In a second article Gloggnitzer *et al.* showed that bacterial infection reduced NMD efficiency and that plant pathogen recognition receptor expression is controlled by NMD [70]. In a third study knockdown of key NMD proteins resulted in increased Semliki Forest virus production in HeLa cells [71]. Depletion of SMG1 substrate Upf1 also resulted in greater accumulation of double-stranded RNA in infected cells. Here we add to these findings by demonstrating that NMD is regulated at multiple levels by TLR4 signalling in mammalian cells. We found that key proteins in NMD were induced at the RNA and protein levels (SMG1, Upf1, Smg7, Smg6 and Upf2) (Figures 2-4 and 2-5). We further demonstrated increased phosphorylation of Upf1 at 2 hour post-LPS treatment (Figure 2-6A-B). These changes led to increased NMD efficiency as demonstrated by decreased expression of the NMD targets (Figure 2-6C-D and Figure S5C-E). The decrease in gas5 expression was clearly dependent on NMD as it was lost in cells from SMG1 heterozygous mice, indicating that SMG1 kinase activity in NMD is rate limiting during an inflammatory response. Further siRNA knockdown of SMG1 or chemical inhibition of NMD blunted the decrease in Gas5 expression in THP-

1 in response to LPS. These findings demonstrate NMD activity is initially regulated by post-transcriptional modification and then later by alteration of proteins levels in response to LPS. This process is similar to regulation of decapping and TTP as discussed above and emerges as a pattern of regulation for RNA decay pathways in our data. Given the varied regulation of transcripts in the RNA degradation pathways across the timecourse feedback mechanisms may be important. One of the most obvious of these is type I interferon; however, only 14 transcripts were up- (bold) or down- (italics) regulated (Table 2-1) according to the interferome database [277] indicating that type I interferon may contribute to regulation of RNA decay pathways but is not solely responsible. Further work will be required to determine the role/s of other feedback mechanisms in the timing of the regulation of RNA decay pathways.

Given that NMD has the potential to regulate up to 10% of all transcripts including those without PTCs it may have a significant role in sculpting the response to LPS. However, it should be noted that a recent paper has described a separate role for Upf1 (and to a more limited extent SMG1) in regulation of response to LPS and other TLR ligands. UPF1 interacts directly with Regnase-1 to allow direction of a subset of pro-inflammatory mRNAs to degradation [278]. This appears to be only partially dependent on SMG1 phosphorylation of UPF1 at only one of sites required for NMD activity so this is likely to represent a role additional to NMD. This pathway was predominantly described in fibroblasts and cell lines, with limited data from myeloid cells included, but it did suggest that this pathway was not as active in either macrophages or dendritic cells but further work will be required to confirm this.

In summary, while separate descriptions of RNA decay regulation in response to inflammation, especially via sequence specific elements, have been described in the literature here we examined broader RNA decay pathways including decapping and deadenylation which form the base of multiple decay pathways. Further this is the first description of the regulation of NMD efficiency during an LPS response. Overall our findings indicate that multiple RNA decay pathways are regulated during the response to LPS in macrophages (Figure S6, Table S3) and that each of these acts on different aspects of the response to fine tune RNA levels and subsequent protein expression. As such regulation of RNA decay is an important regulated mechanism during the LPS response in macrophages though future work will be required to establish mechanistic links between individual RNA decay pathways and their impact on the inflammatory response to LPS. Further work will be required to determine if regulation of RNA decay pathways also occurs in other LPS responsive cell types.

2.5 Conclusion
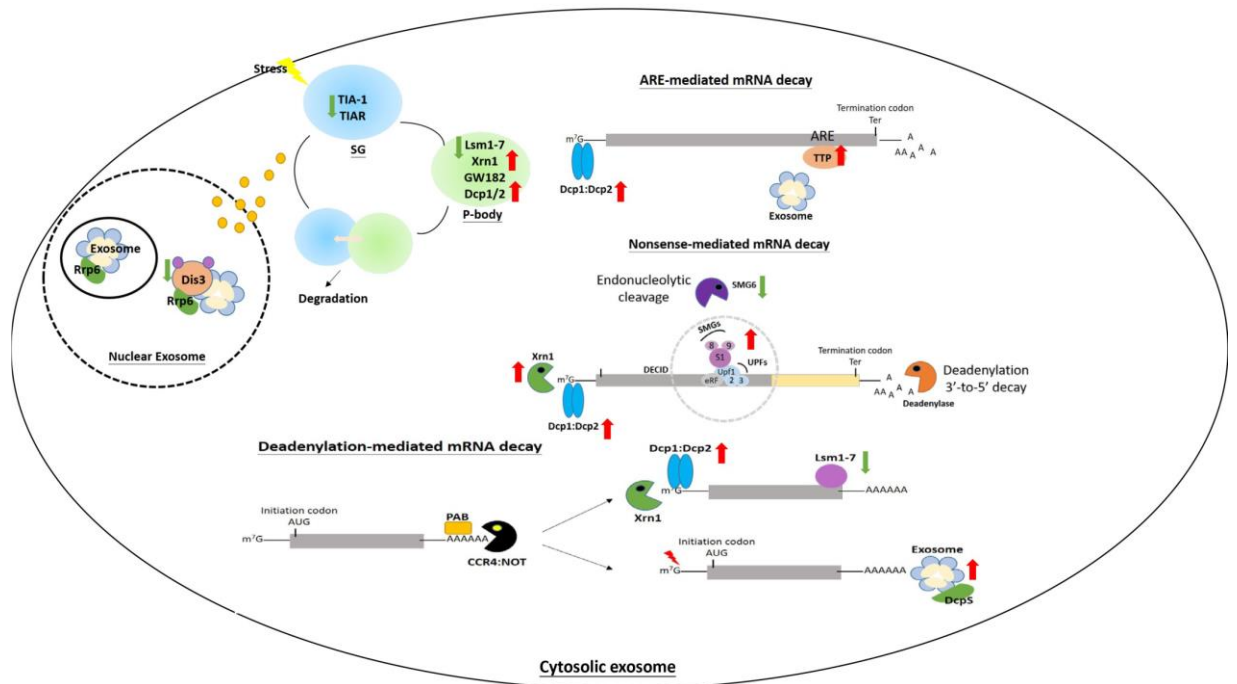
Figure 2-7: Diagrammatic summary of the RNA decay pathways regulated during the macrophages response to LPS. Red arrows indicate upregulation and green arrows downregulation during the response. SG- stress granules, ARE- AU-rich element, P-body – processing body.

Chapter 3- Co-ordinated intron retention in the regulation of innate immunity

3.1 Introduction

Detained introns are a subset of retained introns which received their name due to the fact they were spliced more slowly than other introns in the same transcripts. There are a few possible outcomes from IR in the mature poly-adenylated mRNA transcript [279]: 1) the retained intron is translated and generates an alternative protein isoform; 2) the retained intron introduces new regulatory elements which can alter the rate of translation and/or the stability of the mRNA, these introns are frequently retained in the 3' or 5' untranslated regions (UTRs) of the mRNA; 3) the retained intron introduces a premature stop codon and the mRNA is targeted to the nonsense mediated decay pathway and 4) the intron is a 'detained intron' which while remaining in the mRNA prevents transport from nucleus to the cytoplasm. In mammals, IR predominantly acts to decrease subsequent protein expression from the intron containing transcript [280, 281]. IR events can retain premature termination codons (PTC) which are recognised by NMD. A study across metazoan species demonstrated that IR events occurred in approximately 75% of multi-exon genes [282].

Detained introns were first described, as a broad class, in stem cells. These introns remain in the otherwise mature RNA and are not exported from the nucleus. As a result, transcripts with detained introns are either directed to nuclear RNA decay or the intron is spliced out and the transcript is exported and translated as the normal transcript [283]. In response to different types of cellular stress including DNA damage and hypoxia, key splicing factors are regulated to increase or decrease detained intron splicing [284]. In

neurons detained introns are used to stockpile mRNA transcripts for rapid splicing and expression in response to neuronal stimulation [285]. Intron retention underlies normal differentiation and cellular functions in haematopoiesis [286].

IR is highly regulated during differentiation and development. Differential IR plays a role in haematopoietic cells including granulocytes [286], erythroblasts and megakaryocyte progenitors [280]. In order to understand the role of IR in the regulation of myeloid differentiation, Wong et al. [286] isolated murine promyelocytes, and granulocytes by fluorescence activated cell sorting (FACS) and performed mRNA sequencing (mRNA-seq) to identify intron-retained transcripts during myeloid differentiation. They also successfully developed the computational platform called IRFinder to identify IR events and measure the ratio of retained introns to correctly spliced introns with great accuracy [281]. Their results indicated that 121 introns were retained from 86 genes with significant differences between promyelocytes and granulocytes, which included 30 alternative IR events in multiple introns of these 86 genes. qPCR validation showed 20 of these IR transcripts were poly-adenylated and mainly presented in the cytoplasm, suggesting they are fully processed and exported mRNA rather than splicing intermediates. A follow-up study has compared IR events in primary erythroid and megakaryocyte (MK) cells versus their progenitors (MEPs) and found an overwhelming loss of IR in erythroid and MK cells compared to MEPs [44]. A similar pattern was also seen in human erythroid differentiation [44]. These findings have highlighted the importance of alternative splicing in fine-tuning gene expression during immune cell differentiation/maturation.

As further analysis on the RNA sequencing dataset is described in chapter 5, we analysed intron retention patterns in LPS treated BMM as there was little data examining the role

of intron retention in innate immunity. In our BMMs intron retention was dramatically increased at 2 hours post-LPS but decreased at 6 hours.   In this chapter, we will address the mechanism and outcomes of co-ordinated IR in response to LPS treatment and this is also the first study to provide evidences that co-ordinated IR is a novel mechanism which controls inflammatory responses.

3.2 Results

3.2.1 Intron retention profile analysis by IRFinder platform

With the same data set described in chapter 2, we examined differentially expressed genes across the timecourse via the IRFinder platform [281] and identified differentially retained introns in individual genes at each time point of LPS treatment (Figure 3-1A). Genes demonstrating the presence of retained introns were clustered based on the profile of intron retention over timecourse of LPS treatment (Figure 3-1B). Firstly, we used k-means clustering to group introns with similar retention profiles and a cumulative IR ratio> 0.1. The IR ratio is the ratio between gene transcripts retaining an intron and the sum of all the transcripts of the same genes. Major clusters were examined and it was clear that a group (C1) had significantly retained introns at 2h post-LPS and that this pattern of IR returned to baseline by the 6h timepoint (Figure 4-1C). Others clusters (C2-to-C6) also demonstrated increased IR events but there were not significant differences between timepoints.

(A)

(B)
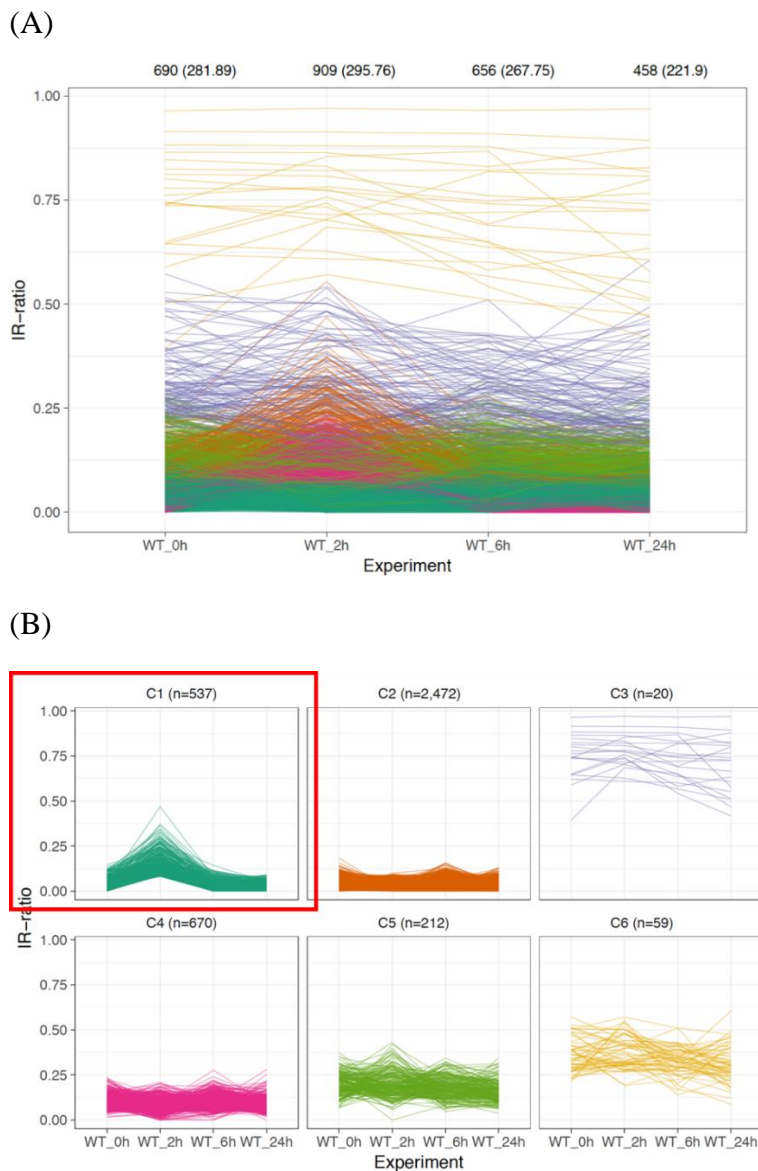
Figure 3-1: IR events increased after 2hrs-LPS treatment. (A) kmeans clustered IR profiles in time-courses (0, 2, 6, and 24 hours) after LPS treatment (k=6 clusters). Shown are only those introns that have a cumulative IR ratio > 0.1 and splice exact > 50 at each time point. Labels on top indicate the total number of IR events at each time point and the cumulative IR ratio in parenthesis. (B) Intron retention profiles as line graphs over the time-courses of the LPS treatment (0, 2, 6, and 24 hours). Red box indicates cluster (n=537 introns) which shows co-ordinated intron retention at 2h post-LPS which is largely resolved by 6h post-LPS. These figure panels were generated by Dr Ulf Schmitz.

3.2.2 IR events increased after 2h post-LPS treatment

In order to investigate functional association of intron-retaining transcripts between IR and spliced transcript expression, we further examined genes in the 2h IR cluster via gene ontology analysis [281]. Unsurprisingly genes were enriched for 'defense responses to other organism' and 'response to virus' (Figure 3-2). Specifically the set was enriched for genes encoding proteins involved in other pathogen recognition pathways (e.g. – caspases 1 and 4, and gasdermin for inflammasome responses; ZBP1 and HIN200 members for detection of nucleic acids and viral infection) [287, 288] and also enriched were genes involved in negative regulation of innate immune responses (Table 3-1).
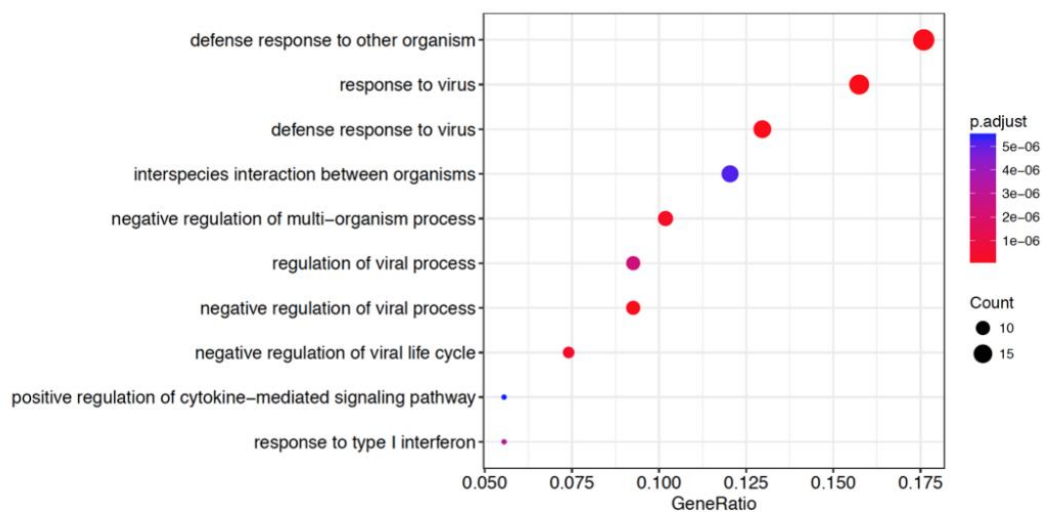
Figure 3-2: Gene ontology was performed to examine genes in the 2h IR clusters.
Gene enriched in the regulating of 'defense response to other organism' and 'response to virus' post-2h LPS treatment. This figure was generated by Dr Ulf Schmitz.

Table 3-1: Genes list of 2h IR clusters by gene ontology analysis.

Gene	Protein	GO-Biological process
Ikbkε	Inhibitor of nuclear factor kappa-B kinase subunit epsilon	-Response to type I interferon -Response to virus
Stat2	Signal transducer and activator of transcription 2	-Cytokine-mediated signalling pathway -Defence response to virus
Irgm2	Immunity-related GTPase family M member 2	-Defence response -Innate immune response
Trim25	E3 ubiquitin/ISG15 ligase TRIM25	-Defence response to virus -Viral process
Dhx58	Probable ATP-dependent RNA helicase DHX58	-Defence response to virus -Viral process
Rsad2	Radical S-adenosyl methionine domain-containing protein 2	-Defence response to virus -Type I interferon signalling pathway
Apobec3	DNA dC->dU-editing enzyme APOBEC-3	-Defence response to virus -Regulation of viral life cycle
Mx1	Interferon-induced GTP-binding protein Mx1	-Defence response to virus -Response to type I interferon
Eif2ak2	Interferon-induced, double-stranded RNA-activated protein kinase	-Response to virus -Innate immune response
Zbp1	Insulin-like growth factor 2 mRNA-binding protein 1	-mRNA transport -Negative regulation of translation
Adar	Double-stranded RNA-specific adenosine deaminase	-Defence response to virus -RNA processing
Oasl2	2'-5'-oligoadenylate synthase-like protein 2	-Defence response to virus -Innate immune response
Oas2	2'-5'-oligoadenylate synthase 2	-Defence response to virus -Type I interferon signalling pathway
Oas1a	2'-5'-oligoadenylate synthase 1A	-Defence response to virus -Innate immune response
Irf7	Interferon regulatory factor 7	-Defence response to virus -Type I interferon signalling pathway
Ddx60	Probable ATP-dependent RNA helicase DDX60	-Defence response to virus -Innate immune response
Pml	Protein PML	-Defence response to virus

		-Response to cytokines
H2-T23	H-2 class I histocompatibility antigen, D-37 alpha chain	-Regulation of natural killer cell mediated immunity -Adaptive immune response
Gsdmd	Gasdermin-D	-Inflammatory response -Innate immune response
Notch2	Neurogenic locus notch homolog protein 2	-Defence response to bacterium -Inflammatory response to antigenic stimulus
Tnfrsf14	Tumour necrosis factor receptor superfamily member 14	-Adaptive immune response -Cell surface receptor signalling pathway
Parp10	Protein mono-ADP-ribosyltransferase PARP10	-Negative regulation of gene expression -Regulation of chromatin assembly
Trim26	Tripartite motif-containing protein 26	-Interferon-gamma-mediated signalling pathway -Innate immune response
Trim14	Tripartite motif-containing protein 14	-Innate immune response -Negative regulation of viral transcription
Nlrc5	Protein NLRC5	-Regulation of kinase activity -Defence response to virus
Casp1	Caspase-1	-Regulation of inflammatory response -Cellular response to cytokine stimulus
Casp4	Caspase-4	-Regulation of inflammatory response -Innate immune response
Tap1	Antigen peptide transporter 1	-Adaptive immune response -Defence response
Trafd1	TRAF-type zinc finger domain-containing protein 1	-Negative regulation of innate immune response
IL-18	Interleukin-18 receptor accessory protein	-Immune response -Inflammatory response
Fcgr2b	Low affinity immunoglobulin gamma Fc region receptor II-b	-Regulation of immune response -Response to bacterium
Rnf31	E3 ubiquitin-protein ligase RNF31	-T cell receptor signalling pathway
Ptprj	Receptor-type tyrosine-protein phosphatase eta	-B cell differentiation -T cell receptor signalling pathway

Cd274	Programmed cell death 1 ligand 1	-Response to cytokine -Immune response
Themis2	Protein THEMIS2	-Inflammatory response -T cell receptor signalling pathway
Pilrb1	Paired immunoglobulin-like type 2 receptor beta	-Myeloid dendritic cell activation
Ifi203	Interferon-activable protein 203	-Activation of innate immune response
Pnpt1	Polyribonucleotide nucleotidyltransferase 1, mitochondrial	-Mitochondrial RNA processing -RNA polyadenylation
Xaf1	XIAP-associated factor 1	-Type I interferon signalling pathway
Psmb9	Proteasome subunit beta type-9	-Regulation of mRNA stability -T cell receptor signalling pathway
H2-Q4	Histocompatibility 2, Q region locus 4	-T cell receptor binding
H2-T24	Histocompatibility 2, T region locus 24	-Positive regulation of T cell mediated cytotoxicity
Otud5	OTU domain-containing protein 5	-Negative regulation of type I interferon production -Protein deubiquitination
Llgl1	Lethal(2) giant larvae protein homolog 1	-Regulation of protein secretion

3.2.3 Validated a set of intron retention event after 2 hours of LPS treatment by qPCR

We next validated a subset of retained introns; each retained intron's data was examined on the IGV platform to confirm levels of individual intron retention (examples in Figure 3-3 right-hand side) [281]. Introns with both strong and moderate levels of retention were chosen for validation (CD274, Herc6, Pnpt1 and Uba7).

CD274, better known as PD-L1, is associated with immune avoidance in cancer. CD274 gene amplification in cancers leads to upregulation of PD-L1 mRNA and protein

expression, while methylation of the gene promoter suppresses its transcription [289]. Herc6 (HECT and RLD Domain Containing E3 Ubiquitin Protein Ligase Family Member 6), is a SG15 E3 ligase and provides conjugation in mouse cells which is required for antiviral activity [290]. Pnpt1 (polynucleotide phosphorylase) is a 3'-5' exoribonuclease and has been documented in the regulation of maintenance of mitochondrial homeostasis, mtRNA import and aging-associated inflammation [291]. Human polynucleotide phosphorylase (hPNPaseold-35) is encoded by the PNPT1 gene which is located at chromosome 2p15-2p16.1. It is also a type I IFN inducible early response gene [292, 293]. Uba7 (ubiquitin-like modifier activating enzyme) can mediate ISGylation which favours the development of an anti-tumour microenvironment by clustering of transcription factors and activating anti-tumour gene expression in breast cancer [294].

Introns known to be transcribed as alternative exons were excluded. Primers to detect the fully spliced transcript and the intron containing transcript were designed and quantitative PCR using oligo dT primed cDNA was performed as described previously [286]. The intron containing version of the transcript was compared to the total transcript level (by measuring exon-exon splicing) and ratio of IR compared to 0h is displayed (Figure 3-3 left-hand side). Results from qPCR showed that the intron-containing variants of CD274, Herc6, Pnpt1 and Uba7 were significantly increased after 2 hours of LPS treatment.

(CD274, also called PD-L1)
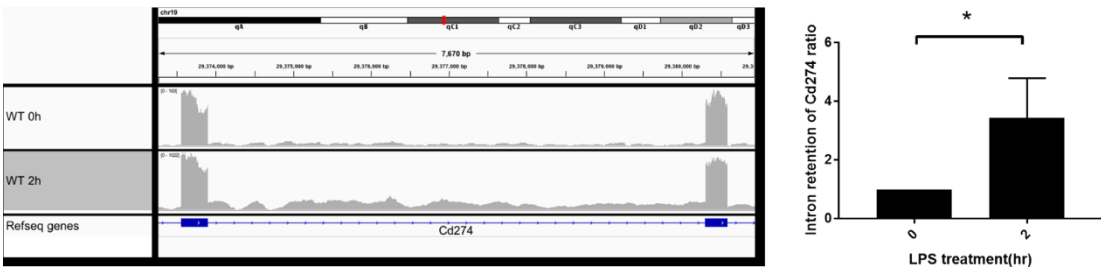
(Herc6)
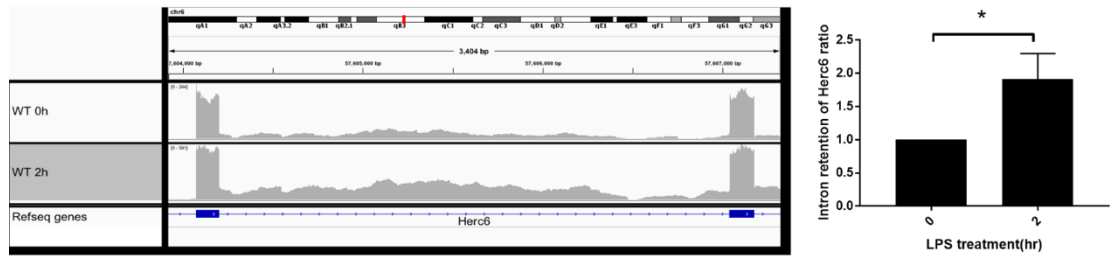
(Pnpt1)
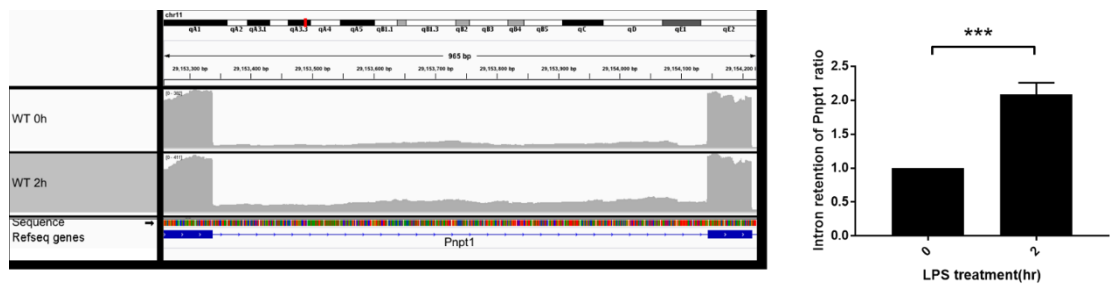
(Uba7)
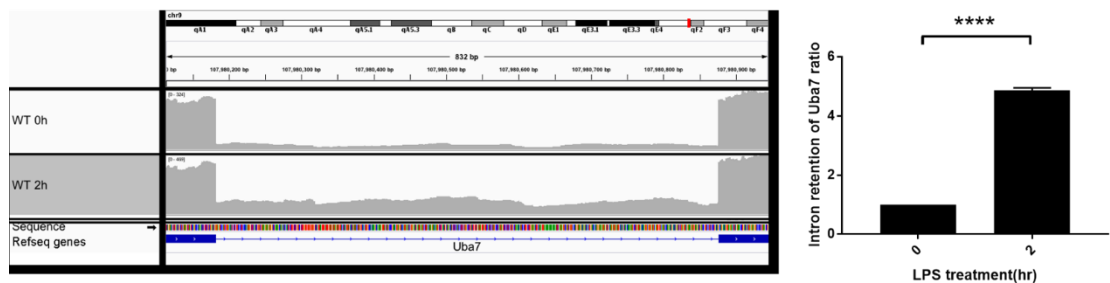
Figure 3-3: Validation for selected genes in response to LPS treatment. Left panel- IGV plots with blue rectangles (exons) and tall grey peaks indicating mapped reads to these exons and in between the reads mapping to the intron. Right panel-qPCR validating the increase in IR ratio at 2h post-LPS. Results from qPCR showed that the intron-containing variants of CD274, Herc6, Pnpt1 and Uba7 were significantly increased after 2 hours of LPS treatment. Graphs show the individual values as the symbols and the error bar show the standard deviation. *$p<0.05$, **$p<0.01$, ***$p<0.001$, ****$p<0.0001$.

3.2.4 NMD loss via SMG1 KO has a limited effect in IR in BMMs in response to LPS treatment.

Given that genes enriched in the '2h IR cluster' could be seen as secondary responses to LPS (i.e. heightened awareness for other pathogens and negative regulation of the immune response) we predicted that the co-ordinated IR was acting as an additional layer of regulation for these transcripts. As described above targeting to either NMD or function as a detained intron are the main possible outcomes for this type of co-ordinated IR. Consequently, we examined whether these transcripts were targeted to the NMD pathway. SMG1 is the key kinase required for NMD and loss of SMG1 blocks NMD function [64]. We have a unique animal model of SMG1 loss in macrophages (Please see chapter 4). *Smg1$^{fl/fl}$* mice have LoxP sites flanking exons 2 to 4 of *Smg1* gene. The gene stays intact unless Cre recombinase (Cre) is expressed in the same cell. *Smg1$^{fl/fl}$* mice were crossed to mice expressing Cre controlled by the LysM promoter, which is active in myeloid lineage cells and tissue macrophages. SMG1, as a key NMD component may be regulated in response to LPS in BMMs from *LysM$^{+/Cre}$Smg1$^{fl/fl}$* mice, we examined whether LPS treatment affected NMD efficiency (Figure 3-4A). We also analysed RNA sequencing data from SMG1 KO macrophages to compared IR events in in the presence and absence of functional NMD (Please see Chapter 5). There were limited differences between wildtype and KO BMMs with IR clustering in KO also displaying a group of ~500 with a peak at 2h post-LPS (Figure 3-4B). This was also validated by realtime PCR and results showed no significant difference in intron retention between BMMs from *LysM$^{+/Cre}$Smg1$^{fl/fl}$* and control group mice. These findings indicated that the transcripts with a retained intron are likely not targeted to NMD. Consequently, these transcripts may contain detained introns.

(A)
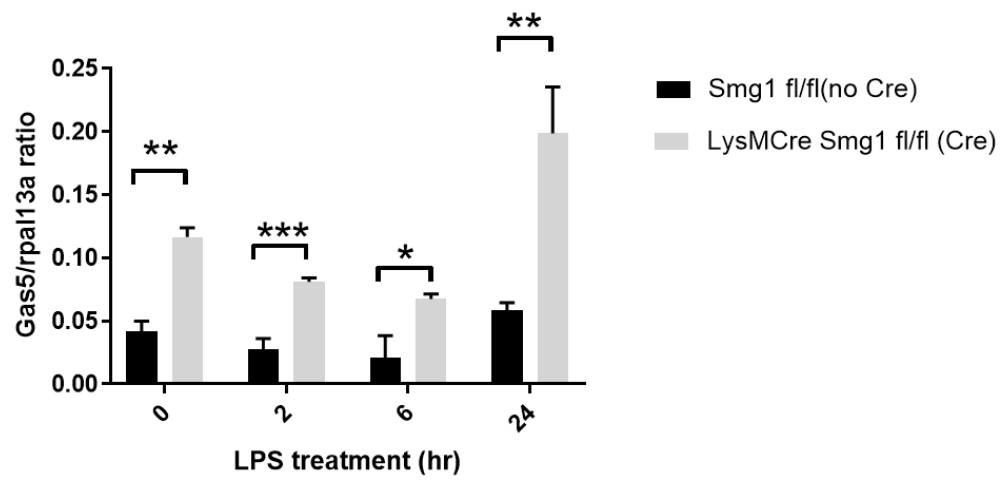
(B)
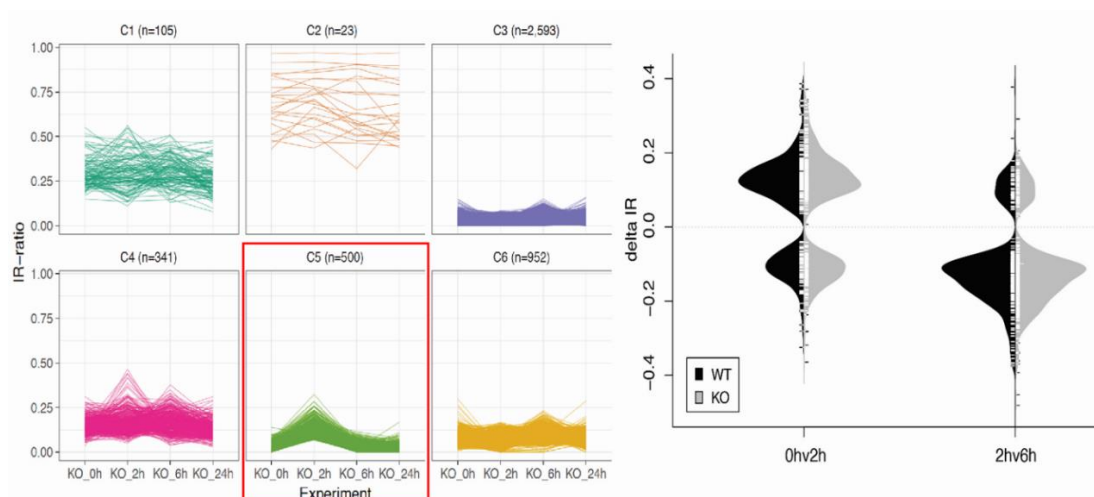
(C)
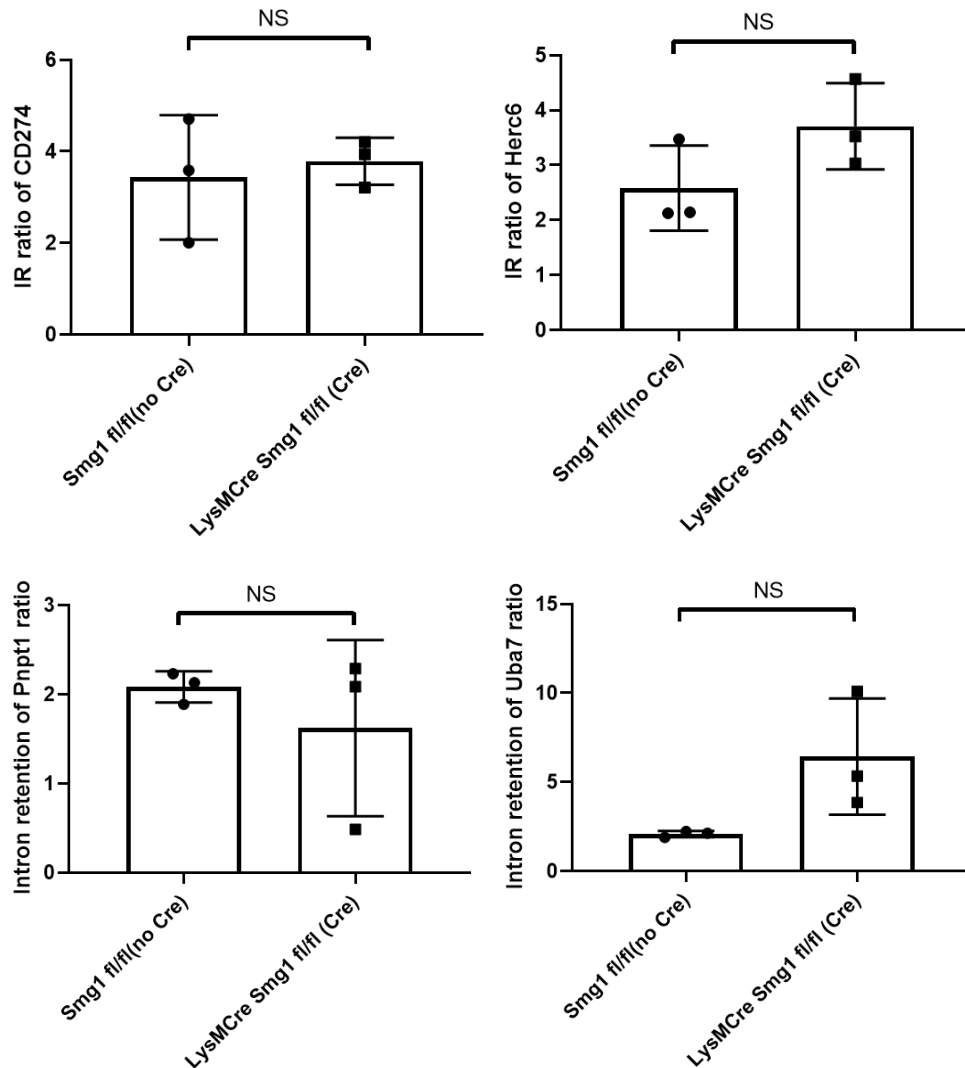
Figure 3-4: NMD loss via SMG1 KO has a limited effect on IR in BMMs in response to LPS. (A)Levels of NMD target RNA in BMMs from wildtype and $LysM^{+/Cre}Smg1^{fl/fl}$ (Cre) animals at indicated time after LPS treatment. (B)Left panel – IR clustering for KO BMMs shows a group of 500 events with a peak at 2h post- LPS. Right panel- Bean plot showing back-to-back changes in IR density highlighting the similarity between WT and KO. This panel was generated by Dr Ulf Schmitz. (C)IR ratio in CD274, Herc6, Pnpt1, Uba7 have no significant difference after 2h post- LPS treatment by qPCR. Graphs show the individual values as the symbols and the error bar show the standard deviation. $*p<0.05$, $**p<0.01$, $***p<0.001$.

3.2.5 Intron retained transcripts localise in the nucleus at 2h post-LPS.

Retention of introns can cause the transcript to be stored in the nucleus until subsequent further splicing occurs; this allows for earlier gene expression and a delay to protein expression. This type of retained intron is referred to as detained introns [279]. Therefore, we determined whether intron containing transcripts are held in the nucleus at 2h post-LPS. RNA was isolated from nuclear and cytoplasmic extracts and tested for the presence of CD274, Herc6, Pnpt1, and Uba7 IR transcripts by realtime PCR. Effectiveness of nuclear separation was confirmed by western blotting for nuclear marker Histone H3 (Figure 3-5 A&B). Neat1 transcript detection was also used to demonstrate nuclear fractionation [285]. Our data showed that the intron-containing variants of CD274, Herc6, Pnpt1, and Uba7 were strongly concentrated in the nucleus with only limited detection in the cytoplasmic fraction (Figure 3-5C). These data supported that these transcripts stayed in the nucleus, and not transported to the cytoplasm, indicating that the retained introns identified are acting as detained introns.

(A&B)
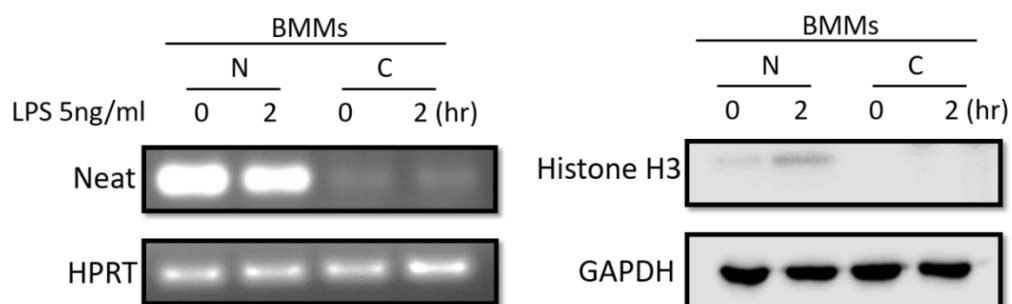
(C)
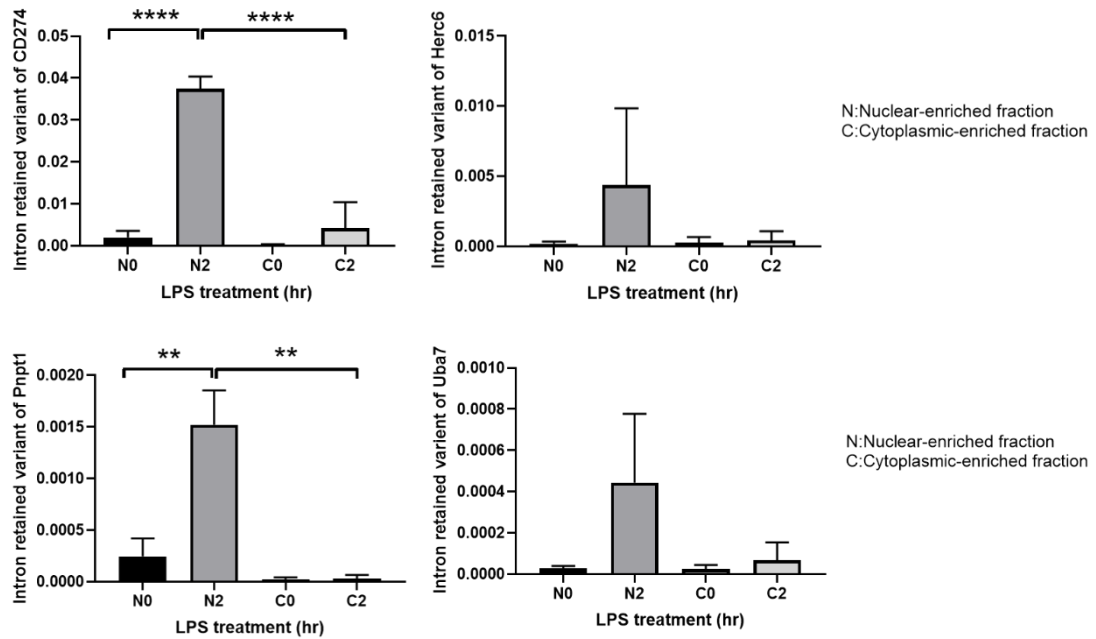
Figure 3-5: Intron retained transcripts are strongly concentrated in the nuclear extracts 2h post-LPS treatment. RNA was isolated from nuclear and cytoplasmic extracts from BMMs at 0 and 2h post-LPS. (A) Neat1 (nuclear) and HPRT used to identify and determine purity of nuclear and cytoplasmic extracts by PCR. (B) Western blotting showed Histone H3 and GAPDH are nuclear and cytoplasmic extracts marker, respectively. (C) The intron retained variant of CD274, Herc6, Pnpt1 and Uba7 were measured by realtime PCR. Data showed that the intron-containing variants of CD274 and Pnpt1 were strongly concentrated in the nucleus with only limited detection in the cytoplasmic fraction. Graphs show the individual values as the symbols and the error bar show the standard deviation. $*p < 0.05$, $**p < 0.01$, $***p < 0.001$, $****p < 0.0001$.

3.3 Discussion

Intron retention (IR) is a regulated process during gene expression, however its regulation during inflammation had not been examined at the start of this project. Intron retention (IR) modulates gene expression levels by altering RNA localisation and efficiency of translation or alters expression of different protein isoforms. Our data showed that at 2h

post-LPS there was a significant increase in intron-retention over the other timepoints. Genes identified as having significantly increased intron retention were enriched for interferon inducible genes (ISGs). We validated intron retention in a subset of these genes by quantitative PCR. These experiments indicated that they appear to be predominantly retained in the nucleus therefore were likely regulatory via acting as detained introns. IFNs are secreted cytokines that activate a signal transduction cascade leading to the induction of hundreds of interferon-stimulated genes (*ISGs*)[295]. From our results, we demonstrated that detained intron transcripts included ISG genes Herc6, Pnpt1 and Uba7.

The type I IFNs are produced by LPS-activated macrophages [4]. The murine genome contains 14 highly related IFN genes and single versions of the more distantly related IFN-β, -ε, and -κ genes [296, 297] . The research of the ability of LPS to induce IFN production and the induction of NF-κB activation of pro-inflammatory gene expression by TLR agonists is well established [298]. However, the role of type I IFNs, particularly IFN, in the induction of macrophage gene expression is not as well defined. In this Chapter, we identified a set of genes enriched in the regulating of 'defense responses to other organism' and 'response to virus' (Figure 3-2) in the 2h IR events after LPS treatment via gene ontology analysis and we also made a list of genes which regulate of innate immune responses (Table 3-1). Some of them are related to IFNs. These findings may indicate the importance of endogenous IFN expression in the induction of ISG expression by LPS in macrophages, but we need to further investigate the links.

Detained introns act an additional layer of regulation which can allow for rapid induction of transcript but a later expression of protein. There is likely a need for a second signal to induce splicing of the detained intron that can assist with whether the proteins are

expressed or not as well so can allow fine tuning of initial response after later signals. To update, polyadenylated-RNA deep sequencing mechanism showed release transcripts within minutes of neuronal stimulation [285]. They found that polyadenylated transcripts retain select introns and are stably accumulated in the cell nucleus in the mouse neocortex. In the future work, we may use this new method to examine more rapid release or increased response to secondary signals during an LPS treatment in bone-marrow derived macrophages.

In the last section of this chapter, we found that intron-containing transcripts were significantly retained in the nucleus not in the cytoplasm, and that loss of SMG1 leading to NMD deficiency did not affect the IR profile at 2h post-LPS. Recent insights demonstrated the role of IR during both monocyte-to-macrophage differentiation and macrophage activation [299]. They found that monocytes and macrophages co-ordinated IR along with nuclear detention, to regulate the expression of pro-inflammatory genes including ID2, IRF7, ENG and LAT. This study supported that macrophage development and activation co-ordinated with IR during innate immunity [299].

We can use the same strategy to investigate whether IR patterns are conserved across species as a regulatory mechanism during inflammation. We can purify monocytes from PBMCs from patients who receiving treatments before and after and analyses gene expression undergoing IR event in human monocyte and macrophages. Also, we can assess the sub-nuclear localisation of introns containing mRNAs during inflammation. Detained introns are stored in nuclear speckles prior to further processing or decay [283]. To assess the sub-nuclear localisation of these transcripts we could perform fluorescent

in situ hybridization of intron containing transcripts. This in return may contribute to potential treatments for controlling inflammation.

3.4 Conclusion

In summary, our study highlights that intron retention is an additional layer of regulation in innate immune responses. Additionally, this study characterised novel pathways controlling innate immune responses. Further we may investigate in the mechanisms undergoing of inflammation related diseases characterised by activated macrophages coupled with IR events during progression.

Chapter 4- The role of SMG1 in regulating innate immunity

4.1 Introduction

SMG1 is a large (3,657 amino acid) member of the phosphatidylinositol 3-kinase-related kinase (PIKK) family that localises to both the nucleus and cytoplasm of mammalian cells. Other family members include ATM, ATR, mTOR and DNA-PK, which are known regulators of DNA damage and cellular stress responses [300, 301]. ATM (Ataxia-Telangiectasia mutated), ATR (Ataxia-Telangiectasia mutated RAD3-related), DNA-PK (DNA-dependent protein kinase catalytic subunit) [302], residue at the apex of the mammalian DDR and phosphorylate an overlapping spectrum of substrates. mTOR (Mechanistic target of rapamycin) is another member of PIKK family with two multiprotein complexes, mTORC1 and mTORC2 [303].

SMG1's globular C-terminal region contains the catalytic site while the elongated N-terminal region consists of α-helical HEAT repeats. SMG1 kinase is required for NMD, a process that ensures rapid degradation of mRNA containing Premature Termination Codons (PTC), to prevent aberrant and potentially deleterious truncated protein production [64]. When a PTC is detected a complex, containing SMG1 and its substrate UPF1, is recruited to the mRNA transcripts and SMG1 phosphorylates UPF1. This interaction results in recruitment of other SMG1 proteins. NMD regulates the level of around 10% of all transcripts in the cells [56, 66]. NMD also controls transcript abundance by regulating alternative splicing (AS) that introduce PTCs; this process is called AS-coupled NMD [63]. SMG1 activity can be regulated by NMD factors UPF2 and UPF3 and also inhibited by SMG8 and SMG9 [304, 305]. In more detail, the kinase

activity of SMG1 is regulated by SMG8 (991 amino acids) and SMG9 (520 amino acids) [304, 305] and they can interact with the SMG1-specific C-terminal insertion as resulting in promoting to bind to UPF1 [306]. SMG1 has also been implicated in the DNA damage response [274, 307], telomere stability [308, 309], resistance to oxidative stress [310], regulation of hypoxic responses [311], transcription regulation [63], membrane dynamics [63], metabolism [63] and apoptosis [312]. SMG1 expression was correlated with promoter hypermethylation in acute myeloid leukaemia and head and neck cancer patients [313, 314]. SMG1 was identified as a significantly mutated gene in human lung adenocarcinoma and familial melanoma [315, 316]. The human protein atlas group analysed malignant lymphoma samples and found that the expression of SMG1 was low or not detectable [317]. McIlwain et al.[63] demonstrated that SMG1 deficient mice died pre-birth and that murine embryonic fibroblasts derived from KO embryos regulated AS-NMD based on RNA sequencing data. Loss of SMG1 led to a significant disruption of AS-coupled NMD in transcripts from a small subset of expressed genes. These transcripts encoded splicing factors and a variety of proteins involved in membrane dynamics/signalling, cell death/DNA repair, regulation of transcription.

In a separate SMG1 mouse model our group found that SMG1 knockout is embryonic lethal from E6.5 and SMG1 heterozygotes ($Smg1^{+/gt}$) show signs of haploinsufficiency including [64] increased rates of cancer development (particularly lymphoma and lung adenocarcinoma) as well as altered pro-inflammatory cytokine production (IL-6, CSF-1 and IL-1β) in tissues and serum prior to onset of disease [64]. This was not due to an alteration in the number of monocytes, granulocytes, neutrophils, B or T cells as these were equivalent to wildtype animals [64]. These were the first data indicating that SMG1 may be involved in regulation of inflammatory responses. Further NMD impairment in

Arabiodopsis showed dependently triggered deregulation of single TNL gene, RPS6 via TIR domain-containing, nucleotide-binding, leucine-rich repeat (TNL) pathways. Also NMD activity is inhibited when bacterial infection of plant and caused stabilisation of NMD-regulated TNL transcripts. This new discovery support NMD can control gene expression in innate immunity of plants via immune-related signalling pathways [318]. However how NMD activity is regulated in response to external stimuli is poorly understood.

In order to address how SMG1 regulates inflammatory responses and may be involved in multiple post-transcriptional regulatory pathways, we have developed a novel model of total SMG1 loss to study the role of SMG1 in TLR mediated responses. This chapter will discuss how SMG1 acts to regulate innate immunity during initial signalling and at post-transcriptional and post-translational levels as well as different regulation between females and males mice.

4.2 Results

4.2.1 Generation of *LysM^{+Cre}Smg1$^{fl/fl}$* mice

The LysM promoter is active in myeloid lineage cells and tissue macrophages and this promoter is frequently used to generate myeloid specific knockouts [319]. Characterisation of LysMCre mice showed knockout of the target gene in 90% of mature macrophages and close to 100% of granulocytes [320]. We generated *LysM$^{+/Cre}$Smg$^{fl/fl}$* (Cre) mice only knocking out SMG1 in myeloid lineage cells under LysM promoter. *Smg1$^{fl/fl}$* mice have LoxP sites flanking exons 2 to 4 of the Smg1 gene (Figure 4-1A). PCR results showed that a DNA fragment size of wt 155 bp; fl 189bp is expected. Our SMG1

is conditional knockout mice which displays only loss of SMG1 function in macrophages, thus genomic DNA extracts from BMMs are two bands, and other genomic DNA from tail only can detect one band (Figure 4-1B left-hand side). We also determined Cre efficiency by measuring the levels of each PCR product in BMM and tail DNA, Cre efficiency ranged from 43% to 80% in total of 9 mice (Figure 4-1B right-hand side) and there was no significant difference between male and female mice. In fact, the number of litters is lower than predicted. This is not surprising because our complete SMG1 knockout mice were early lethal and SMG1 heterozygous mice showed a decreased growth rate of cells [64]. Therefore, we have only smaller proportion of overall pool analysed. qPCR (Figure 4-1C) and western blotting (Figure 4-1D) showed that Smg1 mRNA expression and protein level is lower in *LysM$^{+/Cre}$Smg1$^{fl/fl}$* (Cre) mice as compared to *Smg1$^{fl/fl}$* (WT) mice. Results indicated SMG1 function loss in BMMs as compared with wild-type mice, indicating that our *LysM^{+Cre}Smg1$^{fl/fl}$* (Cre) mice therefore can provide cells totally knocking out SMG1 knocked out only in myeloid lineage.
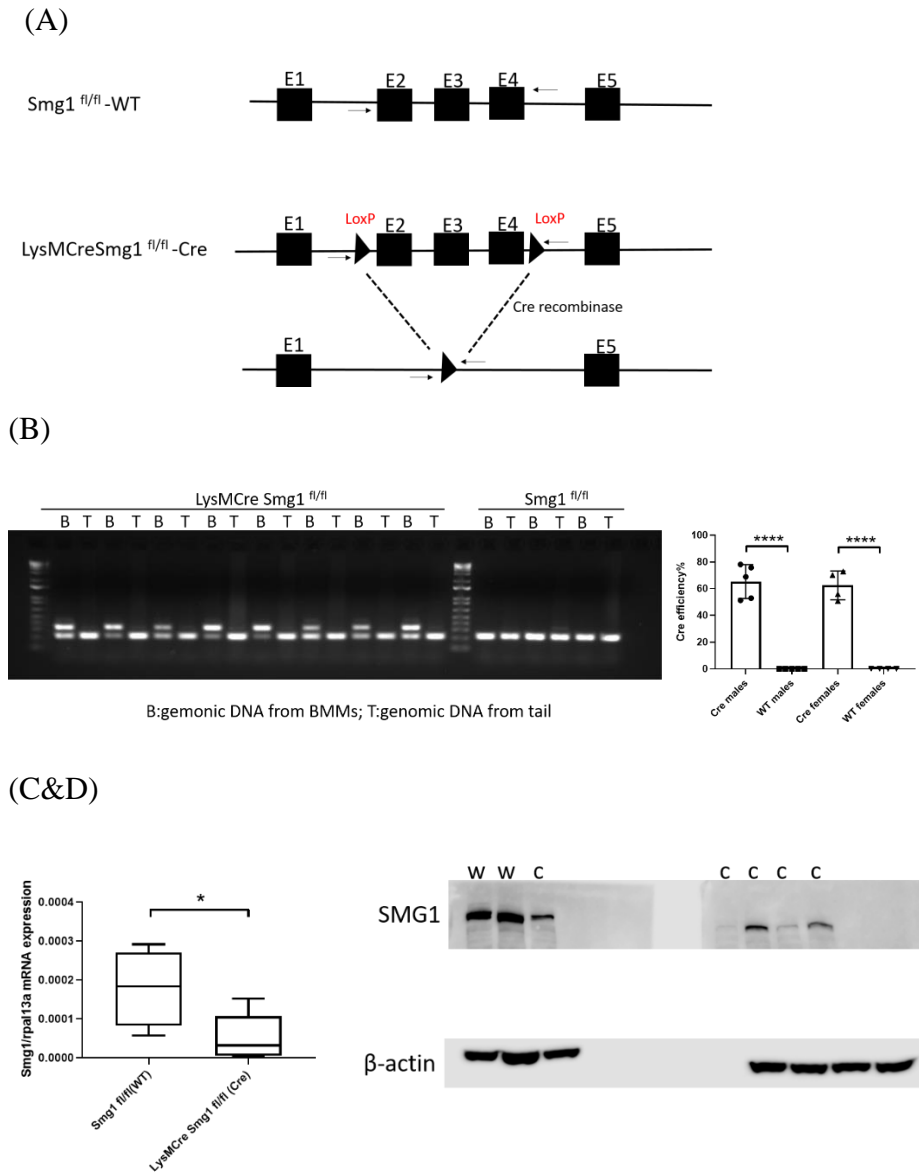
Figure 4-1: Diagram of making the mouse (*LysM^{+Cre}Smg^{fl/fl}* mice). (A) Making mouse diagram-introducing of *LysM^{+Cre}Smg1^{fl/fl}* (Cre) mice. (B) Genotyping showing Smg1 only knockout in myeloid cells (genomic DNA from tail and BMM) and Cre efficiency% between males and females *LysM^{+Cre}Smg^{fl/fl}* (Cre) and *Smg1^{fl/fl}* (WT) mice. (C) Smg1 mRNA expression and (D) protein levels in BMMs between *LysM^{+Cre}Smg1^{fl/fl}* (Cre) and *Smg1^{fl/fl}* (WT) (w: wild-type mice; c: cre mice). All the mice ages were 8-10 weeks old. Graphs show the individual values as the symbols and the error bar show the standard deviation. *$p<0.05$, **$p<0.01$, ***$p<0.001$.

4.2.2 Smg1 deficiency alters toll-like receptor induced inflammatory gene expression

In preliminary data gathered while the group was based at QIMR Berghofer, the LPS response in BMM from $Smg1^{+/gt}$ and wildtype mice was compared. BMMs from $Smg1^{+/gt}$ showed less induction of the pro-inflammatory cytokines IL-6, IL-1β and IFNβ mRNA at early timepoints (Figure 4-2A) compared to BMM from wildtype littermates. However, IFNβ mRNA levels were slightly elevated at later timepoints. These data were confirmed using BMMs from $LysM^{+Cre}Smg1^{fl/fl}$ (Cre) mice and showed lower pro-inflammatory cytokine mRNA levels at early timepoints (Figure 4-2B). However, when the colony of mice was moved to the Ingham Institute in 2015 this phenotype was less apparent – They are relatively less stressed in the new environment and have longer lifespan, as well as take more time to produce cytokines after LPS treatment. This has resulted in an altered phenotype.

IFN-γ is a cytokine which is elevated in humans and other animals with bacterial infection, leading to LPS-induced production of antibacterial mediators, including nitrite oxide (NO), by macrophages [321]. Next, we examined whether IFN-γ primes macrophages stimulated by LPS treatment to produce the antibacterial mediator NO. Later, we also tested nitric oxide production via nitrite assay in BMMs from $LysM^{+Cre}Smg1^{fl/fl}$ (Cre) and $Smg1^{fl/fl}$ (WT) mice. In detail, the IFNs have been reported to augment many macrophage-specific effector functions among the LPS-stimulated cytokines [322]. Our results showed that BMMs from $LysM^{+Cre}Smg1^{fl/fl}$ (Cre) mice produced more nitric oxide in a dose-dependent manner with LPS-stimulated BMMs prior to IFNγ (500ng/ml) induction as compared with wild-type littermates (Figure 4-2C).
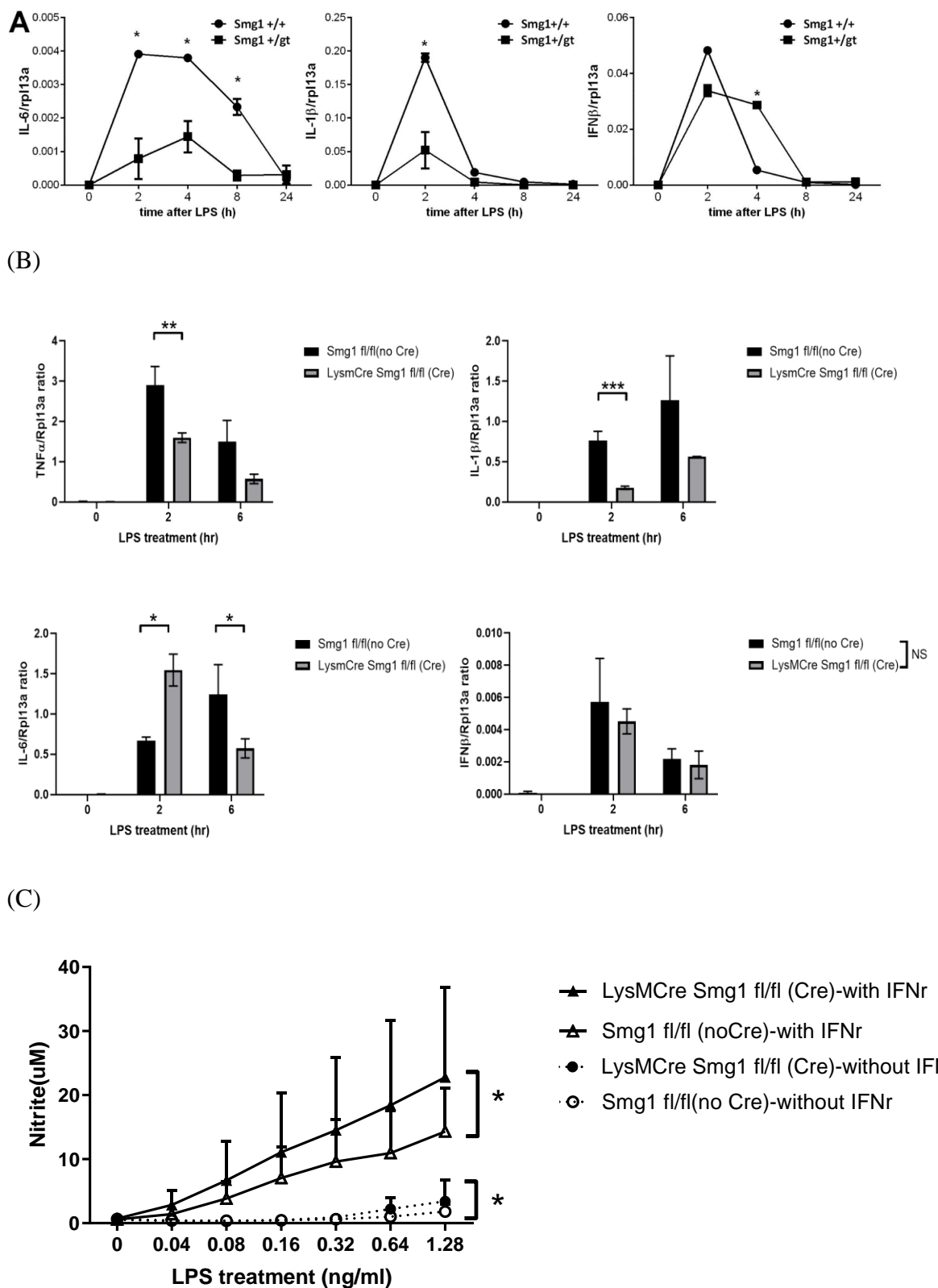
Figure 4-2: Loss of Smg1 alters responses to TLR4/LPS activation. (A) Cytokine mRNA was

measured by qPCR and/or cytokine bead assay in *Smg1*[+/gt] and control litters (Data was generated

at QIMR) (B) Pro-inflammatory cytokine mRNAs were measured by qPCR in BMMs from *LysM^{+Cre}Smg1$^{fl/fl}$* (Cre) and *Smg1$^{fl/fl}$* (WT) mice. (Data was generated at QIMR) (C) Nitrite assay as a measure of nitric oxide production in a dose-dependent in BMMs treated with LPS treatment after 24 hours from *LysM^{+Cre}Smg1$^{fl/fl}$* (Cre) mice and wildtype littermates prior to IFNγ (500ng/ml) induction. All the mice ages were 8-10 weeks old. Graphs show the individual values as the symbols and the error bar show the standard deviation. *$p<0.05$, **$p<0.01$, ***$p<0.001$.

4.2.3 Sex difference affect pro-inflammatory cytokine production in response to LPS treatment in SML mice

While investigating the phenotype of the Ingham Institute colony we discovered that male and female mice showed a different phenotype after SMG1 loss. BMMs from *LysM^{+Cre}Smg1$^{fl/fl}$* (Cre) male mice showed less induction of the pro-inflammatory cytokines TNFα, IFNβ and IL-6 during an LPS treatment, however; TNFα, IFNβ and IL-6 pro-inflammatory cytokine production were up-regulated in BMMs from *LysM^{+Cre}Smg1$^{fl/fl}$* (Cre) female mice 2h post-LPS treatment (Figure 4-3A). From the literature, females display better response to innate and adaptive immune responses than males and are less susceptible to many infectious diseases [323, 324]. Next, we tested whether Cre efficiency may affect pro-inflammatory cytokine production between females and males. BMMs from *LysMCreSmg1$^{fl/fl}$* (Cre) male mice (ID: 3336, 3333, 3286, 3285 with different cre efficiency ranging from 50% to 80%) showed that Cre efficieny did not affect pro-inflammatory cytokine production (TNFα, IFNβ and IL-6) individually. In males BMMs, less than a half of Smg1 function did not mediate pro-inflammatory cytokine production (Figure 4-3B) and not stable in response to LPS treatment (IL-6). These data indicate that Cre efficiency did not affect pro-inflammatory cytokine production in males and less than 50% of Smg1 knockout in macrophages did

not significantly alter response to LPS treatment. Regarding to BMMs from *LysMCreSmg1^{fl/fl}* female mice (ID: 3898, 4021, 4028 with different cre efficiency ranging from 50% to 70%), results showed that pro-inflammatory cytokine did not depend on cre efficiency in females and consistently stable responses were induced during an LPS treatment (Figure 4-3C). In summary, BMMs from *LysM^{+Cre}Smg1^{fl/fl}* (Cre) female mice consistently produced cytokines in response to LPS treatment and did not depend on how much of percentage of Cre efficiency individually. Additionally, there is not a difference in overall Cre efficiency between male and female mice.

(A)
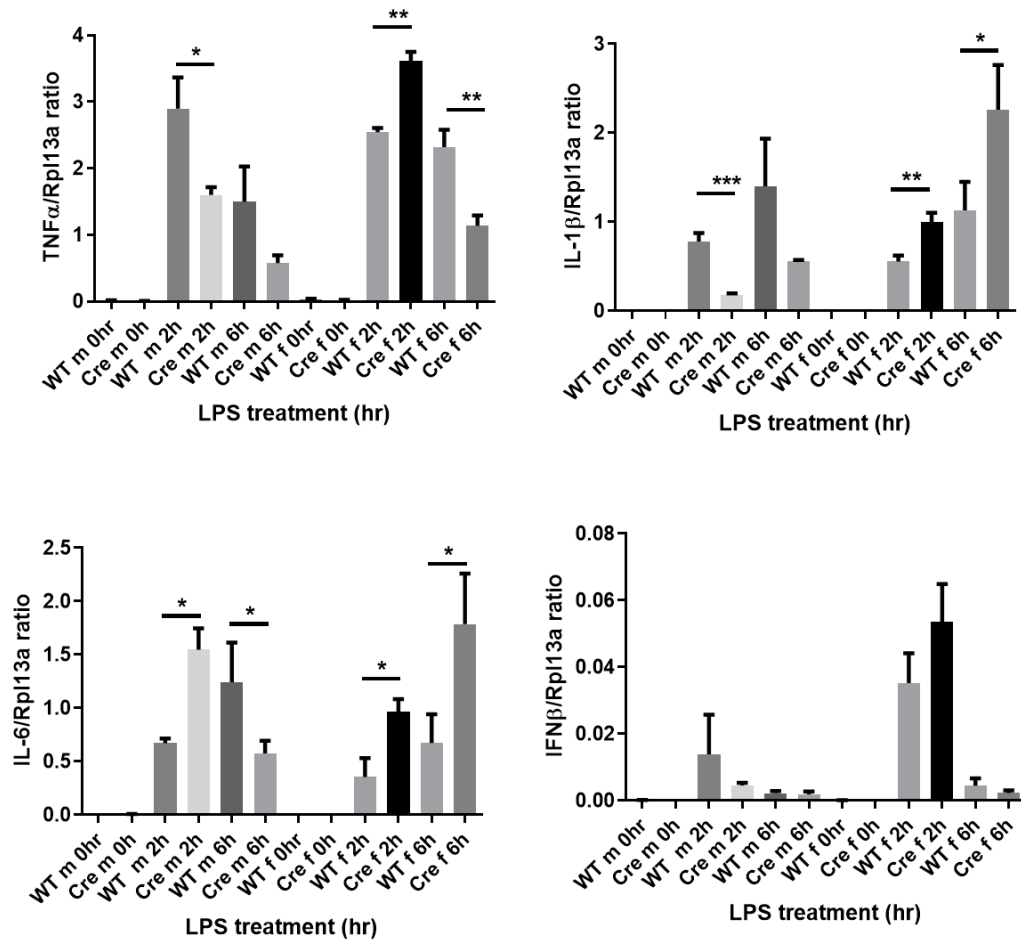
(B)
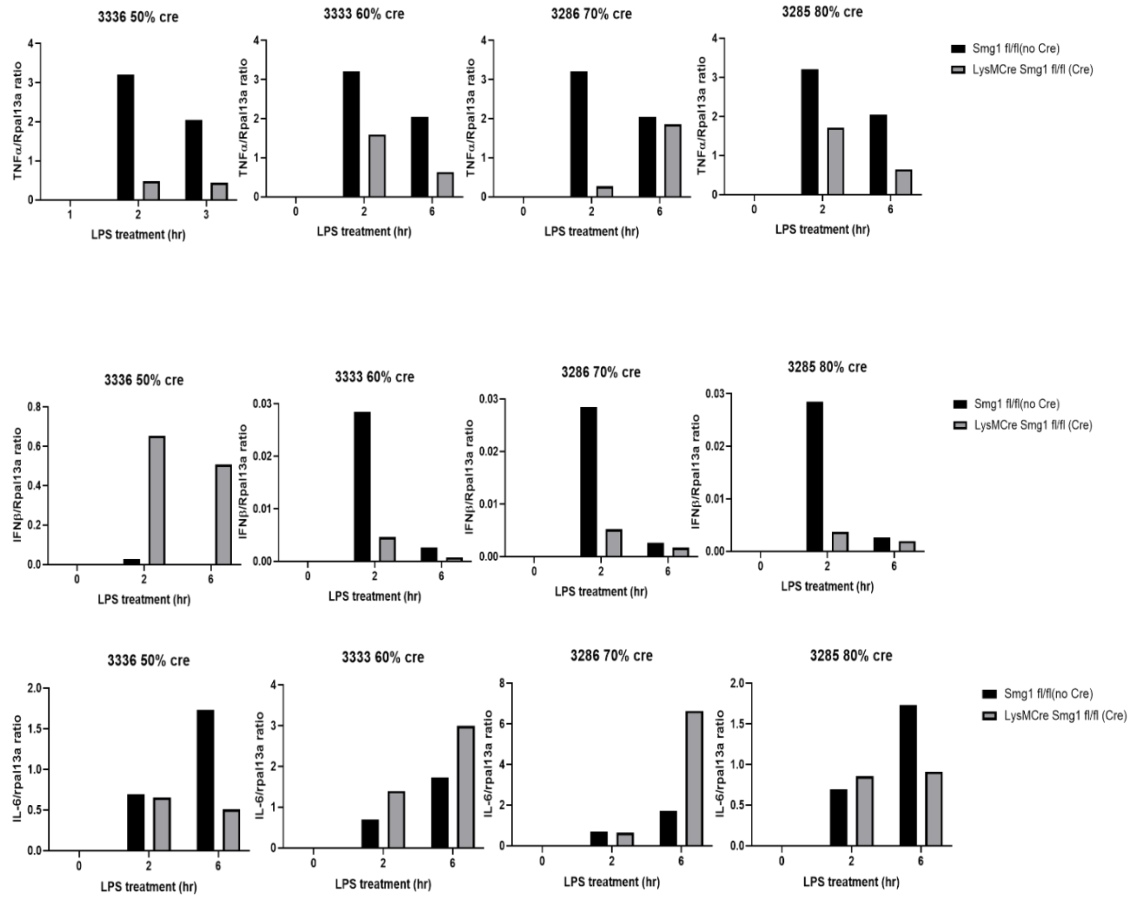
(C)
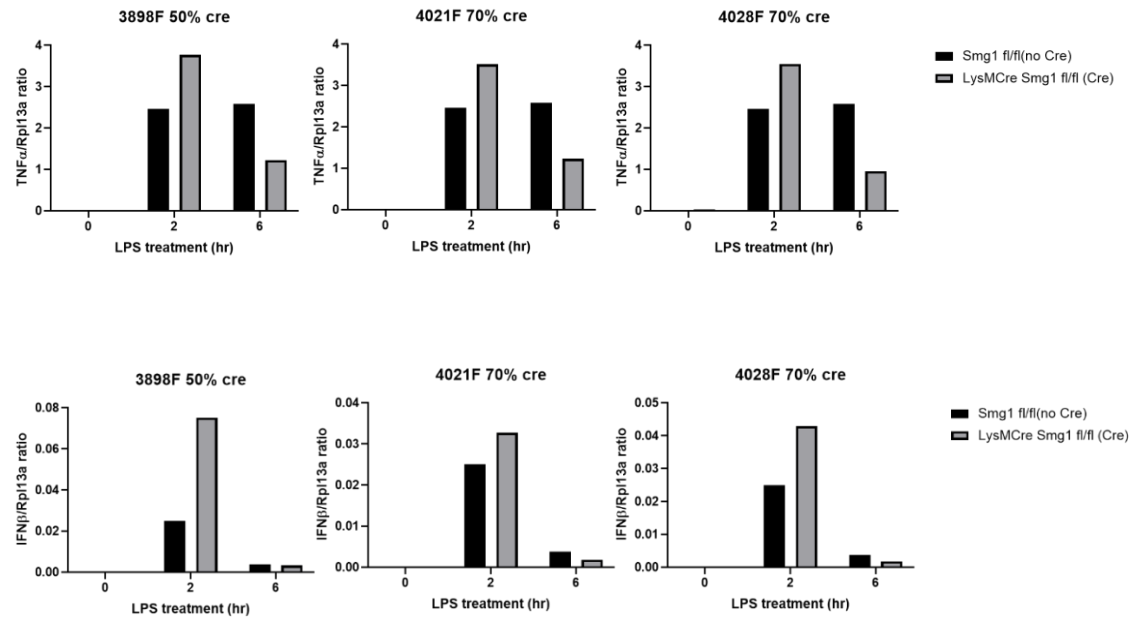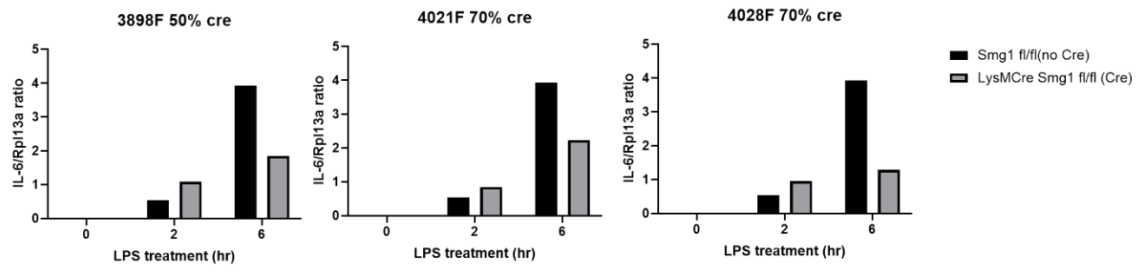
Figure 4-3: Cre efficiency affects pro-inflammatory cytokine production in macrophages from *LysM⁺ᶜʳᵉSmg1 ᶠˡ/ᶠˡ* (Cre) females and males mice during a LPS treatment. (A) Cytokine mRNA was measured by qPCR (TNFα, IFNβ, IL-6 and IL-1β) in *LysM⁺ᶜʳᵉSmg1 ᶠˡ/ᶠˡ* (Cre) and *Smg1ᶠˡ/ᶠˡ* (WT) female and male mice. (B) Pro-inflammatory cytokine production (TNFα, IFNβ and IL-6) in BMMs from *LysM⁺ᶜʳᵉSmg1 ᶠˡ/ᶠˡ* (Cre) male (B) and female (C) mice during an LPS treatment. All the mice ages were 8-10 weeks old. Graphs show the individual values as the symbols and the error bar show the standard deviation. $*p<0.05$, $**p<0.01$, $***p<0.001$.

4.2.4 Loss of Smg1 may affect X-linked genes regulation in innate immunity

Several genes located on the X chromosome are involved in the regulating innate immune responses [323, 325]. This is may be the link to sex differences in the LPS response between male and female mice lacking SMG1. Next, we tested whether Smg1 loss alters X-chromosome encoded immune gene expression. We selected genes which are involved in the process of macrophage differentiation from the haematopoietic stem cell (i.e., IL3RA) [326, 327], macrophage polarisation (i.e., IL13RA1) [328], genes required for the activation of the intracellular oxidative burst in phagocytes (i.e., CYBB) [329, 330], and genes involved in TLR/IL-1R signalling pathways (i.e., IRAK1) [331], as well as regulation of adaptive immunity (i.e., IL2RG) [332]. Results showed that IL3RA and IL13RA1 genes were regulated after LPS treatment of BMMs from *LysM⁺ᶜʳᵉSmg1 ᶠˡ/ᶠˡ*

(Cre) female mice. However, others X-linked genes did not have altered gene regulation during LPS treatment (Figure 4-4A).

We also examined whether loss of SMG1 may be implicated X chromosome inactivation [323, 333]. In humans, each cell of the female contains two X chromosomes (XX) and heterologous in males (XY). Therefore a double dose of all X-linked genes when compared to XY males, who carry a single X chromosome. For genes on the X chromosome, X-inactivation is required to ensure only a single copy functions in each sex and one copy has to be silent, which is called dosage-compensation. Inactivation is initially under the control by the X-inactive specific transcript (Xist) gene [323, 333]. qPCR was performed to examine genes-related to X chromosome inactivation (Xist, Eif1, Rasal, and Upf1) in BMMs from *LysM+CreSmg1 fl/fl* (Cre) female mice and *Smg1fl/fl* (control). Eif1, Rasal and Upf1 are required for upregulation of Xist mRNA during embryonic stem cells (ES) differentiation [333].

We found that loss of SMG1 affects pro-inflammatory cytokine production by up-regulating of Xist regulation post-2 hours LPS treatment (Eif1 and Rasa1), but not involve in mRNA degradation (Upf1). In summary, loss of Smg1 may be involved in the regulation of innate immunity with potential sex differences affecting pro-inflammatory cytokine production in response to LPS treatment. However, these results require further experiments to confirm and provide a clear link to mechanism.

(A)
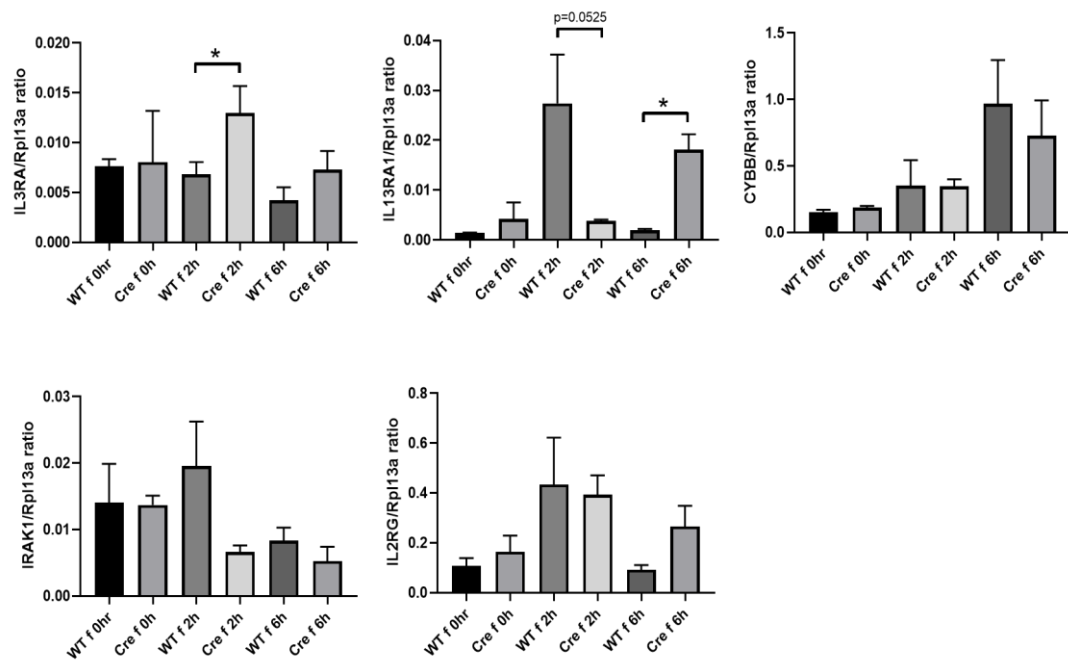
(B)
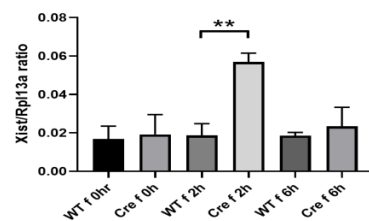
(C)
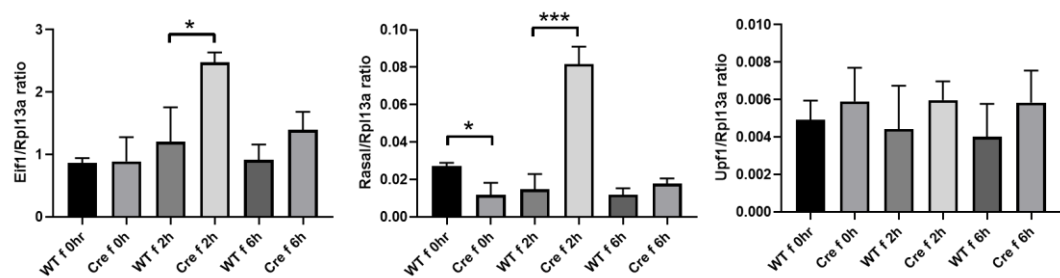
Figure 4-4: Loss of Smg1 altered toll-like receptor induced Xist regulation and X chromosome inactivation, but does not affect X-linked gene expression with potential sex differences during an LPS treatment. (A) mRNA expression was measured by qPCR (IL3RA, IL13RA1, CYBB, IRAK1 and IL2RG) in BMMs from $LysM^{+Cre}Smg1^{fl/fl}$ (Cre) female mice.(B) Xist gene expression

and (C) its downstream (Eif1, Rasal, and Upf1) gene expression in BMMs from $LysM^{+Cre}Smg1$ $^{fl/fl}$ (Cre) female mice were tested by qPCR. Graphs show the individual values as the symbols and the error bar show the standard deviation. $*p<0.05$, $**p<0.01$, $***p<0.001$.

4.2.5 Loss of Smg1 induced inflammatory gene expression in female mice due to change of Toll-like receptor 4 level after LPS treatment at early time point (2 hours)

We next tested TLR4 mRNA expression and protein level in BMMs from $LysM^{+Cre}Smg1$ $^{fl/fl}$ (Cre) and $Smg1^{fl/fl}$ (WT) female and male mice. Results from qPCR (Figure 4-5A) showed increased TLR4 mRNA expression among BMMs from females in contrast Cre males at 2 hours post-LPS treatment had decreased TLR4 mRNA. For protein levels (Figure 4-5B), BMMs from $LysM^{+Cre}Smg1^{fl/fl}$ (Cre) female mice showed an increased TLR4 protein level after 2h-LPS treatment but not as significantly as mRNA levels and in BMM from male mice there was not significant difference between Cre and WT expression of TLR4 protein. As the difference in TLR4 protein expression is small in female mice this may explain some of the increased cytokine production but is unlikely to explain all of the difference between Cre and WT mice.

(A)
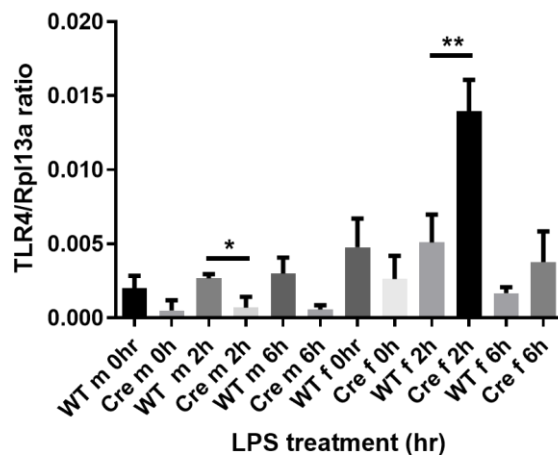
(B)
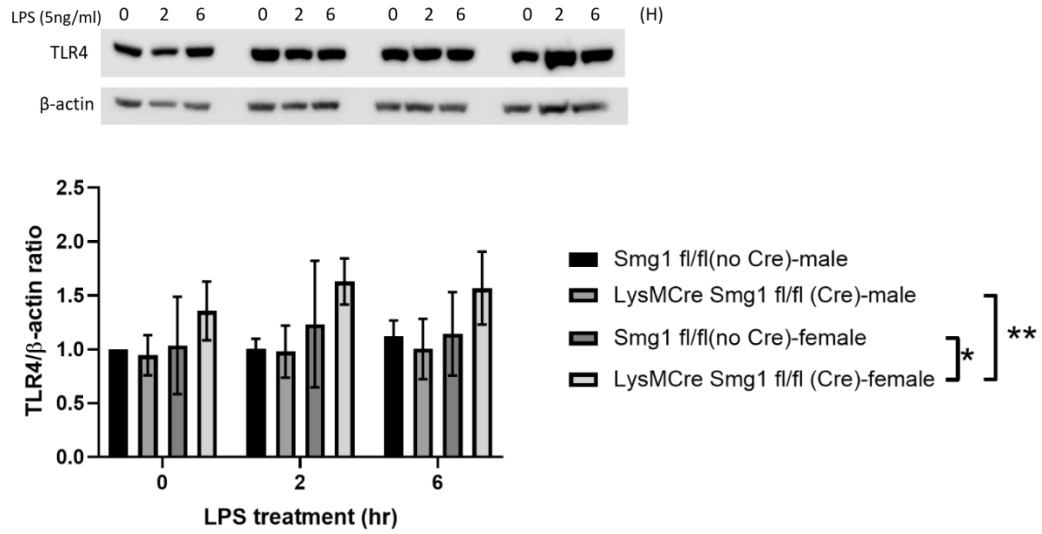
Figure 4-5: Loss of SMG1 alters TLR4 receptor in female SML mice. (A)TLR4 mRNA expression and (B) protein level were measured by qPCR and western blotting in BMMs from $LysM^{+Cre}Smg1^{fl/fl}$ (Cre) and $Smg1^{fl/fl}$ (WT) mice between females and males during an LPS treatment (BMMs from 3 individual mice). All the mice ages were 8-10 weeks old. Graphs show the individual values as the symbols and the error bar show the standard deviation. *$p<0.05$, **$p<0.01$.

4.3 Discussion

We have identified the protein kinase SMG1 as a regulator of TLR responses and we commenced examining the mechanism by which this may be occurring. To do this we generated mice lacking SMG1 in myeloid cells ($LysM^{+Cre}Smg1^{fl/fl}$) and control littermates ($Smg1^{fl/fl}$). We treated BMM from Smg1 deficient mice and wild-type mice with LPS and measured their pro-inflammatory cytokine responses. BMMs from $LysM^{+Cre}Smg^{fl/fl}$ (Cre) male mice showed less induction of the pro-inflammatory cytokines IL-1β, IFNβ, and TNFα (Figure 4-2B) (Figure 4-1A). This is because $LysM^{+Cre}Smg1^{fl/fl}$ (Cre) mice having

an altered phenotype in different animal housing environment after the shift from QIMR to the Ingham Institute.

Reproducibility and replicability are crucial in all fields of experimental research and altered phenotyping of rodents' based on their environment is a significant concern [334]. There are several potential possibilities need to be considered when determining the impact of environment on a set genetic background: housing condition, NH_3 and CO_2 levels, light (intensity, wavelength, photoperiod and flicker frequency), sounds, age size and structure/enrichment, diets, water treatment, presence/absence of pathogens and human presence/interaction, general stress levels [335-337]. Additionally, human interaction and physical environmental factors are regards as part of the stimuli to laboratory animals, and may affect behaviour and physiology or even alter phenotypes in different animal houses. This difference might induce stress responses when the animals are unable to maintain its homeostasis in the presence of stimuli, particularly in animal models that are susceptible to stress and external stimuli such as SMG1 and ATM mice.

Specifically related to our finding that housing impacts the phenotype of Smg1 mice; mice lacking another PIKK family member, ATM, also show housing impacts on phenotype. Ataxia-telangiectasia is an autosomal recessive disorder associated with a high incidence of lymphoid malignancies, neurological degeneration, immunodeficiency, radiation sensitivity, and genetic instability [338]. Ataxia-telangiectasia is caused by biallelic mutations in the ATM gene [338, 339]. Loss of ATM leads to chromosomal breakage and rearrangements as well as increased radiation sensitivity [340, 341]. ATM knockout mice ($Atm^{-/-}$) phenotype and lifespan can differ significantly between different laboratories. One lab developed ATM deficient mice with early lymphomas and lifespans

that were short (2-5 months) [342], however others showed delayed phenotypes and half of mice can be alive after 7 to 12 months [343, 344]. These differences can be observed even with mice with identical genetic backgrounds from the same original strains. These results suggest other factors besides genetic diversity are contributing to disease penetrance. Environmental factors such as housing conditions and diet maybe another factors [345]. Of particular relevance to ATM is the mouse microbiome [346]. The authors performed 16s rRNA high-throughput sequence analysis to identify mucosa-associated bacterial from ATM deficient strains from 2 UCLA mouse colonies in SPF conditions with either sterile (SPF-S) or nonsterile (SPF-N) food, water, and bedding. They found these 2 colonies harbour distinct microbial communities. *Lactobacillus johnsonii* was higher and more cancer-resistant mouse colony of ATM deficient mice from SPF-N, indicating housing condition can impact of microbiome on cancer development via its ability to reduce systemic inflammation and genotoxicity.

Immunodeficiency and autoinflammatory associated animal models such as ATM and SMG1 deficient mice are more susceptible and sensitive to any slight of environmental changes. Momoko Otaki et al. [347] found that macrophage phenotype in wild-type mice was altered after changing to an enriched environment (EE) (double-size of cage, and enrichment with novel physical exercise objects and accessories). There were significantly greater percentages of enriched environment macrophages phagocytosing *S. aureus* and apoptotic neutrophils as compared to macrophages from mice housed in a standard environment. Also after co-culture with *S. aureus*, enriched environmental macrophages can produce more chemokines such as MIP-2, KC and MCP-1. Another recent studies have shown EE is able to elicit anti-inflammatory and neuromodulatory effects in central nervous system via interaction with various immune components and

glial cells [348]. These interactions also affect immune response pathways including secretion muscle fibers released interleukin (IL)-6, reduced monocytes and macrophages expression of Toll-like receptors, modulation of hippocampal T cells, priming of microglia, and upregulation of mitogen-activated protein kinase phosphatase-1. These findings indicating that EE is one of potential factors for cytokine production and further modulate brain function.

The QIMR Berghofer animal house is a very large facility holding tens of thousands of mice, it is relatively noisy and there are many different people moving throughout the facility for long hours each day. In contrast the Ingham facility is smaller housing only hundreds of mice at a time and has a smaller staff and more separated procedure rooms keeping the holding areas quieter. Overall the Ingham environment is likely to be significantly less 'stressful' for mice and this may in turn result in an altered immune phenotype. However, we did still detect a subtler phenotype in SMG1 deficient mice that intriguingly differed between the sexes.

BMMs from $LysM^{+Cre}Smg1^{fl/fl}$ (Cre) male mice showed less induction of the pro-inflammatory cytokines IL-1β, IFNβ, and TNFα, while increased pro-inflammatory cytokines production only was observed in BMMs from $LysM^{+Cre}Smg1^{fl/fl}$ (Cre) female mice compared with controls. This data indicates Smg1 deficiency alters toll-like receptor induced inflammatory gene expression in a sex-specific manner. These were the first data indicating that SMG1 may be involved in regulation of inflammatory responses differently between females and males.

Sex differences have been documented with the variation in the incidence of autoimmune

diseases and malignancies, susceptibility to infectious disease and responses to vaccination. Females develop stronger innate and adaptive immune responses than males [323, 324] and also respond better to various type of vaccination as well as being less susceptible to bacterial or viral infections [349, 350]. Males have a two-fold higher mortality rate to various infection diseases and malignant cancers according to epidemiological studies [351], whereas females are more susceptible to autoimmune diseases, making up 80% of total patients. There has been debate on whether this phenomenon in humans is related to sex alone, behavioural gender norms or a combination of both.

To examine the role of base sex biology there are increasing studies examining sex differences in immune responses. Several factors are also considered for the sex-based disparity in immune responses such as genetics (surrounding XX vs XY chromosomes) and hormonal mediators [323, 349]. X-linked genetic polymorphisms can modulate sex-based differences in innate immunity [352]. Several genes on the X chromosome regulate innate immune responses and these genes encode proteins including PRRs (i.e, TLR7 or TLR8), cytokine receptors and macrophage polarisation (eg. IL2RG and IL13RA1), TLR/IL-1R signalling pathways (eg., IRAK1), activation of phagocytes (eg., CYBB), and adaptive immunity (eg., IL2RG, FOXP3, and CD40L). We tested whether Smg1 loss may alter X-linked genes regulation in innate immunity between females and males mice as compared to wild-type groups. Results showed that BMMs from $LysM^{+Cre}Smg1^{fl/fl}$ (Cre) female mice indicated that the regulation of the bulk of these genes (IL3RA, IL13RA1) were up-regulated of BMMs from Cre mice during an LPS treatment, but CYBB, IRAK1 and IL2RG genes did not differ between Cre and WT BMMs (Figure 4-4A).

Also, SMG1 loss may be implicated in broader X chromosome inactivation [323, 333]. To date, acute inflammation responses is attenuated by Xist in female murine macrophages cell line J774A.1 and human AML193 monocytes by colocalising with the p65 subunit. This interaction led to reducing nuclear migration of NF-κB [353]. qPCR was performed to examine genes-related to X chromosome inactivation (Xist, Eif1, Rasal, and Upf1). Loss of SMG1 resulted in upregulation of Xist, Eif1 and Rasa1 at 2h post-LPS treatment. This indicates that there may be alterations to X inactivation in response to LPS treatment but only when SMG1 levels are limiting (Figure 4-4C).

In the end of this Chapter, results from qPCR and western blots showed slightly increased TLR4 mRNA expression and protein level among BMMs from female but not male $LysM^{+Cre}Smg1^{fl/fl}$ (Cre) mice at 2 hours post-LPS treatment (Figure 4-5). Put it together, Smg1 is involved in sex-specific regulation of innate immunity and potentially in Xist regulation of post-transcriptional level, not translation and further affecting pro-inflammatory cytokine production in response to LPS treatment.

4.4 Conclusion

In summary, this chapter provides the regulation during immune responses between female and male mice when loss of SMG1 function in bone marrow derived macrophages. This is also the first data indicating that Smg1 is involved in sex-specific regulation of innate immunity. For future studies, we can perform macrophages transcriptome to analysis the different regulation of male and females BMMs during an LPS treatment and its related mechanism. Additionally, we also can investigate the points where SMG1 regulates TLRs induced signalling cascades between male and females. This can answer

Smg1 may specifically alter immune response via TLR4 signalling or is also involved in different TLRs and further regulates other immune responses during inflammation.

Chapter 5- Understanding the role of SMG1 in inflammation following LPS treatment by RNA-sequencing analysis

5.1 Introduction

In this chapter, I report additional experiments aimed at addressing the role of SMG1 in inflammation during LPS treatment. RNA sequencing (RNA-seq) is a transcriptomic technique commonly used to compare gene expression between different conditions such as drug treatment versus non-treated samples or between timepoints and demonstrates which genes are up- or down-regulated. This technology not only accurately provides measurements of the levels of transcripts in samples [354], it can also identify alternative splicing [35], allele specific expression [355] and RNA editing [356] depending on the experimental design. Indeed, RNA-seq has been commonly used in clinical studies to identify relationships between clinical features and changes in gene expression which can explain the mechanism of disease progression [357-359].

As described in the previous chapter of this thesis, $Smg1^{fl/fl}$ mice have LoxP sites flanking exons 2 to 4 of the $Smg1$ gene. The gene stays intact unless Cre recombinase (Cre) is expressed in the same cell. $Smg1^{fl/fl}$ mice were crossed to mice expressing Cre under control of the LysM promoter. Preliminary data showed that BMMs from $LysM^{+Cre}Smg1^{fl/fl}$ (Cre) mice had altered toll-like receptor induced inflammatory gene expression, including less induction of IL-6, IL-1β, and IFNβ mRNA expression at early timepoints after LPS exposure as compared to wildtype littermates (see figure 4-2). However, our $LysM^{+Cre}Smg1^{fl/fl}$ (Cre) mice had an altered phenotype following relocation from QIMR to the Ingham Institute.

This chapter describes a side experiment from chapter 4: The role of SMG1 in the regulation of immunity. Chapter 5 aimed to use RNA sequencing to analyse gene expression which is regulated by SMG1 in innate immunity after LPS stimulated TLR4 signalling. BMMs from $LysM^{+Cre}Smg1^{fl/fl}$ (Cre) and $Smg1^{fl/fl}$ (WT) male mice were treated with LPS treatment for 0, 2, 6 and 24h as described previously and RNA extracted. Library preparation and sequencing was performed at the Western Sydney University Next Generation Sequencing Facility (please see chapter 2 and 6 material and methods for more details). Quality Control, normalisation, mapping and initial expression level analysis were performed by our collaborators at The University of Melbourne. (Professor Christine Wells and her groups) [259, 262]. Data was loaded onto the Stemformatics platform for visualisation (*https://www.stemformatics.org*). Data available on the Stemformatics platform reference S4M-7004. Next, we utilised online gene ontology tools to identify characteristics of sets of genes. PANTHER [360] and GORILLA [260] are the two common used online resources for gene function classification and genome-wide data analysis such as gene function, ontology, pathways and statistical analysis tools that enable biologists to analyse large-scale, genome-wide data from sequencing (for more information, please see 5-2 as below).

We next performed validation experiments on candidates. However, our results showed that the majority of the differences between BMMs from $LysM^{+Cre}Smg1^{fl/fl}$ (Cre) and $Smg1^{fl/fl}$ (WT) male mice in response to LPS treatment from the RNA sequencing data set did not validate in independent samples. As discussed later we hypothesise that the point at which these experiments were performed (very shortly after change of housing facility) meant that the new phenotype described in chapter 4 had not yet stabilised and as such limited insight can be obtained from the RNA sequencing data from the $LysM^{+Cre}Smg1$

fl/fl mice with respect to innate immune responses.

5.2 Bio-informatics methods

5.2.1 Gene Ontology (GO) enrichment profiling

Gene Ontology profiling was used to identify statistically significantly over-represented GO terms in our datasets based on RNA seq. Biological and functional gene enriched pathways were identify by the two common online resources- PANTHER (*http://www.pantherdb.org/*) and GORILLA (*http://cbl-gorilla.cs.technion.ac.il/*) [261, 360].

5.2.1.1 GO enrichment analysis- GORILLA

GORILLA is a website-based program that identifies enriched GO terms in a target list of genes compared to a background list of genes. It can also identify enriched GO terms in ranked list genes, without requiring the user to provide explicit target and background sets. GORILLA employs a flexible threshold statistical approach to discover GO terms that are significantly enriched at the top of a ranked gene list as compared to background list. Additionally, the output of the enrichment analysis is visible as a hierarchical structure which can provide the user with a clear picture of the relationships between enriched GO terms in each condition. Moreover, three hierarchically structured ontologies are used that show candidate genes in terms of their associated biological processes, cellular components and molecular functions. In terms of statistics, GO terms enrichment analysis provides an enrichment score and p-value for the over/under representation of a particular term in a given gene list.

5.2.1.2 GO enrichment analysis- PANTHER

The PANTHER (Protein ANnotation Through Evolutionary Relationship) classification system is an online platform that combines gene function, ontology, pathways and statistical analysis tools. This enables users to analyse data from gene expression [361, 362], genome-wide association studies [363, 364], and proteomics [365, 366]. Therefore, users can easily perform analysis at a genome-wide level. The novelty of PANTHER is that it combines both phylogenetic and functional data to annotate subfamilies of shared function and sequences of related genes [367].

The PANTHER system is composed of three functional units. Firstly, the core module is the PANTHER protein library, which contains all protein-coding genes from 82 complete genomes organised into PANTHER defined families and subfamilies. Each family or subfamily is represented by a statistical model annotated with Gene ontology (GO) terms, a phylogenetic tree and a MSA (multiple sequence alignment). The second PANTHER pathway module contains 176 expert-curated pathways. All pathways are linked to phylogenetic information and statistical models through the protein library. The third section is the website-based tools which allow the experimental analysis to be visualised (please find more details in chapter 2).

5.3 Results

As described in previous chapters, BMMs from *Smg1* deficient and wild-type mice were cultured and treated with LPS at different time points (0, 2, 6 and 24 hr) and analysed by RNA sequencing (all details are published and in chapter 2). Over 500 genes showed expression changes stimulated by LPS, ranging from GTPase activity, cell-matrix

adhesion, defence response, immune system process, cytokine production and intracellular signal transduction. Expected changes in response to LPS were examined and described in chapter 2.

Gene Ontology profiling was used to identify statistically over-represented GO terms in our datasets. Biological and functional gene enriched pathways were identify by the two common online resources- PANTHER (*http://www.pantherdb.org/*) and GORILLA (*http://cbl-gorilla.cs.technion.ac.il/*) platforms. GORILLA analysis was performed using a single ranked gene list based on the calculated differential gene expression p-value for paired samples. For analysis (Figure 5-1), the cut-off for GORILLA and PANTHER gene ontology term inclusion was set at 10^{-4} for initial inclusion and FDR q-values were calculated to account for multiple testing. Heat maps were generated via the Stemformatics platform (https://www.stemformatics.org/) using Pearsons correlation (Figure 5-2). Data available on the Stemformatics platform reference S4M-7004.
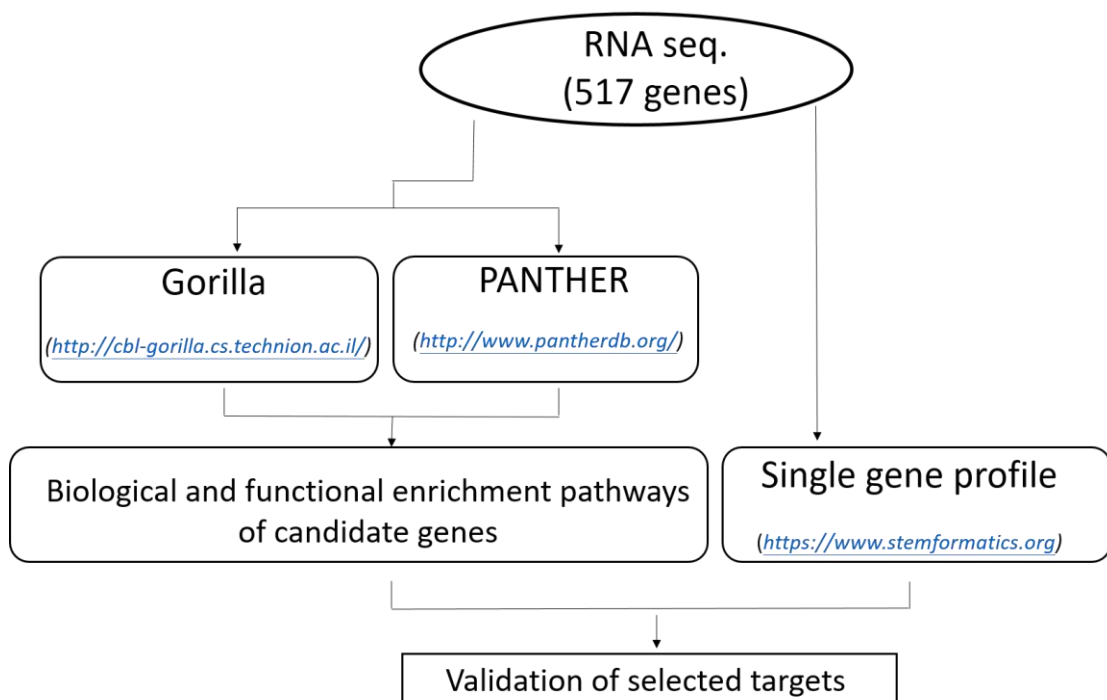
Figure 5-1: Flowchart of the methodology for data analysis.
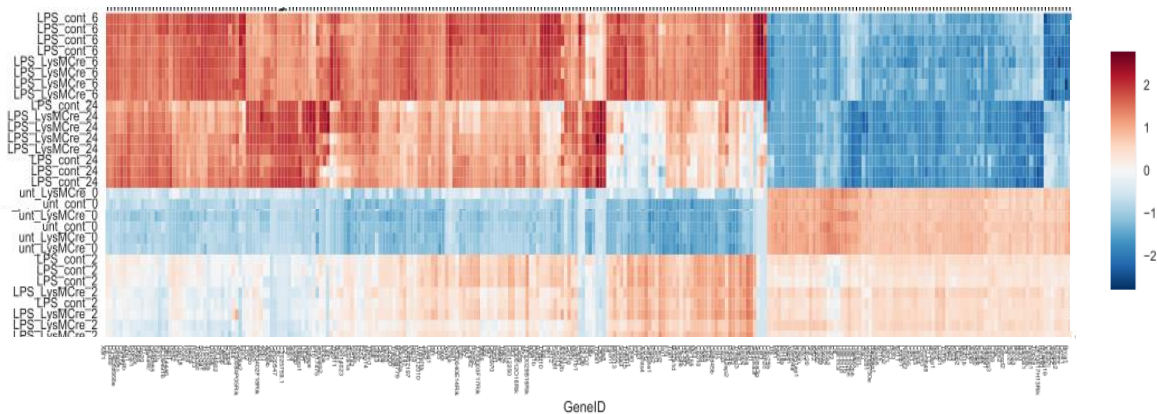
Figure 5-2: Heat-map generated from RNA seq. Heat-map was generated from RNA sequencing data and shows immune-related genes with regulated over the time-course of the LPS treatment (0, 2, 6, 24 hours). All the mice ages are between 8-10 weeks old. Colours indicate the range of each gene's expression in response to LPS treatment, see key on right hand side.

5.3.1 GO terms RNA seq. analysis at 0 hour basal level background.

Firstly, we analysed gene enriched processing pathways using the GORILLA website comparing *LysM*[+/Cre]*Smg1*^{fl/fl} (Cre) and *Smg1*^{fl/fl} (WT) mice at baseline with a p-value cut-off of 0.0001. GORILLA analysis revealed that gene clusters involved in biological processing with positive regulation of GTPase activity (Arhgap27, Ect2, Usp6nl, Tbc1d16), lymph vessel morphogenesis (Pkd1, Vegfa), cell-matrix adhesion (Cd34, Itgal, Itga8, Itgb3) and osteoclast fusion (Cd109) were upregulated in Smg1 deficient BMMs compared to control (Figure 5-3 and Table 5-1). In terms of functional processing GTPase regulator activity (Arhgap27, Ect2, Usp6nl, Tbc1d16), nucleoside-triphosphatase regulator activity (Arhgap27, Ect2, Usp6nl) enzyme regulator activity and molecular function regulator (Sh3bp5, Arhgap27, Oaz1, Dmpk, Usp6nl, Ect2, Tbc1d16, Cd109), vascular endothelial growth factor receptor (Itgb3) and extracellular matrix binding

(Tgfbi, Itgb3), SH3 domain binding (Sh3bp5, Adam10) pathways were upregulated in Smg1 deficient BMMs compared to control, while a gene cluster related to SH3 domain binding is upregulated (Figure 5-4 and Table 5-2). We also used the PANTHER classification system to identify proteins/genes regulated at the basal level between *LysM*[+Cre]*Smg1*^{fl/fl} (Cre) and *Smg1*^{fl/fl} (WT) mice and predicted candidate genes with enrichment analysis with a p-value cut-off of 0.0001. However, we could not find any enriched pathways with same p-value cut off via the PANTHER platform.

Later, we combined the results of gene enriched pathways from GO analysis and examined the single gene profiles using the stemformatics platform to confirm the gene expression analysis. Results confirmed that 14 up-regulated genes (Dmpk, Usp6nl, Ugt1a10, Ibtk, Furin, Fgd2, Wbscr16, Cx3cr1, Cd34, Itga8, Id1, Ang, Pkd212, Cd109) and 11 down-regulated genes (Arhgap6, Arhgap25, Rab4a, Faf2, Vegfa, Tubb2b, Cpe, Il11ra1, Pdefa, Dcstamp, Prkci) were significantly altered at the basal level between *LysM*[+Cre]*Smg1*^{fl/fl} (Cre) and *Smg*^{fl/fl} (WT) mice BMMs (Table 5-3). Interestingly, a small number of proinflammatory cytokine genes were regulated in Smg1 deficient BMMs at basal level as compared to wild-type group. For example, IL17ra1, IL2rg, Dock4 are up-regulated, while Cx3cr1, IL11ra1 are down-regulated in Smg1 BMMs as compared to control.
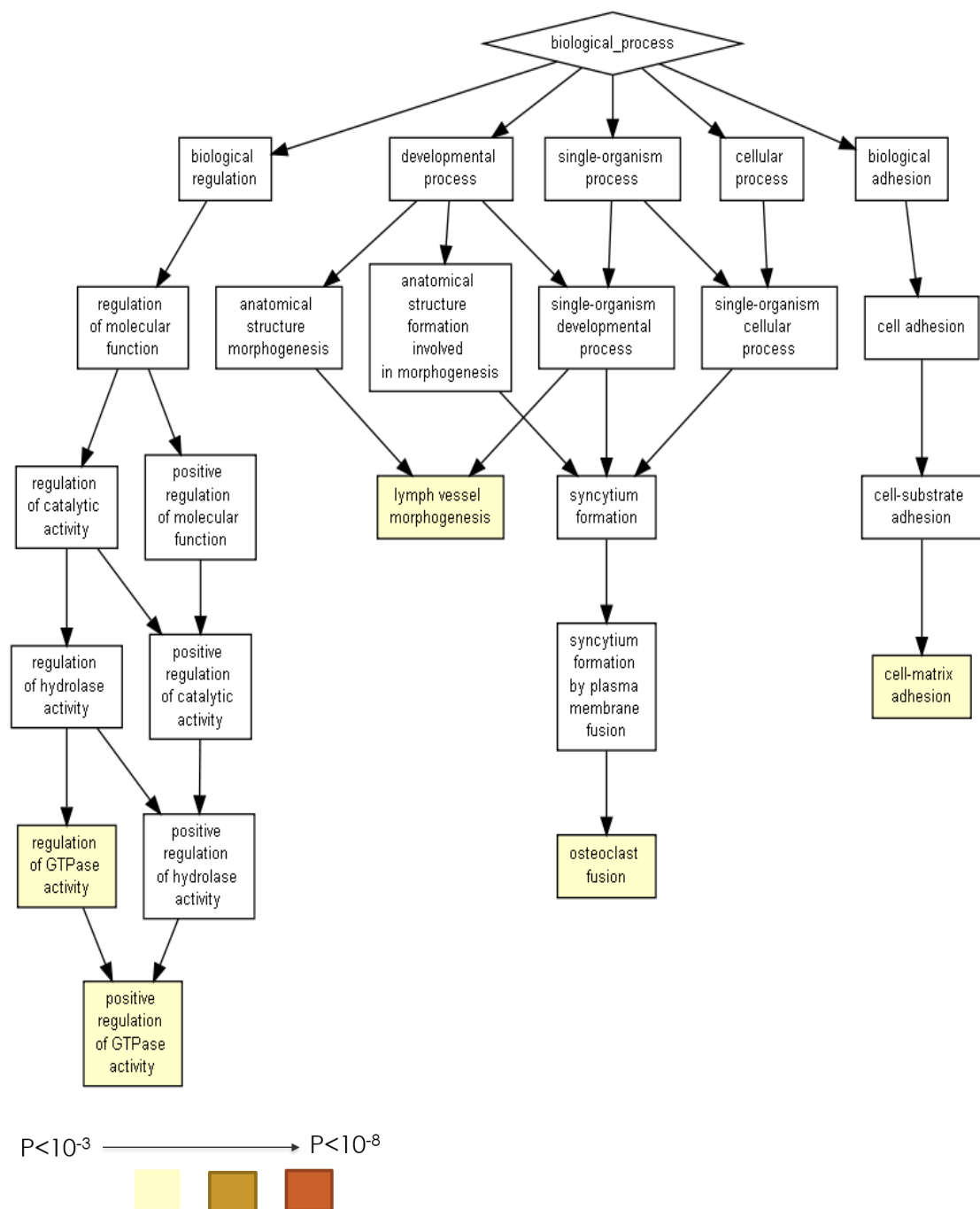
Figure 5-3: Gene ontology process enrichment analysis by GORILLA. Figure depicts pathways which are enriched for changed gene expression at basal level by cut-off 0.0001. Colours of the boxes indicate the significance of the enrichment. The yellow colour boxes are more significant the enrichment of genes in these pathways.

Table 5-1: The process enrichment analysis list generated by GORILLA at basal level background between *LysM^{+Cre}Smg1$^{fl/fl}$* (Cre) and *Smg1$^{fl/fl}$* (WT) mice with -10^{-4} cut-off.

Enriched pathways	P-value	Genes
Positive regulation of GTPase activity	4.88E-05	Arhgap27, Arhgap6, Ect2, Usp6nl, Rasa1, Tbc1d16, Picalm, Rgs16
Lymph vessel morphogenesis	6.75E-05	Pkd1, Vegfa
Regulation of GTPase activity	6.84E-05	Rasgrp3, Arhgap27, Arhgap6, Ect2, Usp6n1, Rasa1, Tbc1d16, Picalm, Rgs16
Cell-matrix adhesion	5.01E-04	Cd34, Itgal, Itga8, Itgb3
Osteoclast fusion	9.90E-04	Dcstamp, Cd109
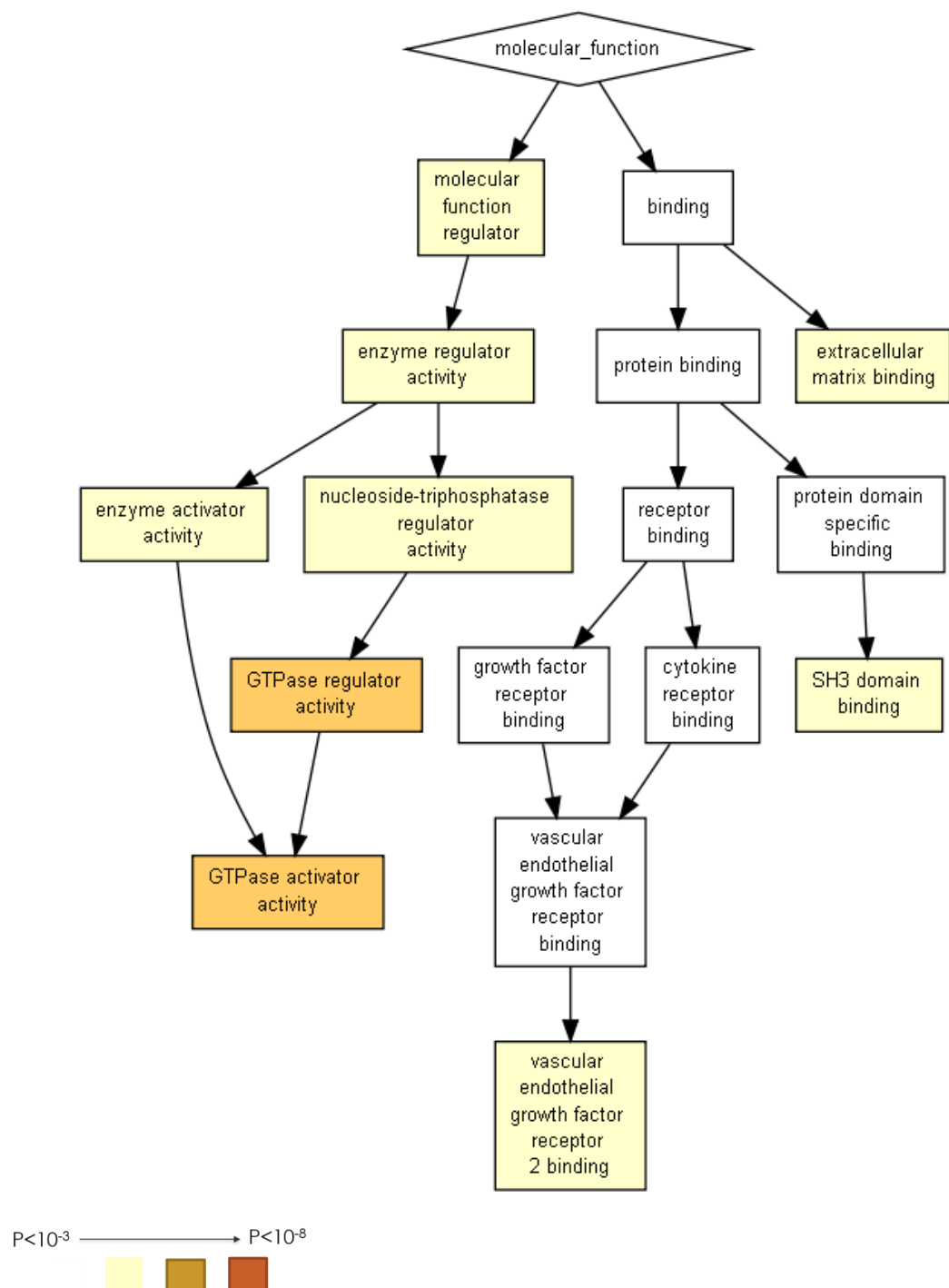
Figure 5-4: Gene ontology functional enrichment analysis by GORILLA. Figure indicates pathways which are enriched for changed gene expression at basal level by cut-off 0.0001. Colours of the boxes indicate the significance of the enrichment, with the darker the colour indicating greater significance (see key in bottom left hand corner).

Table 5-2: The functional enrichment analysis generated by GORILLA at basal level background between $LysM^{+Cre}Smg1^{fl/fl}$ (Cre) and $Smg1^{fl/fl}$ (WT) mice with -10^{-4} cut-off.

Enriched pathways	P-value	Genes
GTPase activator activity	3.07E-06	Rasgrp3, Arhgap27, Arhgap6, Ect2, Usp6n1, Rasa1, Tbc1d16, Rasa1, Tbc1d16, Arhgap25, Acap1, Rgs16
GTPase regulator activity	5.59E-06	Rasgrp3, Arhgap27, Arhgap6 ,Ect2, Usp6n1, Rasa1, Tbc1d16, Arhgap25, Acap1, Rgs16
Nucleoside-triphosphatase regulator activity	1.83E-05	Rasgrp3, Arhgap27, Arhgap6, Ect2, Usp6n1, Rasa1, Tbc1d16, Arhgap25, Acap1, Rgs16
Enzyme regulator activity	3.15E-05	Sh3bp5, Arhgap27, Rpl23, Oaz1, Arhgap25, Acap1, Dmpk, Ercc6, Rasgrp3, Arhgap6, Usp6n1, Ect2, Rasa1, Tbc1d16, Cd109, Rgs16
Enzyme activator activity	7.82E-05	Rasgrp3, Arhgap27, Arhgap6, Ect2, Usp6n1, Rasa1, Tbc1d16, Arhgap25, Acap1, Rgs16, Ercc6
SH3 domain binding	8.48E-04	Sh3bp5, Arhgap27, Arhgap6, Evl, Picalm, Adam10
Molecular function regulator	2.26E-04	Sh3bp5, Rpl23, Arhgap27, Oaz1, Vegfa, Arhgap25, Acap1, Dmpk, Ercc6, Rasgrp3, Arhgap6, Rasa1, Usp6n1, Ect2, Tbc1d16, Cd109, Rgs16
Vascular endothelial growth factor receptor	6.64E-04	Vegfa, Itgb3
Extracellular matrix binding	8.75E-04	Tgfbi, Vegfa, Itgb3

Table 5-3: Single gene profiles of candidate targets genes were analysed and confirmed up- or down-regulated expression in response to LPS treatment at basal level between $LysM^{+Cre}Smg1^{fl/fl}$ (Cre) and $Smg1^{fl/fl}$ (WT) mice is indicated.

	Genes		Functions	(up- or down-)	
Diff(0)	Arhgap6	Rho GTPase activating protein 6	positive regulation of GTPase activity		■
	Arhgap25	Rho GTPase activating protein 25	GTPase activator activity		■
	Dmpk	Dystrophia myotonica protein kinase	intracellular polyamine levels	■	
	Usp6nl	usp6 n-terminal like	positive regulation of GTPase activity	■	
	Ugt1a10	UDP-glucuronosyltransferase	monosaccharide metabolic process	■	
	Rab4a	rab4a,member ras oncogene family	enzyme regulator activity		■
	Ibtk	inhibitor of bruton agammaglobulinemia tyrosine kinase	enzyme regulator activity	■	
	Faf2	fas associated factor family member 2	enzyme regulator activity		■
	Vegfa	vascular endothelial growth factor a	Lymph vessel morphogenesis		■
	Tubb2b	tublin,beta 2b class iib	nervous system development		■
	Furin	furin(paired basic amino acid cleaving enzyme)	peptide hormone processing	■	
	Cpe	carboxypeptidase e	peptide hormone processing		■
	il11ra1	interleukin 11 receptor,alpha chain 1	growth factor		■
	Fgd2	fyve,rhogef and ph domain containing 2	growth factor	■	
	Wbscr16	william-beuren syndrome chromosome region 16	growth factor	■	
	Pdefa	platelet derived growth factor,alpha	chemotaxis		■
	Cx3cr1	chemokine(c-x3-c) receptor 1	chemotaxis	■	
	CD34	Cd34 antigen	cell-matrix adhesion	■	
	Itga8	intergrin alpha 8	cell-matrix adhesion	■	
	Idl	inhibitor of DNA binding 1	system development		■
	Ang	angiogenin,ribonuclease	system development		■
	Pkd212	polycystic kidney disease2-like 2	detection of mechanical stimulus	■	
	CD109	Cd109 antigen	Osteoclast fusion	■	
	Dcstamp	dentrocyte expressed seven trans membrane protein	cell-matrix adhesion		■
	Prkci	protein kinase c,iota	establishment of monopolar cell polarity		■

5.3.2 Baseline up-regulated genes in SMG1 deficient mice include nonsense mediated decay targets.

As discussed previously, SMG1 kinase activity is required for NMD activity [64]. Loss of NMD activity can lead to increased expression of NMD targets. We examined whether genes identified as up-regulated at baseline were likely targets of NMD. Unsurprisingly a number of the genes (Ugt1a10, IBTK, Furin, Fgd2, Wbscr6, CD34, Itga8, Eif4a2,

Gtf2a2) are predicted to be targeted to NMD, indicating that loss of SMG1 mediated NMD activity at basal level background (Table 5-4). This data indicates that NMD is decreased in SMG1 deficient cells and that this is captured in the RNA sequencing data.

Table 5-4: Predicted or known NMD targets transcripts at basal line in Smg1 deficient mice

Gene	NMD target identified	Reference
Ugt1a10	Predicted NMD targeted transcripts	https://www.ncbi.nlm.nih.gov/IEB/Research/Acembly/av.cgi?db=human&q=UGT1A_
DMPK	One known NMD targeted transcript + Possible target CUG repeats in 3'UTR	https://asia.ensembl.org/Mus_musculus/Gene/Summary?db=core;g=ENSMUSG00000035941;r=9:85687360-85749334 + EG. https://www.pnas.org/content/105/7/2646
IBTK	Known NMD targeted transcripts	https://asia.ensembl.org/Mus_musculus/Gene/Summary?db=core;g=ENSMUSG00000035941;r=9:85687360-85749334
furin	Known NMD targeted transcripts	https://jcp.bmj.com/content/early/2020/07/12/jclinpath-2020-206788 and http://m.ensembl.org/Mus_musculus/Transcript/Summary?g=ENSMUSG00000030530;r=7:80396310-80399469;t=ENSMUST00000153446

Fgd2	Predicted NMD targeted transcripts and multiple IR transcripts	https://asia.ensembl.org/Mus_musculus/Gene/Summary?db=core;g=ENSMUSG00000024013;r=17:29360914-29379661
Wbscr6	2 NMD target transcripts	https://asia.ensembl.org/Mus_musculus_C57BL_6NJ/Gene/Summary?db=core;g=MGP_C57BL6NJ_G0030586;r=5:143839075-143921864
CD34	1 NMD targeted transcript	https://asia.ensembl.org/Mus_musculus/Gene/Summary?db=core;g=ENSMUSG00000016494;r=1:194938819-194961279
Itga8	1 NMD targeted transcript	https://asia.ensembl.org/Mus_musculus/Gene/Summary?db=core;g=ENSMUSG00000026768;r=2:12106632-12301922
Eif4a2	Known NMD targeted transcripts	Gene regulated by Smg1-dependent AS-NMD [63]
Gtf2a2	Known NMD targeted transcripts	Gene regulated by Smg1-dependent AS-NMD [63]

5.3.3 GO terms RNA seq. analysis at 2 hour after LPS treatment.

At 2hrs post-LPS treatment, our GORILLA analysis showed 39 enriched pathways between $LysM^{+Cre}Smg1^{fl/fl}$ (Cre) and $Smg^{fl/fl}$ (WT) mice BMMs. The majority of gene clusters were involved in defense responses (Itgax, Gm4321, Zbp1, Lat1, Irf8, Tnfsf4, Zc3hav1, Batf2, Igtp, Ifitm3, Il1rn, Fcgr1, Irgm1, Arid5a), response to interferon-beta (Ifnb1, Ifit3, Ifi47, Ifitm3), innate immune response (Ifnb1, Mb21d1), response to

external biotic stimulus (Ifnb1, Itgax, Zbp1, Irf8, Tnfsf4, Batf2, Ifit3, Ifitm3, Arid5a) are downregulated after 2h-post of LPS treatment in Smg1 deficient BMMs compared to control (Supplementary Figure 1 and Table 5-5). In terms of functional enrichment, 2'-5'-oligoadenylate synthetase activity (Oasl2) was downregulated in Smg1 deficient BMMs as compared to control at 2h post-LPS (Figure 5-5 and Table 5-6). For comparison, we analysed the same dataset via PANTHER. We did not observed any enrichment using $p<0.0001$ cutoff. We also performed single gene profiling using the stemformatics platform, which confirmed two up-regulated genes (Hmgb2, Cd244) and 9 down-regulation genes (Gm543i, Itgax, Irf8, Arid5a, Degs2, F3, Mul1, Slamf8, Gna15) differed at 2hr post-LPS treatment in $LysM^{+Cre}Smg1^{fl/fl}$ (Cre) BMMs compared to $Smg1^{fl/fl}$ (WT) BMMs (Table 5-7).

Table 5-5: The top 10 of process enrichment analysis generated by GORILLA at 2 hours after LPS treatment between $LysM^{+Cre}Smg1^{fl/fl}$ (Cre) and $Smg1^{fl/fl}$ (WT) mice-10^{-4} cut-off.

Enriched pathways	P-value	Genes
Defense response	2.13E-9	Itgax, Gm5431, IFnb1, Zbp1, Lat, Irf8, Tnfsf4, Zc3hav1, Ifit3, Batf2, Ifi47, Igtp, Ifitm3, Il1rn, Fcgr1, Irgm1, Oasl2, Mb21d1, Hmgb2, Lyz2, Arid5a
Response to other organism	1.42E-7	Ifnb1, Itgax, Zbp1, Irf8, Tnfsf4, Oasta, Zc3hav1, Batf2, Ifit3, Ifitm3, Fcgr1, Oasl2, Mb21d1, Hmgb2, Lyz2
Response to interferon-beta	1.54E-7	Ifnb1, Ifi47, Gm543i, Igtp, Ifitm3, Irgm1, Ifit3
Defense response to other organism	4.08E-7	Ifnb1, Itgax, Zbp1, Irf8, Zc3hav1, Batf2, Ifit3, Ifitm3,

		Fcgri, Oasl2, Mb21d1, Hmgb2, Lyz2
Immune response	1.03E-6	Ifnb1, Zbp1, Lat, Irf8, Tnfsf4, Zc3hav1, Cd274, Ifit3, Il1rn, Ifitm3, Irgm1, Fcgr1, Oasl2, Mb21d1, Hmgb2, Nrros, Arid5a
Cellular response to interferon-beta	1.11E-6	Ifnb1, Ifi47, Gm543i, Igtp, Irgm1, Ifit3
Innate immune response	1.14E-6	Ifnb1, Zbp1, Tnfs4, Zc3hav1, Ifit3, Ifitm3, Fcgr1, Irgm1, Oasl2, Mb21d1, Hmgb2, Nrros, Arid5a
Response to virus	1.99E-6	Itgax, Ifnb1, Zbp1, Ifitm3, Oasl2, Mb21d1, Tnfsf4, Oasta, Zc3hav1, Ifit3
Response to external biotic stimulus	3.07E-6	Ifnb1, Itgax, Zbp1, Irf8, Tnfsf4, Oasta, Zc3hav1, Batf2, Ifit3, Ifitm3, Fcgr1, Oasl2, Mb21d1, Hmgb2, Lyz2, Arid5a
Response to biotic stimulus	5.14E-6	Ifnb1, Itgax, Zbp1, Irf8, Tnfsf4, Oasta, Zc3hav1, Batf2, Ifit3, Ifitm3, Fcgr1, Oasl2, Mb21d1, Hmgb2, Lyz2, Arid5a
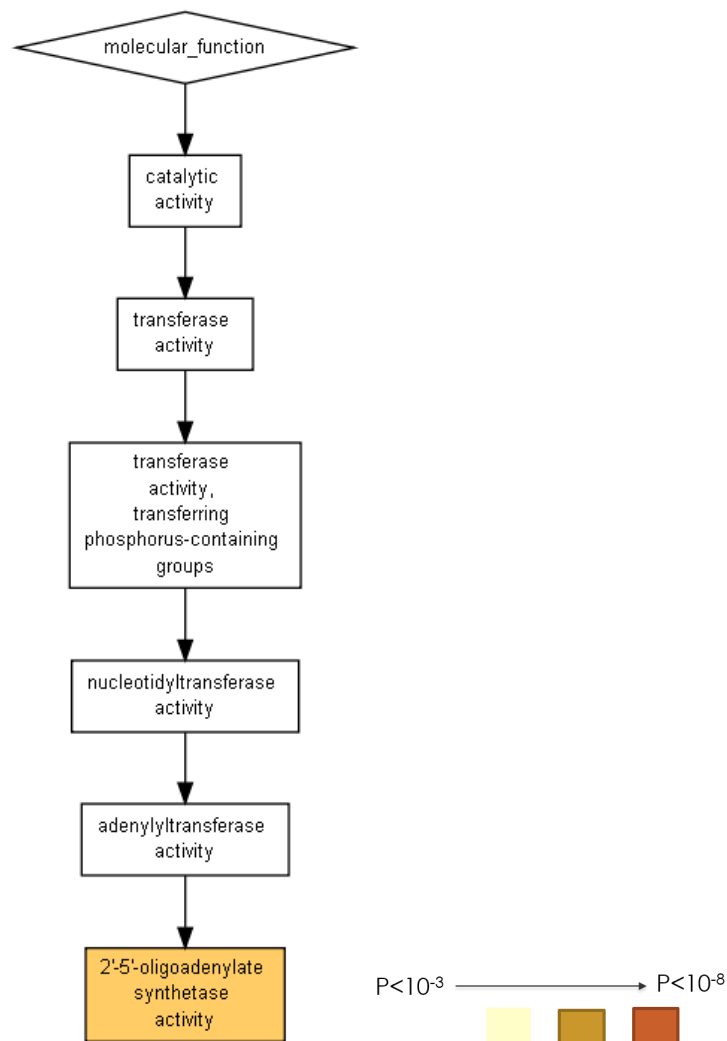
Figure 5-5: Gene ontology functional enrichment analysis using the GORILLA after 2h post-LPS treatment. Figure depicts pathways which are enriched for changed gene expression at 2h post-LPS compared to 0h time point by cut-off 0.0001. Colours of the boxes indicate the significance of the enrichment. The yellow colour boxes are more significant the enrichment of genes in these pathways.

Table 5-6: The functional enrichment analysis generated by GORILLA at 2 hours after LPS treatment between $LysM^{+Cre}Smg1^{fl/fl}$ (Cre) and $Smg1^{fl/fl}$ (WT) mice-10^{-4} cutoff.

Enriched pathways	P-value	Genes
2'-5'-oligoadenylate synthetase activity	8E-6	Oasl2, Oasig, Oasta

Table 5-7: Single gene profile of validated Candidate targets gene expression are up- or down- regulated in response to LPS treatment at 2 hours between $LysM^{+Cre}Smg1^{fl/fl}$ (Cre) and $Smg1^{fl/fl}$ (WT) mice.

	Genes		Functions	(up- or down-)	
Diff(2)	Gm5431	predicted gene 5431	Response to interferon-beta		
	Itgax	integrin alpha x	Defense response		
	Irf8	interferon regulatory factor 8	Defense response		
	Hmgb2	high mobility group box 2	Defense response		
	Arid5a	at rich interactive domain 5a	Defense response		
	Degs2	degenerative spematocyte homolog2	Sphinganine metabolic process		
	F3	coagulation factor iii	Regulation of multicellular organismal process		
	Mul1	mitochondrial ubiquitin ligase activator of nfb1	Cellular response to dsRNA		
	Slamf8	SLAM family member 8	intracellular signal transduction		
	Cd244	natural killer cell receptor 2B4	intracellular signal transduction		
	Gna15	guanine nucleotide-binding protein subunit alpha-15	intracellular signal transduction		

5.3.4 GO terms RNA seq. analysis at 6 hour after LPS treatment

At 6 hours after LPS treatment, the serine family amino acid metabolic process (Psat1, Txnrd1, Srr) and negative regulation of mitochondrial membrane permeability involved in apoptotic process pathways (Bnip3, Acaa2) were identified using GORILLA (p<0.0001) (Figure 5-6 and Table 5-8). Txnrd1, Srr and Bnip3 gene expression are up-regulated in Smg1 deficient BMMs compared to control while Acaa2 and Srr gene

expression are down-regulated. However, we could not find any functional pathways enriched.

Using PANTHER with p<0.0001 cut-off, we identified five gene clusters enriched for biological process pathways, these were chromatin organisation (Suds3, H2afy, Prmt10, Bahd1, Usp22, Cbx4), organelle organisation (Stk4, Slamf8, Cd244, Gna15, Ccl12, Wsb2, Nikiras1, Rapgef2, Scr, Gab2, Rrd1, Gna13, Il23a, Mapk14, Pi4kb, Stat1, Cdk17, Map2k1, Stk4, Rap2c, Sgk1), nucleobase-containing compound metabolic and primary metabolic process (Tbc1d13, Suds3, Rlf, Tsr1, Tcf4, H2afy, Zfp212, Sbno1, Prmt10, Atad1, Igf2bp3, Rasa2, Phf6, Bahd1, Rragc, Hist3h2a, Stat5b, St18, Ampd3, Prpf4, Clock, Pphln1, Cnot7, Tbcel, Dgka, Igf2bp3) were upregulated in response to LPS treatment in Smg1 BMMs as compared to control (Supplementary Figure 2 and Table 5-9). Additionally, we examined each gene from the GO analysis above via single gene profile. We found that there were nine up-regulated genes (Gclc, Wdr75, Tsr1, Tspyl2, Txnrd1, Rasa2, St18, Ampd3, B3galnt2, Tbce1, Usp53) and 12 down-regulated genes (Psat1, Prmt10, Bahd1, Cbx4, Igf2bp3, Stat5b, Prpf4, Prnp, Ggtg1, Dgka, Slc25a36, Chst) between $LysM^{+Cre}Smg1^{fl/fl}$ (Cre) and $Smg1^{fl/fl}$ (WT) BMMs at 6hrs after LPS treatment (Table 5-10).

Figure 5-6: Gene ontology process enrichment analysis by GORILLA after 6h post-LPS treatment. Figure depicts pathways which are enriched for changed gene expression at 2h post-LPS compared to 0h time point by cut-off 0.0001. Colours of the boxes indicate the significance of the enrichment, with the darker the colour indicating greater significance.

Table 5-8: The process enrichment analysis generated by GORILLA at 6 hours after LPS treatment between *LysM^{+Cre}Smg1$^{fl/fl}$* (Cre) and *Smg1$^{fl/fl}$* (WT) mice with -10^{-4} cutoff.

Enriched pathways	P-value	Genes
Serine family amino acid metabolic process	4.59E-4	Psat1,Txnrd1,Srr,Gclc
Negative regulation of mitochondrial membrane permeability involved in apoptotic process	7.71E-4	Bnip3,Acaa2

Table 5-9: The biological process enrichment analysis generated by PANITHER at 6 hours after LPS treatment between *LysM^{+Cre}Smg1$^{fl/fl}$* (Cre) and *Smg1$^{fl/fl}$* (WT) mice with -10^{-4} of cutoff.

Enriched pathways	P-value	Genes
Chromatin organisation	3.31E-02	Suds3, H2afy, Tspyl2, Prmt10, Bahd1, Hist3h2a, Usp22, Wdr75, Cbx4
Organelle organisation	4.10E-02	Stk4, Slamf8, Cd244, Gna15, Ccl12, Wsb2, Nkiras1, Rapgef2, Src, Gab2, Dmpk, Rnd1, Gna13, Nek6, Il23a, Gsg2, Rps6ka2, Nbn, Fgf13, Rrad, Mapk14, Ifnb1, Pi4kb, Stat1, Cdk17, Map2k1, Rasal3, STK4, Rap2c, Sgk1
Nucleobase-containing compound metabolic process	4.64E-02	Tbc1d13, Suds3, Rlf, Tsr1, Tcf4, H2afy, Tspyl2, Mta3, Zfp212, Sbno1, Prmt10, Atad1, Igf2bp3, Rasa2, Phf6, Phf2, Bahd1, Rragc, His3h2a, Zzz3, Rad51, Stat5b, St18, Ampd3, Prpf4, Clock, Pphln1, Wdr75, Cnot7
Primary metabolic process	1.13E-03	Tbc1d13, Suds3, Rlf, Ak4, Tsr1, Prnp, Cdyl, Tcf4, Dtx2, Gclc, Txnrd1, H2afy, Tspl2, B3galnt2, Mta3, Ggta1, Wars, Zfp212, Sbno1, Prmt10, Atad1, Dgka,

			Igf2bp3, Rasa2, Dtx4, Tbcel, Phf6, Slc25a36, Usp53
Metabolic process		1.83E-02	Tbc1d13, Chst14, Suds3, Rif, Ak4, Tsr1, Prnp, Cdyl, Tcf4, Dtx2, Gclc, Txnrd1, H2afy, Tspyl2, B3galnt2, Mta3, Ggta1, Wars, Zfp212, Sbno1, Acaa2, Prmt10, Atad1, Dgka, Igf2bp3, Rasa2, Dtx4, Tbcel, Phf6, Slc25a36

Table 5-10: Confirmed candidate targets gene expression are up- or down- regulated in response to LPS treatment at 6 hours between $LysM^{+Cre}Smg1^{fl/fl}$ (Cre) and $Smg1^{fl/fl}$ (WT) mice.

	Genes		Functions	(up- or down-)	
Diff(6)	Psat1	phosphoserine aminotransferase 1	Serine family amino acid metabolic process		
	Gclc	glutamine-cysteine liganse,catalytic submit	Serine family amino acid metabolic process		
	Prmt10	putative protein arginine N-methyltranferase	Chromatin organization		
	Bahd1	bromo adjacent homology domain-containing 1 protein	Chromatin organization		
	Wdr75	WD repeat-containing protein 75	Chromatin organization		
	Cbx4	E3 sumo-protein ligase CBX4	Chromatin organization		
	Tsr1	pre-mRNA processing protein TSR1 homolog	Nucleobase-containing compound metabolic process		
	Igf2bp3	insulin-like growth factor 2 mRNA binding protein	Nucleobase-containing compound metabolic process		
	Rasa2	ras protein activator like 2	Nucleobase-containing compound metabolic process		
	Stat5b	signal transducer and activator of transcription 5B	Nucleobase-containing compound metabolic process		
	St18	suppression of tumorignicity 18	Nucleobase-containing compound metabolic process		
	Ampd3	AMP deaminase 3	Nucleobase-containing compound metabolic process		
	Prpf4	U4/U6 small nuclear ribonucleoprotein	Nucleobase-containing compound metabolic process		
	Prnp	major prior protein	primary metabolic process		
	B3galnt2	UDP-GaLNA:beta-1,3-N-acetylgalatosaminyltransferase	primary metabolic process		
	Ggtg1	N-acetyllatosaminide alpha-1,3-galacatosyltransferase	primary metabolic process		
	Dgka	diacylglycerol kinase alpha mRNA-binding protein	primary metabolic process		
	Tbce1	tublin-specific chaperone cofactor E-like protein	primary metabolic process		
	Slc25a36	solute carrier family 25 member 36	primary metabolic process		
	Usp53	inactive ubiqutin carboxylterminal hydrolase 53	primary metabolic process		
	Chst	carbohydrate sulfotransferase	metabolic process		

5.3.5 GO terms RNA seq. analysis at 24 hour after LPS treatment

At 24 hours post LPS treatment, our GO analysis showed that negative regulation of multicellular organismal process (Jak2, Ism1, Adam17, Gpr18, Arg1, Col4a2, Cd38, Arg2, Trpm4, Ufd1l, Pde5a, Cx3ce1, Adora2b, Dcn, Il20rb, Inhba, Cd24a, Pilrb1, Met, Ifrd1, IL6) signal transduction and regulation of system process (Jak2, Il13ra1, Bcl2a1, Bcl2a1b, Il1r1, Il1f6, Cd38, Gcnt2, Pde5a, Spata, Il1r12, Dcn, Sla,Il20rb, Gpr141, Niacr1, Notch4, Pilrb2, Clec4d, Pilrb1, Pde10a, Gpr18, Trpm4, Cx4cr1, Il1f9, Olfr99, Adora2b, Ift57, Ccr7, Gipr, Inhba, Afp, Inpp5b, Met, Sema3c, IL6), cellular modified amino acid metabolic process (ERO1l, Aldh1l1, P4hb, Egln3, Gch1, Plod2, Ggh, Gstt4, Gstt2, Mthfs), negative regulation of collateral spouting (Fgf13, Ulk1, Spg20), regulation of immune system process and lymphocyte proliferation (Ccr7, Jak3, Il20rb, Ticam1, Arg1, Cd38, Arg2, Pde5a, Bmi1, Samsn1, Clec4d, Pspc1) were enriched pathways in *LysM$^{+/Cre}$Smg1$^{fl/fl}$;Smg1$^{fl/fl}$* BMMs identified by GORILLA analysis (p<0.0001) (Supplementary Figure 3 and Table 5-11). The functionally enriched pathways identified genes involved in transmembrane transporter activity and signalling receptor activity (Slc29a3, Slc35b1, Bcl2a1d, Surf1, Aqp9, Bcl2a1b, Slc6a12, Slc1a2, Kcna3, Abcc4, Slc7a2, Tmem38b, Prelid2, Ccr7, Il13ra1, Gpr18, Cd302, Il20rb, Il1r1, Gpr141, Niacr1, Cx3cr1, Il1r12, Olfr99, Adora2b, Met) and intramolecular oxidoredutase activity (Ddt, Pdia6, Ecil, P4hb, Ecil, Qsox1) were upregulated in Smg1 deficient BMMs compared to control (Figure 5-7 and Table 5-12). Additionally, PANTHER analysis (p<0.0001) revealed gene clusters involved in pteridine-containing compound metabolic process (Ggh, Mthfd1, Mthfs, Gch1) and metabolic process (Rbpms, Alg8, Acpp, Zfp819, Srsf10, Inhba, Plod2, Rhot1, Spsb1, Denr, Magohb, Ttc19, Rhoq, Rab32, Cnot7, Pdk1, Naa16, Dgat2, Myst2, Frd1, Smurf2, Dna2, Rasa2, Bdp1, Acsbg1, Lox, Mtmr7, Pign, Pola2,

Tra2a) were upregulated in Smg1 deficient BMMs as compared to control. On the top of that, genes involved in the RNA splicing (Rbpms, Gm12355, Magohb, Tra2a) were upregulated at 24 hours post LPS treatment in Smg1 deficient BMMs (Table 5-13). We further analysed the single gene profile of each candidate geneconfirming 10 up-regulated genes (Afp, Ticam1, Mavs, Gstt2, Gstt3, Egln3, IL-6, Fanca, Ulk1, Gpr18) and 8 down-regulated genes (F11r, Srgap2, Mfge8, Syngr1, Tle6, Aldh1l1, Plod2, Dock5) that were significantly altered in BMMs 24hrs post LPS treatment (Table 5-14).

Table 5-11: The top ten of process enrichment analysis generated by GORILLA at 24 hours after LPS treatment between $LysM^{+Cre}Smg1^{fl/fl}$ (Cre) and $Smg1^{fl/fl}$ (WT) mice with -10^{-4} cutoff

Enrichment pathways	P-value	Genes
Negative regulation of multicellular organismal process	6.34E-7	Jak2, Ism1, Jak3, Srgap2, Aatk, Adam17, Gpr18, Arg1, Col4a2, Ulk1, Cd38, Anpep, Arg2, Prkacb, Trpm4, Ufd1l, Pde5a, Evl, Cx3cr1, Nrp1, Calcr1, Dock5, Adora2b, Pros1, Gpnmb, Cd63, Xdh, Dcn, C1qc, Il20rb, Zfp36, Rab11fip5, Mef2c, Gas6, Inhba, Fgf13, Tgfbr2, Cd24a, Pilrb1, Gnas, Met, Spg20, Ifrd1, IL6, Hdac5
Signal transduction	1.37E-6	Jak2, Nfatc2, Jak3, Srgap2, Aatk, Il13ra1, Bcl2a1d, Eril, Bcl2a1b, Il1r1, Il1f6, Ulk1, Spsb2, Aes, Cd38, Gcnt2, Prkacb, Rftn2, Pde5a, Kras, Fam13b, Spata13, Nrp1, Il1rl2, Calcrl, Dock5, Gpnmb, Ccny, Dcn, Sla, Gng10, Malt1, Il20rb, Lrrc4, Zfp36, Gpr141,

		Niacr1, Pdk2, Pdk1, Gas6, Notch4, Pilrb2, Clec4d, Cd24a, Pilrb1, Pde10a, Gnas, Map2k6, Ptplad1, Mavs, Rhoq, Srgap3, Itga4, Adam17, Gpr18, Ticam1, Arhgef3, Col14a2, Arhgap19, Anpep, Plxnb3, Trpm4, Ralgps4, Baiap2, Arhgef10l, Cx3cr1, Hip1, Il1f9, Olfr99, Adora2b, Ift57, Ccnd1, Jmjd6, Arhgap39, Fbxw4, Ccr7, Thra, Rasa2, Sh3bp1, Unc5b, Mef2c, Srsf3, Tmem231, Gipr, Inhba, Afp, Rhou, Fgf13, Tgfbr2, Inpp5b, Met, Rxra, Sema3c, IL6
Regulation of system process	2.87E-6	Jak2, Thra, Rab11fip5, Mef2c, Niacr1, Cd38, Anpep, Acpp, Arg2, Gas6, Inhba, Trpm4, Pde5a, Gnas, Calcr1, Dock5, Gch1, Adora2b, Sp4, Scn1b, IL6
Cellular modified amino acid metabolic process	3.37E-6	Ethe1, Ero1l, Aldh1l1, P4hb, Mthfd1l, Gstt3, Ahcyl2, Egln3, Gch1, Plod2, Ggh, Gstt4, Mthfs, Gstt2
Regulation of multicellular organismal process	3.77E-6	Jak2, Jak3, Srgap2, Aatk, F11r, Il1r1, Arg1, Il1f6, Ulk1, Cd38, Arg2, Fanca, Gcnt2, Prkacb, Ufd1l, Pde5a, Timp2, Nrp1, Eif4g2, Il1rl2, Calcr1, Tle6, Dock5, Gch1, Gpnmb, Xdh, Cd63, Ppib, Dcn, Malt1, Il20rb, Rab11fip5, Zfp36, Niacr1, Por, Gas6, Notch4, Ddt, Cd24a, Pilrb1, Pdlim7, Gnas, Scn1b, Sp4, Mavs, Ism1, Adam17, Gpr18, Ticam1, Co14a2, Atxn1l, Smurf2, Anpep, Plxnb3, Trpm4,

		Baiap2, Evl, Cx3cr1, Il1f9, Adora2b, Myrf, Pros1, Ccnd1, Bmil, Ccr7, Thra, Sh3bp1, C1qc, Panx1, Mef2c, Acpp, Clec5a, Inhba, Fgf13, Tgfbr2, Met, Spa20, Ifrd1, Rxra, Sema3c, IL6, Hdac5
Cell surface receptor signalling pathway	5.46E-6	Jak2, Jak3, Nfatc2, Il13ra1, Bc12a1d, Bc12a1b, Il1r1, Il1f6, Aes, Cd38, Gcnt2, Rftn2, Kras, Nrp1, Calcr1, Ccny, Dcn, Sla, Malt1, Lrrc4, Pdk1, Pdk2, Gas6, Notch4, Pilrb2, Cd24a, Clec4d, Pilrb1, Rhoq, Adam17, Itga4, Ticam1, Co14a2, Plxnb3, Baiap2, Cx3cr1, Il1f9, Adora2b, Ift57, Ccnd1, Jmjd6, Fbxw4, Sh3bp1, Srsf3, Mef2c, Tmem231, Gipr, Inhba, Tgfbr2, Met, Sema3c, IL6
Negative regulation of collateral spouting	1.42E-5	Fgf13, Ulk1, Spg20, Ifrd1
Regulation of immune system process	1.8E-5	Nfatc2, Jak3, Bcl2a1d, Adam17, Itga4, Gpr18, Ticam1, Smpd13b, Arg1, Il1r1, Atxn1l, Samsn1, Cd38, Fanca, Arg2, H2-Ob, Trpm4, Ufd1l, Rfn2, Pde5a, Il1rl2, Adora2, Bmi1, Gpnmb, Ccr7, H2-Ab1, Slc7a2, Clqc, Malt1, Il20rb, Zfp36, Mef2c, C1qa, Niacr1, C1qb, Gas6, Inhba, Ddt, Tgfbr2, Clec4d, Cd24a, Pilrb1, Gnas, Mavs, Matr3, Cnot7, IL6, Pspc1
Regulation of lymphocyte proliferation	3.47E-5	Ccr7, Jak3, Nfatc2, H2-Ab1,Il20rb,Ticam1,Arg1,Mef2c,Cd38

		,Arg2,Pde5a,Tgfbr2,Cd24a,Bmi1,Gpnmb,IL6
Regulation of mononuclear cell proliferation	4.06E-5	Ccr7, Jak3, Nfatc2, H2-Ab1, Il20rb, Ticam1, Arg1, Mef2c, Cd38, Arg2, Pde5a, Tgfbr2, Cd24a, Bmi1, Gpnmb, IL6
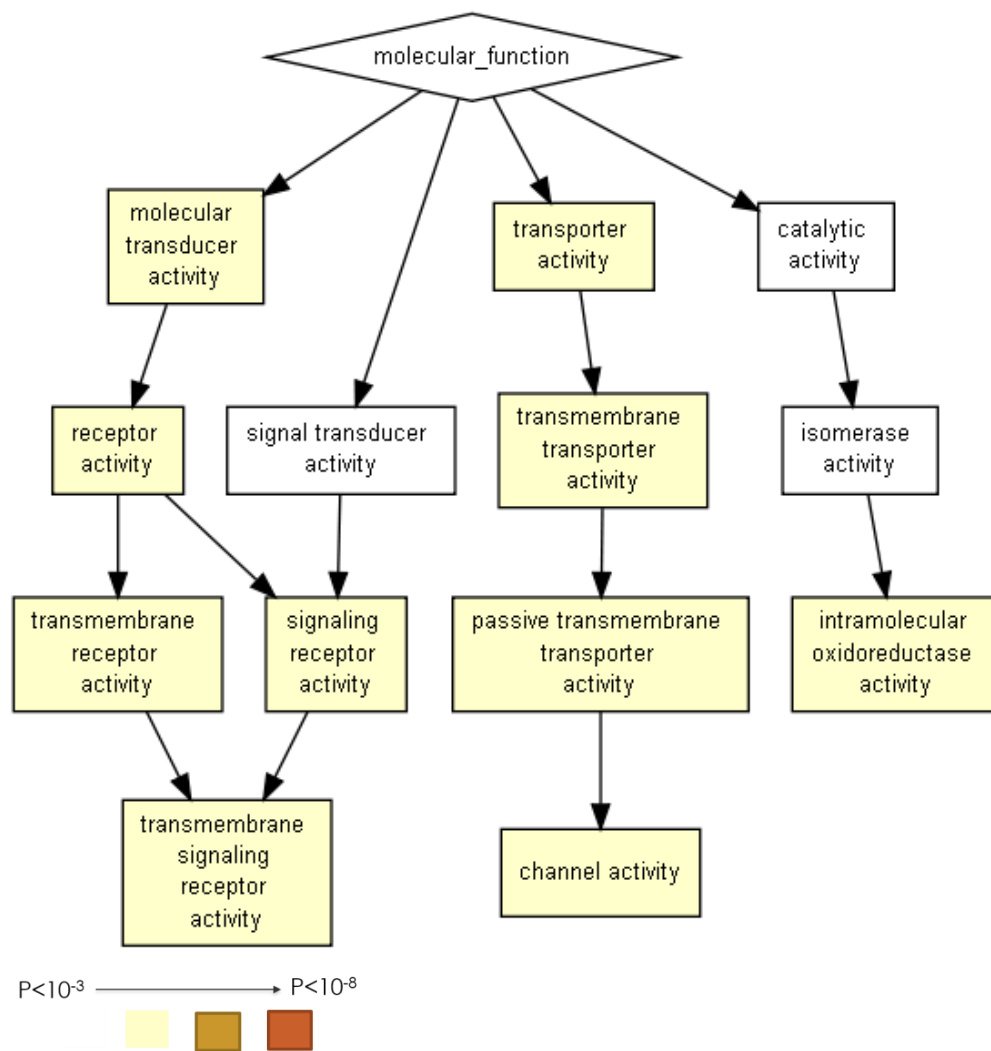
Figure 5-7: Gene ontology functional enrichment analysis using by GORILLA after 24h post-LPS treatment. Figure depicts pathways which are enriched for changed gene expression at 2h post-LPS compared to 0h time point by cut-off 0.0001. Colours of the boxes indicate the significance of the enrichment, with the darker the colour indicating greater significance.

Table 5-12: The functional enrichment analysis generated by GORILLA at 24 hours after LPS treatment between *LysM^{+Cre}Smg1^{fl/fl}* (Cre) and *Smg1^{fl/fl}* (WT) mice with -10^{-4} cutoff.

Enriched pathways	P-value	Genes
Transmembrane transporter activity	2.47E-5	Slc29a3, Slc35b1, Bcl2a1d, Surf1, Aqp9, Bcl2a1b, Slc30a1, Slc6a12, Slc25a45, Slc1a2, Trpm4, Trpm7, Slc44a1, Abcd1, Slc25a51, Kcna3, Kcnk13, Abcc4, Slc45a4, Slc9a9, Slc7a2, Ttyh2, Gas6, Slc30a9, Abcb9, Tmem38b, Slc7a6, Scn1b, Slc25a53, Slc35a3
Transporter activity	8.15E-5	Slc35b1, Slc29a3, Bcl2a1d, Surf1, Aqp9, Bcl2a1b, Slc30a1, Slc6a12, Slc6a1a2, Slc25a45, Trpm4, Trpm7, Ap1b1, Calcr1, Slc44a1, Stard5, Abcb1b, Slc25a51, Kcna3, Kcnk13, Abcc4, Slc45a4, Slc9a9, Slc7a2, Prelid2, Panx1, Ttyh2, Gas6, Atp8b4, Slc30a9, Abcb9, Tmem38b, Slc7a6, Scn1b, Slc25a53, Slc35a3
Transmembrane receptor activity	3.63E-4	Ccr7, Il13ra1, Gpr18, Cd302, Il20rb, Unc5b, Il1r1, Gpr141, Niacr1, Plxnb3, Tgfbr2, Nrp1, Cx3cr1, Calcrl, Il1rl2, Olfr99, Adora2b, Met
Transmembrane signalling receptor activity	3.63E-4	Ccr7, Il13ra1, Gpr18, Cd302, Il20rb, Unc5b, Il11r1, Gpr141, Niacr1, Gipr, Plxnb3, Tgfbr2, Nrp1, Cx3cr1, Calcr1, Il1rl2, Olfr99, Adora2b, Met

Signalling receptor activity	4.21E-4	Ccr7, Thra, Il13ra1, Gpr18, Cd302, Il20rb, Unc5b, Il1r1, Gpr141, Niacr1, Gipr, Plxnb3, Tgfbr2, Nrp1, Calcr1, Il1rl2, Olfr99, Adora2b, Met, Rxra
Positive transmembrane transporter activity	5.6E-4	Ttyh2, Gas6, Trpm4, Trpm7, Bcl2a1d, Aqp9, Bcl2a1b, Tmem38b, Panx1, Scn1b, Kcna3, Kcnk13
Channel activity	5.6E-4	Ttyh2, Gas6, Trpm4, Trpm7, Bcl2a1d, Aqp9, Bcl2a1b, Tmem38b, Panx1, Scn1b, Kcna3, Kcnk13
Molecular transducer activity	8.05E-4	Il13ra1, Cd302, Gpr18, Il1r1, Plxnb3, Prkacb, Nrp1, Cx3cr1, Calcr1, Il1rl2, Olfr99, Adora2b, Ccnd1, Ccr7, Thra, Il20rb, Unc5b, Gpr141, Niacr1, Gipr, Notch4, Tgfbr2, Cd5l, Met, Rxra
Intramolecular oxidoreductase activity	8.46E-4	Ddt, Pdia6, Eci1, P4hb, Ero1l, Qsox1
Receptor activity	9.94E-4	Ccr7, Thra, Il13ra1, Gpr18, Cd302, Il20rb, Unc5b, Il1r1, Gpr141, Niacr1, Gipr, Plxnb3, Notch4, Tgfbr2, Nrp1, Cx3cr1, Cd5l, Calcr1, Il1rl2, Olfr99, Adora2b, Met, Rxra

Table 5-13: The biological process enrichment analysis generated by PANITHER at 24 hours after LPS treatment between $LysM^{+Cre}Smg1^{fl/fl}$ (Cre) and $Smg1^{fl/fl}$ (WT) mice-10^{-4} of cutoff.

Enriched pathways	P-value	Genes
Pteridine-containing compound metabolic process	1.16E-04	Ggh, Mthfd1l, Mthfs, Gch1
Metabolic process	3.61E-04	Rbpms, Nfatc2, Atp8b4, Rxra, Alg8, Gm98, Acpp, Zfp819, Srsf10, Inhba, Naprt1, Arhgap19, Ggh, Plod2, Rhot1, Xdh, Spsb1, Pdk2, Dpp8, Etv3, Abcb9, Denr, Gm12355, Arhgef10l, Magohb, Thra, Rcbtb2, Ttc19, Naa25, Rhoq, Rab32, Sh3bp1, Pspc1, Lipa, Pdk1, Pigf, Slc29a3, Surf1, Dennd4a, Eci1, Plxnb3, Adarb1, Uchl1, Oxct1, Zfp654, Ckb, Gnas, Expi, Mef2c, Zfp36, Arg1, Acsl5, Naa16, Dgat2, Myst2, Hip1, Nudt4, Cnot7, Baiasp2, Zdhc2, Ifrd1, Smurf2, Dna2, Pdk1, Rasa2, Bdp1, Slc35a3, Mettl2, Cct3, Evi5l, Slc1a2, Man1c1, Chst14, Swi5, Ethe1, Timp2, Rhou, Degs2, Pdf, Ahnak2, Spsb2, Tmem208, Abcc4, Arg1, Atp10d, Ahcyl2, Acsbg1, Lox, Ctsa, Mthfd1l, Inpp5b, Srsf3, Dpy19l4, Mtmr7, Cd68, Cyp4v3, Srsf7, Wasl, Sp4, Fbxw4, Pdxk, Thg1l, Cars2, Zfp558, Sephs1, Mthfs, Slc45a4, Hsd3b7, Arg2, Ak4, Gch1, Pign, Pigz, Pola2, Tra2a
Coenzyme metabolic process	2.12E-05	Naprt1, Ggh, Oxct1, Ahcyl2, Mthfd1l, Pdxk, Mthfs, Gch1

RNA splicing	1.04E-03	Rbpms, Srsf10, Gm12355, Magohb, Pspc1, Ahnak2, Srsf3, Srsf7, Tra2a
Primary metabolic process	4.60E-05	Rbpms, Atp8b4, Rxra, Alg8, Gm98, Acpp, Zfp819, Srsf10, Inhba, Naprt1, Ggh, Plod2, Rhot1, Xdh, Spsb1, Pdk2, Dpp8, Abcb9, Denr, Gm12355, Arhgef10l, Magohb, Rcbtb2, Ttc19, Naa25, Rhoq, Rab32, Pspc1, Lipa, Pigf
Cellular amino acid metabolic process	3.16E-04	Ggh, Pdk2, Arg1, Pdk1, Slc1a2, Ethe1, Ahcyl2, Mthfd1l, Cars2, Sephs1, Mthfs, Arg2
Response to stimulus	4.05E-04	Nfatc2, Itgb8, H2-Ob, Inhba, Arhgap19, Rhot1, Clec4d, Thra, Met, Rhoq, Rab32, Pdk1, Bcl2a1b, Il13ra1, Plxnb3, Adarb1, Sla, Gnas, Bcl2a1d, Map2k6, Smurf2, P4hb, Rasa2, H2-Ab1, Olfr99, Swi5, Timp2, Rhou, Cd63, Sema3c
Sensory perception	1.12E-03	Hpcal1, Pde5a, Inpp5b

Table 5-14: Selected candidate targets gene expression are up- or down- regulated in response to LPS treatment at 24 hours between $LysM^{+Cre}Smg1^{fl/fl}$ (Cre) and $Smg1^{fl/fl}$ (WT) mice.

	Genes		Functions	(up- or down-)	
Diff(24)	F11r	f11 receptor	Regulation of multicellular organismal process		■
	Afp	alpha fetoprotein	Signal transduction	■	
	Ticam1	toll-like receptor adaptor molecular 1	Cell surface receptor signaling pathway	■	
	Srgap2	slit-robo rho gtpase activating protein2	Signal transduction		■
	Mfge8	milk fat globule-egf factor 8 protein	Regulation of multicellular organismal process		■
	Syngr1	synaptogyrin1	Regulation of multicellular organismal process		■
	Tle6	transducin-like enhancer of split 6,homolog of drosophila	Regulation of multicellular organismal process		■
	Mavs	mitochondrial antiviral signaling protein	Regulation of immune system process	■	
	Aldh1l1	aldehyde dehydrogenases	Cellular modified amino acid metabolic process		■
	Gstt3	glutathinone s-transferase,theta 3	Cellular modified amino acid metabolic process	■	
	Gstt2	glutathinone s-transferase,theta 2	Cellular modified amino acid metabolic process	■	
	Plod2	procollagen lysine,2-oxoglutarate-5-dioxygenase 2	Cellular modified amino acid metabolic process		■
	Egln3	egl nine homolog 3	Cellular modified amino acid metabolic process	■	
	IL6	interleukin6	Regulation of immune system process	■	
	Fanca	fanconi anemia,complementation group a	Regulation of multicellular organismal process	■	
	Dock5	dedicator of cytokinesis 5	Signal transduction		■
	Ulk1	unc-51 like kinase 1	negative regulation of multicellular organismal process	■	
	Gpr18	g protein-coupled receptor 18	negative regulation of multicellular organismal process	■	

5.3.6 Validation of gene expression changes by quantitative PCR

Next, we attempted validation of our RNA-seq data by quantitative real time PCR (qPCR). (Table 5-15). In summary, gene oncology analysis illustrated that gene clusters altered between genotypes at basal level were GTPase regulation activity and nucleoside-triphosphatase regulator activity, defense response, at 2hr post-LPS - response to interferon-beta and at 6 hour post-LPS treatment- immune and defense response. Therefore we selected candidates which could be divided into three groups where gene function is related to immune and defense responses (Figure 5-8), GTPase regulator activity (Figure 5-9) and others (Figure 5-10). Also we made a conclusion figure to summarise the outcome of validation experiments for the selected genes (Table 5-16).

Table 5-15: Selected targets from dataset analysis and related information

Gene	Enriched pathways	Functions	
Cx3cr1	*G protein-coupled receptor activity* and *chemokine receptor activity*	- Receptor for the CX3C chemokine fractalkine (CX3CL1) -Binds to CX3CL1 and mediates both its adhesive and migratory functions. -Acts as coreceptor with CD4 for HIV-1 virus envelope protein (in vitro).	[368]
IL11ra1	*Obsolete signal transducer activity* and *cytokine receptor activity*	-Receptor for interleukin-11. -Utilises IL6ST for initiating signal transmission. -May be involved in the control of proliferation and/or differentiation of skeletogenic progenitor or other mesenchymal cells. -Essential for the normal development of craniofacial bones and teeth.	[369]
IL6	*Signalling receptor binding* and *growth factor activity*	-Involves in the regulation of immune response,hematopoiesis,platelet production,acute phase reaction and bone resorption (susceptibility factor for osteopenia) -Plays a role in the aggressiveness of non hodgkin lymphoma by stimulating MMP2 and MMP9	[370]
IRF8	*DNA-binding transcription factor activity*	-Specifically binds to the upstream regulatory region of type I IFN and IFN-inducible MHC class I genes (the interferon consensus sequence (ICS)). -Plays a negative regulatory role in cells of the immune system. -Involves in CD8(+) dendritic cell differentiation by forming a complex with the BATF-JUNB heterodimer in immune cells, leading to recognition of AICE sequence (5'-TGAnTCA/GAAA-3'), an immune-specific regulatory element, followed by cooperative binding of BATF and IRF8 and activation of genes (By similarity).	[371]

		-Positively regulates macroautophagy in dendritic cells	
Cd244	*Innate lymphoid cell differentiation pathways*	-Heterophilic receptor of the signalling lymphocytic activation molecule (SLAM) family; its ligand is CD48. -Involves in the regulation and interconnection of both innate and adaptive immune response. -Acts as activating natural killer (NK) cell receptor. -Activating function implicates association with SH2D1A and FYN. -Downstreaming signalling involves predominantly VAV1, and, to a lesser degree, INPP5D/SHIP1 and CBL. -Stimulates NK cell cytotoxicity, production of IFN-gamma and granule exocytosis. -Acts as costimulator in NK activation by enhancing signals by other NK receptors such as NCR3 and NCR1. -Involves in the regulation of CD8 (+) T-cell proliferation. -Inhibits inflammatory responses in dendritic cells (DCs).	[372]
Slamf8	*Leukocyte chemotaxis involved in inflammatory response*	-A member of the CD2 family of cell surface proteins involved in lymphocyte activation. -May play a role in B-lineage commitment and/or modulation of signalling through the B-cell receptor.	[373]
Itgax	*Defense response*	-A receptor for fibrinogen. -Recognises the sequence G-P-R in fibrinogen. -Mediates cell-cell interaction during inflammatory responses. -Plays an important role of monocyte adhesion and chemotaxis.	[374]

Usp6nl	*GTPase activator activity* and *Rab GTPase binding*	-Acts as a GTPase-activating protein for RAB5A and RAB43. -Involves in receptor trafficking. -In complex with EPS8 inhibits internalisation of EGFR. -Involved in retrograde transport from the endocytic pathway to the Golgi apparatus. -Involved in the transport of Shiga toxin from early and recycling endosomes to the trans-Golgi network. -Required for structural integrity of the Golgi complex.	[375]
Tubb2b	*GTP binding* and *structural constituent of cytoskeleton*	-Major constituent of microtubules. -Binds two moles of GTP, one at an exchangeable site on the beta chain and one at a non-exchangeable site on the alpha chain. -Plays a critical role in proper axon guidance in both central and peripheral axon tracts. -Implicates in neuronal migration	[376]
Srgap2	*Protein homodimerisation activity* and *Rac GTPase binding*	-Binds and deforms membranes, and regulates actin dynamics to regulate cell migration and differentiation. -Plays an important role in different aspects of neuronal morphogenesis and migration mainly during development of the cerebral cortex.	[377]
Arhgap25	*GTPase activator activity*	-Involves in actin remodelling, cell polarity, and cell migration	[378]
Gna15	*GTP binding* and *obsolete signal transducer activity*	-Heterotrimeric G proteins are membrane bound GTPases that are linked to 7-TM receptors. -Each G protein contains an alpha-, beta- and gamma-subunit and is bound to GDP in the 'off' state. -Ligand binding causes a receptor conformational change, detaching the G protein and switching it 'on'.	[379]

F3	*Phospholipid binding* and *cytokine receptor activity*	-encodes coagulation factor III which is a cell surface glycoprotein. -This factor enables cells to initiate the blood coagulation cascades, and it functions as the high-affinity receptor for the coagulation factor VII.	[380]
F11r	*PDZ domain binding*	-Plays a role in epithelial tight junction formation. -Plays a role in regulating monocyte transmigration involved in integrity of epithelial barrier. -Ligand for integrin alpha-L/beta-2 involved in memory T-cell and neutrophil transmigration. -Involves in platelet activation	[381]
Ulk1	*Transferase activity, transferring phosphorus-containing groups* and *protein tyrosine kinase activity*	-Involves in autophagy in response to starvation. -Acts upstream of phosphatidylinositol 3-kinase PIK3C3 to regulate the formation of autophagophores, the precursors of autophagosomes. -Part of regulatory feedback loops in autophagy. -Acts both as a downstream effector and negative regulator of mammalian target of rapamycin complex 1 (mTORC1) via interaction with RPTOR. -Activated via phosphorylation by AMPK, leading to negatively regulate AMPK activity.	[382]
Ttyh2	*Chloride channel activity*	-Probable large-conductance Ca^{2+}-activated chloride channel. -May play a role in Ca^{2+} signal transduction. -May be involved in cell proliferation and cell aggregation.	[383]
Bahd1	*Chromatin binding* and *transcription regulatory region sequence-specific DNA binding*	-Acts as a transcription repressor and has the ability to promote the formation of large heterochromatic domains. -May act by recruiting heterochromatin proteins such as CBX5 (HP1 alpha), HDAC5 and MBD1.	[384]

		-Represses IGF2 expression by binding to its CpG-rich P3 promoter and recruiting heterochromatin proteins.	
Furin	*Serine-type endopeptidase activity* and *serine-type endopeptidase inhibitor activity*	-Ubiquitous endoprotease within constitutive secretory pathways capable of cleavage at the RX (K/R)R consensus motif. -Mediates processing of TGFB1, an essential step in TGF-beta-1 activation.	[385]

5.3.6.1 Validation of Genes which are enriched pathways in the regulating in immune and defence responses when loss of Smg1 during an LPS treatment.

Previously, increased basal cytokine levels (IL6, CSF1, IL-1β), oxidative damage to tissues and chronic inflammation were observed in Smg1 heterozygous mice possibly due to the dysregulation of immune responses and stress signalling [5]. Therefore, we chose Cx3cr1, IL11ra1, IRF8, CD244 and Slamf8 that are involved in the regulation of immune responses and cytokine production for validation.

RNA seq. data showed Cx3cr1 gene expression is higher in KO BMMs, but down-regulated during LPS treatment. As compared to qPCR, our results found that a higher Cx3cr1 mRNA expression can be observed in KO BMMs mice as compared to WT BMMs during an LPS treatment. For IL11RA1, gene expression was expected to be lower in KO BMMs, and overall trend being down-regulation during LPS treatment. As validated by qPCR, IL11ra1 mRNA expression is down-regulated in KO BMMs as compare with control group during LPS treatment. Regarding to CD244, gene expression is higher in KO BMMs and overall trend in response to LPS treatment is down-regulated. As compared to qPCR, validated at baseline, but did not show at 2 and 6- post LPS. Validation results showed that initially CD244 mRNA expression is higher basal expression in BMMs from *LysM*$^{+Cre}$*Smg1*$^{fl/fl}$ (Cre) mice as compared to control group,

and the expression pattern is different to *Smg1^{fl/fl}* (WT) mice, which means that there is an imbalance regulation of CD244 between *LysM^{+Cre}Smg1^{fl/fl}* (Cre) and *Smg1^{fl/fl}* (WT) mice. In contrast, IRF8, and Slamf8 did not show significant regulation in validation samples from RNA seq. data and validation data.
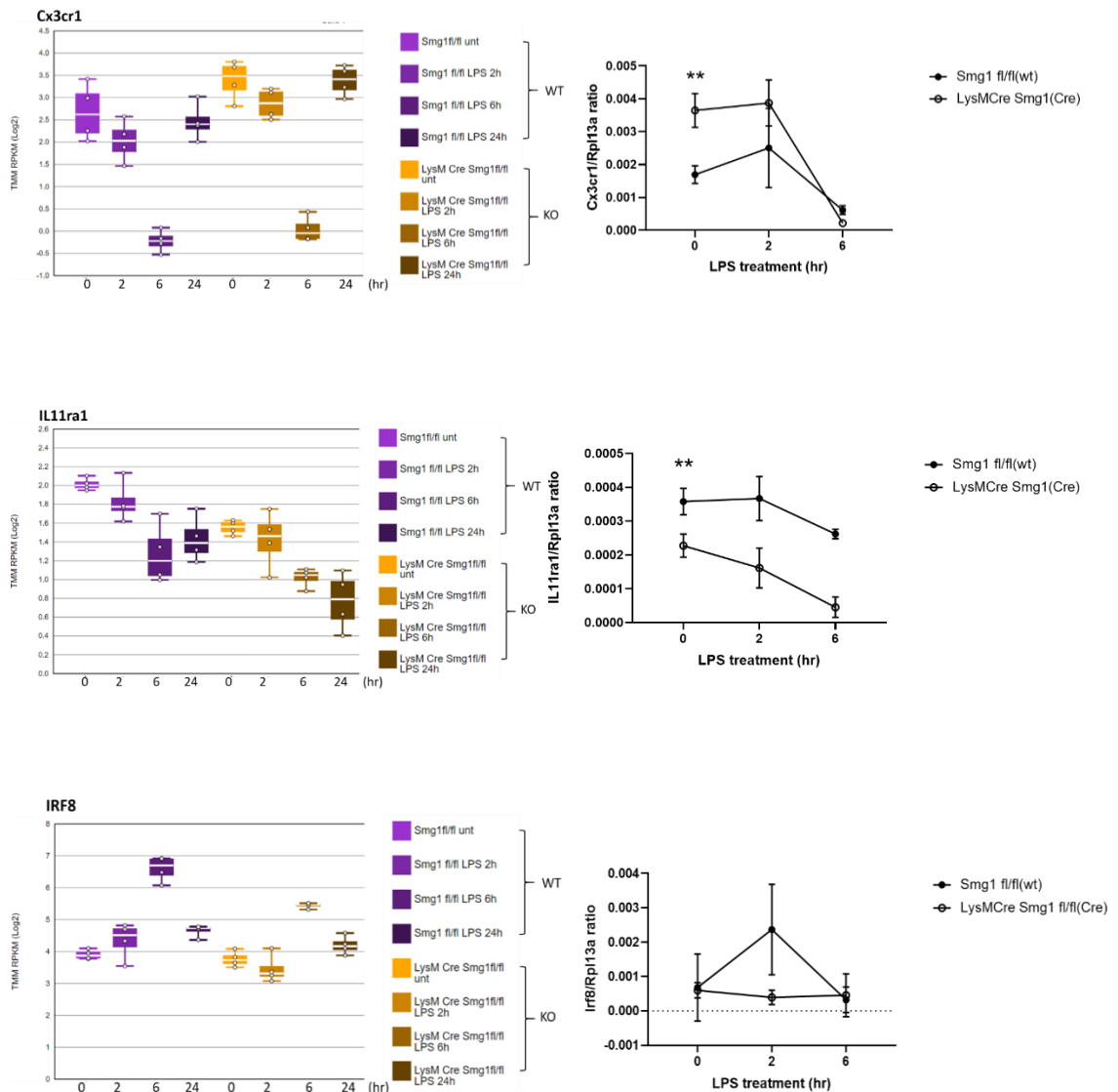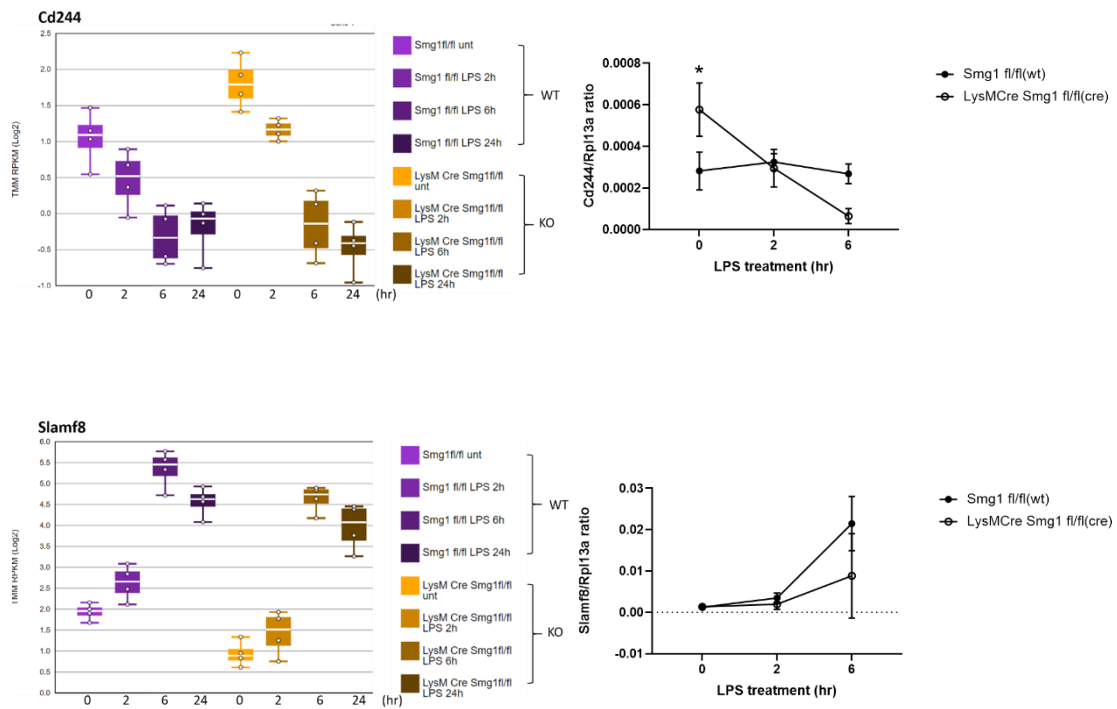
Figure 5-8: Single gene profiles (left hand side) and qPCR results (right hand side) of selected gene in the regulation of expected defence and immune responses in response to LPS between *LysM*^{+Cre}*Smg1*^{fl/fl} (Cre) and *Smg1*^{fl/fl} (WT) BMMs. Single gene profiles were generated with the stemformatics platform for genes to be validated. Each graph shows the level of gene expression in a log scale on the y-axis the timecourse of LPS treatment at 0, 2 and 6 hours across the x-axis. For each data group the white line shows the average expression, the white dots the individual data points for each replicate sample and the error bars the full range of the independent samples. The expression pattern of a subset of genes was validated by quantitative PCR. The level of each gene was compared to the control gene (rpl13a) in 2-4 samples from mice at 0, 2, 6 hours after LPS treatment. Bars indicate the mean and error bars the standard error of the mean. *$p<0.05$, **$p<0.01$, ***$p<0.001$.

5.3.6.2 Validation of Genes which are enriched pathways as GTPase regulators when loss of Smg1 during an LPS treatment.

Secondly, a subset of genes with regulated GTP activity included Usp6nl, Arhgap25, Tubb2b, Srgap2, Gna15 were selected for the following validation. Briefly, the qPCR results did not validate a change in expression for any of the genes examined (Figure 5-9).
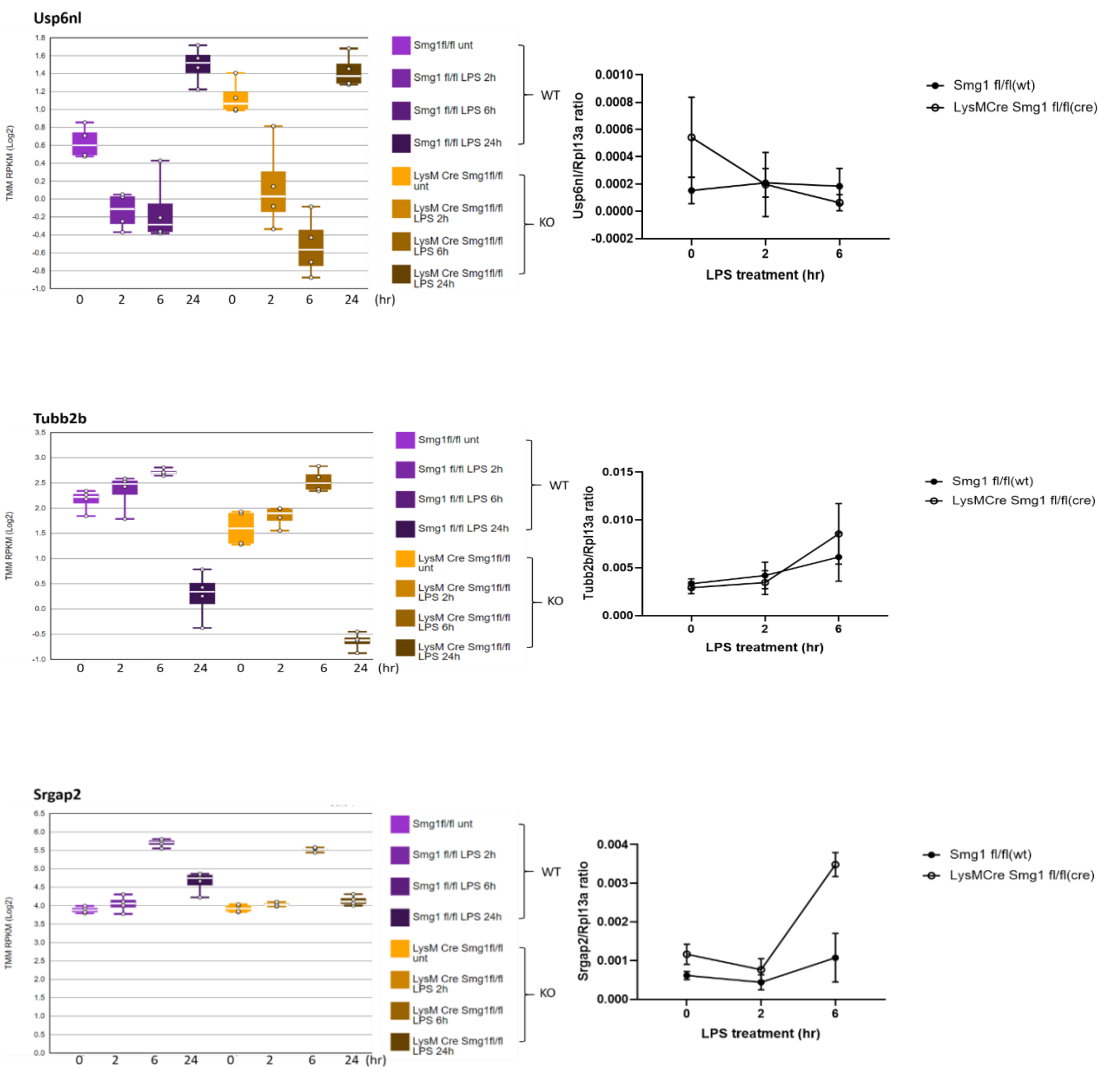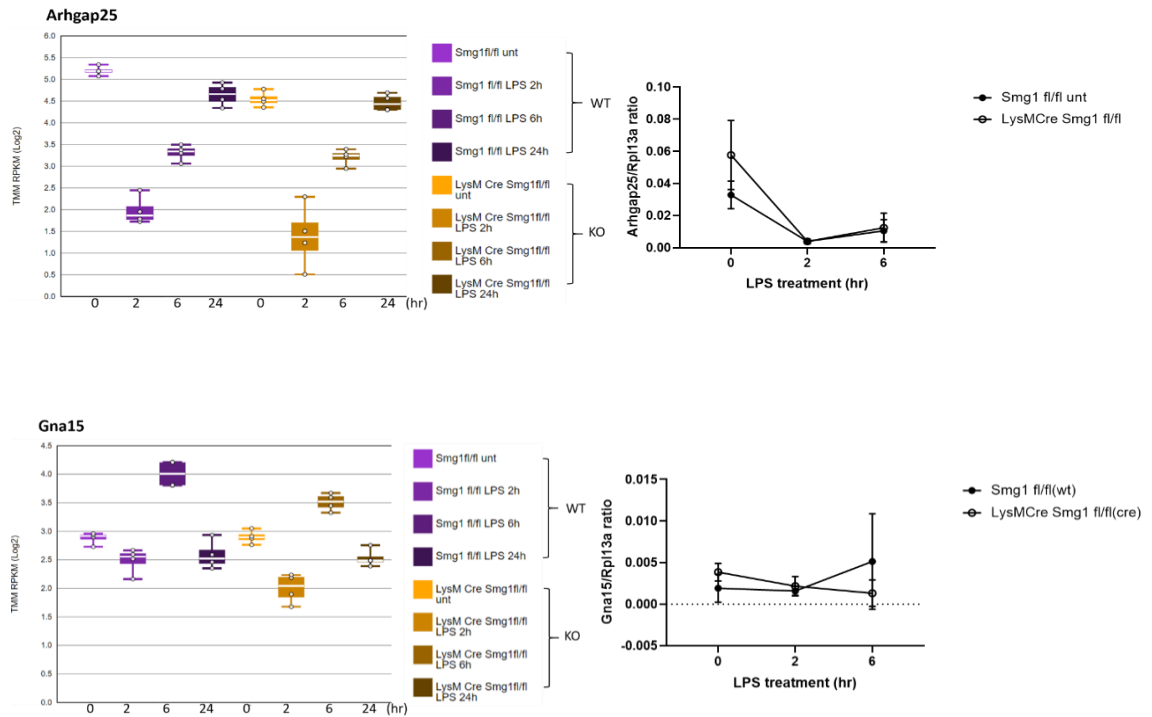
Figure 5-9: Single gene profiles (left hand side) and qPCR results (right hand side) of selected gene in the regulation of GTPase regulation activity in response to LPS between $LysM^{+Cre}Smg1^{fl/fl}$ (Cre) and $Smg1^{fl/fl}$ (WT) BMMs. Single gene profiles were generated with the stemformatics platform for genes to be validated. Each graph shows the level of gene expression in a log scale on the y-axis the timecourse of LPS treatment at 0, 2 and 6 hours across the x-axis. For each data group the white line shows the average expression, the white dots the individual data points for each replicate sample and the error bars the full range of the independent samples. The expression pattern of a subset of genes was validated by quantitative PCR. The level of each gene was compared to the control gene (rpl13a) in 2-4 samples from independent mice at 0, 2, 6 hours after LPS treatment.

5.3.6.3 Validation of Other Genes which are enriched with loss of Smg1 during an LPS treatment

Last group of targets, we selected Furin, Bahd1, Ulk1, Ttyh2 and F11r. Of these only furin expression validated, this is unsurprising as discussed above Furin is a known NMD

target. Furin, is the pro-protein convertase enzyme, which knocked out of the function only in macrophages showed an elevated IL-1β levels and reduced numbers of splenocytes [385].
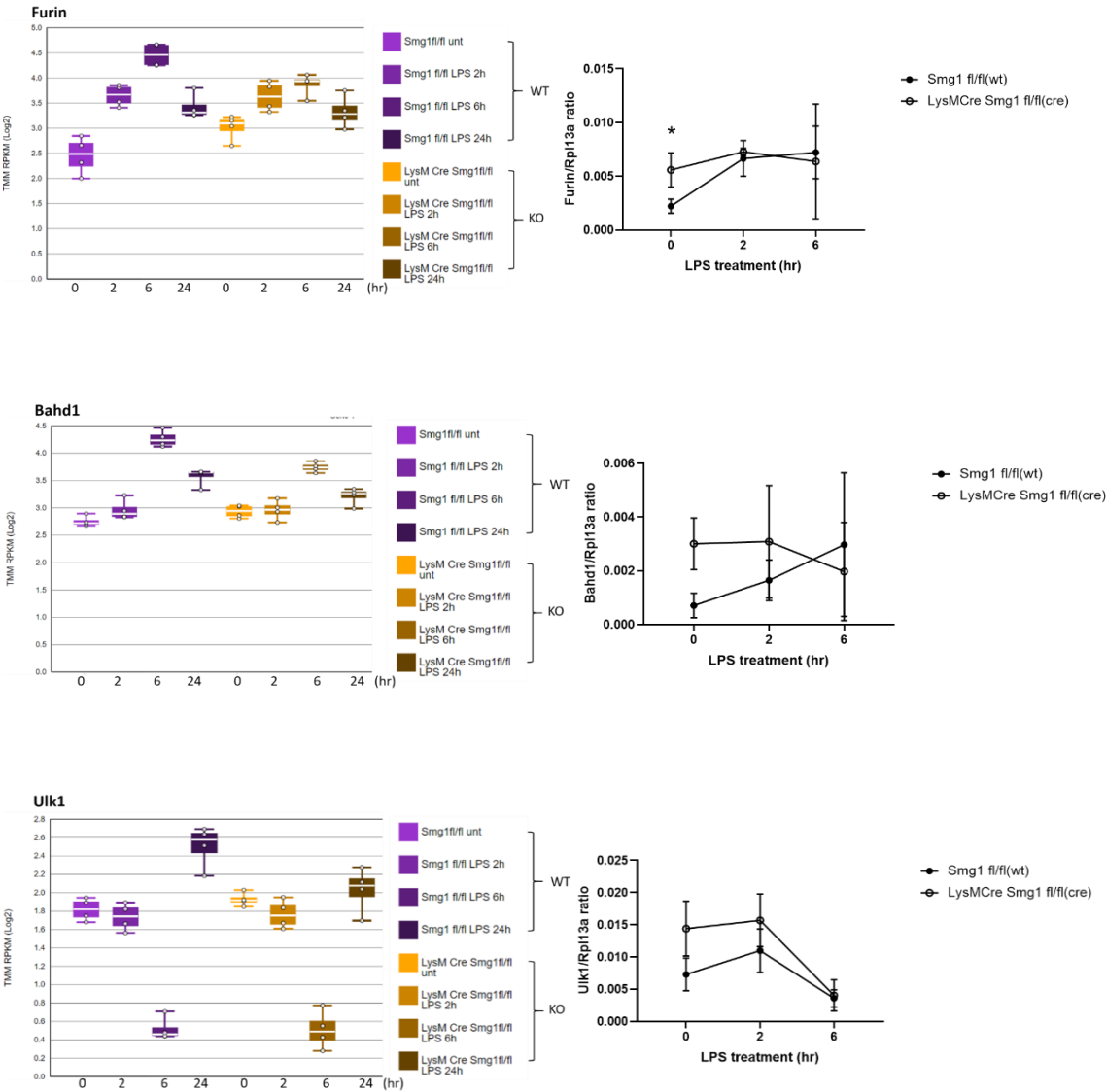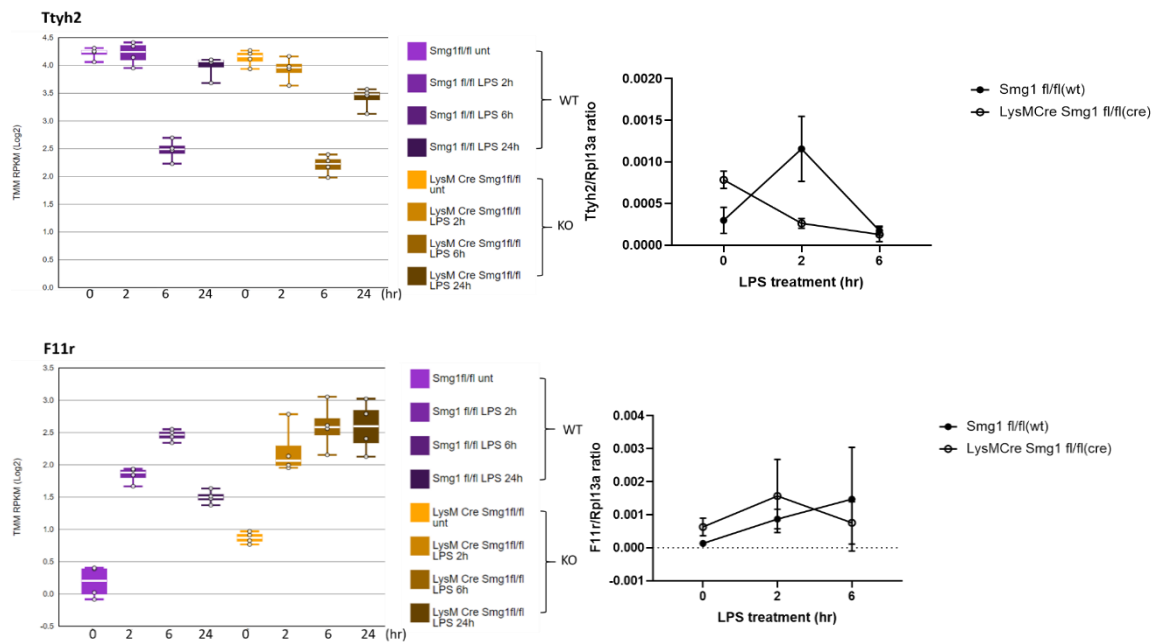
Figure 5-10: Single gene profiles (left hand side) and qPCR results (right hand side) of selected gene in the regulation of cell-cell interaction and adhesion, monocyte transmigration, Ca^{2+} signal transduction, and to autophagy in response to LPS between $LysM^{+Cre}Smg1^{fl/fl}$ (Cre) and $Smg1^{fl/fl}$ (WT) BMMs. Single gene profiles were generated with the stemformatics platform for genes to be validated. Each graph shows the level of gene expression in a log scale on the y-axis the timecourse of LPS treatment at 0, 2 and 6 hours across the x-axis. For each data group the white line shows the average expression, the white dots the individual data points for each replicate sample and the error bars the full range of the independent samples. The expression pattern of a subset of genes was validated by quantitative PCR. The level of each gene was compared to the control gene (rpl13a) in 2-4 samples from independent mice at 0, 2, 6 hours after LPS treatment. Bars indicate the mean and error bars the standard error of the mean. *$p<0.05$, **$p<0.01$, ***$p<0.001$.

Table 5-16: Summary the validation outcomes of selected genes

Gene	Expected	Did or did not validate
Cx3cr1	Gene expression is expected to be higher in KO BMMs, but overall trend is down-regulated during an LPS treatment.	v
IL11ra1	Gene expression is expected to be lower in KO BMMs, and overall trend is down-regulated during an LPS treatment.	v
IRF8	Gene expression is expected to be lower in KO BMMs, and overall trend is up-regulated during an LPS treatment.	x
Cd244	Gene expression is expected to be higher in KO BMMs, and overall trend is down-regulated during an LPS treatment.	X(2,6h) v(0h)
Slamf8	Gene expression is expected to be lower in KO BMMs, and overall trend is up-regulated during an LPS treatment.	x
Usp6nl	Gene expression is expected to be higher in KO BMMs, and overall trend is down-regulated during an LPS treatment.	x
Tubb2b	Gene expression is expected to be lower in KO BMMs, and overall trend is up-regulated during an LPS treatment.	x
Srgap2	Gene expression is expected to be lower in KO BMMs, and overall trend is up-regulated during an LPS treatment.	x
Arhgap25	Gene expression is expected to be lower in KO BMMs, and overall trend is up-regulated during an LPS treatment.	x
Gna15	Gene expression is expected to be lower in KO BMMs, and overall trend is up-regulated during an LPS treatment.	x
F11r	Gene expression is expected to be higher in KO BMMs, and overall trend is up-regulated during an LPS treatment.	x
Ulk1	Gene expression is expected to be higher in KO BMMs, and overall trend is down-regulated during an LPS treatment.	x
Ttyh2	Gene expression is expected to be lower in KO BMMs, and overall trend is down-regulated during an LPS treatment.	x
Bahd1	Gene expression is expected to be higher in KO BMMs, and overall trend is up-regulated during an LPS treatment.	x
Furin	Gene expression is expected to be lower in KO BMMs, and overall trend is up-regulated during an LPS treatment.	v

5.4 Discussion

In summary, the bulk of the genes that appeared different between Smg1 deficient and wildtype BMM did not validate and we decided not to do further studies are related to those genes or this set of data generally. As described in chapter 4, after shifting our Smg1 deficient mice from QMIR to Ingham Institute, we found that while initial data were comparable with previous results over time the phenotype of the mice changed with a decreased impact of SMG1 loss and sex-specific differences. The samples for analysis by RNA sequencing were generated from mice bred in the 3-6 months after the mice were established at the Ingham Institute, with hindsight we realise that at this point it is unlikely the mice showed the phenotype of either the QIMR colony or the Ingham colony as described in chapter 4. Therefore this transitional phenotype at the timepoint examined may explain why much of the RNA sequencing findings did not validate via qPCR on independent samples.

However, a small number of genes did validate as different between SMG1 deficient and wildtype BMM, including targets of NMD (ie, Furin) and particularly those that differed at baseline (ie. Cx3cr1, IL11RA1, CD244). Furin is a modulator of the T-cell dependent adaptive immunity. Furin is up-regulated upon cellular activation via IL-12/STAT4 pathway in T helper type I cells [386, 387] and Th1/Th2 balance. Loss of Furin function in T cells showed aberrant polarisation of T helper cells due to insufficient protective cell-mediated host-defence. This led to the spontaneous development of autoimmunity in old mice [388, 389]. Loss of Furin function in myeloid cells in vivo results in a reduced number of splenocytes and increased IL-1β production. After LPS treatment, results showed increased serum pro-inflammatory cytokine production and accelerated mortality in macrophages [385]. This study concluded that Furin attenuates inflammation. As Furin

is a target of NMD it is unsurprising that it is upregulated upon loss of SMG1. As noted above we found several genes predicted to be NMD targets (Ugt1a10, IBTK, Furin, Fgd2, Wbscr6, CD34, Itga8, Eif4a2, Gtf2a2) upregulated at baseline. These data supports that NMD is decreased in Smg1 KO cells.

Cx3cr1 is a chemokine receptor that is present on most early myeloid lineage cell [390, 391] and has been identified as a key regulator of macrophage function at sites of inflammation [392, 393]. Cx3cr1 and its receptor which is named Fractalkine, plays an important role in osteoclast maturation and Cx3cr1 knockout mice showed a slight increase in trabecular and cortical bone thickness by increasing osteoid formation rate [394]. Fractalkine/ Cx3cr1 can induce adhesion and migration of leukocytes [395]. IL11ra1, a member cytokine in the IL-6 family, and can exhibit pleotropic functions such as bone development, tissue repair, tumour regulation and haematopoiesis [396, 397]. CD244 (SLAMF44 or 2B4), is natural killer cell receptor of SLAMF family, has been documented to participated in the modulating of myeloid cell and lymphocyte development, and T and B cell responses to microbes and parasites [373].

5.5 Conclusion

For this Chapter, we showed how to analyse RNA-seq. data of BMM from $LysM^{+/Cre}Smg1^{fl/fl}$ and $Smg1^{fl/fl}$ mice (wild-type) treated with LPS treatment at dedicated time points by gene ontology tools to find out gene enriched clusters during an LPS treatment between SMG1 deficient and wildtype BMM. However, $LysM^{+/Cre}Smg1^{fl/fl}$ mice had an altered phenotype in different housing and environment after shift from QIMR to Ingham Institute. Therefore, we could not repeat the data same as from QIMR after we validated targets which are regulating of innate immunity and GTPase activity.

In summary, a few of genes did validate as different between SMG1 deficient and wildtype BMM, including targets of NMD (ie, Furin) and particularly those that differed at baseline (ie. Cx3cr1, IL11RA1, CD244).

These findings support that loss of Smg1 regulates innate immunity. In the future, we may examine Cx3cr1 and IL11RA1 function in SMG1 KO macrophages and investigate the related pathways which may be involved and further modulate down-stream signalling pathways.

Chapter 6- Final discussion

While the effect of LPS on the immune system and toll-like receptor activation has been studied for over 20 years mechanisms involved in moderation of inflammatory responses are still relatively poorly understood compared to mechanisms activating inflammation. For my thesis, we have addressed post-transcriptional gene expression regulation in response to LPS, below are a summary of key findings of the thesis.

1. Multiple components of different RNA decay pathways are regulated in response to LPS treatment.

2. Co-ordinated intron retention and the use of detained introns is an additional level of regulation of LPS responses.

3. Loss of SMG1 altered LPS responses in a sex-specific manner.

4. Mouse housing has a significant impact on the phenotype of SMG1 deficient mice.

The final discussion reviews the broad findings and discusses major challenges remaining in this field and approaches to further investigation.

6.1 The role of RBPs proteins in the regulating of gene expression beyond their specific target mRNA

Messenger RNAs (mRNAs) are produced in the nucleus of a cell and then exported into cytoplasm to produce proteins. Once this process has finished, the template is destroyed. The rate at which the messenger RNA is made depends on the balance between its production (transcription) and its degradation (mRNA decay). Recent studies have shown

that the rate at which each mRNA is degraded is specific for every gene, but little is known about how this is regulated including in inflammation. In our work as described in chapter 2, a number of key regulators of RNA decay pathways were identified as regulated at their gene expression and protein level in macrophages during LPS treatment. RNA decay pathways include nonsense-mediated decay, the RNA decay exosome, P-body localised deadenylation, decapping and degradation, and AU-rich element targeted decay mediated by tristetraprolin. Our results showed that a set of RNA binding proteins (RBPs) that participate in RNA decay pathways including nonsense-mediated decay, the RNA decay exosome, P-body localised deadenylation, decapping and degradation, and AU-rich element targeted decay mediated by tristetraprolin (TTP), are co-ordinately regulated in response to inflammatory stimuli.

There are interesting implications that RNA decay rates may alter more than just the mRNA specifically being degraded at that point in time. Recent evidence suggests that the speed at which mRNA is destroyed in the cytoplasm can influence how much of it is made in the nucleus, i.e., different kinds of virus infections can affect the rate at which RNAs are destroyed, and further stop protein production. For example, many viruses including alpha and gamma herpesviruses, influenza A virus, and SARS coronavirus could accelerate host mRNA degradation through the use of viral proteins that trigger endonucleolytic cleavage of mRNAs in the cytoplasm speeding up the destruction of messenger RNA to gain control over the host cell [398]. Messenger RNAs are coated with proteins, which are released when the RNA is destroyed. Gilbertson et al.[399] found that many RNA-binding proteins indeed return to the nucleus when RNA is destroyed. However, the mechanism is still unknown. This new link between messenger RNA destruction and production may provide new light on how cells use different signals to

control the production of their own genes while restricting pathogens from taking over. The implication of our findings in regard to broader transcriptional regulation would be a significant new area of study.

While mRNA decay is often considered the terminal stage of gene expression, the different steps of mRNA decay (deadenylation, decapping, and exonuclease degradation) take place with transcript-specific rates, and thus contribute to determining the overall decay rate. As noted above this work demonstrated significant regulation of RBPs. An attractive hypothesis is that one or more RNA binding proteins (RBPs) could differentially regulate each step of mRNA decay and traffick between the cytoplasm and the nucleus. These findings can provide a new sight that RBPs proteins may play a key role in transmitting the signal between the cytoplasm and the nucleus to control the production messenger RNA.

6.2 How is m6A RNA modification regulated in macrophages after LPS treatment?

The m6A process is a key regulator of RNA modification due to mediation of mRNA turnover and translation. The m6A RNA modification is deposited by the METTL3/14 complex in the nucleus. This modification may be erased by demethylases FTO and ALKBH5. Subsequently, m6A-containing mRNAs are recognised by YTHDF1-3, thereby controlling their translation and decay. These modifications have been reported to regulate RNA transcript processing, and inflammatory, antitumour immune responses and antiviral immunity [400].

As discussed in Chapter 2, we identified key regulators of RNA decay pathways in

macrophages during LPS treatment. However, the role of m6A methylation in regulating mRNA fate and function of innate and adaptive immunity and their impact on inflammatory responses is poorly understood. Therefore, we could investigate the members of m6A modification regulators to be regulated in activation of TLR4 signalling. We could use molecular and cellular biology approaches to knockdown or mutant single m6A regulator in macrophages and identify cluster genes that display change the level of gene expression during an LPS treatments by transcriptome. We could also examine the mRNA expression and protein level of each m6A regulators in bone marrow derived macrophages in response to LPS treatment. Also, RNA m6A methylation has been reparted as a regulator to participate in cancer growth and metastasis in macrophges. Therefore, we could also generate animal model to address the role of m6A modification in the regulating in response to LPS treatment. Then we could extend understanding how is gene expression regulated by m6A modification during inflammation.

Generally, the role of RNA modifications such as m6A are poorly udnerstood. Cataloguing the range of modifications that occur and determining the roles they play in regulating RNA metabolism is a major challenge for the field of RNA biology in years to come.

6.3 The phosphorylation of splicing factors related to IR in the LPS response

Intron retention (IR) is a new insight into post-transcriptional gene regulation in vertebrates. It has been challenging to detect IR events that are targeted to NMD as this leads to rapid degradation of the transcripts with introns. IR regulation during inflammation had not been previously examined, which we addressed in chapter 3. Genes

identified as having significantly increased intron retention were enriched for interferon inducible genes and those involved in pattern recognition receptor pathways for example caspase-1 and IRF8. We validated intron retention in a subset of these genes by quantitative PCR. These experiments confirmed that introns being retained included those that were not incorporated into known protein isoforms suggesting that they are playing a regulatory role in this context.

To date, our knowledge of regulation of alternative splicing including intron retention indicates it is largely controlled by components of the spliceosome, associated RNA binding proteins and the kinases and phosphatases that modulate their activity [409]. Splicing can either occur concurrently with transcription or post-transcriptionally. The serine-arginine rich splicing factors (SRSF) are RNA binding proteins important in splicing regulation and their phosphorylation state alters splicing efficiency. They have also been implicated in regulating intron retention [281]. The phosphorylation state of SRSF proteins is balanced by the action of kinases and phosphatases. Kinases which phosphorylate SRSF proteins predominantly come from 3 families (SR, CLK, DYRK families) and dephosphorylation is controlled by the phosphatases PP1 and PP2A. Future works should include identification of splicing factors whose regulation contributes to the increased intron retention at 2h post-LPS and also the splicing factors involved in resolution of IR by 6h – i.e. those that may be involved in removing detained introns.

Detained introns are stored in nuclear speckles prior to further processing or decay [283]. Nuclear speckles or splicing speckles (also called interchromatin granule clusters) are dynamic subnuclear structures for splicing factor storage and modification [410]. In nuclear speckles additional splicing to remove the retained intron is coupled to nuclear

export and translation. Mislocalisation of transcripts leads to degradation by nuclear DNA decay pathways. For further work, we can examine whether intron retained transcripts localise to nuclear speckles as described for other detained introns. Additionally, future work should determine the timecourse of localisation of regulatory splicing and nuclear export factors to sites of intron-retaining transcripts and the timeline in which activation of spliceosomes occurs to remove the retained/detained introns. These combined future experiments will describe the mechanisms by which inflammation induced IR events are coordinated by the activity of the cellular splicing and RNA metabolism machinery.

6.4 The importance role of NMD in the regulating of gene expression upon inflammatory responses

Nonsense-mediated mRNA decay (NMD) is a RNA surveillance pathway to reduce errors in gene expression by degrading transcripts with premature termination codons (PTCs) and prevents non-functional or toxic protein production. Recognition of PTCs during NMD requires UPF1 phosphorylation via SMG1. To understand the role of SMG1 in regulating of LPS responses, we investigated whether SMG1 regulates toll-like receptor induced signalling pathways (Chapter 4) and examined how SMG1 controls RNA metabolism during inflammation (Chapter 5) by using molecular and cellular biology approaches and RNA sequencing.

For chapter 4 results, we found that BMMs from $LysM^{+/Cre}Smg1^{fl/fl}$ (Cre) male mice showed less induction of the pro-inflammatory cytokines IL-1β, IFNβ, and TNFα, while increased pro-inflammatory cytokine production was observed in BMMs from $LysM^{+/Cre}Smg1^{fl/fl}$ female mice as compared with control. Also post-LPS treatment there was slightly lower TLR4 protein level in Smg1 deficient male mice BMMs compared to

female mice. Thus, Smg1 deficiency alters toll-like receptor induced inflammatory gene expression in a sex-dependent manner. For future work, we could investigate whether SMG1 loss alters cytokine production as induced by other TLRs. This work should also include analysis of signalling pathways downstream of TLR4 in macrophages from male vs female mice to try and determine the mechanistic interaction of SMG1 with these pathways.

There are known difference in broad immune response capability between males and females. Innate detection of nucleic acids by PRRs differs between females and males. The TLR7 gene, encoded on the X chromosome, may escape X inactivation resulting in higher expression levels of TLR7 in females than males [401]. Peripheral blood mononuclear cells (PBMC) from human females displayed higher production of IFNα after stimulation with TLR7 ligands [402]. More IL-10 production [403] and higher levels of IFN regulatory factor 5 (IRF5) were detected in plasmacytoid dendritic cells (pDCs) from female humans compared to males [404]. In contrast, PBMCs from human males produced more TNFα after LPS stimulation [405, 406]. In mice, there is a greater rate of phagocytosis and higher levels of TLR2, TLR3, and TLR4 in peritoneal macrophages from female mice [407]. However, macrophages from male mice had greater pro-inflammatory cytokine production than macrophages from female mice. In contrast, a different study suggested that peritoneal macrophages from male mice were had higher levels of TLR4 and produced more CXC-chemokine ligand 10 (CXCL10) after LPS stimulation [408]. As these few studies show results have been inconsistent, with mouse work exact housing conditions are rarely described and not standardised across institutes. Greater investigation of the impacts of housing on inflammatory phenotypes is going to be essential for validating many studies involving inflammatory phenotypes including

infections, autoimmunity and neurodegeneration. This will require significant co-operation between research groups/institutions and acknowledgement of the limitations of mouse models. For our ongoing work, we could investigate the response to TLR4 in male and female mice from peritoneal and bone marrow sources to determine the impact of culture methods and microenvironment on sex differences. This would allow us to understand what distinct regulation with potential sex differences occurs in the two reservoirs of macrophages and further address if there what mechanism involved in the process.

BMMs from *LysM*$^{+/Cre}$*Smg1*$^{fl/fl}$ (Cre) mice, either male or female mice, showed altered pro-inflammatory cytokine IL-1β, IFNβ, and TNFα production in response to LPS treatment compared to control mice indicating that SMG1 may affect both MyD88- and TRIF-dependent pathways as well as potentially post-transcriptional and feedback pathways. We expect that SMG1 will at least act to control NF-κB activation and translation via regulation of NMD but other points of regulation may also exist. Therefore, we could compare protein levels and activation status of NF-κB pathway components by western blot to address the role of SMG1 in the regulating of innate immunity between males and females. Based on a relatively limited literature to examine sex-specific immune responses in either animal models or in human, what the impact of this is and at a high level how this should be addressed in the future.

6.5 Conclusion

For my thesis, we have identified the regulation of the components of RNA decay pathways during LPS treatment. Subsequently, we demonstrated that co-ordinated intron retention and the use of detained introns may be an additional level of regulation in LPS

responses. These findings can open up new areas of research on post-transcriptional regulation of innate immunity and how these pathways are regulated and can be manipulated. Also, post-transcriptional gene expression can be regulated via nonsense-mediated decay, which can precisely control the timing and level of gene expression as well as eliminating unstable or toxic protein production. We used animal models to address the role of SMG1 in response to inflammatory stimuli. Loss of SMG1 may alter regulation of innate immunity with potential sex differences affecting pro-inflammatory cytokine production in response to LPS treatment. In summary, my projects aimed to address post-transcriptional gene expression regulation in response to inflammatory stimuli. Understanding post-transcriptional gene expression at the level of RNA biology, will be helpful in the development of a new generation of drugs to treat cancer, autoimmune disorders and infectious diseases.

Chapter 7-Materials and Methods

7.1 Materials

7.1.1 Cell lines

7.1.1.1 THP-1(ATCC TIB-202)

THP-1 is a human monocytic cell line derived from an acute monocytic leukemia patient and is commonly used as a model for human monocytes. This cell line is known to produce lysozyme and can phagocytose latex beads and lacks surface and cytoplasmic immunoglobulin. THP-1 cells can be differentiated into a macrophage-like cell by treatment with phorbol-12-myristate-13 acetate (PMA) [411]. THP-1 was purchased from the ATCC (Manassas, VA).

7.1.1.2 RAW264.7 (ATCC TIB-71)

The murine macrophage-like cell line RAW264.7 was established from the tumour cells of a mouse infected with Abelson leukaemia virus [412] and is a good model for murine macrophages as they display many macrophage characteristics such as the ability to respond to a range of microbial products (LPS, bacterial DNA and peptidoglycan) (Sigma Aldrich, Castle Hill, NSW) as well as to murine cytokines [413, 414]. This cell line was purchased from the ATCC (Manassas, VA).

7.1.2 Primary Cells

7.1.2.1 Mouse models background and utilised

The LysM promoter is active in myeloid lineage cells and tissue macrophages and we used cre-recombination to flank exons 2 to 4 of the Smg1 gene. Therefore, these $LysM^{+/Cre}Smg1^{fl/fl}$ (Cre) mice can provide cells with SMG1 knocked out only in myeloid lineage. In this thesis we describe the isolation of macrophages from $Smg1^{fl/fl}$ mice with (SMG1 knockout) or without (SMG1 wild-type) Cre expression to dissect SMG1 regulated inflammatory responses [64].

7.1.2.2 Mouse background

SMG1- mice in which a genetrap cassette has been inserted between exons 4 and 5 of the SMG1 gene preventing expression of the SMG1 gene-on mixed 129/C57 background [64].

SMB- SMG1 mice backcrossed for over 20 generations to a C57BL/6J (Jax labs) background

SCC- In which exons 2-4 of the Smg1 gene are flanked by LoxP sites with no loss of gene expression until crossed to a Cre recombinase expressing line or cells are isolated and exposed to Cre recombinase ex vivo.

SML-(SCC x LysM Cre)-Smg$^{fl/fl}$ mice are crossed to mice heterozygous for Cre expression driven by LysM promoter to generate myeloid specific knockout animals.

7.1.2.3 Bone Marrow Derived Macrophages (BMMs)

Bone marrow derived macrophages were derived from the femur and tibia bone marrow cells of adult mice (8-10 weeks old). Cells were flushed from the femoral cavity using a 27 G needle with RPMI1640 medium (Thermo Fisher Scientific, Waltham, MA). Subsequently, cells were cultured on bacteriological plastic (Millipore, Castle Hill, NSW), 10% FBS for 7-10 days in the presence of 10000 U/ml recombinant hCSF-1 (PEPROTECH, Rocky Hill, USA), which induces differentiation into macrophages [415]. Later we treated with LPS (Sigma Aldrich, Castle Hill, NSW) on BMMs with RPMI1640, 10%FBS and hCSF-1 and performed experiments.

7.1.2.4 Animal husbandry

Mice were bred in- house and 8-10 week old mice were used to isolate bone marrow cells. All mice were housed in a perpetual 12 hour light/dark cycle and fed *ad libidum* under specific pathogen-free (SPF) conditions. All animal experiments were approved by the animal ethics committees of Western Sydney University or The University of Queensland and were conducted in accordance with the 'Australian Code for the Care and Use of Animals for Scientific Purposes (2013)'.

7.2 Methods

7.2.1 Cell Culture

7.2.1.1 Culture conditions

For routine culture RAW264.7 and THP-1 were grown in RPMI (Thermo Fisher Scientific, Waltham, MA) supplemented with 10% fetal bovine serum (Gibco, North Ryde, NSW), 100 U/mL penicillin and 100 μg/mL streptomycin (Gibco, North Ryde NSW) , 10mM Hepes (Gibco, North Ryde, NSW), 1mM Sodium Pyruvate (Gibco, North Ryde, NSW), 0.05mM β-mercaptoethanol (Sigma Aldrich, Castle Hill, NSW) in a humidified incubator at 37°C and 5% CO_2. BMMs were cultured in RPMI (Thermo Fisher Scientific, Waltham, MA) supplemented with 10% fetal bovine serum (Gibco, North Ryde, NSW) 100 U/mL penicillin and 100 μg/mL streptomycin (Gibco, North Ryde, NSW) and plus hCSF-1 (PEPROTECH, Rocky Hill, USA) which induces differentiation into macrophages. FBS was batch tested for low immunogenicity or inhibition of inflammatory responses, and ability to support BMM differentiation. A single batch was used for all experiments described in this thesis.

7.2.2 DNA isolation from ear clip

7.2.2.1 Genotyping was achieved via PCR and analysed by agarose gel

Electrophoresis (Labpro Scientific, Narangba QLD). In general, PCR reactions were performed in a T100 Thermal Cycler (BioRad, Gladesville NSW). The reaction mixes (Thermo Fisher Scientific, Waltham, MA) comprised of 1x PCR buffer, 2.5mM $MgCl_2$, 0.25mM dNTPs (Invitrogen, Cincinnati, USA), 1μM of each primer and 0.5U Taq DNA

polymerase (Thermo Fisher Scientific, Waltham, MA), 1μl of DNA extraction and sterile water up to 20μL. PCR conditions for each strain are shown below. PCR reactions were analysed by agarose gel electrophoresis (7.2.1.2.2) where 18μl of PCR products in 2μl 10x loading dye and run 80V for 40 mins.

Strain	Primer sequences	PCR conditions
SML	06F- ccactgagggttacactcacat 85R- ctgggctggtgataaaaccta 87R- gtttgtcttaagggcttttcca	95°C10 mins **95°C45sec** **57°C45sec 35cycles** **72°C1min** 72°C10min
SMG1	3066-cccagaaatgccagattacg 3067-cttgggctgccagaatttctc 3068-ttacagtcggccaggctgac	95C 10 mins **95C 30sec** **62C 1min 35cycles** **72C 1min** 72C 7min
SMB	Lac Z up- gtcacactacgtctgaacgt Lac Z down- ctgcaccattcgcgttacg	95°C10 mins **95°C30sec** **55°C30sec 35cycles** **72°C1min** 72°C10min

7.2.2.2 Agarose Gel electrophoresis

1% and 2% (w/v) agarose (Astral Scientific, Australia) in 1x TAE and 0.5μg/mL ethidium bromide gels were routinely run at 80V for 40 mins. The apparent sizes of DNA samples were compared with 1Kb Plus ladder size standard (Invitrogen, Cincinnati, USA). The bands were visualised under UV using Gel Doc-It^{TM} Imaging System.

7.2.3 Harvesting cells

RAW264.7 and BMMs cells are harvested from bacteriological plastic by squirting with a syringe and 18G needle in medium or PBS. THP-1 were removed from tissue culture flasks, followed by PBS washing and collected. For RAW264.7, we only used passages before 12.

7.3 Assays

7.3.1 Quantification of DNA & RNA

DNA and RNA concentrations were measured spectrophotometrically using the NanoDrop 2000 Spectrophotometer. The absorbance of 1.5μl of undiluted sample was measured at A260 and A280. An A260 = 1.0 was taken to be equivalent to a DNA concentration of 50ng/μL and RNA concentration of 40ng/μL. A sample with an A260/A280 ratio between 1.8- 2.0 was considered to be pure.

7.3.2 RNA isolation

Day1: Cell were treated with LPS (5ng/ml) (Sigma Aldrich, Castle Hill, NSW) for 0, 2, 6 and 24 hours and harvested cell lysates following by two times 1ml PBS wash. The cells were suspended in 1 mL of TRIzol reagent (Thermo Fisher Scientific, Waltham, USA) in a 1.5ml tube. The tubes were incubated at room temperature for 10 minutes before 200μL of chloroform was added and the tubes were shaken vigorously for 15 seconds and incubated at room temperature for an additional 10 minutes followed by centrifugation at 13,500 rpm for 30 minutes at 4℃. The upper aqueous phase was retained

in a new 1.5 mL microfuge tube and 500μL of isopropanol was added and vortexed. The tubes were incubated at 4℃ in the cold room overnight. Day2: The tubes were centrifuged at 13,500 rpm, 4℃, for 30 minutes. The supernatant was decanted and the pellet was resuspended in ice cold 75% ethanol and centrifuged at 13,500 rpm, for 1 minutes followed by 100% ethanol and centrifugation. The supernatant was removed, and the pellets were dried in a laminar flow hood for 20 minutes with the tubes inverted. The pellets were then resuspended in RNAase-free water (Life Technologies, North Ryde, NSW) and absorbance measurements made on a spectrophotometer (section 7.3.1)

7.3.3 qPCR analysis

RNA was isolated from cells using Tri-reagent (see 7.3.2). RNA was then treated to remove contaminating DNA. 2μg of RNA was incubated with 2μl DNase buffer and 1μl DNase (Ambion, Austin, USA) at 37°C for 30 mins. Subsequently, EDTA was added to a final concentration of 5mM and heat inactivated at 75°C for 10 mins. Reverse transcriptase (RT) reactions were performed in 20μl including 2μl RNA, 500ng of oligo-dT, 0.5mM dNTPs, 0.01 M DTT, buffer and superscript III (Gibco, North Ryde, NSW). Initially, RNA and oligo dT were denatured at 70°C for 10 mins, cooled in ice and the remainder of the reagents added. Reactions were incubated at 50℃ for 50 mins and 70℃ for 10 mins. PCR reactions were performed in 20μl. Each reaction contained 0.4 μM of each forward and reverse primers, 0.4mM dNTPs, buffer and 1.25U Taq polymerase (Invitrogen, Carisbad, USA). Standard cycling conditions for PCR were 94℃ 3mins, 35 cycles of 94℃ 15 secs, 55℃ 30 secs, 72℃ 1 min followed by 72℃ 10 mins. PCR was analysed by using an Applied Biosystems QuantStudio (Thermo Fisher Scientific, Waltham, MA). Primers list used for PCR reactions are shown as Table 7.2.

7.3.4 Quantitative real-time PCR (qPCR)

For confirmation of RNA-seq data, selected genes were analysed by qPCR analysis. mRNA expression was quantified by real-time PCR using the SYBR green detection system (Invitrogen, Cincinnati, USA) and was performed using the Quantstudio 12k Flex (Life technology) real-time PCR machine and software. Real time PCR was performed in a 20μl reaction including SYBR Green master mix (Applied Biosystems, Foster City USA), 4μM primers (Sigma Aldrich, Castle Hill, NSW) and cDNA (200 ng RNA each sample). PCR conditions were as follows 50℃ for 2 mins, 90℃ for 10 mins and then 40 cycles of 95℃ 15 secs, 60℃ 1 mins. Gene expression was normalised with either hHPRT or mRpal13a. Depending on where were the samples from, either from patients or mice. Housekeeping genes for LPS treatment were optimised and selected for stable expression during inflammatory responses by the laboratory prior to the start of this PhD project. T The difference in cycle threshold ($\sqrt{Ct}$) between the target gene and housekeeping gene was determined. The conversion to expression values is $=2^{-\sqrt{Ct}}$ as each cycle represented doubling of the template copy number. Standard deviations (sd) in the expression values were calculated by the following equations. $Sd_{gene}^2 + sd_{Rpal13a}^2 = \sqrt{.}\sqrt{\sqrt{}} + \sqrt{Ct} = X$. maximum error $= 2^{-x}$. Sd of expression value $= 2^{-\sqrt{Ct}} - 2^{-x}$.

Table 7-1: Sequences of primers used for qPCR (Rpl13a and IFNβ primers are sourced from indicated references, others are mainly designed for this thesis).

Target Gene	Forward Primer 5'-3'	Reverse Primer 5'-3'	Ref
Rpl13a	GAGGTCGGGTGGAAGTACCA	TGCATCTTGGCCTTTTCCTT	[416]
IFNβ	CCACAGCCCTCTCCATCAAC	TGAAGTCCGCCCTGTAGGTG	[417]

Gene	Forward	Reverse	
TNFα	AGCCCCCAGTCTGTATCCTT	CTCCCTTTGCAGAACTCAGG	
Upf2	ACTGAGCCGGAGAAGAAACA	CTGGTGGCTTATCTGGCATT	
Smg7	GCTCCAAGGCAGAACTGAAC	TCCCAATGGGTCCAAAATTA	
Upf3b	AGGAAACCGGAAAAAGGAGA	ATCATGCGCTCCTGATCTCT	
Upf1	AACAGAAGGCGCTAGTGGAA	TGCTGCGGTCATAGACAGAC	
Dcp1a	CCAGCTGAAGCTCCTACCAC	CTGTGGGGTCAACCTGAGTT	
Lsm1	ACCAGACTGGAGGCAGAGAA	TGGCATCCATGAAAGAATGA	
TTP	CCCTCTGCAACTCTGGTCTC	TGGCTTTGGCTATTTGCTTT	
Dis3	GCAAGAGCAGGGAGAGAATG	ACACGTGAAGGCTGGTATCC	
Cnot7	GTTGGGCTTGTAACCTGGA	GTTGACGTTCCTGGAGGGTA	
Stau1	GCACAGAGATGCCAAGAACA	GGCCCACTGGAGTTATCAGA	
Xrn1	CCACTTCAGACTAACAAGCCA	GGGAGGCAGTTTCAACATGAG	
Dcp2	GACCAGCTTGCTCGCTTGTA	TTGGACTTGGGAGTCATGTCA	
Zc3h12a	ACGAAGCCTGTCCAAGAATCC	TAGGGGCCTCTTTAGCCACA	
Exosc5	CGTGCAGACGCCAATTTACTC	GACAGCAGGTTTTGCTCACA	
Exosc7	CTACATCGTTCATGGAGTGCAG	GCAGACCCACTGGTGTTAGAC	
Smg1	GACGAGCCTACAATCCATCCT	CAAACTCTGCAACCACCCA	
IRAK1	GCTGTGGACACCGATACCTT	GCTACACCCACCCACAGAGT	
IL-17	GGA GAA AGC GGA TAC CAA	TGT GAG GAC TAC CGA GCC	
F11r	GTTCCCATTGGAGTTGCTGT	GGGAGAGGAGAAGCCAGAGT	
ATF3	CTAGAATCCCAGCAGCCAAG	GGCCAGCTAGGTCATCTGAG	
METTL3	ggctgtggcagaaaagaaag	gacttcttagccggctcctt	
Virma	cctttattcgggttctgcaa	agggatagagcacaggagca	
Wtap	gcaagagtgcaccactcaaa	cattttgggcttgttccagt	

Alkbh5	ggaacctgtgctttctctgc	tgctcagggattttgtttcc	
YTHDC1	cggtaccacatgaagcaaga	ggtctctgtcccgatcacat	
YTHDF1	ttggtggcacagttgttgat	accattgccagaaaggacac	
YTHDF2	tgcaagcagtgttccaaaag	gatcctgcaatgccattctt	
Hnrnpa2b1	tggaggtagccctggttatg	tcctcccatgttcctgctac	
Hnrnpc	agtctgaggcaggtgcagat	cccacaaacgcctaggtaaa	
Casp1_E4I5	ATCCTTCAGAGgtgctgtgc	cctcagggttcttcagcttg	
Casp1 E4E5	CCCTTTAGAAAAAGCCCAGAA	GATCCTCCAGCAGCAACTTC	
CD274_E1I1	CTGCAGgtaagggagcatct	gacccagctacctacccaca	
CD274 E1E2	AAATCGTGGTCCCCAAGC	GAACTATCTGCAGGCGAGGA	
Uba7 E1E2	CCAGGCAGCTGTATGTACTGG	GCAGGCCACATAGCAAGACT	
Uba7_E1I1	CCAGGCAGCTgtaagtctca	ggaccaaaggtctggaagc	
Pnpt1 E1E2	TGTAGACCTGGGACACAGAAAA	CATCAGCAAATCTTGCCAGT	
Pnpt1_E1I1	CACAGgtgagaaacggtgtg	gatttgacttctggggctga	
Herc6 E1E2	TTCAGCAACCACAGGGTGTA	CTCACCAGGTCAACATGCAG	
Herc6_E1I1	AGAGTACCGAAAGGCCAGgt	aacagggttccagcttctga	

7.3.5 RNA-sequencing (RNA-seq)

RNA was isolated using Qiagen RNeasy kits according to the manufacturer's instructions. RNA samples were run on the labchip to determine contaminations and then proceeded with DNAse treatment (Turbo DNase, Invitrogen, Cincinnati, USA). RNA integrity number (RIN value) was checked with a Bioanalyser (Agilent, Santa Clara – USA) to decide the fragmentation time for each sample. Concentration of samples were determined with Quant-iT RiboGreen assay (ThermoFisher Scientific) and normalised to the same total concentration of 250ng before proceeding to library preparation. Next, RNA was depleted, fragmented, 1st and 2nd strand synthesised, adenylated, ligated and

then enriched following Illumina Truseq Stranded RNA Library prep (Gold) kit protocol (Illumina, USA). The DNA fragment was enriched using the following PCR conditions – 98℃ for 30 sec, (98℃ for 10sec, 60℃ for 30 sec, 72℃ for 30 sec) x 10 cycles, 72℃ for 5 min. The final library was cleaned using AMPure XP beads (Beckman Coulter, USA) and checked on the 4200 TapeStation (Agilent, USA) to determine fragment size and concentration. Libraries were normalised to the same concentration (2nM), pooled together and sequenced at 12pM on the Illumina HiSeq2500 platform at Western Sydney University-NGS facility (Hawkesbury, Australia).

Reads were aligned using the standard Stemformatics RNA-Seq data processing pipeline (https://www.stemformatics.org/Stemformatics_data_methods.pdf) [259, 262] Summarised count data was counts per million (CPM) normalised and log transformed prior to differential expression analysis using the limma and voom packages (https://f1000research.com/articles/5-1408/v2). Multiple pairwise contrasts between samples were performed and top tables of significant differential expression probes by empirical Bayes moderated t-test were produced. Gene Ontology profiling was used to identify statistically over-represented GO terms in our datasets based on RNA seq. Biological and functional gene enriched pathways were identify by the two common online resources-Panther (http://www.pantherdb.org/) and GOrilla (http://cbl-gorilla.cs.technion.ac.il/) platforms [261, 360]. Gorilla analysis was performed using a single ranked gene list based on the calculated differential gene expression p-value for paired samples. The cut-off for GOrilla gene ontology term inclusion was set at 10^{-4} for initial inclusion and FDR q-values were calculated to account for multiple testing (see GOrilla website [260, 261]) Heat maps were generated via the Stemformatics platform

using Pearsons correlation. Dataset available on the Stemformatics platform reference S4M-7004. All analysis results were shown as Chapter 5.

7.3.6 Polysome Profile Analysis

BMMs were stimulated with 5 ng/ml LPS (*E. coli* LPS) (Sigma Aldrich, Castle Hill, NSW) for 2h and before harvesting cells, 10 μg/ml of cycloheximide (Sigma Aldrich, Castle Hill, NSW) was added for 10 mins. Cells were washed twice with PBS media and lysed in Polysome lysis buffer (0.5% (v/v) NP40, 10mM HEPES, pH 7.6, 10mM NaCl, 3mM $CaCl_2$, 5mM $MgCl_2$, 1mM DTT, 100Mm KCl, complete protease inhibitors(Roche, Millers Point, NSW). Nuclei were removed by centrifugation (9300xg, 4°C, 10 mins) and then the cytoplasmic lysate was loaded onto a 10-50% continuous sucrose gradient (10mM NaCl, 20mM Tris-HCl, pH 7.5, 5mM $MgCl_2$) and centrifuged at 55,000xg, 75 mins using a SW55i rotor (Invitrogen, Cincinnati, USA). The base of the centrifuge tube was punctured with an 18G needle and fractions of approximately 400μl were collected in RNase-free eppendorfs starting from the bottom of the gradient, and UV absorbance was monitored at 260nm to identify fractions containing monosomes and polysomes. Samples of total RNA were extracted with TRIzol reagent (see section 7.3.2) (Thermo Fisher Scientific, Waltham, USA) from each fraction and the analysis the relative amount of intron retention genes and HPRT mRNAs was measured by real time-PCR (see section 7.3.4).

7.3.7 Western Blotting

7.3.7.1 Whole cell extracts for Western Blotting

Cells were lysed in 50mM Tris-Cl pH7.5, 150mM NaCl, 0.5% Triton X-100, 2mM EDTA, 2mM EGTA 25mM NaF, 10% glycerol, 1mM sodium pyrophosphate, 10mM sodium fluoride, 1mM sodium molybdate and 1x protease inhibiters (Roche, Millers Point, NSW) for 30 minutes on ice followed by clearing at 13200rpm at 4°C.

7.3.7.2 Protein Assay

The concentrations of western extracts were determined using the BCA Protein Assay Kit (Pierce, Rockford USA) according to manufacture's instructions. Briefly, assay reagents A and B were mixed at 50:1 ratio. 10μl of diluted western extract, lysis buffer and bovine serum albumin standards were incubated with 200μl of mixed reagent S with 5μl of diluted protein samples and then add 200μl reagent B at 37°C for 30 mins on the bench. Absorbance at 750nm was determined using a bio-strategy SpectraMax M2^e plate reader (Molecular Devices, California USA).

7.3.8 Immunoblotting

Proteins were separated by SDS-PAGE using 4-12% polyacrylamide gels (Invitrogen, Cincinnati, USA). The gels were transferred to PVDF membranes in 25mM Tris, 150mM Glycine and 20% methanol at 75V for 90 minutes at 4°C. The membrane was blocked in TBS-Tween with 5% skim milk for 1 hour at room temperature followed by incubation with primary antibody in 1% skim milk powder (w/v) in TBS-Tween overnight 4°C .

Membranes were then washed in TBS-Tween buffer 3 times with agitation for 10 minutes, followed by incubation with secondary antibody (see below) in 1% skim milk powder (w/v) in TBS-Tween for 1 hour at room temperature. Membranes were then washed with TBS-Tween 3 times for 5, 10, and 20 mins and then incubated with ECL Reagent (Amersham, Buckinghamshire UK) for 1 mins, drained and imaged using the Odyssey Fc Imaging System (Millennium Science NSW).

Antibody conditions were as bellow: the primary antibodies and dilutions used were rabbit anti-DCP1a (Abcam) 1:1000 (#ab183709), mouse-anti-DIS3 (Abcam) 1:1000 (#ab214083), rabbit anti-Xrn1 (Abcam) 1:1000 (#ab70259), rabbit anti-EST1A (Abcam) 1:1000 (#ab87539), rabbit anti-Staufen1 (Abcam) 1:1000 (#ab73478), rabbit anti-UPF1 (MBL) 1:1000 (#MBRN108PW), rabbit phospho (S/T)Q (cell signalling Technologies) 1:1000 (#2851), rabbit anti-Phospho-NF-κB p65 (cell signalling) 1:1000 (#93H1), rabbit anti-NF-κB p65 (cell signalling) 1:1000 (#3034), mouse-anti-β-actin (cell signalling) 1:2500 (#3700S), mouse anti-TLR4 (Abcam) 1:1000 (#ab22048), rabbit anti-P-TBK1 (cell signalling) 1:1000 (#5483S), rabbit anti-TBK1 (cell signalling) 1:1000 (#3504P), and mouse anti-β-actin (Cell Signaling Technologies) 1:5000 (#3700). The anti-SMG1 antibodies were generated in house and have been described previously [125]. Anti-Rabbit (#7074) and anti-mouse (#7076) horse radish peroxidase tagged secondary antibodies were sourced from cell signalling Technologies.

7.3.9 Immunoprecipitation

10 million cells were lysed in 0.1% Triton (v/v), 1M Tris-HCl pH7.4, 1M NaCl with phosphatase and protease inhibitors (Roche, Millers Point, NSW) and incubated on ice

for 30 mins. Samples were then homogenised with a 21G needle and incubated for a further 15 mins. Samples were centrifuged at 14,000g for 10 mins and the supernatant was collected. 1mg of protein lysate was incubated with antibody (1:1000) overnight at 4°C . Protein G agarose (40μl of beads/mg protein) (Merck Millipore, Germany) was added and incubation continued for 30 mins.

7.3.10 Nuclear and Cytoplasmic RNA extraction

Cells ($4x10^7$) were pelleted in a cold room centrifuge at 2500rpm for 5 mins followed by washing twice with 0.7ml PBS. The cell pellet was resuspended in200μl HWB (1ml HWB+10μl DALC+ 10μl PMSF+5μl vanadate+ 20μl 50 PI (500μl/sample)). 200μl LB (1ml HWB+ 10μl DALC+ 10μl PMSF+ 5μl vanadate+ 20ul 50 PI (500μl/sample+10μl 10% NP40) was added and left on ice for 5 mins. Cell lysis was confirmed by microscopic observation on an haemacytometer. The lysate was centrifuged at 2500rpm and supernatant was transferred to a new tube referred to as the cytoplasmic extract. The nuclear pellet was washed by resuspension in 800μl HWB and centrifuged at 2500rpm for 5mins. The pellet was resuspended in 150μl NEB (1ml NWB+ 10μl DALC+ 10μl PMSF+ 5μl vanadate+ 20μl 50 PI (500μl /sample) and left 10mins on ice following by full speed (14000 rpm) to remove nuclei and corrected nuclear extract to new tube. RNA was extracted from each cytoplasmic and nuclei supernatant using 1ml of TRIzol reagent (Thermo Fisher Scientific, Waltham, USA) (see section 7.2.2.2).

7.3.11 Nitrite assay

Nitrite is measured as an estimate of the amount of NO production during an immune responses. Day1: 4×10^5 BMMs/well were plated in 96-well plates in 200μl of culture medium overnight. Day2: Cell were pre-treated with 500 ng/ml IFNγ (Sigma Aldrich, Castle Hill, NSW) for 2 hours prior to 5ng/ml LPS (Sigma Aldrich, Castle Hill, NSW) treatment overnight. Supernatant was collected and analysed by additional of an equal volume of Griess Reagent(1% sulphanilamide (p-aminobenzenesulfonamide)(w/v)+ 0.1% N-(1-napthyl) ethylenediamine diHCl(w/v)+2.1% phosphoric acid(v/v)) (Sigma Aldrich, Castle Hill, NSW). The reaction was incubated at room temperature for 5mins and then the absorbance measured at 540nm. This method of detection of nitric oxide has been described previously [418].

7.3.12 Statistical Analysis

Graphing and statistical evaluation was performed using GraphPad Prism 8 (GraphPad Software, USA). Data are presented as mean ± standard error of the mean from at least three independent experiments by an unpaired two-tailed student T tests. Differences were considered to be significant if $p \leq 0.05$.

7.3.13 Solutions

PBS- 137mM NaCl, 2.7 mM KCl, 10 Mm buffered phosphate solution pH7.4

TE- 10mM Tris-HCl pH8 + 1mM EDTA

Phosphatase Inhibitors- 1mM sodium vanadate, 1mM sodium pyrophosphate, 10 mM sodium fluoride, 1mM sodium molybdate

MOPS- 0.02M MOPS, 5mM Sodium Acetate, 1mM Disodium EDTA

DNA loading Dye- 0.125% bromophenol blue(w/v), TE Buffer, 50% glycerol(v/v)

HWB- 1.19g 10mM HEPES pH7.4+ 0.75ml 1.5mM $MgCl_2$ +0.373g 10mM KCl

NEB- 0.477g 20mM HEPES pH7.8+ 2.454g 0.42M NaCl+ 20% glycerol+ 40μl 0.2mM EDTA+ 150μl 1.5mM $MgCl_2$

200 Mm Vanadate- 7.36g Sodium Ortho vanadate to 200ml water

50x TAE buffer- 242 g Tris base+ 57.1 ml glacial acetic acid+ 100 ml of 500 mM EDTA (pH 8.0) solution, and up to 1 litre of final volume.

Chapter 8-Bibliography

1. Berget SM, Moore C, Sharp PA. Spliced segments at the 5' terminus of adenovirus 2 late mRNA. Proc Natl Acad Sci U S A. 1977;74(8):3171-5. PubMed PMID: 269380; PubMed Central PMCID: PMCPMC431482.

2. Chow LT, Gelinas RE, Broker TR, Roberts RJ. An amazing sequence arrangement at the 5' ends of adenovirus 2 messenger RNA. Cell. 1977;12(1):1-8. PubMed PMID: 902310.

3. Douglas AG, Wood MJ. RNA splicing: disease and therapy. Brief Funct Genomics. 2011;10(3):151-64. doi: 10.1093/bfgp/elr020. PubMed PMID: 21628314.

4. Lerner MR, Boyle JA, Mount SM, Wolin SL, Steitz JA. Are snRNPs involved in splicing? Nature. 1980;283(5743):220-4. PubMed PMID: 7350545.

5. Rozovski U, Keating M, Estrov Z. The significance of spliceosome mutations in chronic lymphocytic leukemia. Leuk Lymphoma. 2013;54(7):1364-6. Epub 2012/12/29. doi: 10.3109/10428194.2012.742528. PubMed PMID: 23270583; PubMed Central PMCID: PMCPMC4176818.

6. Matera AG, Wang Z. A day in the life of the spliceosome. Nat Rev Mol Cell Biol. 2014;15(2):108-21. doi: 10.1038/nrm3742. PubMed PMID: 24452469; PubMed Central PMCID: PMCPMC4060434.

7. Graubert TA, Shen D, Ding L, Okeyo-Owuor T, Lunn CL, Shao J, et al. Recurrent mutations in the U2AF1 splicing factor in myelodysplastic syndromes. Nat Genet. 2011;44(1):53-7. doi: 10.1038/ng.1031. PubMed PMID: 22158538; PubMed Central PMCID: PMCPMC3247063.

8. Quesada V, Conde L, Villamor N, Ordonez GR, Jares P, Bassaganyas L, et al. Exome sequencing identifies recurrent mutations of the splicing factor SF3B1 gene in chronic

lymphocytic leukemia. Nat Genet. 2011;44(1):47-52. doi: 10.1038/ng.1032. PubMed PMID: 22158541.

9. Rosati E, Baldoni S, De Falco F, Del Papa B, Dorillo E, Rompietti C, et al. NOTCH1 Aberrations in Chronic Lymphocytic Leukemia. Front Oncol. 2018;8:229. Epub 2018/07/13. doi: 10.3389/fonc.2018.00229. PubMed PMID: 29998084; PubMed Central PMCID: PMCPMC6030253.

10. Adamia S, Pilarski PM, Belch AR, Pilarski LM. Aberrant splicing, hyaluronan synthases and intracellular hyaluronan as drivers of oncogenesis and potential drug targets. Curr Cancer Drug Targets. 2013;13(4):347-61. PubMed PMID: 23517594.

11. Cooper TA, Wan L, Dreyfuss G. RNA and disease. Cell. 2009;136(4):777-93. doi: 10.1016/j.cell.2009.02.011. PubMed PMID: 19239895; PubMed Central PMCID: PMCPMC2866189.

12. Padgett RA. New connections between splicing and human disease. Trends Genet. 2012;28(4):147-54. doi: 10.1016/j.tig.2012.01.001. PubMed PMID: 22397991; PubMed Central PMCID: PMCPMC3319163.

13. Wang GS, Cooper TA. Splicing in disease: disruption of the splicing code and the decoding machinery. Nat Rev Genet. 2007;8(10):749-61. doi: 10.1038/nrg2164. PubMed PMID: 17726481.

14. Bernier FP, Caluseriu O, Ng S, Schwartzentruber J, Buckingham KJ, Innes AM, et al. Haploinsufficiency of SF3B4, a component of the pre-mRNA spliceosomal complex, causes Nager syndrome. Am J Hum Genet. 2012;90(5):925-33. doi: 10.1016/j.ajhg.2012.04.004. PubMed PMID: 22541558; PubMed Central PMCID: PMCPMC3376638.

15. Czeschik JC, Voigt C, Alanay Y, Albrecht B, Avci S, Fitzpatrick D, et al. Clinical and mutation data in 12 patients with the clinical diagnosis of Nager syndrome. Hum

Genet. 2013;132(8):885-98. doi: 10.1007/s00439-013-1295-2. PubMed PMID: 23568615.

16. Gordon CT, Petit F, Oufadem M, Decaestecker C, Jourdain AS, Andrieux J, et al. EFTUD2 haploinsufficiency leads to syndromic oesophageal atresia. J Med Genet. 2012;49(12):737-46. doi: 10.1136/jmedgenet-2012-101173. PubMed PMID: 23188108.

17. Lefebvre S, Burglen L, Reboullet S, Clermont O, Burlet P, Viollet L, et al. Identification and characterization of a spinal muscular atrophy-determining gene. Cell. 1995;80(1):155-65. PubMed PMID: 7813012.

18. Lines MA, Huang L, Schwartzentruber J, Douglas SL, Lynch DC, Beaulieu C, et al. Haploinsufficiency of a spliceosomal GTPase encoded by EFTUD2 causes mandibulofacial dysostosis with microcephaly. Am J Hum Genet. 2012;90(2):369-77. doi: 10.1016/j.ajhg.2011.12.023. PubMed PMID: 22305528; PubMed Central PMCID: PMCPMC3276671.

19. Luquetti DV, Hing AV, Rieder MJ, Nickerson DA, Turner EH, Smith J, et al. "Mandibulofacial dysostosis with microcephaly" caused by EFTUD2 mutations: expanding the phenotype. Am J Med Genet A. 2013;161A(1):108-13. doi: 10.1002/ajmg.a.35696. PubMed PMID: 23239648; PubMed Central PMCID: PMCPMC3535578.

20. Mordes D, Luo X, Kar A, Kuo D, Xu L, Fushimi K, et al. Pre-mRNA splicing and retinitis pigmentosa. Mol Vis. 2006;12:1259-71. PubMed PMID: 17110909; PubMed Central PMCID: PMCPMC2683577.

21. Neuenkirchen N, Chari A, Fischer U. Deciphering the assembly pathway of Sm-class U snRNPs. FEBS Lett. 2008;582(14):1997-2003. doi: 10.1016/j.febslet.2008.03.009. PubMed PMID: 18348870.

22. Petit F, Escande F, Jourdain AS, Porchet N, Amiel J, Doray B, et al. Nager syndrome:

confirmation of SF3B4 haploinsufficiency as the major cause. Clin Genet. 2014;86(3):246-51. doi: 10.1111/cge.12259. PubMed PMID: 24003905.

23. Voigt C, Megarbane A, Neveling K, Czeschik JC, Albrecht B, Callewaert B, et al. Oto-facial syndrome and esophageal atresia, intellectual disability and zygomatic anomalies - expanding the phenotypes associated with EFTUD2 mutations. Orphanet J Rare Dis. 2013;8:110. doi: 10.1186/1750-1172-8-110. PubMed PMID: 23879989; PubMed Central PMCID: PMCPMC3727992.

24. Busch A, Hertel KJ. Evolution of SR protein and hnRNP splicing regulatory factors. Wiley Interdiscip Rev RNA. 2012;3(1):1-12. doi: 10.1002/wrna.100. PubMed PMID: 21898828; PubMed Central PMCID: PMCPMC3235224.

25. Wang Z, Burge CB. Splicing regulation: from a parts list of regulatory elements to an integrated splicing code. RNA. 2008;14(5):802-13. doi: 10.1261/rna.876308. PubMed PMID: 18369186; PubMed Central PMCID: PMCPMC2327353.

26. Wang Z, Xiao X, Van Nostrand E, Burge CB. General and specific functions of exonic splicing silencers in splicing control. Mol Cell. 2006;23(1):61-70. doi: 10.1016/j.molcel.2006.05.018. PubMed PMID: 16797197; PubMed Central PMCID: PMCPMC1839040.

27. Ladd AN, Cooper TA. Finding signals that regulate alternative splicing in the post-genomic era. Genome Biol. 2002;3(11):reviews0008. PubMed PMID: 12429065; PubMed Central PMCID: PMCPMC244920.

28. Bhatt DM, Pandya-Jones A, Tong AJ, Barozzi I, Lissner MM, Natoli G, et al. Transcript dynamics of proinflammatory genes revealed by sequence analysis of subcellular RNA fractions. Cell. 2012;150(2):279-90. Epub 2012/07/24. doi: 10.1016/j.cell.2012.05.043. PubMed PMID: 22817891; PubMed Central PMCID: PMCPMC3405548.

29.   Hao S, Baltimore D. RNA splicing regulates the temporal order of TNF-induced gene expression. Proc Natl Acad Sci U S A. 2013;110(29):11934-9. Epub 2013/07/03. doi: 10.1073/pnas.1309990110. PubMed PMID: 23812748; PubMed Central PMCID: PMCPMC3718113.

30.   Expert-Bezancon A, Sureau A, Durosay P, Salesse R, Groeneveld H, Lecaer JP, et al. hnRNP A1 and the SR proteins ASF/SF2 and SC35 have antagonistic functions in splicing of beta-tropomyosin exon 6B. J Biol Chem. 2004;279(37):38249-59. doi: 10.1074/jbc.M405377200. PubMed PMID: 15208309.

31.   Sanford JR, Wang X, Mort M, Vanduyn N, Cooper DN, Mooney SD, et al. Splicing factor SFRS1 recognizes a functionally diverse landscape of RNA transcripts. Genome Res. 2009;19(3):381-94. doi: 10.1101/gr.082503.108. PubMed PMID: 19116412; PubMed Central PMCID: PMCPMC2661799.

32. Grigoryev YA. Post-Transcriptional Mechanisms of Gene Regulation and Information Control in Immunity. California: Proquest, Umi Dissertation Publishing; 2012. p. 284.

33. Ip JY, Tong A, Pan Q, Topp JD, Blencowe BJ, Lynch KW. Global analysis of alternative splicing during T-cell activation. RNA. 2007;13(4):563-72. doi: 10.1261/rna.457207. PubMed PMID: 17307815; PubMed Central PMCID: PMCPMC1831861.

34.   Rodrigues R, Grosso AR, Moita L. Genome-wide analysis of alternative splicing during dendritic cell response to a bacterial challenge. PLoS One. 2013;8(4):e61975. Epub 2013/04/25. doi: 10.1371/journal.pone.0061975. PubMed PMID: 23613991; PubMed Central PMCID: PMCPMC3629138.

35.   Wang ET, Sandberg R, Luo S, Khrebtukova I, Zhang L, Mayr C, et al. Alternative isoform regulation in human tissue transcriptomes. Nature. 2008;456(7221):470-6. doi:

10.1038/nature07509. PubMed PMID: 18978772; PubMed Central PMCID: PMCPMC2593745.

36. Nilsen TW, Graveley BR. Expansion of the eukaryotic proteome by alternative splicing. Nature. 2010;463(7280):457-63. doi: 10.1038/nature08909. PubMed PMID: 20110989; PubMed Central PMCID: PMCPMC3443858.

37. Pan Q, Bakowski MA, Morris Q, Zhang W, Frey BJ, Hughes TR, et al. Alternative splicing of conserved exons is frequently species-specific in human and mouse. Trends Genet. 2005;21(2):73-7. doi: 10.1016/j.tig.2004.12.004. PubMed PMID: 15661351.

38. Hashimoto M, Nagao JI, Ikezaki S, Tasaki S, Arita-Morioka KI, Narita Y, et al. Identification of a Novel Alternatively Spliced Form of Inflammatory Regulator SWAP-70-Like Adapter of T Cells. Int J Inflam. 2017;2017:1324735. doi: 10.1155/2017/1324735. PubMed PMID: 28523202; PubMed Central PMCID: PMCPMC5421089.

39. Banks L. The Role of the Akt2 Isoform in Th17 Differentiation in Vitro and Peripheral Cd4 T Cell Immune Responses in Vivo. Publicly Accessible Penn Dissertations. 2014;1203.

40. Bihl MP, Heinimann K, Rudiger JJ, Eickelberg O, Perruchoud AP, Tamm M, et al. Identification of a novel IL-6 isoform binding to the endogenous IL-6 receptor. Am J Respir Cell Mol Biol. 2002;27(1):48-56. doi: 10.1165/ajrcmb.27.1.4637. PubMed PMID: 12091245.

41. Heinhuis B, Plantinga TS, Semango G, Kusters B, Netea MG, Dinarello CA, et al. Alternatively spliced isoforms of IL-32 differentially influence cell death pathways in cancer cell lines. Carcinogenesis. 2016;37(2):197-205. doi: 10.1093/carcin/bgv172. PubMed PMID: 26678222.

42. Lee TL, Chang ML, Lin YJ, Tsai MH, Chang YH, Chuang CM, et al. An

alternatively spliced IL-15 isoform modulates abrasion-induced keratinocyte activation. J Invest Dermatol. 2015;135(5):1329-37. doi: 10.1038/jid.2015.17. PubMed PMID: 25615554.

43. Luzina IG, Lockatell V, Todd NW, Keegan AD, Hasday JD, Atamas SP. Splice isoforms of human interleukin-4 are functionally active in mice in vivo. Immunology. 2011;132(3):385-93. doi: 10.1111/j.1365-2567.2010.03393.x. PubMed PMID: 21219317; PubMed Central PMCID: PMCPMC3044904.

44. Hong C, Luckey MA, Ligons DL, Waickman AT, Park JY, Kim GY, et al. Activated T cells secrete an alternatively spliced form of common gamma-chain that inhibits cytokine signaling and exacerbates inflammation. Immunity. 2014;40(6):910-23. doi: 10.1016/j.immuni.2014.04.020. PubMed PMID: 24909888; PubMed Central PMCID: PMCPMC4143255.

45. Le Hir H, Gatfield D, Izaurralde E, Moore MJ. The exon-exon junction complex provides a binding platform for factors involved in mRNA export and nonsense-mediated mRNA decay. EMBO J. 2001;20(17):4987-97. doi: 10.1093/emboj/20.17.4987. PubMed PMID: 11532962; PubMed Central PMCID: PMCPMC125616.

46. Le Hir H, Seraphin B. EJCs at the heart of translational control. Cell. 2008;133(2):213-6. doi: 10.1016/j.cell.2008.04.002. PubMed PMID: 18423193.

47. Ishigaki Y, Li X, Serin G, Maquat LE. Evidence for a pioneer round of mRNA translation: mRNAs subject to nonsense-mediated decay in mammalian cells are bound by CBP80 and CBP20. Cell. 2001;106(5):607-17. PubMed PMID: 11551508.

48. Chiu SY, Lejeune F, Ranganathan AC, Maquat LE. The pioneer translation initiation complex is functionally distinct from but structurally overlaps with the steady-state translation initiation complex. Genes Dev. 2004;18(7):745-54. doi: 10.1101/gad.1170204. PubMed PMID: 15059963; PubMed Central PMCID: PMCPMC387415.

49. Choe J, Oh N, Park S, Lee YK, Song OK, Locker N, et al. Translation initiation on mRNAs bound by nuclear cap-binding protein complex CBP80/20 requires interaction between CBP80/20-dependent translation initiation factor and eukaryotic translation initiation factor 3g. J Biol Chem. 2012;287(22):18500-9. doi: 10.1074/jbc.M111.327528. PubMed PMID: 22493286; PubMed Central PMCID: PMCPMC3365721.

50. Gewandter JS, Bambara RA, O'Reilly MA. The RNA surveillance protein SMG1 activates p53 in response to DNA double-strand breaks but not exogenously oxidized mRNA. Cell Cycle. 2011;10(15):2561-7. Epub 2011/06/28. doi: 10.4161/cc.10.15.16347. PubMed PMID: 21701263; PubMed Central PMCID: PMCPMC3180194.

51. Huntzinger E, Kashima I, Fauser M, Sauliere J, Izaurralde E. SMG6 is the catalytic endonuclease that cleaves mRNAs containing nonsense codons in metazoan. RNA. 2008;14(12):2609-17. Epub 2008/11/01. doi: 10.1261/rna.1386208. PubMed PMID: 18974281; PubMed Central PMCID: PMCPMC2590965.

52. Schneider C, Leung E, Brown J, Tollervey D. The N-terminal PIN domain of the exosome subunit Rrp44 harbors endonuclease activity and tethers Rrp44 to the yeast core exosome. Nucleic Acids Res. 2009;37(4):1127-40. Epub 2009/01/09. doi: 10.1093/nar/gkn1020. PubMed PMID: 19129231; PubMed Central PMCID: PMCPMC2651783.

53. Anders KR, Grimson A, Anderson P. SMG-5, required for C.elegans nonsense-mediated mRNA decay, associates with SMG-2 and protein phosphatase 2A. EMBO J. 2003;22(3):641-50. Epub 2003/01/30. doi: 10.1093/emboj/cdg056. PubMed PMID: 12554664; PubMed Central PMCID: PMCPMC140740.

54. Chiu SY, Serin G, Ohara O, Maquat LE. Characterization of human Smg5/7a: a protein with similarities to Caenorhabditis elegans SMG5 and SMG7 that functions in the dephosphorylation of Upf1. RNA. 2003;9(1):77-87. Epub 2003/01/30. doi:

10.1261/rna.2137903. PubMed PMID: 12554878; PubMed Central PMCID: PMCPMC1370372.

55. Ohnishi T, Yamashita A, Kashima I, Schell T, Anders KR, Grimson A, et al. Phosphorylation of hUPF1 induces formation of mRNA surveillance complexes containing hSMG-5 and hSMG-7. Mol Cell. 2003;12(5):1187-200. Epub 2003/11/26. doi: 10.1016/s1097-2765(03)00443-x. PubMed PMID: 14636577.

56. Okada-Katsuhata Y, Yamashita A, Kutsuzawa K, Izumi N, Hirahara F, Ohno S. N- and C-terminal Upf1 phosphorylations create binding platforms for SMG-6 and SMG-5:SMG-7 during NMD. Nucleic Acids Res. 2012;40(3):1251-66. Epub 2011/10/04. doi: 10.1093/nar/gkr791. PubMed PMID: 21965535; PubMed Central PMCID: PMCPMC3273798.

57. Franks TM, Singh G, Lykke-Andersen J. Upf1 ATPase-dependent mRNP disassembly is required for completion of nonsense- mediated mRNA decay. Cell. 2010;143(6):938-50. Epub 2010/12/15. doi: 10.1016/j.cell.2010.11.043. PubMed PMID: 21145460; PubMed Central PMCID: PMCPMC3357093.

58. Glavan F, Behm-Ansmant I, Izaurralde E, Conti E. Structures of the PIN domains of SMG6 and SMG5 reveal a nuclease within the mRNA surveillance complex. EMBO J. 2006;25(21):5117-25. Epub 2006/10/21. doi: 10.1038/sj.emboj.7601377. PubMed PMID: 17053788; PubMed Central PMCID: PMCPMC1630413.

59. Eberle AB, Lykke-Andersen S, Muhlemann O, Jensen TH. SMG6 promotes endonucleolytic cleavage of nonsense mRNA in human cells. Nat Struct Mol Biol. 2009;16(1):49-55. Epub 2008/12/09. doi: 10.1038/nsmb.1530. PubMed PMID: 19060897.

60. Singh G, Rebbapragada I, Lykke-Andersen J. A competition between stimulators and antagonists of Upf complex recruitment governs human nonsense-mediated mRNA

decay. PLoS Biol. 2008;6(4):e111. Epub 2008/05/02. doi: 10.1371/journal.pbio.0060111. PubMed PMID: 18447585; PubMed Central PMCID: PMCPMC2689706.

61.   Ivanov PV, Gehring NH, Kunz JB, Hentze MW, Kulozik AE. Interactions between UPF1, eRFs, PABP and the exon junction complex suggest an integrated model for mammalian NMD pathways. EMBO J. 2008;27(5):736-47. Epub 2008/02/08. doi: 10.1038/emboj.2008.17. PubMed PMID: 18256688; PubMed Central PMCID: PMCPMC2265754.

62.   Behm-Ansmant I, Gatfield D, Rehwinkel J, Hilgers V, Izaurralde E. A conserved role for cytoplasmic poly(A)-binding protein 1 (PABPC1) in nonsense-mediated mRNA decay. EMBO J. 2007;26(6):1591-601. Epub 2007/02/24. doi: 10.1038/sj.emboj.7601588. PubMed PMID: 17318186; PubMed Central PMCID: PMCPMC1829367.

63.   McIlwain DR, Pan Q, Reilly PT, Elia AJ, McCracken S, Wakeham AC, et al. Smg1 is required for embryogenesis and regulates diverse genes via alternative splicing coupled to nonsense-mediated mRNA decay. Proc Natl Acad Sci U S A. 2010;107(27):12186-91. doi: 10.1073/pnas.1007336107. PubMed PMID: 20566848; PubMed Central PMCID: PMCPMC2901484.

64.   Roberts TL, Ho U, Luff J, Lee CS, Apte SH, MacDonald KP, et al. Smg1 haploinsufficiency predisposes to tumor formation and inflammation. Proc Natl Acad Sci U S A. 2013;110(4):E285-94. doi: 10.1073/pnas.1215696110. PubMed PMID: 23277562; PubMed Central PMCID: PMCPMC3557096.

65.   Linde L, Kerem B. Introducing sense into nonsense in treatments of human genetic diseases. Trends Genet. 2008;24(11):552-63. doi: 10.1016/j.tig.2008.08.010. PubMed PMID: 18937996.

66.   Isken O, Maquat LE. The multiple lives of NMD factors: balancing roles in gene and genome regulation. Nat Rev Genet. 2008;9(9):699-712. doi: 10.1038/nrg2402.

PubMed PMID: 18679436; PubMed Central PMCID: PMCPMC3711694.

67. Usuki F, Yamashita A, Shiraishi T, Shiga A, Onodera O, Higuchi I, et al. Inhibition of SMG-8, a subunit of SMG-1 kinase, ameliorates nonsense-mediated mRNA decay-exacerbated mutant phenotypes without cytotoxicity. Proc Natl Acad Sci U S A. 2013;110(37):15037-42. doi: 10.1073/pnas.1300654110. PubMed PMID: 23983263; PubMed Central PMCID: PMCPMC3773753.

68. Inoue K, Khajavi M, Ohyama T, Hirabayashi S, Wilson J, Reggin JD, et al. Molecular mechanism for distinct neurological phenotypes conveyed by allelic truncating mutations. Nat Genet. 2004;36(4):361-9. doi: 10.1038/ng1322. PubMed PMID: 15004559.

69. Wachter A, Hartmann L. NMD: nonsense-mediated defense. Cell host & microbe. 2014;16(3):273-5. doi: 10.1016/j.chom.2014.08.015. PubMed PMID: 25211070.

70. Gloggnitzer J, Akimcheva S, Srinivasan A, Kusenda B, Riehs N, Stampfl H, et al. Nonsense-mediated mRNA decay modulates immune receptor levels to regulate plant antibacterial defense. Cell host & microbe. 2014;16(3):376-90. doi: 10.1016/j.chom.2014.08.010. PubMed PMID: 25211079.

71. Balistreri G, Horvath P, Schweingruber C, Zund D, McInerney G, Merits A, et al. The host nonsense-mediated mRNA decay pathway restricts Mammalian RNA virus replication. Cell host & microbe. 2014;16(3):403-11. doi: 10.1016/j.chom.2014.08.007. PubMed PMID: 25211080.

72. Garcia D, Garcia S, Voinnet O. Nonsense-mediated decay serves as a general viral restriction mechanism in plants. Cell host & microbe. 2014;16(3):391-402. doi: 10.1016/j.chom.2014.08.001. PubMed PMID: 25155460.

73. Usuki F, Yamashita A, Higuchi I, Ohnishi T, Shiraishi T, Osame M, et al. Inhibition of nonsense-mediated mRNA decay rescues the phenotype in Ullrich's disease. Ann

Neurol. 2004;55(5):740-4. doi: 10.1002/ana.20107. PubMed PMID: 15122717.

74. Furniss D, Critchley P, Giele H, Wilkie AO. Nonsense-mediated decay and the molecular pathogenesis of mutations in SALL1 and GLI3. Am J Med Genet A. 2007;143A(24):3150-60. doi: 10.1002/ajmg.a.32097. PubMed PMID: 18000979.

75. Hall GW, Thein S. Nonsense codon mutations in the terminal exon of the beta-globin gene are not associated with a reduction in beta-mRNA accumulation: a mechanism for the phenotype of dominant beta-thalassemia. Blood. 1994;83(8):2031-7. PubMed PMID: 8161774.

76. Brichta L, Garbes L, Jedrzejowska M, Grellscheid SN, Holker I, Zimmermann K, et al. Nonsense-mediated messenger RNA decay of survival motor neuron 1 causes spinal muscular atrophy. Hum Genet. 2008;123(2):141-53. doi: 10.1007/s00439-007-0455-7. PubMed PMID: 18172693.

77. Karam R, Carvalho J, Bruno I, Graziadio C, Senz J, Huntsman D, et al. The NMD mRNA surveillance pathway downregulates aberrant E-cadherin transcripts in gastric cancer cells and in CDH1 mutation carriers. Oncogene. 2008;27(30):4255-60. doi: 10.1038/onc.2008.62. PubMed PMID: 18427545.

78. Li A, Swift M. Mutations at the ataxia-telangiectasia locus and clinical phenotypes of A-T patients. Am J Med Genet. 2000;92(3):170-7. PubMed PMID: 10817650.

79. Yoshinaga M, Takeuchi O. Post-transcriptional control of immune responses and its potential application. Clin Transl Immunology. 2019;8(6):e1063. Epub 2019/06/27. doi: 10.1002/cti2.1063. PubMed PMID: 31236273; PubMed Central PMCID: PMCPMC6580065.

80. Khabar KS. Rapid transit in the immune cells: the role of mRNA turnover regulation. J Leukoc Biol. 2007;81(6):1335-44. Epub 2007/04/03. doi: 10.1189/jlb.0207109. PubMed PMID: 17400611; PubMed Central PMCID: PMCPMC7166898.

81. Al-Haj L, Khabar KS. Cloning of cytokine 3' untranslated regions and posttranscriptional assessment using cell-based GFP assay. Methods Mol Biol. 2012;820:91-104. Epub 2011/12/02. doi: 10.1007/978-1-61779-439-1_6. PubMed PMID: 22131027.

82. Schott J, Stoecklin G. Networks controlling mRNA decay in the immune system. Wiley Interdiscip Rev RNA. 2010;1(3):432-56. Epub 2011/10/01. doi: 10.1002/wrna.13. PubMed PMID: 21956941.

83. Shaw G, Kamen R. A conserved AU sequence from the 3' untranslated region of GM-CSF mRNA mediates selective mRNA degradation. Cell. 1986;46(5):659-67. Epub 1986/08/29. doi: 10.1016/0092-8674(86)90341-7. PubMed PMID: 3488815.

84. Beisang D, Bohjanen PR. Perspectives on the ARE as it turns 25 years old. Wiley Interdiscip Rev RNA. 2012;3(5):719-31. Epub 2012/06/27. doi: 10.1002/wrna.1125. PubMed PMID: 22733578; PubMed Central PMCID: PMCPMC4126804.

85. Ivanov P, Anderson P. Post-transcriptional regulatory networks in immunity. Immunol Rev. 2013;253(1):253-72. Epub 2013/04/05. doi: 10.1111/imr.12051. PubMed PMID: 23550651; PubMed Central PMCID: PMCPMC6989036.

86. Wang J, Guo Y, Chu H, Guan Y, Bi J, Wang B. Multiple functions of the RNA-binding protein HuR in cancer progression, treatment responses and prognosis. Int J Mol Sci. 2013;14(5):10015-41. Epub 2013/05/15. doi: 10.3390/ijms140510015. PubMed PMID: 23665903; PubMed Central PMCID: PMCPMC3676826.

87. Hao S, Baltimore D. The stability of mRNA influences the temporal order of the induction of genes encoding inflammatory molecules. Nat Immunol. 2009;10(3):281-8. doi: 10.1038/ni.1699. PubMed PMID: 19198593; PubMed Central PMCID: PMCPMC2775040.

88. Peng SS, Chen CY, Xu N, Shyu AB. RNA stabilization by the AU-rich element

binding protein, HuR, an ELAV protein. EMBO J. 1998;17(12):3461-70. Epub 1998/06/17. doi: 10.1093/emboj/17.12.3461. PubMed PMID: 9628881; PubMed Central PMCID: PMCPMC1170682.

89. Chen YL, Huang YL, Lin NY, Chen HC, Chiu WC, Chang CJ. Differential regulation of ARE-mediated TNFalpha and IL-1beta mRNA stability by lipopolysaccharide in RAW264.7 cells. Biochem Biophys Res Commun. 2006;346(1):160-8. Epub 2006/06/09. doi: 10.1016/j.bbrc.2006.05.093. PubMed PMID: 16759646.

90. Taylor GA, Carballo E, Lee DM, Lai WS, Thompson MJ, Patel DD, et al. A pathogenetic role for TNF alpha in the syndrome of cachexia, arthritis, and autoimmunity resulting from tristetraprolin (TTP) deficiency. Immunity. 1996;4(5):445-54. Epub 1996/05/01. doi: 10.1016/s1074-7613(00)80411-2. PubMed PMID: 8630730.

91. Carballo E, Lai WS, Blackshear PJ. Feedback inhibition of macrophage tumor necrosis factor-alpha production by tristetraprolin. Science. 1998;281(5379):1001-5. Epub 1998/08/14. doi: 10.1126/science.281.5379.1001. PubMed PMID: 9703499.

92. Carballo E, Lai WS, Blackshear PJ. Evidence that tristetraprolin is a physiological regulator of granulocyte-macrophage colony-stimulating factor messenger RNA deadenylation and stability. Blood. 2000;95(6):1891-9. Epub 2000/03/09. PubMed PMID: 10706852.

93. Lu JY, Sadri N, Schneider RJ. Endotoxic shock in AUF1 knockout mice mediated by failure to degrade proinflammatory cytokine mRNAs. Genes Dev. 2006;20(22):3174-84. Epub 2006/11/07. doi: 10.1101/gad.1467606. PubMed PMID: 17085481; PubMed Central PMCID: PMCPMC1635151.

94. Sadri N, Schneider RJ. Auf1/Hnrnpd-deficient mice develop pruritic inflammatory skin disease. J Invest Dermatol. 2009;129(3):657-70. Epub 2008/10/03. doi:

10.1038/jid.2008.298. PubMed PMID: 18830269; PubMed Central PMCID: PMCPMC4074411.

95. Stoecklin G, Stubbs T, Kedersha N, Wax S, Rigby WF, Blackwell TK, et al. MK2-induced tristetraprolin:14-3-3 complexes prevent stress granule association and ARE-mRNA decay. EMBO J. 2004;23(6):1313-24. Epub 2004/03/12. doi: 10.1038/sj.emboj.7600163. PubMed PMID: 15014438; PubMed Central PMCID: PMCPMC381421.

96. Perry RP, Kelley DE, Friderici K, Rottman F. The methylated constituents of L cell messenger RNA: evidence for an unusual cluster at the 5' terminus. Cell. 1975;4(4):387-94. PubMed PMID: 1168101.

97. Wei CM, Gershowitz A, Moss B. Methylated nucleotides block 5' terminus of HeLa cell messenger RNA. Cell. 1975;4(4):379-86. PubMed PMID: 164293.

98. Dubin DT, Taylor RH. The methylation state of poly A-containing messenger RNA from cultured hamster cells. Nucleic Acids Res. 1975;2(10):1653-68. PubMed PMID: 1187339; PubMed Central PMCID: PMCPMC343535.

99. Meyer KD, Saletore Y, Zumbo P, Elemento O, Mason CE, Jaffrey SR. Comprehensive analysis of mRNA methylation reveals enrichment in 3' UTRs and near stop codons. Cell. 2012;149(7):1635-46. doi: 10.1016/j.cell.2012.05.003. PubMed PMID: 22608085; PubMed Central PMCID: PMCPMC3383396.

100. Lewis BP, Burge CB, Bartel DP. Conserved seed pairing, often flanked by adenosines, indicates that thousands of human genes are microRNA targets. Cell. 2005;120(1):15-20. doi: 10.1016/j.cell.2004.12.035. PubMed PMID: 15652477.

101. Meyer KD, Jaffrey SR. Rethinking m(6)A Readers, Writers, and Erasers. Annu Rev Cell Dev Biol. 2017;33:319-42. Epub 2017/08/02. doi: 10.1146/annurev-cellbio-100616-060758. PubMed PMID: 28759256; PubMed Central PMCID: PMCPMC5963928.

102. Liu J, Yue Y, Han D, Wang X, Fu Y, Zhang L, et al. A METTL3-METTL14 complex mediates mammalian nuclear RNA N6-adenosine methylation. Nat Chem Biol. 2014;10(2):93-5. doi: 10.1038/nchembio.1432. PubMed PMID: 24316715; PubMed Central PMCID: PMCPMC3911877.

103. Zhao BS, Roundtree IA, He C. Post-transcriptional gene regulation by mRNA modifications. Nat Rev Mol Cell Biol. 2017;18(1):31-42. Epub 2016/11/04. doi: 10.1038/nrm.2016.132. PubMed PMID: 27808276; PubMed Central PMCID: PMCPMC5167638.

104. Mauer J, Luo X, Blanjoie A, Jiao X, Grozhik AV, Patil DP, et al. Reversible methylation of m(6)Am in the 5' cap controls mRNA stability. Nature. 2017;541(7637):371-5. Epub 2016/12/22. doi: 10.1038/nature21022. PubMed PMID: 28002401; PubMed Central PMCID: PMCPMC5513158.

105. Zheng G, Dahl JA, Niu Y, Fedorcsak P, Huang CM, Li CJ, et al. ALKBH5 is a mammalian RNA demethylase that impacts RNA metabolism and mouse fertility. Mol Cell. 2013;49(1):18-29. Epub 2012/11/28. doi: 10.1016/j.molcel.2012.10.015. PubMed PMID: 23177736; PubMed Central PMCID: PMCPMC3646334.

106. Jia G, Fu Y, Zhao X, Dai Q, Zheng G, Yang Y, et al. N6-methyladenosine in nuclear RNA is a major substrate of the obesity-associated FTO. Nat Chem Biol. 2011;7(12):885-7. Epub 2011/10/18. doi: 10.1038/nchembio.687. PubMed PMID: 22002720; PubMed Central PMCID: PMCPMC3218240.

107. Roundtree IA, Evans ME, Pan T, He C. Dynamic RNA Modifications in Gene Expression Regulation. Cell. 2017;169(7):1187-200. Epub 2017/06/18. doi: 10.1016/j.cell.2017.05.045. PubMed PMID: 28622506; PubMed Central PMCID: PMCPMC5657247.

108. Bokar JA, Shambaugh ME, Polayes D, Matera AG, Rottman FM. Purification and

cDNA cloning of the AdoMet-binding subunit of the human mRNA (N6-adenosine)-methyltransferase. RNA. 1997;3(11):1233-47. PubMed PMID: 9409616; PubMed Central PMCID: PMCPMC1369564.

109. Meng J, Lu Z, Liu H, Zhang L, Zhang S, Chen Y, et al. A protocol for RNA methylation differential analysis with MeRIP-Seq data and exomePeak R/Bioconductor package. Methods. 2014;69(3):274-81. doi: 10.1016/j.ymeth.2014.06.008. PubMed PMID: 24979058; PubMed Central PMCID: PMCPMC4194139.

110. Ping XL, Sun BF, Wang L, Xiao W, Yang X, Wang WJ, et al. Mammalian WTAP is a regulatory subunit of the RNA N6-methyladenosine methyltransferase. Cell Res. 2014;24(2):177-89. doi: 10.1038/cr.2014.3. PubMed PMID: 24407421; PubMed Central PMCID: PMCPMC3915904.

111. Schwartz S, Mumbach MR, Jovanovic M, Wang T, Maciag K, Bushkin GG, et al. Perturbation of m6A writers reveals two distinct classes of mRNA methylation at internal and 5' sites. Cell Rep. 2014;8(1):284-96. doi: 10.1016/j.celrep.2014.05.048. PubMed PMID: 24981863; PubMed Central PMCID: PMCPMC4142486.

112. Patil DP, Chen CK, Pickering BF, Chow A, Jackson C, Guttman M, et al. m(6)A RNA methylation promotes XIST-mediated transcriptional repression. Nature. 2016;537(7620):369-73. doi: 10.1038/nature19342. PubMed PMID: 27602518; PubMed Central PMCID: PMCPMC5509218.

113. Pendleton KE, Chen B, Liu K, Hunter OV, Xie Y, Tu BP, et al. The U6 snRNA m(6)A Methyltransferase METTL16 Regulates SAM Synthetase Intron Retention. Cell. 2017;169(5):824-35 e14. doi: 10.1016/j.cell.2017.05.003. PubMed PMID: 28525753; PubMed Central PMCID: PMCPMC5502809.

114. Patil DP, Pickering BF, Jaffrey SR. Reading m(6)A in the Transcriptome: m(6)A-Binding Proteins. Trends Cell Biol. 2018;28(2):113-27. Epub 2017/11/07. doi:

10.1016/j.tcb.2017.10.001. PubMed PMID: 29103884; PubMed Central PMCID: PMCPMC5794650.

115. Alarcon CR, Goodarzi H, Lee H, Liu X, Tavazoie S, Tavazoie SF. HNRNPA2B1 Is a Mediator of m(6)A-Dependent Nuclear RNA Processing Events. Cell. 2015;162(6):1299-308. doi: 10.1016/j.cell.2015.08.011. PubMed PMID: 26321680; PubMed Central PMCID: PMCPMC4673968.

116. Kaufmann SHE, Medzhitov R, Gordon S. The innate immune response to infection. Washington, D.C.: ASM Press; 2004. xv, 465 p. p.

117. Winkler R, Gillis E, Lasman L, Safra M, Geula S, Soyris C, et al. Publisher Correction: m6A modification controls the innate immune response to infection by targeting type I interferons. Nat Immunol. 2019;20(2):243. Epub 2019/01/13. doi: 10.1038/s41590-019-0314-4. PubMed PMID: 30635652.

118. Rubio RM, Depledge DP, Bianco C, Thompson L, Mohr I. RNA m(6) A modification enzymes shape innate responses to DNA by regulating interferon beta. Genes Dev. 2018;32(23-24):1472-84. Epub 2018/11/23. doi: 10.1101/gad.319475.118. PubMed PMID: 30463905; PubMed Central PMCID: PMCPMC6295168.

119. Motwani M, Pesiridis S, Fitzgerald KA. DNA sensing by the cGAS-STING pathway in health and disease. Nat Rev Genet. 2019;20(11):657-74. Epub 2019/07/31. doi: 10.1038/s41576-019-0151-1. PubMed PMID: 31358977.

120. Yang H, Wang H, Ren J, Chen Q, Chen ZJ. cGAS is essential for cellular senescence. Proc Natl Acad Sci U S A. 2017;114(23):E4612-E20. Epub 2017/05/24. doi: 10.1073/pnas.1705499114. PubMed PMID: 28533362; PubMed Central PMCID: PMCPMC5468617.

121. Doidge R, Mittal S, Aslam A, Winkler GS. Deadenylation of cytoplasmic mRNA by the mammalian Ccr4-Not complex. Biochem Soc Trans. 2012;40(4):896-901. doi:

10.1042/BST20120074. PubMed PMID: 22817755.

122. Wahle E, Winkler GS. RNA decay machines: deadenylation by the Ccr4-not and Pan2-Pan3 complexes. Biochim Biophys Acta. 2013;1829(6-7):561-70. doi: 10.1016/j.bbagrm.2013.01.003. PubMed PMID: 23337855.

123. Coller JM, Gray NK, Wickens MP. mRNA stabilization by poly(A) binding protein is independent of poly(A) and requires translation. Genes Dev. 1998;12(20):3226-35. Epub 1998/10/24. doi: 10.1101/gad.12.20.3226. PubMed PMID: 9784497; PubMed Central PMCID: PMCPMC317214.

124. Sheth U, Parker R. Decapping and decay of messenger RNA occur in cytoplasmic processing bodies. Science. 2003;300(5620):805-8. Epub 2003/05/06. doi: 10.1126/science.1082320. PubMed PMID: 12730603; PubMed Central PMCID: PMCPMC1876714.

125. Brown JA, Roberts TL, Richards R, Woods R, Birrell G, Lim YC, et al. A novel role for hSMG-1 in stress granule formation. Mol Cell Biol. 2011;31(22):4417-29. doi: 10.1128/MCB.05987-11. PubMed PMID: 21911475; PubMed Central PMCID: PMCPMC3209244.

126. Caponigro G, Parker R. Multiple functions for the poly(A)-binding protein in mRNA decapping and deadenylation in yeast. Genes Dev. 1995;9(19):2421-32. Epub 1995/10/01. doi: 10.1101/gad.9.19.2421. PubMed PMID: 7557393.

127. Morrissey JP, Deardorff JA, Hebron C, Sachs AB. Decapping of stabilized, polyadenylated mRNA in yeast pab1 mutants. Yeast. 1999;15(8):687-702. Epub 1999/07/07. doi: 10.1002/(SICI)1097-0061(19990615)15:8<687::AID-YEA412>3.0.CO;2-L. PubMed PMID: 10392446.

128. Wilusz CJ, Gao M, Jones CL, Wilusz J, Peltz SW. Poly(A)-binding proteins regulate both mRNA deadenylation and decapping in yeast cytoplasmic extracts. RNA.

2001;7(10):1416-24. Epub 2001/10/30. PubMed PMID: 11680846; PubMed Central PMCID: PMCPMC1370185.

129. Teixeira D, Sheth U, Valencia-Sanchez MA, Brengues M, Parker R. Processing bodies require RNA for assembly and contain nontranslating mRNAs. RNA. 2005;11(4):371-82. Epub 2005/02/11. doi: 10.1261/rna.7258505. PubMed PMID: 15703442; PubMed Central PMCID: PMCPMC1370727.

130. Lai HC, James A, Luff J, De Souza P, Quek H, Ho U, et al. Regulation of RNA degradation pathways during the lipopolysaccharide response in Macrophages. J Leukoc Biol. 2020. Epub 2020/08/24. doi: 10.1002/JLB.2AB0420-151RR. PubMed PMID: 32829531.

131. Singh RK, Cooper TA. Pre-mRNA splicing in disease and therapeutics. Trends Mol Med. 2012;18(8):472-82. Epub 2012/07/24. doi: 10.1016/j.molmed.2012.06.006. PubMed PMID: 22819011; PubMed Central PMCID: PMCPMC3411911.

132. Lopez-Bigas N, Audit B, Ouzounis C, Parra G, Guigo R. Are splicing mutations the most frequent cause of hereditary disease? FEBS Lett. 2005;579(9):1900-3. Epub 2005/03/29. doi: 10.1016/j.febslet.2005.02.047. PubMed PMID: 15792793.

133. Ritter SY, Subbaiah R, Bebek G, Crish J, Scanzello CR, Krastins B, et al. Proteomic analysis of synovial fluid from the osteoarthritic knee: comparison with transcriptome analyses of joint tissues. Arthritis Rheum. 2013;65(4):981-92. Epub 2013/02/13. doi: 10.1002/art.37823. PubMed PMID: 23400684; PubMed Central PMCID: PMCPMC3618606.

134. Nuhrenberg TG, Langwieser N, Binder H, Kurz T, Stratz C, Kienzle RP, et al. Transcriptome analysis in patients with progressive coronary artery disease: identification of differential gene expression in peripheral blood. J Cardiovasc Transl Res. 2013;6(1):81-93. Epub 2012/11/29. doi: 10.1007/s12265-012-9420-5. PubMed PMID:

23188564.

135. Evsyukova I, Somarelli JA, Gregory SG, Garcia-Blanco MA. Alternative splicing in multiple sclerosis and other autoimmune diseases. RNA Biol. 2010;7(4):462-73. Epub 2010/07/20. doi: 10.4161/rna.7.4.12301. PubMed PMID: 20639696; PubMed Central PMCID: PMCPMC3070910.

136. Douglas KB, Windels DC, Zhao J, Gadeliya AV, Wu H, Kaufman KM, et al. Complement receptor 2 polymorphisms associated with systemic lupus erythematosus modulate alternative splicing. Genes Immun. 2009;10(5):457-69. Epub 2009/04/24. doi: 10.1038/gene.2009.27. PubMed PMID: 19387458; PubMed Central PMCID: PMCPMC2714407.

137. Kan SH, Mancini G, Gallagher G. Identification and characterization of multiple splice forms of the human interleukin-23 receptor alpha chain in mitogen-activated leukocytes. Genes Immun. 2008;9(7):631-9. Epub 2008/08/30. doi: 10.1038/gene.2008.64. PubMed PMID: 18754016.

138. Tuller T, Atar S, Ruppin E, Gurevich M, Achiron A. Common and specific signatures of gene expression and protein-protein interactions in autoimmune diseases. Genes Immun. 2013;14(2):67-82. Epub 2012/11/30. doi: 10.1038/gene.2012.55. PubMed PMID: 23190644.

139. Hozumi N, Tonegawa S. Evidence for somatic rearrangement of immunoglobulin genes coding for variable and constant regions. 1976 [classical article]. J Immunol. 2004;173(7):4260-4. Epub 2004/09/24. PubMed PMID: 15383553.

140. Tonegawa S, Steinberg C, Dube S, Bernardini A. Evidence for somatic generation of antibody diversity. Proc Natl Acad Sci U S A. 1974;71(10):4027-31. Epub 1974/10/01. doi: 10.1073/pnas.71.10.4027. PubMed PMID: 4215074; PubMed Central PMCID: PMCPMC434321.

141. Dranoff G. Cytokines in cancer pathogenesis and cancer therapy. Nat Rev Cancer. 2004;4(1):11-22. Epub 2004/01/07. doi: 10.1038/nrc1252. PubMed PMID: 14708024.

142. Clark R, Kupper T. Old meets new: the interaction between innate and adaptive immunity. J Invest Dermatol. 2005;125(4):629-37. Epub 2005/09/28. doi: 10.1111/j.0022-202X.2005.23856.x. PubMed PMID: 16185260.

143. Haseeb M, Anwar MA, Choi S. Molecular Interactions Between Innate and Adaptive Immune Cells in Chronic Lymphocytic Leukemia and Their Therapeutic Implications. Front Immunol. 2018;9:2720. Epub 2018/12/14. doi: 10.3389/fimmu.2018.02720. PubMed PMID: 30542344; PubMed Central PMCID: PMCPMC6277854.

144. Sasmono RT, Oceandy D, Pollard JW, Tong W, Pavli P, Wainwright BJ, et al. A macrophage colony-stimulating factor receptor-green fluorescent protein transgene is expressed throughout the mononuclear phagocyte system of the mouse. Blood. 2003;101(3):1155-63. Epub 2002/10/24. doi: 10.1182/blood-2002-02-0569. PubMed PMID: 12393599.

145. Langermans JA, Van der Hulst ME, Nibbering PH, Hiemstra PS, Fransen L, Van Furth R. IFN-gamma-induced L-arginine-dependent toxoplasmastatic activity in murine peritoneal macrophages is mediated by endogenous tumor necrosis factor-alpha. J Immunol. 1992;148(2):568-74. Epub 1992/01/15. PubMed PMID: 1729374.

146. Nathan C. Metchnikoff's Legacy in 2008. Nat Immunol. 2008;9(7):695-8. Epub 2008/06/20. doi: 10.1038/ni0708-695. PubMed PMID: 18563074.

147. Nahrendorf M, Swirski FK. Abandoning M1/M2 for a Network Model of Macrophage Function. Circ Res. 2016;119(3):414-7. Epub 2016/07/28. doi: 10.1161/CIRCRESAHA.116.309194. PubMed PMID: 27458196; PubMed Central PMCID: PMCPMC4965179.

148. Nathan CF, Murray HW, Wiebe ME, Rubin BY. Identification of interferon-gamma

as the lymphokine that activates human macrophage oxidative metabolism and antimicrobial activity. J Exp Med. 1983;158(3):670-89. Epub 1983/09/01. doi: 10.1084/jem.158.3.670. PubMed PMID: 6411853; PubMed Central PMCID: PMCPMC2187114.

149. Gordon S, Martinez FO. Alternative activation of macrophages: mechanism and functions. Immunity. 2010;32(5):593-604. Epub 2010/06/01. doi: 10.1016/j.immuni.2010.05.007. PubMed PMID: 20510870.

150. Atri C, Guerfali FZ, Laouini D. Role of Human Macrophage Polarization in Inflammation during Infectious Diseases. Int J Mol Sci. 2018;19(6). Epub 2018/06/21. doi: 10.3390/ijms19061801. PubMed PMID: 29921749; PubMed Central PMCID: PMCPMC6032107.

151. Mosser DM, Edwards JP. Exploring the full spectrum of macrophage activation. Nat Rev Immunol. 2008;8(12):958-69. Epub 2008/11/26. doi: 10.1038/nri2448. PubMed PMID: 19029990; PubMed Central PMCID: PMCPMC2724991.

152. Biswas SK, Mantovani A. Macrophage plasticity and interaction with lymphocyte subsets: cancer as a paradigm. Nat Immunol. 2010;11(10):889-96. Epub 2010/09/22. doi: 10.1038/ni.1937. PubMed PMID: 20856220.

153. Grohmann U, Belladonna ML, Vacca C, Bianchi R, Fallarino F, Orabona C, et al. Positive regulatory role of IL-12 in macrophages and modulation by IFN-gamma. J Immunol. 2001;167(1):221-7. Epub 2001/06/22. doi: 10.4049/jimmunol.167.1.221. PubMed PMID: 11418652.

154. Armstrong L, Jordan N, Millar A. Interleukin 10 (IL-10) regulation of tumour necrosis factor alpha (TNF-alpha) from human alveolar macrophages and peripheral blood monocytes. Thorax. 1996;51(2):143-9. Epub 1996/02/01. doi: 10.1136/thx.51.2.143. PubMed PMID: 8711645; PubMed Central PMCID:

PMCPMC473022.

155. Albina JE, Mills CD, Henry WL, Jr., Caldwell MD. Temporal expression of different pathways of 1-arginine metabolism in healing wounds. J Immunol. 1990;144(10):3877-80. Epub 1990/05/15. PubMed PMID: 2332635.

156. Hibbs JB, Jr., Vavrin Z, Taintor RR. L-arginine is required for expression of the activated macrophage effector mechanism causing selective metabolic inhibition in target cells. J Immunol. 1987;138(2):550-65. Epub 1987/01/15. PubMed PMID: 2432129.

157. Mills CD. Macrophage arginine metabolism to ornithine/urea or nitric oxide/citrulline: a life or death issue. Crit Rev Immunol. 2001;21(5):399-425. Epub 2002/04/11. PubMed PMID: 11942557.

158. Mills CD. M1 and M2 Macrophages: Oracles of Health and Disease. Crit Rev Immunol. 2012;32(6):463-88. Epub 2013/02/23. doi: 10.1615/critrevimmunol.v32.i6.10. PubMed PMID: 23428224.

159. Li Y, Karlin A, Loike JD, Silverstein SC. Determination of the critical concentration of neutrophils required to block bacterial growth in tissues. J Exp Med. 2004;200(5):613-22. Epub 2004/09/09. doi: 10.1084/jem.20040725. PubMed PMID: 15353554; PubMed Central PMCID: PMCPMC2212745.

160. Beyer M, Mallmann MR, Xue J, Staratschek-Jox A, Vorholt D, Krebs W, et al. High-resolution transcriptome of human macrophages. PLoS One. 2012;7(9):e45466. Epub 2012/10/03. doi: 10.1371/journal.pone.0045466. PubMed PMID: 23029029; PubMed Central PMCID: PMCPMC3448669.

161. Vogel DY, Glim JE, Stavenuiter AW, Breur M, Heijnen P, Amor S, et al. Human macrophage polarization in vitro: maturation and activation methods compared. Immunobiology. 2014;219(9):695-703. Epub 2014/06/12. doi: 10.1016/j.imbio.2014.05.002. PubMed PMID: 24916404.

162. Italiani P, Mazza EM, Lucchesi D, Cifola I, Gemelli C, Grande A, et al. Transcriptomic profiling of the development of the inflammatory response in human monocytes in vitro. PLoS One. 2014;9(2):e87680. Epub 2014/02/06. doi: 10.1371/journal.pone.0087680. PubMed PMID: 24498352; PubMed Central PMCID: PMCPMC3912012.

163. Martinez FO, Gordon S, Locati M, Mantovani A. Transcriptional profiling of the human monocyte-to-macrophage differentiation and polarization: new molecules and patterns of gene expression. J Immunol. 2006;177(10):7303-11. Epub 2006/11/04. doi: 10.4049/jimmunol.177.10.7303. PubMed PMID: 17082649.

164. Vogel DY, Vereyken EJ, Glim JE, Heijnen PD, Moeton M, van der Valk P, et al. Macrophages in inflammatory multiple sclerosis lesions have an intermediate activation status. J Neuroinflammation. 2013;10:35. Epub 2013/03/05. doi: 10.1186/1742-2094-10-35. PubMed PMID: 23452918; PubMed Central PMCID: PMCPMC3610294.

165. Ambarus CA, Noordenbos T, de Hair MJ, Tak PP, Baeten DL. Intimal lining layer macrophages but not synovial sublining macrophages display an IL-10 polarized-like phenotype in chronic synovitis. Arthritis Res Ther. 2012;14(2):R74. Epub 2012/04/13. doi: 10.1186/ar3796. PubMed PMID: 22494514; PubMed Central PMCID: PMCPMC3446447.

166.Tarique AA, Logan J, Thomas E, Holt PG, Sly PD, Fantino E. Phenotypic, functional, and plasticity features of classical and alternatively activated human macrophages. Am J Respir Cell Mol Biol. 2015;53(5):676-88. Epub 2015/04/15. doi: 10.1165/rcmb.2015-0012OC. PubMed PMID: 25870903.

167. Verreck FA, de Boer T, Langenberg DM, Hoeve MA, Kramer M, Vaisberg E, et al. Human IL-23-producing type 1 macrophages promote but IL-10-producing type 2 macrophages subvert immunity to (myco)bacteria. Proc Natl Acad Sci U S A.

2004;101(13):4560-5. Epub 2004/04/09. doi: 10.1073/pnas.0400983101. PubMed PMID: 15070757; PubMed Central PMCID: PMCPMC384786.

168. Verreck FA, de Boer T, Langenberg DM, van der Zanden L, Ottenhoff TH. Phenotypic and functional profiling of human proinflammatory type-1 and anti-inflammatory type-2 macrophages in response to microbial antigens and IFN-gamma- and CD40L-mediated costimulation. J Leukoc Biol. 2006;79(2):285-93. Epub 2005/12/07. doi: 10.1189/jlb.0105015. PubMed PMID: 16330536.

169. Kawasaki T, Kawai T. Toll-like receptor signaling pathways. Front Immunol. 2014;5:461. Epub 2014/10/14. doi: 10.3389/fimmu.2014.00461. PubMed PMID: 25309543; PubMed Central PMCID: PMCPMC4174766.

170. Adamia S, Crainie M, Kriangkum J, Mant MJ, Belch AR, Pilarski LM. Abnormal expression of hyaluronan synthases in patients with Waldenstrom's macroglobulimenia. Semin Oncol. 2003;30(2):165-8. doi: 10.1053/sonc.2003.50042. PubMed PMID: 12720129.

171. Cai X, Chiu YH, Chen ZJ. The cGAS-cGAMP-STING pathway of cytosolic DNA sensing and signaling. Mol Cell. 2014;54(2):289-96. Epub 2014/04/29. doi: 10.1016/j.molcel.2014.03.040. PubMed PMID: 24766893.

172. Bell JK, Mullen GE, Leifer CA, Mazzoni A, Davies DR, Segal DM. Leucine-rich repeats and pathogen recognition in Toll-like receptors. Trends Immunol. 2003;24(10):528-33. Epub 2003/10/14. doi: 10.1016/s1471-4906(03)00242-4. PubMed PMID: 14552836.

173. O'Neill LA, Greene C. Signal transduction pathways activated by the IL-1 receptor family: ancient signaling machinery in mammals, insects, and plants. J Leukoc Biol. 1998;63(6):650-7. Epub 1998/06/10. PubMed PMID: 9620655.

174. Kawai T, Akira S. The role of pattern-recognition receptors in innate immunity:

update on Toll-like receptors. Nat Immunol. 2010;11(5):373-84. Epub 2010/04/21. doi: 10.1038/ni.1863. PubMed PMID: 20404851.

175. Celhar T, Magalhaes R, Fairhurst AM. TLR7 and TLR9 in SLE: when sensing self goes wrong. Immunol Res. 2012;53(1-3):58-77. Epub 2012/03/22. doi: 10.1007/s12026-012-8270-1. PubMed PMID: 22434514.

176. Ozinsky A, Underhill DM, Fontenot JD, Hajjar AM, Smith KD, Wilson CB, et al. The repertoire for pattern recognition of pathogens by the innate immune system is defined by cooperation between toll-like receptors. Proc Natl Acad Sci U S A. 2000;97(25):13766-71. Epub 2000/11/30. doi: 10.1073/pnas.250476497. PubMed PMID: 11095740; PubMed Central PMCID: PMCPMC17650.

177. Hayashi F, Smith KD, Ozinsky A, Hawn TR, Yi EC, Goodlett DR, et al. The innate immune response to bacterial flagellin is mediated by Toll-like receptor 5. Nature. 2001;410(6832):1099-103. Epub 2001/04/27. doi: 10.1038/35074106. PubMed PMID: 11323673.

178. Blasius AL, Beutler B. Intracellular toll-like receptors. Immunity. 2010;32(3):305-15. Epub 2010/03/30. doi: 10.1016/j.immuni.2010.03.012. PubMed PMID: 20346772.

179. Alexopoulou L, Holt AC, Medzhitov R, Flavell RA. Recognition of double-stranded RNA and activation of NF-kappaB by Toll-like receptor 3. Nature. 2001;413(6857):732-8. Epub 2001/10/19. doi: 10.1038/35099560. PubMed PMID: 11607032.

180. Heil F, Hemmi H, Hochrein H, Ampenberger F, Kirschning C, Akira S, et al. Species-specific recognition of single-stranded RNA via toll-like receptor 7 and 8. Science. 2004;303(5663):1526-9. Epub 2004/02/21. doi: 10.1126/science.1093620. PubMed PMID: 14976262.

181. Hemmi H, Kaisho T, Takeuchi O, Sato S, Sanjo H, Hoshino K, et al. Small anti-viral compounds activate immune cells via the TLR7 MyD88-dependent signaling pathway.

Nat Immunol. 2002;3(2):196-200. Epub 2002/01/29. doi: 10.1038/ni758. PubMed PMID: 11812998.

182. Hemmi H, Takeuchi O, Kawai T, Kaisho T, Sato S, Sanjo H, et al. A Toll-like receptor recognizes bacterial DNA. Nature. 2000;408(6813):740-5. Epub 2000/12/29. doi: 10.1038/35047123. PubMed PMID: 11130078.

183. Yarovinsky F, Zhang D, Andersen JF, Bannenberg GL, Serhan CN, Hayden MS, et al. TLR11 activation of dendritic cells by a protozoan profilin-like protein. Science. 2005;308(5728):1626-9. Epub 2005/04/30. doi: 10.1126/science.1109893. PubMed PMID: 15860593.

184. Koblansky AA, Jankovic D, Oh H, Hieny S, Sungnak W, Mathur R, et al. Recognition of profilin by Toll-like receptor 12 is critical for host resistance to Toxoplasma gondii. Immunity. 2013;38(1):119-30. Epub 2012/12/19. doi: 10.1016/j.immuni.2012.09.016. PubMed PMID: 23246311; PubMed Central PMCID: PMCPMC3601573.

185. Oldenburg M, Kruger A, Ferstl R, Kaufmann A, Nees G, Sigmund A, et al. TLR13 recognizes bacterial 23S rRNA devoid of erythromycin resistance-forming modification. Science. 2012;337(6098):1111-5. Epub 2012/07/24. doi: 10.1126/science.1220363. PubMed PMID: 22821982.

186. Taylor KR, Trowbridge JM, Rudisill JA, Termeer CC, Simon JC, Gallo RL. Hyaluronan fragments stimulate endothelial recognition of injury through TLR4. J Biol Chem. 2004;279(17):17079-84. Epub 2004/02/07. doi: 10.1074/jbc.M310859200. PubMed PMID: 14764599.

187. Frantz S, Kobzik L, Kim YD, Fukazawa R, Medzhitov R, Lee RT, et al. Toll4 (TLR4) expression in cardiac myocytes in normal and failing myocardium. J Clin Invest. 1999;104(3):271-80. Epub 1999/08/03. doi: 10.1172/JCI6709. PubMed PMID: 10430608;

PubMed Central PMCID: PMCPMC408420.

188. O'Neill LA, Bowie AG. The family of five: TIR-domain-containing adaptors in Toll-like receptor signalling. Nat Rev Immunol. 2007;7(5):353-64. Epub 2007/04/26. doi: 10.1038/nri2079. PubMed PMID: 17457343.

189. Luo L, Lucas RM, Liu L, Stow JL. Signalling, sorting and scaffolding adaptors for Toll-like receptors. J Cell Sci. 2019;133(5). Epub 2020/01/01. doi: 10.1242/jcs.239194. PubMed PMID: 31889021.

190. Viriyakosol S, Tobias PS, Kitchens RL, Kirkland TN. MD-2 binds to bacterial lipopolysaccharide. J Biol Chem. 2001;276(41):38044-51. Epub 2001/08/14. doi: 10.1074/jbc.M105228200. PubMed PMID: 11500507.

191. Zanoni I, Ostuni R, Marek LR, Barresi S, Barbalat R, Barton GM, et al. CD14 controls the LPS-induced endocytosis of Toll-like receptor 4. Cell. 2011;147(4):868-80. Epub 2011/11/15. doi: 10.1016/j.cell.2011.09.051. PubMed PMID: 22078883; PubMed Central PMCID: PMCPMC3217211.

192. Barton GM, Medzhitov R. Toll-like receptor signaling pathways. Science. 2003;300(5625):1524-5. Epub 2003/06/07. doi: 10.1126/science.1085536. PubMed PMID: 12791976.

193. Deguine J, Barton GM. MyD88: a central player in innate immune signaling. F1000Prime Rep. 2014;6:97. Epub 2015/01/13. doi: 10.12703/P6-97. PubMed PMID: 25580251; PubMed Central PMCID: PMCPMC4229726.

194. Akira S, Hoshino K. Myeloid differentiation factor 88-dependent and -independent pathways in toll-like receptor signaling. J Infect Dis. 2003;187 Suppl 2:S356-63. Epub 2003/06/07. doi: 10.1086/374749. PubMed PMID: 12792852.

195. Zughaier SM, Zimmer SM, Datta A, Carlson RW, Stephens DS. Differential induction of the toll-like receptor 4-MyD88-dependent and -independent signaling

pathways by endotoxins. Infect Immun. 2005;73(5):2940-50. Epub 2005/04/23. doi: 10.1128/IAI.73.5.2940-2950.2005. PubMed PMID: 15845500; PubMed Central PMCID: PMCPMC1087371.

196. Takeda K, Akira S. TLR signaling pathways. Semin Immunol. 2004;16(1):3-9. Epub 2004/01/31. doi: 10.1016/j.smim.2003.10.003. PubMed PMID: 14751757.

197. Yamamoto M, Akira S. [TIR domain--containing adaptors regulate TLR-mediated signaling pathways]. Nihon Rinsho. 2004;62(12):2197-203. Epub 2004/12/16. PubMed PMID: 15597785.

198. Kawai T, Adachi O, Ogawa T, Takeda K, Akira S. Unresponsiveness of MyD88-deficient mice to endotoxin. Immunity. 1999;11(1):115-22. Epub 1999/08/06. doi: 10.1016/s1074-7613(00)80086-2. PubMed PMID: 10435584.

199. Yamamoto M, Sato S, Hemmi H, Sanjo H, Uematsu S, Kaisho T, et al. Essential role for TIRAP in activation of the signalling cascade shared by TLR2 and TLR4. Nature. 2002;420(6913):324-9. Epub 2002/11/26. doi: 10.1038/nature01182. PubMed PMID: 12447441.

200. Fitzgerald KA, Palsson-McDermott EM, Bowie AG, Jefferies CA, Mansell AS, Brady G, et al. Mal (MyD88-adapter-like) is required for Toll-like receptor-4 signal transduction. Nature. 2001;413(6851):78-83. Epub 2001/09/07. doi: 10.1038/35092578. PubMed PMID: 11544529.

201. Liaunardy-Jopeace A, Gay NJ. Molecular and cellular regulation of toll-like receptor-4 activity induced by lipopolysaccharide ligands. Front Immunol. 2014;5:473. Epub 2014/10/24. doi: 10.3389/fimmu.2014.00473. PubMed PMID: 25339952; PubMed Central PMCID: PMCPMC4186342.

202. Hoshino K, Takeuchi O, Kawai T, Sanjo H, Ogawa T, Takeda Y, et al. Cutting edge: Toll-like receptor 4 (TLR4)-deficient mice are hyporesponsive to lipopolysaccharide:

evidence for TLR4 as the Lps gene product. J Immunol. 1999;162(7):3749-52. Epub 1999/04/14. PubMed PMID: 10201887.

203. Hou L, Sasaki H, Stashenko P. Toll-like receptor 4-deficient mice have reduced bone destruction following mixed anaerobic infection. Infect Immun. 2000;68(8):4681-7. Epub 2000/07/19. doi: 10.1128/iai.68.8.4681-4687.2000. PubMed PMID: 10899873; PubMed Central PMCID: PMCPMC98410.

204. O'Brien AD, Rosenstreich DL, Scher I, Campbell GH, MacDermott RP, Formal SB. Genetic control of susceptibility to Salmonella typhimurium in mice: role of the LPS gene. J Immunol. 1980;124(1):20-4. Epub 1980/01/01. PubMed PMID: 6985638.

205. Woods JP, Frelinger JA, Warrack G, Cannon JG. Mouse genetic locus Lps influences susceptibility to Neisseria meningitidis infection. Infect Immun. 1988;56(8):1950-5. Epub 1988/08/01. doi: 10.1128/IAI.56.8.1950-1955.1988. PubMed PMID: 3397181; PubMed Central PMCID: PMCPMC259506.

206. Roger T, Froidevaux C, Le Roy D, Reymond MK, Chanson AL, Mauri D, et al. Protection from lethal gram-negative bacterial sepsis by targeting Toll-like receptor 4. Proc Natl Acad Sci U S A. 2009;106(7):2348-52. Epub 2009/02/03. doi: 10.1073/pnas.0808146106. PubMed PMID: 19181857; PubMed Central PMCID: PMCPMC2650125.

207. Park BS, Lee JO. Recognition of lipopolysaccharide pattern by TLR4 complexes. Exp Mol Med. 2013;45:e66. Epub 2013/12/07. doi: 10.1038/emm.2013.97. PubMed PMID: 24310172; PubMed Central PMCID: PMCPMC3880462.

208. Wells CA, Chalk AM, Forrest A, Taylor D, Waddell N, Schroder K, et al. Alternate transcription of the Toll-like receptor signaling cascade. Genome Biol. 2006;7(2):R10. Epub 2006/03/02. doi: 10.1186/gb-2006-7-2-r10. PubMed PMID: 16507160; PubMed Central PMCID: PMCPMC1431733.

209. Jaresova I, Rozkova D, Spisek R, Janda A, Brazova J, Sediva A. Kinetics of Toll-like receptor-4 splice variants expression in lipopolysaccharide-stimulated antigen presenting cells of healthy donors and patients with cystic fibrosis. Microbes Infect. 2007;9(11):1359-67. Epub 2007/09/25. doi: 10.1016/j.micinf.2007.06.009. PubMed PMID: 17890129.

210. Iwami KI, Matsuguchi T, Masuda A, Kikuchi T, Musikacharoen T, Yoshikai Y. Cutting edge: naturally occurring soluble form of mouse Toll-like receptor 4 inhibits lipopolysaccharide signaling. J Immunol. 2000;165(12):6682-6. Epub 2000/12/20. doi: 10.4049/jimmunol.165.12.6682. PubMed PMID: 11120784.

211. LeBouder E, Rey-Nores JE, Rushmere NK, Grigorov M, Lawn SD, Affolter M, et al. Soluble forms of Toll-like receptor (TLR)2 capable of modulating TLR2 signaling are present in human plasma and breast milk. J Immunol. 2003;171(12):6680-9. Epub 2003/12/10. doi: 10.4049/jimmunol.171.12.6680. PubMed PMID: 14662871.

212. Takeuchi O, Akira S. Pattern recognition receptors and inflammation. Cell. 2010;140(6):805-20. Epub 2010/03/23. doi: 10.1016/j.cell.2010.01.022. PubMed PMID: 20303872.

213. Janssens S, Burns K, Tschopp J, Beyaert R. Regulation of interleukin-1- and lipopolysaccharide-induced NF-kappaB activation by alternative splicing of MyD88. Curr Biol. 2002;12(6):467-71. Epub 2002/03/23. doi: 10.1016/s0960-9822(02)00712-1. PubMed PMID: 11909531.

214. De Arras L, Alper S. Limiting of the innate immune response by SF3A-dependent control of MyD88 alternative mRNA splicing. PLoS Genet. 2013;9(10):e1003855. Epub 2013/11/10. doi: 10.1371/journal.pgen.1003855. PubMed PMID: 24204290; PubMed Central PMCID: PMCPMC3812059.

215. Burns K, Janssens S, Brissoni B, Olivos N, Beyaert R, Tschopp J. Inhibition of

interleukin 1 receptor/Toll-like receptor signaling through the alternatively spliced, short form of MyD88 is due to its failure to recruit IRAK-4. J Exp Med. 2003;197(2):263-8. Epub 2003/01/23. doi: 10.1084/jem.20021790. PubMed PMID: 12538665; PubMed Central PMCID: PMCPMC2193806.

216. Akira S, Takeda K. Toll-like receptor signalling. Nat Rev Immunol. 2004;4(7):499-511. doi: 10.1038/nri1391. PubMed PMID: 15229469.

217. Takeda K, Kaisho T, Akira S. Toll-like receptors. Annu Rev Immunol. 2003;21:335-76. Epub 2003/01/14. doi: 10.1146/annurev.immunol.21.120601.141126. PubMed PMID: 12524386.

218. Liew FY, Xu D, Brint EK, O'Neill LA. Negative regulation of toll-like receptor-mediated immune responses. Nat Rev Immunol. 2005;5(6):446-58. Epub 2005/06/02. doi: 10.1038/nri1630. PubMed PMID: 15928677.

219. Seabra MC, Wasmeier C. Controlling the location and activation of Rab GTPases. Curr Opin Cell Biol. 2004;16(4):451-7. Epub 2004/07/21. doi: 10.1016/j.ceb.2004.06.014. PubMed PMID: 15261679.

220. Zerial M, McBride H. Rab proteins as membrane organizers. Nat Rev Mol Cell Biol. 2001;2(2):107-17. Epub 2001/03/17. doi: 10.1038/35052055. PubMed PMID: 11252952.

221. Bucci C, Chiariello M. Signal transduction gRABs attention. Cell Signal. 2006;18(1):1-8. Epub 2005/08/09. doi: 10.1016/j.cellsig.2005.07.001. PubMed PMID: 16084065.

222. Wang Y, Chen T, Han C, He D, Liu H, An H, et al. Lysosome-associated small Rab GTPase Rab7b negatively regulates TLR4 signaling in macrophages by promoting lysosomal degradation of TLR4. Blood. 2007;110(3):962-71. Epub 2007/03/31. doi: 10.1182/blood-2007-01-066027. PubMed PMID: 17395780.

223. Wang D, Lou J, Ouyang C, Chen W, Liu Y, Liu X, et al. Ras-related protein Rab10

facilitates TLR4 signaling by promoting replenishment of TLR4 onto the plasma membrane. Proc Natl Acad Sci U S A. 2010;107(31):13806-11. Epub 2010/07/21. doi: 10.1073/pnas.1009428107. PubMed PMID: 20643919; PubMed Central PMCID: PMCPMC2922283.

224. Janssens S, Burns K, Vercammen E, Tschopp J, Beyaert R. MyD88S, a splice variant of MyD88, differentially modulates NF-kappaB- and AP-1-dependent gene expression. FEBS Lett. 2003;548(1-3):103-7. Epub 2003/07/30. doi: 10.1016/s0014-5793(03)00747-6. PubMed PMID: 12885415.

225. Loiarro M, Capolunghi F, Fanto N, Gallo G, Campo S, Arseni B, et al. Pivotal Advance: Inhibition of MyD88 dimerization and recruitment of IRAK1 and IRAK4 by a novel peptidomimetic compound. J Leukoc Biol. 2007;82(4):801-10. Epub 2007/06/06. doi: 10.1189/jlb.1206746. PubMed PMID: 17548806.

226. Wang C, Chen T, Zhang J, Yang M, Li N, Xu X, et al. The E3 ubiquitin ligase Nrdp1 'preferentially' promotes TLR-mediated production of type I interferon. Nat Immunol. 2009;10(7):744-52. Epub 2009/06/02. doi: 10.1038/ni.1742. PubMed PMID: 19483718.

227. Peng J, Yuan Q, Lin B, Panneerselvam P, Wang X, Luan XL, et al. SARM inhibits both TRIF- and MyD88-mediated AP-1 activation. Eur J Immunol. 2010;40(6):1738-47. Epub 2010/03/23. doi: 10.1002/eji.200940034. PubMed PMID: 20306472.

228. Kobayashi K, Hernandez LD, Galan JE, Janeway CA, Jr., Medzhitov R, Flavell RA. IRAK-M is a negative regulator of Toll-like receptor signaling. Cell. 2002;110(2):191-202. Epub 2002/08/02. doi: 10.1016/s0092-8674(02)00827-9. PubMed PMID: 12150927.

229. Kinjyo I, Hanada T, Inagaki-Ohara K, Mori H, Aki D, Ohishi M, et al. SOCS1/JAB is a negative regulator of LPS-induced macrophage activation. Immunity. 2002;17(5):583-91. Epub 2002/11/16. doi: 10.1016/s1074-7613(02)00446-6. PubMed PMID: 12433365.

230. Nakagawa R, Naka T, Tsutsui H, Fujimoto M, Kimura A, Abe T, et al. SOCS-1 participates in negative regulation of LPS responses. Immunity. 2002;17(5):677-87. Epub 2002/11/16. doi: 10.1016/s1074-7613(02)00449-1. PubMed PMID: 12433373.

231. Palsson-McDermott EM, Doyle SL, McGettrick AF, Hardy M, Husebye H, Banahan K, et al. TAG, a splice variant of the adaptor TRAM, negatively regulates the adaptor MyD88-independent TLR4 pathway. Nat Immunol. 2009;10(6):579-86. Epub 2009/05/05. doi: 10.1038/ni.1727. PubMed PMID: 19412184.

232. Saitoh T, Tun-Kyi A, Ryo A, Yamamoto M, Finn G, Fujita T, et al. Negative regulation of interferon-regulatory factor 3-dependent innate antiviral response by the prolyl isomerase Pin1. Nat Immunol. 2006;7(6):598-605. Epub 2006/05/16. doi: 10.1038/ni1347. PubMed PMID: 16699525.

233. Kwon JW, Kwon HK, Shin HJ, Choi YM, Anwar MA, Choi S. Activating transcription factor 3 represses inflammatory responses by binding to the p65 subunit of NF-kappaB. Sci Rep. 2015;5:14470. Epub 2015/09/29. doi: 10.1038/srep14470. PubMed PMID: 26412238; PubMed Central PMCID: PMCPMC4585983.

234. Fukao T, Tanabe M, Terauchi Y, Ota T, Matsuda S, Asano T, et al. PI3K-mediated negative feedback regulation of IL-12 production in DCs. Nat Immunol. 2002;3(9):875-81. Epub 2002/08/03. doi: 10.1038/ni825. PubMed PMID: 12154357.

235. Kayagaki N, Phung Q, Chan S, Chaudhari R, Quan C, O'Rourke KM, et al. DUBA: a deubiquitinase that regulates type I interferon production. Science. 2007;318(5856):1628-32. Epub 2007/11/10. doi: 10.1126/science.1145918. PubMed PMID: 17991829.

236. Burns K, Clatworthy J, Martin L, Martinon F, Plumpton C, Maschera B, et al. Tollip, a new component of the IL-1RI pathway, links IRAK to the IL-1 receptor. Nat Cell Biol. 2000;2(6):346-51. Epub 2000/06/15. doi: 10.1038/35014038. PubMed PMID: 10854325.

237. Bulut Y, Faure E, Thomas L, Equils O, Arditi M. Cooperation of Toll-like receptor 2 and 6 for cellular activation by soluble tuberculosis factor and Borrelia burgdorferi outer surface protein A lipoprotein: role of Toll-interacting protein and IL-1 receptor signaling molecules in Toll-like receptor 2 signaling. J Immunol. 2001;167(2):987-94. Epub 2001/07/07. doi: 10.4049/jimmunol.167.2.987. PubMed PMID: 11441107.

238. Zhang G, Ghosh S. Negative regulation of toll-like receptor-mediated signaling by Tollip. J Biol Chem. 2002;277(9):7059-65. Epub 2001/12/26. doi: 10.1074/jbc.M109537200. PubMed PMID: 11751856.

239. Tanaka T, Grusby M, Kaisho T. PDLIM2-Mediated Termination of Transcription Factor NF-KappaB Activation by Intranuclear Sequestration and Degradation of the P65 Subunit. Nature immunology. 2007;8:584-91. doi: 10.1038/ni1464.

240. Yu Y, Hayward GS. The ubiquitin E3 ligase RAUL negatively regulates type i interferon through ubiquitination of the transcription factors IRF7 and IRF3. Immunity. 2010;33(6):863-77. Epub 2010/12/21. doi: 10.1016/j.immuni.2010.11.027. PubMed PMID: 21167755; PubMed Central PMCID: PMCPMC3012379.

241. Boone DL, Turer EE, Lee EG, Ahmad RC, Wheeler MT, Tsui C, et al. The ubiquitin-modifying enzyme A20 is required for termination of Toll-like receptor responses. Nat Immunol. 2004;5(10):1052-60. Epub 2004/08/31. doi: 10.1038/ni1110. PubMed PMID: 15334086.

242. Zhou F, Zhang X, van Dam H, Ten Dijke P, Huang H, Zhang L. Ubiquitin-specific protease 4 mitigates Toll-like/interleukin-1 receptor signaling and regulates innate immune activation. J Biol Chem. 2012;287(14):11002-10. Epub 2012/01/21. doi: 10.1074/jbc.M111.328187. PubMed PMID: 22262844; PubMed Central PMCID: PMCPMC3322833.

243. Chuang TH, Ulevitch RJ. Triad3A, an E3 ubiquitin-protein ligase regulating Toll-

like receptors. Nat Immunol. 2004;5(5):495-502. Epub 2004/04/27. doi: 10.1038/ni1066. PubMed PMID: 15107846.

244. Yoshida H, Jono H, Kai H, Li JD. The tumor suppressor cylindromatosis (CYLD) acts as a negative regulator for toll-like receptor 2 signaling via negative cross-talk with TRAF6 AND TRAF7. J Biol Chem. 2005;280(49):41111-21. Epub 2005/10/19. doi: 10.1074/jbc.M509526200. PubMed PMID: 16230348.

245. Brint EK, Xu D, Liu H, Dunne A, McKenzie AN, O'Neill LA, et al. ST2 is an inhibitor of interleukin 1 receptor and Toll-like receptor 4 signaling and maintains endotoxin tolerance. Nat Immunol. 2004;5(4):373-9. Epub 2004/03/09. doi: 10.1038/ni1050. PubMed PMID: 15004556.

246. Wald D, Qin J, Zhao Z, Qian Y, Naramura M, Tian L, et al. SIGIRR, a negative regulator of Toll-like receptor-interleukin 1 receptor signaling. Nat Immunol. 2003;4(9):920-7. Epub 2003/08/20. doi: 10.1038/ni968. PubMed PMID: 12925853.

247. Garlanda C, Riva F, Polentarutti N, Buracchi C, Sironi M, De Bortoli M, et al. Intestinal inflammation in mice deficient in Tir8, an inhibitory member of the IL-1 receptor family. Proc Natl Acad Sci U S A. 2004;101(10):3522-6. Epub 2004/03/03. doi: 10.1073/pnas.0308680101. PubMed PMID: 14993616; PubMed Central PMCID: PMCPMC373495.

248. Diehl GE, Yue HH, Hsieh K, Kuang AA, Ho M, Morici LA, et al. TRAIL-R as a negative regulator of innate immune cell responses. Immunity. 2004;21(6):877-89. Epub 2004/12/14. doi: 10.1016/j.immuni.2004.11.008. PubMed PMID: 15589175.

249. Wang W, Huang X, Xin HB, Fu M, Xue A, Wu ZH. TRAF Family Member-associated NF-kappaB Activator (TANK) Inhibits Genotoxic Nuclear Factor kappaB Activation by Facilitating Deubiquitinase USP10-dependent Deubiquitination of TRAF6 Ligase. J Biol Chem. 2015;290(21):13372-85. Epub 2015/04/12. doi:

10.1074/jbc.M115.643767. PubMed PMID: 25861989; PubMed Central PMCID: PMCPMC4505586.

250. Zhao W, Wang L, Zhang M, Yuan C, Gao C. E3 ubiquitin ligase tripartite motif 38 negatively regulates TLR-mediated immune responses by proteasomal degradation of TNF receptor-associated factor 6 in macrophages. J Immunol. 2012;188(6):2567-74. Epub 2012/02/11. doi: 10.4049/jimmunol.1103255. PubMed PMID: 22323536.

251. Zhang J, Shen B. SHP limits TLR signaling, an inducible transcriptional corepressor. Cell Mol Immunol. 2011;8(6):445-6. Epub 2011/08/24. doi: 10.1038/cmi.2011.31. PubMed PMID: 21860408; PubMed Central PMCID: PMCPMC4012932.

252. McEvoy AN, Murphy EA, Ponnio T, Conneely OM, Bresnihan B, FitzGerald O, et al. Activation of nuclear orphan receptor NURR1 transcription by NF-kappa B and cyclic adenosine 5'-monophosphate response element-binding protein in rheumatoid arthritis synovial tissue. J Immunol. 2002;168(6):2979-87. Epub 2002/03/09. doi: 10.4049/jimmunol.168.6.2979. PubMed PMID: 11884470.

253. Akira S. TLR signaling. Curr Top Microbiol Immunol. 2006;311:1-16. PubMed PMID: 17048703.

254. Carpenter S, Ricci EP, Mercier BC, Moore MJ, Fitzgerald KA. Post-transcriptional regulation of gene expression in innate immunity. Nat Rev Immunol. 2014;14(6):361-76. doi: 10.1038/nri3682. PubMed PMID: 24854588.

255. Medzhitov R, Horng T. Transcriptional control of the inflammatory response. Nat Rev Immunol. 2009;9(10):692-703. doi: 10.1038/nri2634. PubMed PMID: 19859064.

256. Khabar KS. Post-transcriptional control during chronic inflammation and cancer: a focus on AU-rich elements. Cell Mol Life Sci. 2010;67(17):2937-55. doi: 10.1007/s00018-010-0383-x. PubMed PMID: 20495997; PubMed Central PMCID: PMCPMC2921490.

257. Stoecklin G, Lu M, Rattenbacher B, Moroni C. A constitutive decay element promotes tumor necrosis factor alpha mRNA degradation via an AU-rich element-independent pathway. Mol Cell Biol. 2003;23(10):3506-15. PubMed PMID: 12724409; PubMed Central PMCID: PMCPMC164766.

258. Curtale G, Rubino M, Locati M. MicroRNAs as Molecular Switches in Macrophage Activation. Front Immunol. 2019;10:799. doi: 10.3389/fimmu.2019.00799. PubMed PMID: 31057539; PubMed Central PMCID: PMCPMC6478758.

259. Choi J, Pacheco CM, Mosbergen R, Korn O, Chen T, Nagpal I, et al. Stemformatics: visualize and download curated stem cell data. Nucleic Acids Res. 2019;47(D1):D841-D6. doi: 10.1093/nar/gky1064. PubMed PMID: 30407577; PubMed Central PMCID: PMCPMC6323943.

260. Eden E, Lipson D, Yogev S, Yakhini Z. Discovering motifs in ranked lists of DNA sequences. PLoS Comput Biol. 2007;3(3):e39. Epub 2007/03/27. doi: 10.1371/journal.pcbi.0030039. PubMed PMID: 17381235; PubMed Central PMCID: PMCPMC1829477.

261. Eden E, Navon R, Steinfeld I, Lipson D, Yakhini Z. GOrilla: a tool for discovery and visualization of enriched GO terms in ranked gene lists. BMC Bioinformatics. 2009;10:48. doi: 10.1186/1471-2105-10-48. PubMed PMID: 19192299; PubMed Central PMCID: PMCPMC2644678.

262. Wells CA, Mosbergen R, Korn O, Choi J, Seidenman N, Matigian NA, et al. Stemformatics: visualisation and sharing of stem cell gene expression. Stem Cell Res. 2013;10(3):387-95. doi: 10.1016/j.scr.2012.12.003. PubMed PMID: 23466562.

263. Tiedje C, Diaz-Munoz MD, Trulley P, Ahlfors H, Laass K, Blackshear PJ, et al. The RNA-binding protein TTP is a global post-transcriptional regulator of feedback control in inflammation. Nucleic Acids Res. 2016;44(15):7418-40. doi: 10.1093/nar/gkw474.

PubMed PMID: 27220464; PubMed Central PMCID: PMCPMC5009735.

264. Matsushita K, Takeuchi O, Standley DM, Kumagai Y, Kawagoe T, Miyake T, et al. Zc3h12a is an RNase essential for controlling immune responses by regulating mRNA decay. Nature. 2009;458(7242):1185-90. doi: 10.1038/nature07924. PubMed PMID: 19322177.

265. Schroder K, Irvine KM, Taylor MS, Bokil NJ, Le Cao KA, Masterman KA, et al. Conservation and divergence in Toll-like receptor 4-regulated gene expression in primary human versus mouse macrophages. Proc Natl Acad Sci U S A. 2012;109(16):E944-53. doi: 10.1073/pnas.1110156109. PubMed PMID: 22451944; PubMed Central PMCID: PMCPMC3341041.

266. Kurosaki T, Popp MW, Maquat LE. Quality and quantity control of gene expression by nonsense-mediated mRNA decay. Nat Rev Mol Cell Biol. 2019. doi: 10.1038/s41580-019-0126-2. PubMed PMID: 30992545.

267. Quek H, Lim YC, Lavin MF, Roberts TL. PIKKing a way to regulate inflammation. Immunol Cell Biol. 2018;96(1):8-20. doi: 10.1111/imcb.1001. PubMed PMID: 29359354.

268. Weischenfeldt J, Damgaard I, Bryder D, Theilgaard-Monch K, Thoren LA, Nielsen FC, et al. NMD is essential for hematopoietic stem and progenitor cells and for eliminating by-products of programmed DNA rearrangements. Genes Dev. 2008;22(10):1381-96. doi: 10.1101/gad.468808. PubMed PMID: 18483223; PubMed Central PMCID: PMCPMC2377192.

269. Yamashita A. Role of SMG-1-mediated Upf1 phosphorylation in mammalian nonsense-mediated mRNA decay. Genes Cells. 2013;18(3):161-75. doi: 10.1111/gtc.12033. PubMed PMID: 23356578.

270. Stein KC, Frydman J. The stop-and-go traffic regulating protein biogenesis: How translation kinetics controls proteostasis. J Biol Chem. 2019;294(6):2076-84. doi:

10.1074/jbc.REV118.002814. PubMed PMID: 30504455; PubMed Central PMCID: PMCPMC6369277.

271. Singh J, Padgett RA. Rates of in situ transcription and splicing in large human genes. Nat Struct Mol Biol. 2009;16(11):1128-33. doi: 10.1038/nsmb.1666. PubMed PMID: 19820712; PubMed Central PMCID: PMCPMC2783620.

272. Martin L, Grigoryan A, Wang D, Wang J, Breda L, Rivella S, et al. Identification and characterization of small molecules that inhibit nonsense-mediated RNA decay and suppress nonsense p53 mutations. Cancer Res. 2014;74(11):3104-13. doi: 10.1158/0008-5472.CAN-13-2235. PubMed PMID: 24662918; PubMed Central PMCID: PMCPMC4040335.

273. Tenekeci U, Poppe M, Beuerlein K, Buro C, Muller H, Weiser H, et al. K63-Ubiquitylation and TRAF6 Pathways Regulate Mammalian P-Body Formation and mRNA Decapping. Mol Cell. 2016;63(3):540. doi: 10.1016/j.molcel.2016.07.009. PubMed PMID: 27494559.

274. Yamashita A, Ohnishi T, Kashima I, Taya Y, Ohno S. Human SMG-1, a novel phosphatidylinositol 3-kinase-related protein kinase, associates with components of the mRNA surveillance complex and is involved in the regulation of nonsense-mediated mRNA decay. Genes Dev. 2001;15(17):2215-28. doi: 10.1101/gad.913001. PubMed PMID: 11544179; PubMed Central PMCID: PMCPMC312771.

275. Huang L, Wilkinson MF. Regulation of nonsense-mediated mRNA decay. Wiley Interdiscip Rev RNA. 2012;3(6):807-28. doi: 10.1002/wrna.1137. PubMed PMID: 23027648.

276. Mendell JT, Sharifi NA, Meyers JL, Martinez-Murillo F, Dietz HC. Nonsense surveillance regulates expression of diverse classes of mammalian transcripts and mutes genomic noise. Nature genetics. 2004;36(10):1073-8. doi: 10.1038/ng1429. PubMed

PMID: 15448691.

277. Rusinova I, Forster S, Yu S, Kannan A, Masse M, Cumming H, et al. Interferome v2.0: an updated database of annotated interferon-regulated genes. Nucleic Acids Res. 2013;41(Database issue):D1040-6. doi: 10.1093/nar/gks1215. PubMed PMID: 23203888; PubMed Central PMCID: PMCPMC3531205.

278. Mino T, Iwai N, Endo M, Inoue K, Akaki K, Hia F, et al. Translation-dependent unwinding of stem-loops by UPF1 licenses Regnase-1 to degrade inflammatory mRNAs. Nucleic Acids Res. 2019. doi: 10.1093/nar/gkz628. PubMed PMID: 31329944.

279. Jacob AG, Smith CWJ. Intron retention as a component of regulated gene expression programs. Hum Genet. 2017;136(9):1043-57. Epub 2017/04/10. doi: 10.1007/s00439-017-1791-x. PubMed PMID: 28391524; PubMed Central PMCID: PMCPMC5602073.

280. Edwards CR, Ritchie W, Wong JJ, Schmitz U, Middleton R, An X, et al. A dynamic intron retention program in the mammalian megakaryocyte and erythrocyte lineages. Blood. 2016;127(17):e24-e34. doi: 10.1182/blood-2016-01-692764. PubMed PMID: 26962124; PubMed Central PMCID: PMCPMC4850870.

281. Middleton R, Gao D, Thomas A, Singh B, Au A, Wong JJ, et al. IRFinder: assessing the impact of intron retention on mammalian gene expression. Genome Biol. 2017;18(1):51. doi: 10.1186/s13059-017-1184-4. PubMed PMID: 28298237; PubMed Central PMCID: PMCPMC5353968.

282. Gerstein MB, Rozowsky J, Yan KK, Wang D, Cheng C, Brown JB, et al. Comparative analysis of the transcriptome across distant species. Nature. 2014;512(7515):445-8. doi: 10.1038/nature13424. PubMed PMID: 25164755; PubMed Central PMCID: PMCPMC4155737.

283. Wegener M, Muller-McNicoll M. Nuclear retention of mRNAs - quality control, gene regulation and human disease. Semin Cell Dev Biol. 2018;79:131-42. Epub

2017/11/06. doi: 10.1016/j.semcdb.2017.11.001. PubMed PMID: 29102717.

284. Boutz PL, Bhutkar A, Sharp PA. Detained introns are a novel, widespread class of post-transcriptionally spliced introns. Genes Dev. 2015;29(1):63-80. Epub 2015/01/07. doi: 10.1101/gad.247361.114. PubMed PMID: 25561496; PubMed Central PMCID: PMCPMC4281565.

285. Mauger O, Lemoine F, Scheiffele P. Targeted Intron Retention and Excision for Rapid Gene Regulation in Response to Neuronal Activity. Neuron. 2016;92(6):1266-78. Epub 2016/12/24. doi: 10.1016/j.neuron.2016.11.032. PubMed PMID: 28009274.

286. Wong JJ, Ritchie W, Ebner OA, Selbach M, Wong JW, Huang Y, et al. Orchestrated intron retention regulates normal granulocyte differentiation. Cell. 2013;154(3):583-95. doi: 10.1016/j.cell.2013.06.052. PubMed PMID: 23911323.

287. O'Neill LA, Bowie AG. Sensing and signaling in antiviral innate immunity. Curr Biol. 2010;20(7):R328-33. Epub 2010/04/16. doi: 10.1016/j.cub.2010.01.044. PubMed PMID: 20392426.

288. Maelfait J, Liverpool L, Bridgeman A, Ragan KB, Upton JW, Rehwinkel J. Sensing of viral and endogenous RNA by ZBP1/DAI induces necroptosis. EMBO J. 2017;36(17):2529-43. Epub 2017/07/19. doi: 10.15252/embj.201796476. PubMed PMID: 28716805; PubMed Central PMCID: PMCPMC5579359.

289. Wang Y, Wang H, Yao H, Li C, Fang JY, Xu J. Regulation of PD-L1: Emerging Routes for Targeting Tumor Immune Evasion. Front Pharmacol. 2018;9:536. Epub 2018/06/19. doi: 10.3389/fphar.2018.00536. PubMed PMID: 29910728; PubMed Central PMCID: PMCPMC5992436.

290. Oudshoorn D, van Boheemen S, Sanchez-Aparicio MT, Rajsbaum R, Garcia-Sastre A, Versteeg GA. HERC6 is the main E3 ligase for global ISG15 conjugation in mouse cells. PLoS One. 2012;7(1):e29870. Epub 2012/01/25. doi:

10.1371/journal.pone.0029870. PubMed PMID: 22272257; PubMed Central PMCID: PMCPMC3260183.

291. Sokhi UK, Bacolod MD, Dasgupta S, Emdad L, Das SK, Dumur CI, et al. Identification of genes potentially regulated by human polynucleotide phosphorylase (hPNPase old-35) using melanoma as a model. PLoS One. 2013;8(10):e76284. Epub 2013/10/22. doi: 10.1371/journal.pone.0076284. PubMed PMID: 24143183; PubMed Central PMCID: PMCPMC3797080.

292. Leszczyniecka M, Kang DC, Sarkar D, Su ZZ, Holmes M, Valerie K, et al. Identification and cloning of human polynucleotide phosphorylase, hPNPase old-35, in the context of terminal differentiation and cellular senescence. Proc Natl Acad Sci U S A. 2002;99(26):16636-41. Epub 2002/12/11. doi: 10.1073/pnas.252643699. PubMed PMID: 12473748; PubMed Central PMCID: PMCPMC139196.

293. Leszczyniecka M, Su ZZ, Kang DC, Sarkar D, Fisher PB. Expression regulation and genomic organization of human polynucleotide phosphorylase, hPNPase(old-35), a Type I interferon inducible early response gene. Gene. 2003;316:143-56. Epub 2003/10/18. doi: 10.1016/s0378-1119(03)00752-2. PubMed PMID: 14563561.

294. Fan JB, Miyauchi S, Xu HZ, Liu D, Kim LJY, Burkart C, et al. Type I Interferon Regulates a Coordinated Gene Network to Enhance Cytotoxic T Cell-Mediated Tumor Killing. Cancer Discov. 2020;10(3):382-93. Epub 2020/01/25. doi: 10.1158/2159-8290.CD-19-0608. PubMed PMID: 31974171; PubMed Central PMCID: PMCPMC7058499.

295. Schoggins JW, Rice CM. Interferon-stimulated genes and their antiviral effector functions. Curr Opin Virol. 2011;1(6):519-25. Epub 2012/02/14. doi: 10.1016/j.coviro.2011.10.008. PubMed PMID: 22328912; PubMed Central PMCID: PMCPMC3274382.

296. Hardy MP, Owczarek CM, Jermiin LS, Ejdeback M, Hertzog PJ. Characterization of the type I interferon locus and identification of novel genes. Genomics. 2004;84(2):331-45. Epub 2004/07/06. doi: 10.1016/j.ygeno.2004.03.003. PubMed PMID: 15233997.

297. van Pesch V, Lanaya H, Renauld JC, Michiels T. Characterization of the murine alpha interferon gene family. J Virol. 2004;78(15):8219-28. Epub 2004/07/16. doi: 10.1128/JVI.78.15.8219-8228.2004. PubMed PMID: 15254193; PubMed Central PMCID: PMCPMC446145.

298. Gessani S, Belardelli F, Pecorelli A, Puddu P, Baglioni C. Bacterial lipopolysaccharide and gamma interferon induce transcription of beta interferon mRNA and interferon secretion in murine macrophages. J Virol. 1989;63(6):2785-9. Epub 1989/06/01. doi: 10.1128/JVI.63.6.2785-2789.1989. PubMed PMID: 2498530; PubMed Central PMCID: PMCPMC250780.

299. Green ID, Pinello N, Song R, Lee Q, Halstead JM, Kwok CT, et al. Macrophage development and activation involve coordinated intron retention in key inflammatory regulators. Nucleic Acids Res. 2020;48(12):6513-29. Epub 2020/05/26. doi: 10.1093/nar/gkaa435. PubMed PMID: 32449925; PubMed Central PMCID: PMCPMC7337907.

300. Lovejoy CA, Cortez D. Common mechanisms of PIKK regulation. DNA Repair (Amst). 2009;8(9):1004-8. Epub 2009/05/26. doi: 10.1016/j.dnarep.2009.04.006. PubMed PMID: 19464237; PubMed Central PMCID: PMCPMC2725225.

301. Denning G, Jamieson L, Maquat LE, Thompson EA, Fields AP. Cloning of a novel phosphatidylinositol kinase-related kinase: characterization of the human SMG-1 RNA surveillance protein. J Biol Chem. 2001;276(25):22709-14. Epub 2001/05/02. doi: 10.1074/jbc.C100144200. PubMed PMID: 11331269.

302. Blackford AN, Jackson SP. ATM, ATR, and DNA-PK: The Trinity at the Heart of the DNA Damage Response. Mol Cell. 2017;66(6):801-17. Epub 2017/06/18. doi: 10.1016/j.molcel.2017.05.015. PubMed PMID: 28622525.

303. Loewith R, Hall MN. Target of rapamycin (TOR) in nutrient signaling and growth control. Genetics. 2011;189(4):1177-201. Epub 2011/12/17. doi: 10.1534/genetics.111.133363. PubMed PMID: 22174183; PubMed Central PMCID: PMCPMC3241408.

304. Arias-Palomo E, Yamashita A, Fernandez IS, Nunez-Ramirez R, Bamba Y, Izumi N, et al. The nonsense-mediated mRNA decay SMG-1 kinase is regulated by large-scale conformational changes controlled by SMG-8. Genes Dev. 2011;25(2):153-64. doi: 10.1101/gad.606911. PubMed PMID: 21245168; PubMed Central PMCID: PMCPMC3022261.

305. Yamashita A, Izumi N, Kashima I, Ohnishi T, Saari B, Katsuhata Y, et al. SMG-8 and SMG-9, two novel subunits of the SMG-1 complex, regulate remodeling of the mRNA surveillance complex during nonsense-mediated mRNA decay. Genes Dev. 2009;23(9):1091-105. doi: 10.1101/gad.1767209. PubMed PMID: 19417104; PubMed Central PMCID: PMCPMC2682953.

306. Deniaud A, Karuppasamy M, Bock T, Masiulis S, Huard K, Garzoni F, et al. A network of SMG-8, SMG-9 and SMG-1 C-terminal insertion domain regulates UPF1 substrate recruitment and phosphorylation. Nucleic Acids Res. 2015;43(15):7600-11. doi: 10.1093/nar/gkv668. PubMed PMID: 26130714; PubMed Central PMCID: PMCPMC4551919.

307. Brumbaugh KM, Otterness DM, Geisen C, Oliveira V, Brognard J, Li X, et al. The mRNA surveillance protein hSMG-1 functions in genotoxic stress response pathways in mammalian cells. Mol Cell. 2004;14(5):585-98. doi: 10.1016/j.molcel.2004.05.005.

PubMed PMID: 15175154.

308. Azzalin CM, Reichenbach P, Khoriauli L, Giulotto E, Lingner J. Telomeric repeat containing RNA and RNA surveillance factors at mammalian chromosome ends. Science. 2007;318(5851):798-801. doi: 10.1126/science.1147182. PubMed PMID: 17916692.

309. Chawla R, Azzalin CM. The telomeric transcriptome and SMG proteins at the crossroads. Cytogenet Genome Res. 2008;122(3-4):194-201. doi: 10.1159/000167804. PubMed PMID: 19188687.

310. Masse I, Molin L, Mouchiroud L, Vanhems P, Palladino F, Billaud M, et al. A novel role for the SMG-1 kinase in lifespan and oxidative stress resistance in Caenorhabditis elegans. PLoS One. 2008;3(10):e3354. doi: 10.1371/journal.pone.0003354. PubMed PMID: 18836529; PubMed Central PMCID: PMCPMC2556085.

311. Chen RQ, Yang QK, Chen YL, Oliveira VA, Dalton WS, Fearns C, et al. Kinome siRNA screen identifies SMG-1 as a negative regulator of hypoxia-inducible factor-1alpha in hypoxia. J Biol Chem. 2009;284(25):16752-8. doi: 10.1074/jbc.M109.014316. PubMed PMID: 19406746; PubMed Central PMCID: PMCPMC2719310.

312. Oliveira V, Romanow WJ, Geisen C, Otterness DM, Mercurio F, Wang HG, et al. A protective role for the human SMG-1 kinase against tumor necrosis factor-alpha-induced apoptosis. J Biol Chem. 2008;283(19):13174-84. doi: 10.1074/jbc.M708008200. PubMed PMID: 18326048; PubMed Central PMCID: PMCPMC2442360.

313. Du Y, Lu F, Li P, Ye J, Ji M, Ma D, et al. SMG1 acts as a novel potential tumor suppressor with epigenetic inactivation in acute myeloid leukemia. Int J Mol Sci. 2014;15(9):17065-76. doi: 10.3390/ijms150917065. PubMed PMID: 25257528; PubMed Central PMCID: PMCPMC4200422.

314. Gubanova E, Brown B, Ivanov SV, Helleday T, Mills GB, Yarbrough WG, et al. Downregulation of SMG-1 in HPV-positive head and neck squamous cell carcinoma due

to promoter hypermethylation correlates with improved survival. Clin Cancer Res. 2012;18(5):1257-67. doi: 10.1158/1078-0432.CCR-11-2058. PubMed PMID: 22247495; PubMed Central PMCID: PMCPMC4010255.

315. Ding L, Getz G, Wheeler DA, Mardis ER, McLellan MD, Cibulskis K, et al. Somatic mutations affect key pathways in lung adenocarcinoma. Nature. 2008;455(7216):1069-75. doi: 10.1038/nature07423. PubMed PMID: 18948947; PubMed Central PMCID: PMCPMC2694412.

316. Robles-Espinoza CD, Harland M, Ramsay AJ, Aoude LG, Quesada V, Ding Z, et al. POT1 loss-of-function variants predispose to familial melanoma. Nat Genet. 2014;46(5):478-81. doi: 10.1038/ng.2947. PubMed PMID: 24686849; PubMed Central PMCID: PMCPMC4266105.

317. Uhlen M, Oksvold P, Fagerberg L, Lundberg E, Jonasson K, Forsberg M, et al. Towards a knowledge-based Human Protein Atlas. Nat Biotechnol. 2010;28(12):1248-50. doi: 10.1038/nbt1210-1248. PubMed PMID: 21139605.

318. Rayson S, Arciga-Reyes L, Wootton L, De Torres Zabala M, Truman W, Graham N, et al. A role for nonsense-mediated mRNA decay in plants: pathogen responses are induced in Arabidopsis thaliana NMD mutants. PLoS One. 2012;7(2):e31917. Epub 2012/03/03. doi: 10.1371/journal.pone.0031917. PubMed PMID: 22384098; PubMed Central PMCID: PMCPMC3284524.

319. Derecki NC, Quinnies KM, Kipnis J. Alternatively activated myeloid (M2) cells enhance cognitive function in immune compromised mice. Brain Behav Immun. 2011;25(3):379-85. doi: 10.1016/j.bbi.2010.11.009. PubMed PMID: 21093578; PubMed Central PMCID: PMCPMC3039052.

320. Clausen BE, Burkhardt C, Reith W, Renkawitz R, Forster I. Conditional gene targeting in macrophages and granulocytes using LysMcre mice. Transgenic Res.

1999;8(4):265-77. PubMed PMID: 10621974.

321. Stich RW, Shoda LK, Dreewes M, Adler B, Jungi TW, Brown WC. Stimulation of nitric oxide production in macrophages by Babesia bovis. Infect Immun. 1998;66(9):4130-6. Epub 1998/08/26. PubMed PMID: 9712758; PubMed Central PMCID: PMCPMC108496.

322. Ulevitch RJ, Tobias PS. Receptor-dependent mechanisms of cell stimulation by bacterial endotoxin. Annu Rev Immunol. 1995;13:437-57. Epub 1995/01/01. doi: 10.1146/annurev.iy.13.040195.002253. PubMed PMID: 7542010.

323. Klein SL, Flanagan KL. Sex differences in immune responses. Nat Rev Immunol. 2016;16(10):626-38. Epub 2016/08/23. doi: 10.1038/nri.2016.90. PubMed PMID: 27546235.

324. Fish EN. The X-files in immunity: sex-based differences predispose immune responses. Nat Rev Immunol. 2008;8(9):737-44. Epub 2008/08/30. doi: 10.1038/nri2394. PubMed PMID: 18728636; PubMed Central PMCID: PMCPMC7097214.

325. Rubtsova K, Marrack P, Rubtsov AV. Sexual dimorphism in autoimmunity. J Clin Invest. 2015;125(6):2187-93. Epub 2015/04/29. doi: 10.1172/JCI78082. PubMed PMID: 25915581; PubMed Central PMCID: PMCPMC4497744.

326. Ebner S, Hofer S, Nguyen VA, Furhapter C, Herold M, Fritsch P, et al. A novel role for IL-3: human monocytes cultured in the presence of IL-3 and IL-4 differentiate into dendritic cells that produce less IL-12 and shift Th cell responses toward a Th2 cytokine pattern. J Immunol. 2002;168(12):6199-207. Epub 2002/06/11. doi: 10.4049/jimmunol.168.12.6199. PubMed PMID: 12055233.

327. Robin C, Ottersbach K, Durand C, Peeters M, Vanes L, Tybulewicz V, et al. An unexpected role for IL-3 in the embryonic development of hematopoietic stem cells. Dev Cell. 2006;11(2):171-80. Epub 2006/08/08. doi: 10.1016/j.devcel.2006.07.002. PubMed

PMID: 16890157.

328. Braune J, Weyer U, Hobusch C, Mauer J, Bruning JC, Bechmann I, et al. IL-6 Regulates M2 Polarization and Local Proliferation of Adipose Tissue Macrophages in Obesity. J Immunol. 2017;198(7):2927-34. Epub 2017/02/15. doi: 10.4049/jimmunol.1600476. PubMed PMID: 28193830.

329. de Oliveira-Junior EB, Bustamante J, Newburger PE, Condino-Neto A. The human NADPH oxidase: primary and secondary defects impairing the respiratory burst function and the microbicidal ability of phagocytes. Scand J Immunol. 2011;73(5):420-7. Epub 2011/01/06. doi: 10.1111/j.1365-3083.2010.02501.x. PubMed PMID: 21204900.

330. Nguyen GT, Green ER, Mecsas J. Neutrophils to the ROScue: Mechanisms of NADPH Oxidase Activation and Bacterial Resistance. Front Cell Infect Microbiol. 2017;7:373. Epub 2017/09/12. doi: 10.3389/fcimb.2017.00373. PubMed PMID: 28890882; PubMed Central PMCID: PMCPMC5574878.

331. Liu PH, Sidi S. Targeting the Innate Immune Kinase IRAK1 in Radioresistant Cancer: Double-Edged Sword or One-Two Punch? Front Oncol. 2019;9:1174. Epub 2019/12/05. doi: 10.3389/fonc.2019.01174. PubMed PMID: 31799178; PubMed Central PMCID: PMCPMC6866135.

332. Heeb LEM, Egholm C, Boyman O. Evolution and function of interleukin-4 receptor signaling in adaptive immunity and neutrophils. Genes Immun. 2020;21(3):143-9. Epub 2020/03/07. doi: 10.1038/s41435-020-0095-7. PubMed PMID: 32139893; PubMed Central PMCID: PMCPMC7274943.

333. Ciaudo C, Bourdet A, Cohen-Tannoudji M, Dietz HC, Rougeulle C, Avner P. Nuclear mRNA degradation pathway(s) are implicated in Xist regulation and X chromosome inactivation. PLoS Genet. 2006;2(6):e94. Epub 2006/06/23. doi: 10.1371/journal.pgen.0020094. PubMed PMID: 16789828; PubMed Central PMCID:

PMCPMC1479048.

334. Mueller FS, Polesel M, Richetto J, Meyer U, Weber-Stadlbauer U. Mouse models of maternal immune activation: Mind your caging system! Brain Behav Immun. 2018;73:643-60. Epub 2018/07/22. doi: 10.1016/j.bbi.2018.07.014. PubMed PMID: 30026057.

335. Clough G. Environmental effects on animals used in biomedical research. Biol Rev Camb Philos Soc. 1982;57(Pt 3):487-523. Epub 1982/08/01. doi: 10.1111/j.1469-185x.1982.tb00705.x. PubMed PMID: 6982731.

336. Mason TJ, Matthews M. Aquatic environment, housing, and management in the eighth edition of the Guide for the Care and Use of Laboratory Animals: additional considerations and recommendations. J Am Assoc Lab Anim Sci. 2012;51(3):329-32. Epub 2012/07/11. PubMed PMID: 22776190; PubMed Central PMCID: PMCPMC3358981.

337. Castelhano-Carlos MJ, Baumans V. The impact of light, noise, cage cleaning and in-house transport on welfare and stress of laboratory rats. Lab Anim. 2009;43(4):311-27. Epub 2009/06/10. doi: 10.1258/la.2009.0080098. PubMed PMID: 19505937.

338. Meyn MS. Ataxia-telangiectasia, cancer and the pathobiology of the ATM gene. Clin Genet. 1999;55(5):289-304. Epub 1999/07/28. doi: 10.1034/j.1399-0004.1999.550501.x. PubMed PMID: 10422797.

339. Uziel T, Savitsky K, Platzer M, Ziv Y, Helbitz T, Nehls M, et al. Genomic Organization of the ATM gene. Genomics. 1996;33(2):317-20. Epub 1996/04/15. doi: 10.1006/geno.1996.0201. PubMed PMID: 8660985.

340. Rotman G, Shiloh Y. ATM: from gene to function. Hum Mol Genet. 1998;7(10):1555-63. Epub 1998/09/15. doi: 10.1093/hmg/7.10.1555. PubMed PMID: 9735376.

341. Ho U, Luff J, James A, Lee CS, Quek H, Lai HC, et al. SMG1 heterozygosity exacerbates haematopoietic cancer development in Atm null mice by increasing persistent DNA damage and oxidative stress. J Cell Mol Med. 2019;23(12):8151-60. Epub 2019/10/01. doi: 10.1111/jcmm.14685. PubMed PMID: 31565865; PubMed Central PMCID: PMCPMC6850945.

342. Barlow C, Hirotsune S, Paylor R, Liyanage M, Eckhaus M, Collins F, et al. Atm-deficient mice: a paradigm of ataxia telangiectasia. Cell. 1996;86(1):159-71. Epub 1996/07/12. doi: 10.1016/s0092-8674(00)80086-0. PubMed PMID: 8689683.

343. Borghesani PR, Alt FW, Bottaro A, Davidson L, Aksoy S, Rathbun GA, et al. Abnormal development of Purkinje cells and lymphocytes in Atm mutant mice. Proc Natl Acad Sci U S A. 2000;97(7):3336-41. Epub 2000/03/15. doi: 10.1073/pnas.050584897. PubMed PMID: 10716718; PubMed Central PMCID: PMCPMC16240.

344. Reliene R, Schiestl RH. Antioxidant N-acetyl cysteine reduces incidence and multiplicity of lymphoma in Atm deficient mice. DNA Repair (Amst). 2006;5(7):852-9. Epub 2006/06/20. doi: 10.1016/j.dnarep.2006.05.003. PubMed PMID: 16781197.

345. Bolhuis JE, Parmentier HK, Schouten WG, Schrama JW, Wiegant VM. Effects of housing and individual coping characteristics on immune responses of pigs. Physiol Behav. 2003;79(2):289-96. Epub 2003/07/02. doi: 10.1016/s0031-9384(03)00090-8. PubMed PMID: 12834801.

346. Yamamoto ML, Maier I, Dang AT, Berry D, Liu J, Ruegger PM, et al. Intestinal bacteria modify lymphoma incidence and latency by affecting systemic inflammatory state, oxidative stress, and leukocyte genotoxicity. Cancer Res. 2013;73(14):4222-32. Epub 2013/07/19. doi: 10.1158/0008-5472.CAN-13-0022. PubMed PMID: 23860718; PubMed Central PMCID: PMCPMC3718495.

347. Otaki M, Hirano T, Yamaguchi Y, Kaida K, Koshika S, Nagata K, et al. Changes in

the function and phenotype of resident peritoneal macrophages after housing in an enriched environment. Int Immunopharmacol. 2018;65:44-9. Epub 2018/10/03. doi: 10.1016/j.intimp.2018.09.037. PubMed PMID: 30273916.

348. Singhal G, Jaehne EJ, Corrigan F, Baune BT. Cellular and molecular mechanisms of immunomodulation in the brain through environmental enrichment. Front Cell Neurosci. 2014;8:97. Epub 2014/04/29. doi: 10.3389/fncel.2014.00097. PubMed PMID: 24772064; PubMed Central PMCID: PMCPMC3982075.

349. Libert C, Dejager L, Pinheiro I. The X chromosome in immune functions: when a chromosome makes the difference. Nat Rev Immunol. 2010;10(8):594-604. Epub 2010/07/24. doi: 10.1038/nri2815. PubMed PMID: 20651746.

350. vom Steeg LG, Klein SL. SeXX Matters in Infectious Disease Pathogenesis. PLoS Pathog. 2016;12(2):e1005374. Epub 2016/02/20. doi: 10.1371/journal.ppat.1005374. PubMed PMID: 26891052; PubMed Central PMCID: PMCPMC4759457.

351. Giefing-Kroll C, Berger P, Lepperdinger G, Grubeck-Loebenstein B. How sex and age affect immune responses, susceptibility to infections, and response to vaccination. Aging Cell. 2015;14(3):309-21. Epub 2015/02/28. doi: 10.1111/acel.12326. PubMed PMID: 25720438; PubMed Central PMCID: PMCPMC4406660.

352. Spolarics Z. In gender-based outcomes, sex hormones may be important but it is in the genes*. Crit Care Med. 2014;42(5):1294-5. Epub 2014/04/17. doi: 10.1097/CCM.0000000000000268. PubMed PMID: 24736343; PubMed Central PMCID: PMCPMC4007312.

353. Shenoda BB, Ramanathan S, Gupta R, Tian Y, Jean-Toussaint R, Alexander GM, et al. Xist attenuates acute inflammatory response by female cells. Cell Mol Life Sci. 2021;78(1):299-316. Epub 2020/03/21. doi: 10.1007/s00018-020-03500-3. PubMed PMID: 32193609; PubMed Central PMCID: PMCPMC7501270.

354. Fu X, Fu N, Guo S, Yan Z, Xu Y, Hu H, et al. Estimating accuracy of RNA-Seq and microarrays with proteomics. BMC Genomics. 2009;10:161. doi: 10.1186/1471-2164-10-161. PubMed PMID: 19371429; PubMed Central PMCID: PMCPMC2676304.

355. Wang X, Sun Q, McGrath SD, Mardis ER, Soloway PD, Clark AG. Transcriptome-wide identification of novel imprinted genes in neonatal mouse brain. PLoS One. 2008;3(12):e3839. doi: 10.1371/journal.pone.0003839. PubMed PMID: 19052635; PubMed Central PMCID: PMCPMC2585789.

356. Wahlstedt H, Daniel C, Enstero M, Ohman M. Large-scale mRNA sequencing determines global regulation of RNA editing during brain development. Genome Res. 2009;19(6):978-86. doi: 10.1101/gr.089409.108. PubMed PMID: 19420382; PubMed Central PMCID: PMCPMC2694479.

357. Kukurba KR, Montgomery SB. RNA Sequencing and Analysis. Cold Spring Harb Protoc. 2015;2015(11):951-69. doi: 10.1101/pdb.top084970. PubMed PMID: 25870306; PubMed Central PMCID: PMCPMC4863231.

358. Chu Y, Corey DR. RNA sequencing: platform selection, experimental design, and data interpretation. Nucleic Acid Ther. 2012;22(4):271-4. doi: 10.1089/nat.2012.0367. PubMed PMID: 22830413; PubMed Central PMCID: PMCPMC3426205.

359. Maher CA, Kumar-Sinha C, Cao X, Kalyana-Sundaram S, Han B, Jing X, et al. Transcriptome sequencing to detect gene fusions in cancer. Nature. 2009;458(7234):97-101. doi: 10.1038/nature07638. PubMed PMID: 19136943; PubMed Central PMCID: PMCPMC2725402.

360. Mi H, Muruganujan A, Casagrande JT, Thomas PD. Large-scale gene function analysis with the PANTHER classification system. Nat Protoc. 2013;8(8):1551-66. doi: 10.1038/nprot.2013.092. PubMed PMID: 23868073.

361. van Baarsen LG, Bos WH, Rustenburg F, van der Pouw Kraan TC, Wolbink GJ,

Dijkmans BA, et al. Gene expression profiling in autoantibody-positive patients with arthralgia predicts development of arthritis. Arthritis Rheum. 2010;62(3):694-704. doi: 10.1002/art.27294. PubMed PMID: 20131234.

362. Verma G, Bhatia H, Datta M. Gene expression profiling and pathway analysis identify the integrin signaling pathway to be altered by IL-1beta in human pancreatic cancer cells: role of JNK. Cancer Lett. 2012;320(1):86-95. doi: 10.1016/j.canlet.2012.01.036. PubMed PMID: 22313544.

363. Shi Y, Zhao H, Shi Y, Cao Y, Yang D, Li Z, et al. Genome-wide association study identifies eight new risk loci for polycystic ovary syndrome. Nat Genet. 2012;44(9):1020-5. doi: 10.1038/ng.2384. PubMed PMID: 22885925.

364. den Hoed M, Eijgelsheim M, Esko T, Brundel BJ, Peal DS, Evans DM, et al. Identification of heart rate-associated loci and their effects on cardiac conduction and rhythm disorders. Nat Genet. 2013;45(6):621-31. doi: 10.1038/ng.2610. PubMed PMID: 23583979; PubMed Central PMCID: PMCPMC3696959.

365. Boyer AP, Collier TS, Vidavsky I, Bose R. Quantitative proteomics with siRNA screening identifies novel mechanisms of trastuzumab resistance in HER2 amplified breast cancers. Mol Cell Proteomics. 2013;12(1):180-93. doi: 10.1074/mcp.M112.020115. PubMed PMID: 23105007; PubMed Central PMCID: PMCPMC3536899.

366. Stutzer I, Selevsek N, Esterhazy D, Schmidt A, Aebersold R, Stoffel M. Systematic proteomic analysis identifies beta-site amyloid precursor protein cleaving enzyme 2 and 1 (BACE2 and BACE1) substrates in pancreatic beta-cells. J Biol Chem. 2013;288(15):10536-47. doi: 10.1074/jbc.M112.444703. PubMed PMID: 23430253; PubMed Central PMCID: PMCPMC3624435.

367. Thomas PD, Campbell MJ, Kejariwal A, Mi H, Karlak B, Daverman R, et al.

PANTHER: a library of protein families and subfamilies indexed by function. Genome Res. 2003;13(9):2129-41. doi: 10.1101/gr.772403. PubMed PMID: 12952881; PubMed Central PMCID: PMCPMC403709.

368. Burgess M, Wicks K, Gardasevic M, Mace KA. Cx3CR1 Expression Identifies Distinct Macrophage Populations That Contribute Differentially to Inflammation and Repair. Immunohorizons. 2019;3(7):262-73. Epub 2019/07/30. doi: 10.4049/immunohorizons.1900038. PubMed PMID: 31356156.

369. Ng B, Dong J, Viswanathan S, Widjaja AA, Paleja BS, Adami E, et al. Fibroblast-specific IL11 signaling drives chronic inflammation in murine fibrotic lung disease. FASEB J. 2020;34(9):11802-15. Epub 2020/07/14. doi: 10.1096/fj.202001045RR. PubMed PMID: 32656894.

370. Fernando MR, Reyes JL, Iannuzzi J, Leung G, McKay DM. The pro-inflammatory cytokine, interleukin-6, enhances the polarization of alternatively activated macrophages. PLoS One. 2014;9(4):e94188. Epub 2014/04/17. doi: 10.1371/journal.pone.0094188. PubMed PMID: 24736635; PubMed Central PMCID: PMCPMC3988054.

371. Jia Y, Han S, Li J, Wang H, Liu J, Li N, et al. IRF8 is the target of SIRT1 for the inflammation response in macrophages. Innate Immun. 2017;23(2):188-95. Epub 2016/12/23. doi: 10.1177/1753425916683751. PubMed PMID: 28008797.

372. Agresta L, Hoebe KHN, Janssen EM. The Emerging Role of CD244 Signaling in Immune Cells of the Tumor Microenvironment. Front Immunol. 2018;9:2809. Epub 2018/12/14. doi: 10.3389/fimmu.2018.02809. PubMed PMID: 30546369; PubMed Central PMCID: PMCPMC6279924.

373. van Driel BJ, Liao G, Engel P, Terhorst C. Responses to Microbial Challenges by SLAMF Receptors. Front Immunol. 2016;7:4. Epub 2016/02/03. doi: 10.3389/fimmu.2016.00004. PubMed PMID: 26834746; PubMed Central PMCID:

PMCPMC4718992.

374. Fink LN, Oberbach A, Costford SR, Chan KL, Sams A, Bluher M, et al. Expression of anti-inflammatory macrophage genes within skeletal muscle correlates with insulin sensitivity in human obesity and type 2 diabetes. Diabetologia. 2013;56(7):1623-8. Epub 2013/04/19. doi: 10.1007/s00125-013-2897-x. PubMed PMID: 23595247.

375. Sun K, He SB, Yao YZ, Qu JG, Xie R, Ma YQ, et al. Tre2 (USP6NL) promotes colorectal cancer cell proliferation via Wnt/beta-catenin pathway. Cancer Cell Int. 2019;19:102. Epub 2019/04/25. doi: 10.1186/s12935-019-0823-0. PubMed PMID: 31015802; PubMed Central PMCID: PMCPMC6469084.

376. Ovalle-Bracho C, Franco-Munoz C, Londono-Barbosa D, Restrepo-Montoya D, Clavijo-Ramirez C. Changes in Macrophage Gene Expression Associated with Leishmania (Viannia) braziliensis Infection. PLoS One. 2015;10(6):e0128934. Epub 2015/06/09. doi: 10.1371/journal.pone.0128934. PubMed PMID: 26052705; PubMed Central PMCID: PMCPMC4460072.

377. Mason FM, Heimsath EG, Higgs HN, Soderling SH. Bi-modal regulation of a formin by srGAP2. J Biol Chem. 2011;286(8):6577-86. Epub 2010/12/15. doi: 10.1074/jbc.M110.190397. PubMed PMID: 21148482; PubMed Central PMCID: PMCPMC3057853.

378. Csepanyi-Komi R, Sirokmany G, Geiszt M, Ligeti E. ARHGAP25, a novel Rac GTPase-activating protein, regulates phagocytosis in human neutrophilic granulocytes. Blood. 2012;119(2):573-82. Epub 2011/11/19. doi: 10.1182/blood-2010-12-324053. PubMed PMID: 22096251.

379. Davignon I, Catalina MD, Smith D, Montgomery J, Swantek J, Croy J, et al. Normal hematopoiesis and inflammatory responses despite discrete signaling defects in Galpha15 knockout mice. Mol Cell Biol. 2000;20(3):797-804. Epub 2000/01/11. doi:

10.1128/MCB.20.3.797-804.2000. PubMed PMID: 10629036; PubMed Central PMCID: PMCPMC85196.

380. Hsu JW, Huang HC, Chen ST, Wong CH, Juan HF. Ganoderma lucidum Polysaccharides Induce Macrophage-Like Differentiation in Human Leukemia THP-1 Cells via Caspase and p53 Activation. Evid Based Complement Alternat Med. 2011;2011:358717. Epub 2009/08/22. doi: 10.1093/ecam/nep107. PubMed PMID: 19696196; PubMed Central PMCID: PMCPMC3135330.

381. Pong WW, Walker J, Wylie T, Magrini V, Luo J, Emnett RJ, et al. F11R is a novel monocyte prognostic biomarker for malignant glioma. PLoS One. 2013;8(10):e77571. Epub 2013/10/23. doi: 10.1371/journal.pone.0077571. PubMed PMID: 24147027; PubMed Central PMCID: PMCPMC3795683.

382. She H, He Y, Zhao Y, Mao Z. Autophagy in inflammation: the p38alpha MAPK-ULK1 axis. Macrophage (Houst). 2018;5. Epub 2018/05/08. PubMed PMID: 29732413; PubMed Central PMCID: PMCPMC5933864.

383. Poczobutt JM, De S, Yadav VK, Nguyen TT, Li H, Sippel TR, et al. Expression Profiling of Macrophages Reveals Multiple Populations with Distinct Biological Roles in an Immunocompetent Orthotopic Model of Lung Cancer. J Immunol. 2016;196(6):2847-59. Epub 2016/02/14. doi: 10.4049/jimmunol.1502364. PubMed PMID: 26873985; PubMed Central PMCID: PMCPMC4779748.

384. Fan H, Guo Y, Tsai YH, Storey AJ, Kim A, Gong W, et al. A conserved BAH module within mammalian BAHD1 connects H3K27me3 to Polycomb gene silencing. Nucleic Acids Res. 2021;49(8):4441-55. Epub 2021/04/07. doi: 10.1093/nar/gkab210. PubMed PMID: 33823544; PubMed Central PMCID: PMCPMC8096256.

385. Cordova ZM, Gronholm A, Kytola V, Taverniti V, Hamalainen S, Aittomaki S, et al. Myeloid cell expressed proprotein convertase FURIN attenuates inflammation.

Oncotarget. 2016;7(34):54392-404. Epub 2016/08/17. doi: 10.18632/oncotarget.11106. PubMed PMID: 27527873; PubMed Central PMCID: PMCPMC5342350.

386. Pesu M, Muul L, Kanno Y, O'Shea JJ. Proprotein convertase furin is preferentially expressed in T helper 1 cells and regulates interferon gamma. Blood. 2006;108(3):983-5. Epub 2006/04/22. doi: 10.1182/blood-2005-09-3824. PubMed PMID: 16627761; PubMed Central PMCID: PMCPMC1895858.

387. Ortutay Z, Oksanen A, Aittomaki S, Ortutay C, Pesu M. Proprotein convertase FURIN regulates T cell receptor-induced transactivation. J Leukoc Biol. 2015;98(1):73-83. Epub 2015/05/01. doi: 10.1189/jlb.2A0514-257RR. PubMed PMID: 25926688.

388. Oksanen A, Aittomaki S, Jankovic D, Ortutay Z, Pulkkinen K, Hamalainen S, et al. Proprotein convertase FURIN constrains Th2 differentiation and is critical for host resistance against Toxoplasma gondii. J Immunol. 2014;193(11):5470-9. Epub 2014/10/31. doi: 10.4049/jimmunol.1401629. PubMed PMID: 25355923; PubMed Central PMCID: PMCPMC4261955.

389. Pesu M, Watford WT, Wei L, Xu L, Fuss I, Strober W, et al. T-cell-expressed proprotein convertase furin is essential for maintenance of peripheral immune tolerance. Nature. 2008;455(7210):246-50. Epub 2008/08/15. doi: 10.1038/nature07210. PubMed PMID: 18701887; PubMed Central PMCID: PMCPMC2758057.

390. Ishii M, Egen JG, Klauschen F, Meier-Schellersheim M, Saeki Y, Vacher J, et al. Sphingosine-1-phosphate mobilizes osteoclast precursors and regulates bone homeostasis. Nature. 2009;458(7237):524-8. Epub 2009/02/11. doi: 10.1038/nature07713. PubMed PMID: 19204730; PubMed Central PMCID: PMCPMC2785034.

391. Fogg DK, Sibon C, Miled C, Jung S, Aucouturier P, Littman DR, et al. A clonogenic bone marrow progenitor specific for macrophages and dendritic cells. Science. 2006;311(5757):83-7. Epub 2005/12/03. doi: 10.1126/science.1117729. PubMed PMID:

16322423.

392. Ishida Y, Gao JL, Murphy PM. Chemokine receptor CX3CR1 mediates skin wound healing by promoting macrophage and fibroblast accumulation and function. J Immunol. 2008;180(1):569-79. Epub 2007/12/22. doi: 10.4049/jimmunol.180.1.569. PubMed PMID: 18097059.

393. Donnelly DJ, Longbrake EE, Shawler TM, Kigerl KA, Lai W, Tovar CA, et al. Deficient CX3CR1 signaling promotes recovery after mouse spinal cord injury by limiting the recruitment and activation of Ly6Clo/iNOS+ macrophages. J Neurosci. 2011;31(27):9910-22. Epub 2011/07/08. doi: 10.1523/JNEUROSCI.2114-11.2011. PubMed PMID: 21734283; PubMed Central PMCID: PMCPMC3139517.

394. Hoshino A, Ueha S, Hanada S, Imai T, Ito M, Yamamoto K, et al. Roles of chemokine receptor CX3CR1 in maintaining murine bone homeostasis through the regulation of both osteoblasts and osteoclasts. J Cell Sci. 2013;126(Pt 4):1032-45. Epub 2012/12/25. doi: 10.1242/jcs.113910. PubMed PMID: 23264747.

395. Imai T, Hieshima K, Haskell C, Baba M, Nagira M, Nishimura M, et al. Identification and molecular characterization of fractalkine receptor CX3CR1, which mediates both leukocyte migration and adhesion. Cell. 1997;91(4):521-30. Epub 1997/12/09. doi: 10.1016/s0092-8674(00)80438-9. PubMed PMID: 9390561.

396. Putoczki T, Ernst M. More than a sidekick: the IL-6 family cytokine IL-11 links inflammation to cancer. J Leukoc Biol. 2010;88(6):1109-17. Epub 2010/07/09. doi: 10.1189/jlb.0410226. PubMed PMID: 20610798.

397. Jones SA, Jenkins BJ. Recent insights into targeting the IL-6 cytokine family in inflammatory diseases and cancer. Nat Rev Immunol. 2018;18(12):773-89. Epub 2018/09/27. doi: 10.1038/s41577-018-0066-7. PubMed PMID: 30254251.

398. Fabian MR, Cieplak MK, Frank F, Morita M, Green J, Srikumar T, et al. miRNA-

mediated deadenylation is orchestrated by GW182 through two conserved motifs that interact with CCR4-NOT. Nat Struct Mol Biol. 2011;18(11):1211-7. Epub 2011/10/11. doi: 10.1038/nsmb.2149. PubMed PMID: 21984185.

399. Gilbertson S, Federspiel JD, Hartenian E, Cristea IM, Glaunsinger B. Changes in mRNA abundance drive shuttling of RNA binding proteins, linking cytoplasmic RNA degradation to transcription. Elife. 2018;7. Epub 2018/10/04. doi: 10.7554/eLife.37663. PubMed PMID: 30281021; PubMed Central PMCID: PMCPMC6203436.

400. Zhang C, Fu J, Zhou Y. A Review in Research Progress Concerning m6A Methylation and Immunoregulation. Front Immunol. 2019;10:922. Epub 2019/05/14. doi: 10.3389/fimmu.2019.00922. PubMed PMID: 31080453; PubMed Central PMCID: PMCPMC6497756.

401. Pisitkun P, Deane JA, Difilippantonio MJ, Tarasenko T, Satterthwaite AB, Bolland S. Autoreactive B cell responses to RNA-related antigens due to TLR7 gene duplication. Science. 2006;312(5780):1669-72. Epub 2006/05/20. doi: 10.1126/science.1124978. PubMed PMID: 16709748.

402. Berghofer B, Frommer T, Haley G, Fink L, Bein G, Hackstein H. TLR7 ligands induce higher IFN-alpha production in females. J Immunol. 2006;177(4):2088-96. Epub 2006/08/05. doi: 10.4049/jimmunol.177.4.2088. PubMed PMID: 16887967.

403. Torcia MG, Nencioni L, Clemente AM, Civitelli L, Celestino I, Limongi D, et al. Sex differences in the response to viral infections: TLR8 and TLR9 ligand stimulation induce higher IL10 production in males. PLoS One. 2012;7(6):e39853. Epub 2012/07/07. doi: 10.1371/journal.pone.0039853. PubMed PMID: 22768144; PubMed Central PMCID: PMCPMC3387221.

404. Griesbeck M, Ziegler S, Laffont S, Smith N, Chauveau L, Tomezsko P, et al. Sex Differences in Plasmacytoid Dendritic Cell Levels of IRF5 Drive Higher IFN-alpha

Production in Women. J Immunol. 2015;195(11):5327-36. Epub 2015/11/01. doi: 10.4049/jimmunol.1501684. PubMed PMID: 26519527; PubMed Central PMCID: PMCPMC4654231.

405. Jaillon S, Berthenet K, Garlanda C. Sexual Dimorphism in Innate Immunity. Clin Rev Allergy Immunol. 2019;56(3):308-21. Epub 2017/10/01. doi: 10.1007/s12016-017-8648-x. PubMed PMID: 28963611.

406. Asai K, Hiki N, Mimura Y, Ogawa T, Unou K, Kaminishi M. Gender differences in cytokine secretion by human peripheral blood mononuclear cells: role of estrogen in modulating LPS-induced cytokine secretion in an ex vivo septic model. Shock. 2001;16(5):340-3. Epub 2001/11/09. doi: 10.1097/00024382-200116050-00003. PubMed PMID: 11699070.

407. Scotland RS, Stables MJ, Madalli S, Watson P, Gilroy DW. Sex differences in resident immune cell phenotype underlie more efficient acute inflammatory responses in female mice. Blood. 2011;118(22):5918-27. Epub 2011/09/14. doi: 10.1182/blood-2011-03-340281. PubMed PMID: 21911834; PubMed Central PMCID: PMCPMC5363818.

408. Laffont S, Rouquie N, Azar P, Seillet C, Plumas J, Aspord C, et al. X-Chromosome complement and estrogen receptor signaling independently contribute to the enhanced TLR7-mediated IFN-alpha production of plasmacytoid dendritic cells from women. J Immunol. 2014;193(11):5444-52. Epub 2014/10/24. doi: 10.4049/jimmunol.1303400. PubMed PMID: 25339659.

409. Naro C, Sette C. Phosphorylation-mediated regulation of alternative splicing in cancer. Int J Cell Biol. 2013;2013:151839. doi: 10.1155/2013/151839. PubMed PMID: 24069033; PubMed Central PMCID: PMCPMC3771450.

410. Galganski L, Urbanek MO, Krzyzosiak WJ. Nuclear speckles: molecular organization, biological function and role in disease. Nucleic Acids Res.

2017;45(18):10350-68. Epub 2017/10/05. doi: 10.1093/nar/gkx759. PubMed PMID: 28977640; PubMed Central PMCID: PMCPMC5737799.

411. Starr T, Bauler TJ, Malik-Kale P, Steele-Mortimer O. The phorbol 12-myristate-13-acetate differentiation protocol is critical to the interaction of THP-1 macrophages with Salmonella Typhimurium. PLoS One. 2018;13(3):e0193601. Epub 2018/03/15. doi: 10.1371/journal.pone.0193601. PubMed PMID: 29538403; PubMed Central PMCID: PMCPMC5851575.

412. Raschke WC, Baird S, Ralph P, Nakoinz I. Functional macrophage cell lines transformed by Abelson leukemia virus. Cell. 1978;15(1):261-7. Epub 1978/09/01. doi: 10.1016/0092-8674(78)90101-0. PubMed PMID: 212198.

413. Cao Y, Chen J, Ren G, Zhang Y, Tan X, Yang L. Punicalagin Prevents Inflammation in LPS-Induced RAW264.7 Macrophages by Inhibiting FoxO3a/Autophagy Signaling Pathway. Nutrients. 2019;11(11). Epub 2019/11/17. doi: 10.3390/nu11112794. PubMed PMID: 31731808; PubMed Central PMCID: PMCPMC6893462.

414. Fan K, Lin L, Ai Q, Wan J, Dai J, Liu G, et al. Lipopolysaccharide-Induced Dephosphorylation of AMPK-Activated Protein Kinase Potentiates Inflammatory Injury via Repression of ULK1-Dependent Autophagy. Front Immunol. 2018;9:1464. Epub 2018/07/11. doi: 10.3389/fimmu.2018.01464. PubMed PMID: 29988556; PubMed Central PMCID: PMCPMC6026648.

415. Sweet MJ, Campbell CC, Sester DP, Xu D, McDonald RC, Stacey KJ, et al. Colony-stimulating factor-1 suppresses responses to CpG DNA and expression of toll-like receptor 9 but enhances responses to lipopolysaccharide in murine macrophages. J Immunol. 2002;168(1):392-9. Epub 2001/12/26. doi: 10.4049/jimmunol.168.1.392. PubMed PMID: 11751985.

416. Mogal A, Abdulkadir SA. Effects of Histone Deacetylase Inhibitor (HDACi);

Trichostatin-A (TSA) on the expression of housekeeping genes. Mol Cell Probes. 2006;20(2):81-6. doi: 10.1016/j.mcp.2005.09.008. PubMed PMID: 16326072.

417. Roberts TL, Idris A, Dunn JA, Kelly GM, Burnton CM, Hodgson S, et al. HIN-200 proteins regulate caspase activation in response to foreign cytoplasmic DNA. Science. 2009;323(5917):1057-60. doi: 10.1126/science.1169841. PubMed PMID: 19131592.

418. Sweet MJ, Stacey KJ, Ross IL, Ostrowski MC, Hume DA. Involvement of Ets, rel and Sp1-like proteins in lipopolysaccharide-mediated activation of the HIV-1 LTR in macrophages. J Inflamm. 1998;48(2):67-83. Epub 1998/07/10. PubMed PMID: 9656143.

Appendix

Supplementary data and this work has been published in Journal of Leukocyte Biology

[130] (chapter 2)

JLB JOURNAL OF LEUKOCYTE BIOLOGY

BRIEF CONCLUSIVE REPORT

Regulation of RNA degradation pathways during the lipopolysaccharide response in Macrophages

Hui-Chi Lai[1,2] | Alexander James[1] | John Luff[3] | Paul De Souza[1,4,6] | Hazel Quek[5] | Uda Ho[7] | Martin F. Lavin[3] | Tara L. Roberts[1,2,3,6] [ID]

[1] Ingham Institute for Applied Medical Research, Liverpool, New South Wales, Australia

[2] South West Sydney Clinical School, UNSW Australia, Liverpool, New South Wales, Australia

[3] The University of Queensland Centre for Clinical Research, Herston, Queensland, Australia

[4] Medical Oncology Department, Liverpool Hospital, Liverpool, New South Wales, Australia

[5] QIMR Berghofer Medical Research Institute, Herston, Queensland, Australia

[6] School of Medicine, Western Sydney University, Macarthur, New South Wales, Australia

[7] School of Biomedical Sciences, Faculty of Medicine, University of Queensland, Brisbane, Queensland, Australia

Correspondence
Dr Tara Roberts, 1 Campbell St Liverpool NSW Australia 2170.
Email: Tara.Roberts@westernsydney.edu.au

Abstract

The innate immune response to LPS is highly dynamic yet tightly regulated. The majority of studies of gene expression have focussed on transcription. However, it is also important to understand how post-transcriptional pathways are regulated in response to inflammatory stimuli as the rate of RNA degradation relative to new transcription is important for overall expression. RNA decay pathways include nonsense-mediated decay, the RNA decay exosome, P-body localized deadenylation, decapping and degradation, and AU-rich element targeted decay mediated by tristetraprolin. Here, bone marrow-derived Mφs were treated with LPS over a time course of 0, 2, 6, and 24 h and the transcriptional profiles were analyzed by RNA sequencing. The data show that components of RNA degradation pathways are regulated during an LPS response. Processing body associated decapping enzyme DCP2 and regulatory subunit DCP1A, and 5′ exonuclease XRN1 and sequence specific RNA decay pathways were upregulated. Nonsense mediated decay was also increased in response to LPS induced signaling, initially by increased activation and at later timepoints at the mRNA and protein levels. This leads to increased nonsense mediated decay efficiency across the 24 h following LPS treatment. These findings suggest that LPS activation of Mφs results in targeted regulation of RNA degradation pathways in order to change how subsets of mRNAs are degraded during an inflammatory response.

KEYWORDS

LPS, nonsense mediated decay, post-transcriptional regulation, RNA decay, toll-like receptors

1 | INTRODUCTION

The TLRs are a well-known signaling pathway in the recognition of pathogen associated molecular patterns (PAMPs); specific molecular patterns that are present in microbial components. The TLR family respond to a range of PAMPs to induce pro-inflammatory cytokine production, up-regulation of co-stimulatory molecules, and sculpting of the adaptive immune response.[1,2]

Abbreviations: ATCC, American Type Culture Collection; ALKBH3, Alpha-Ketoglutarate Dependent Dioxygenase; ATF4, Activating transcription factor 4; bp, base pair; BSA, Bovine serum albumin; BMM, Bone marrow macrophages; C57BL/6, C57 black 6 mouse strain; cDNA, complementary deoxyribonucleic acid; CO₂, Carbon dioxide; Cre, Cre recombinase; CNOT7, CCR4-NOT Transcription Complex Subunit 7; DCP1A, mRNA-decapping enzyme 1A; DCP2, Decapping mRNA 2; DIS3, Exosome complex exonuclease RRP44; DMSO, Dimethyl sulfoxide; DNA, Deoxyribonucleic acid; dNTPs, Deoxynucleotide; DTT, Dithiothreitol; EST1A, Telomerase-binding protein; E. coli, Escherichia coli; EDTA, Ethylenediaminetetraacetate; GAPDH, Glyceraldehyde 3-phosphate dehydrogenase; GAS1, Growth arrest specific 1; GAS5, Growth arrest specific 5; GTPase, Guanine triphosphatase; HCl, Hydrochloric acid; hr, hour; IF, Immunofluorescence; IRF3, Interferon regulatory factor 3; IKKα/IKKβ, IKB Kinase a/ IKB Kinase β; IL-6, Interleukin 6; IL-1β, Interleukin 1 beta; KDa, kilo Dalton; L, Litre; LPS, Lipopolysaccharide; Luc7l, Putative RNA-binding protein Luc7-like 1; M, Molar; MEF, Mouse embryonic fibroblast; MET, Mesenchymal epithelial transition; MgCl₂, Magnesium chloride; min, minute; mRNA, messenger ribonucleic acid; MW, Molecular weight; MyD88, Myeloid differentiation primary response 88; M-CSF, Macrophage colony-stimulating factor; NaCl, Sodium chloride; NF-κB, Nuclear Factor kappa-light-chain-enhancer of activated B cells; NMD, Nonsense mediated decay; PBS, Phosphate buffer saline; PCR, Polymerase chain reaction; PTC, Premature termination codon; qRT-PCR, Quantitative reverse transcriptase polymerase chain reaction; RNA, Ribonucleic acid; rpm, round per minute; SMG1, SMG1 Phosphatidylinositol 3-Kinase-Related Kinase; SMG5, SMG5 Nonsense Mediated MRNA Decay Factor; SMG6, SMG6 Nonsense Mediated MRNA Decay Factor; SMG7, SMG7 Nonsense Mediated MRNA Decay Factor; STALUFEN1, STAU1-mediated mRNA decay protein; TBK1, TANK-binding kinase 1; TRIF, TIR-domain-containing adapter-inducing interferon-β; TNFα, Tumor necrosis factor alpha; UPF1, RNA Helicase And ATPase; TBL2, Transducin Beta Like 2; TGM2, Transglutaminase 2; TTP, Tristetraprolin; UPF3B, Up-Frameshift Suppressor 3 Homolog On Chromosome X; WT, Wild-type; XRN1, 5′-3′ Exoribonuclease 1.

In this study, we focused on TLR4 signaling. TLR4 is activated by LPS and can recruit adaptor proteins MyD88 and TRIF. MyD88 binds to the cytoplasmic portion of TLRs through interaction between individual Toll-IL 1 receptor (TIR) domains. Upon stimulation, MyD88 downstream signaling leads to activation of MAPKs and NF-κB, and induction of the transcription of cytokines and immune regulatory genes.[1] In addition to MyD88-dependent signaling, TLR4 also activates the MyD88–independent pathway (TRIF-dependent) that leads to activation of IRF3 via TBK1 and IKKα/IKKβ and induces type I IFN production.[2]

Gene expression is controlled at multiple steps including transcription, splicing, mRNA export, RNA stability, and rate of translation.[3] Compared to induction of gene expression,[4] there is less known about how post-transcriptional pathways are regulated in response to inflammatory stimuli. Alternative splicing results in the generation of different protein isoforms and incorporation of additional regulatory elements and is important for innate immune regulation.[5,6] Regulatory elements can control the stability of the mRNA transcript, in innate immunity particularly adenylate/uridylate-rich (AU-rich) elements that control mRNA stability of many cytokines including TNFα, IL-6, and IL-1β.[7] Other elements such as the constitutive decay element in TNFα have also been described.[8] miRNA can also regulate RNA degradation and translation rates in inflammatory responses in Mφs.[9] Regulation of RNA decay pathways more broadly has not been described in response to TLR signaling with most studies describing how these pathways may target viral transcripts. RNA decay also plays an essential role in post-transcriptional regulation of gene expression. The rate of RNA degradation of specific transcripts compared to new transcription is important for overall expression. Pathways controlling RNA decay include the RNA decay exosome, P-body localized deadenylation, decapping and degradation, quality control systems including nonsense-mediated decay, and AU-rich element targeted decay mediated by tristetraprolin (TTP) (Table 1). In eukaryotes, 5'-cap and 3'-poly (A) tail are considered features that protect from the attack of exonucleases and these 2 structures can interact with the cytoplasmic proteins eIF4E and the poly (A)-binding protein (PABP), respectively. As a result, mRNA transcripts are protected from exonucleases leading to enhanced translation. The process of RNA decay frequently starts with deprotection of the mRNA transcript, that is, decapping and deadenylation. mRNA may subsequently be degraded by the XRN1 exonuclease or alternatively, the exosome complex degrades mRNA in the 3' to 5' direction. RNA decay can occur co-translationally or in cytoplasmic foci called processing bodies (P-bodies). P-bodies are sites where mRNAs are targeted to decay factors and are either degraded or shuttled to other cytoplasmic foci called stress granules where some transcripts are stored for later translation.[10] Sequence-specific RNA decay pathways or quality control pathways direct mRNAs to these sites of degradation. RNA decay in immunity has predominantly been studied in relation to infection with RNA viruses.[11,12] Here, we have examined the regulation of key RNA decay pathways during the time course of the response to the bacterial component LPS in Mφs. These results highlight targeted regulation of these pathways during innate immunity as an additional layer of control on inflammatory processes.

2 | MATERIALS AND METHODS

2.1 | Isolation and culture bone marrow-derived Mφs

C57BL/6J mice were bred in house and 6–8-week-old mice were used to isolate bone marrow cells. SMG1 heterozygous mice have been described previously.[13] All mice were housed in a perpetual 12 h light/dark cycle and fed ad libitum under specific pathogen-free (SPF) conditions. All animal experiments were approved by the animal ethics committees of Western Sydney University or The University of Queensland and were conducted in accordance with the "Australian Code for the Care and Use of Animals for Scientific Purposes (2013)." Bone marrow derived Mφs (BMMs) were isolated as described previously[14] with minor modifications. Briefly, bone marrow cells were flushed from mouse tibiae and femurs with media. The cells were then plated in 10-cm dishes with 10 ml of RPMI supplemented with 10% FBS, 100 U/ml penicillin, and 100 μg/ml streptomycin, and cultured in a humidified incubator at 37°C and 5% CO_2 in the presence of 10 ng/ml M-CSF (Peprotech). At day 5, cells were washed and fresh media supplied. After 7 days differentiation, BMMs were stimulated with LPS (E coli LPS, Sigma) 5 ng/ml for 0, 2, 6, and 24 h to generate quadruplicate ($n = 4$) samples for each timepoint.

2.2 | Cell culture for THP-1 human myeloid cells

THP-1 (ATCC TIB-202) were grown in RPMI (Thermo Fisher Scientific, Waltham, MA) supplemented with 10% FBS, 100 U/ml penicillin, and 100 μg/ml streptomycin, 10 mM Hepes, 1 mM Sodium Pyruvate, 0.05 mM β-mercaptoethanol (Sigma) in a humidified incubator at 37°C and 5% CO_2. siRNA knockdown was performed as described previously.[15] NMDI 14 (Sigma–Aldrich) was dissolved in DMSO and incubated overnight with THP-1 at indicated concentrations.

2.3 | RNA-sequencing (RNA-seq)

RNA was isolated using Qiagen RNeasy kits according to the manufacturer's instructions. RNA samples were run on the lab-chip to determine contaminations and then proceeded with DNAse treatment (Turbo DNase, Invitrogen). RNA integrity number (RIN value) was checked with a Bioanalyser (Agilent, Santa Clara – USA) to decide the fragmentation time for each sample. Concentration for samples were determined with Quant-iT RiboGreen assay (ThermoFisher Scientific) and normalized to the same total concentration of 250 ng before proceeding to library preparation. Next, RNA was depleted, fragmented, first and second strand synthesized, adenylated, ligated, and then enriched following Illumina Truseq Stranded RNA Library prep (Gold) kit protocol (Illumina, USA). The DNA fragment was enriched using the following PCR conditions: – 98°C for 30 s, (98°C for 10 s, 60°C for 30 s, 72°C for 30 s) × 10 cycles, 72°C for 5 min. The final library was cleaned using AMPure XP beads (Beckman Coulter, USA) and checked on the 4200 TapeStation (Agilent, USA) to determine fragment size and concentration. Libraries were normalized to the same concentration (2 nM), pooled together, and sequenced at 12 pM on the

TABLE 1 Genes regulated by LPS and related to RNA decay pathways

Regulation by RNA decay pathways	Genes
Deadenylation (Ccr4-NOT Complex) (17)	Cnot1, Cnot2, Cnot3, Cnot4, Cnot6, Cnot7, Cnot8, Rqcd1 (Cnot9), Cnot10, *Pam*, Cnot6l, *Pan2 (Ampd3)*, Pan3, Tob1, Tob2, **Btg1**, Btg2
Core Exosome (9)	Dis3, Exosc1, Exosc2, Exosc3, Exosc4, Exosc5, Exosc7, Exosc8, Exosc9
Exosome-Associated Factors (8)	C1d, Mphosph6, Exosc10, *Pabpc1*, Skiv2l2, **Papd7**, Skiv2l, *Zcchc7*
Element/sequence specific (2)	Dhx36, *Pabpc1*
Decapping (16)	Xrn1, Xrn2, Dcp1a, **Dcp2**, Edc3, Dcp1b, Dcps, Wdr61 (Ski8), Ttc37, *Lsm1*, Lsm2, Lsm3, Lsm4, Lsm5, Lsm6, Edc4
P-bodies and stress granules (3)	Xrn1, Ddx6, *Pat1*
RNA degradosome (3)	Eno1, *Eno2*, Eno3
Nonsense-mediated decay (8)	Upf1, Upf2, Upf3a, Upf3b, Smg1, Smg5, Smg6, Smg7
Other (4)	Hspd1, Naa38, Hspa9, Wdr61

Bold, up-regulated > 1.5-fold by IFN. Italics, down-regulated > 1.5-fold by IFN (according to interferome database, www.interferome.org).

Illumina HiSeq2500 platform at Western Sydney University-NGS facility (Hawkesbury, Australia).

Reads were aligned using the standard Stemformatics RNA-Seq data processing pipeline (https://www.stemformatics.org/Stemformatics_data_methods.pdf).[16,17] Summarized count data were CPM (counts per million) normalized and log transformed prior to differential expression analysis using the limma and voom packages (https://f1000research.com/articles/5-1408/v2). Multiple pairwise contrasts between samples were performed and top tables of significant differential expression probes by empirical Bayes moderated t-test were produced. Gene Ontology profiling was used to identify statistically over-represented GO terms in our datasets based on RNA seq. Biological and functional gene enriched pathways were identify by the 2 common online resources-Panther (http://www.pantherdb.org/) and GOrilla (http://cbl-gorilla.cs.technion.ac.il/) platforms.[18,19] Gorilla analysis was performed using a single ranked gene list based on the calculated differential gene expression p-value for paired samples. Cut-off for GOrilla gene ontology term inclusion was set at 10^{-4} for initial inclusion and FDR q-values were calculated to account for multiple testing (see GOrilla website,[19,20]). Heat maps were generated via the Stemformatics platform using Pearsons correlation. Dataset available on the Stemformatics platform reference S4M-7004.

2.4 | Quantitative PCR

RNA was isolated using TriReagent (Sigma) according to the manufacturer's instructions with minor modifications as described previously.[21] Real time PCR reactions were performed as described previously[15] and analyzed using an Applied Biosystems QuantStudio (ThermoFisher). Primer sequences are listed in Table S2.

2.5 | Statistical analysis

Graphing and statistical evaluation was performed using GraphPad Prism 8 (GraphPad Software, USA). Data are presented as mean ± SEM from at least 3 independent experiments by an unpaired 2-tailed Student's T-test. Differences were considered to be significant if $p \leq 0.05$.

2.6 | Western blotting and immunoprecipitation

Western blotting was performed as described previously.[22] The primary Abs and dilutions used were rabbit anti-DCP1a (Abcam) 1:1000 (#ab183709), mouse-anti-DIS3 (Abcam) 1:1000 (#ab214083), rabbit anti-Xrn1 (Abcam) 1:1000 (#ab70259), rabbit anti-EST1A (Abcam) 1:1000 (#ab87539), rabbit anti-Staufen1 (Abcam) 1:1000 (#ab73478), rabbit anti-UPF1 (MBL) 1:1000 (#MBRN108PW), rabbit phospho (S/T)Q (Cell Signalling Technologies) 1:1000 (#2851), and mouse anti-β-actin (Cell Signalling Technologies) 1:5000 (#3700). The anti-SMG1 Abs were generated in house and have been described previously.[10] Anti-Rabbit (#7074) and anti-mouse (#7076) HRP tagged secondary Abs were sourced from Cell Signalling Technologies. Immunoprecipitations were performed as described previously.[21] Anti-UPF1 (#MBRN108PW, note: not all lots of this Ab work for immunoprecipitation) and protein G beads were purchased from MBL and Millipore, respectively.

3 | RESULTS

3.1 | RNA degradation pathways are regulated during an LPS response

We performed RNA sequencing to analyze gene expression changes during the LPS response.[16,17] Quadruplicate samples from BMM treated with LPS for 0, 2, 6 and 24 h were analyzed (schematic of the experimental process is shown in Fig. 1A). We examined differentially expressed genes across the time course including performing gene ontology analysis via the GOrilla platform,[19,20] example output for the 2 h timepoint is shown in Supplementary Fig. S1. This demonstrated the expected increase in pathways associated with innate immune responses and regulation of cytokine production (among multiple immune related pathways). We also validated the regulation of key cytokines involved in LPS responses, as seen in RNA sequencing data (Supplementary Fig. S2A), by real-time PCR (Supplementary Fig. S2A and B) that indicated that Mφs were responding to LPS as expected within this dataset. In addition to immune related genes, we were interested to note that the RNA metabolism gene ontology
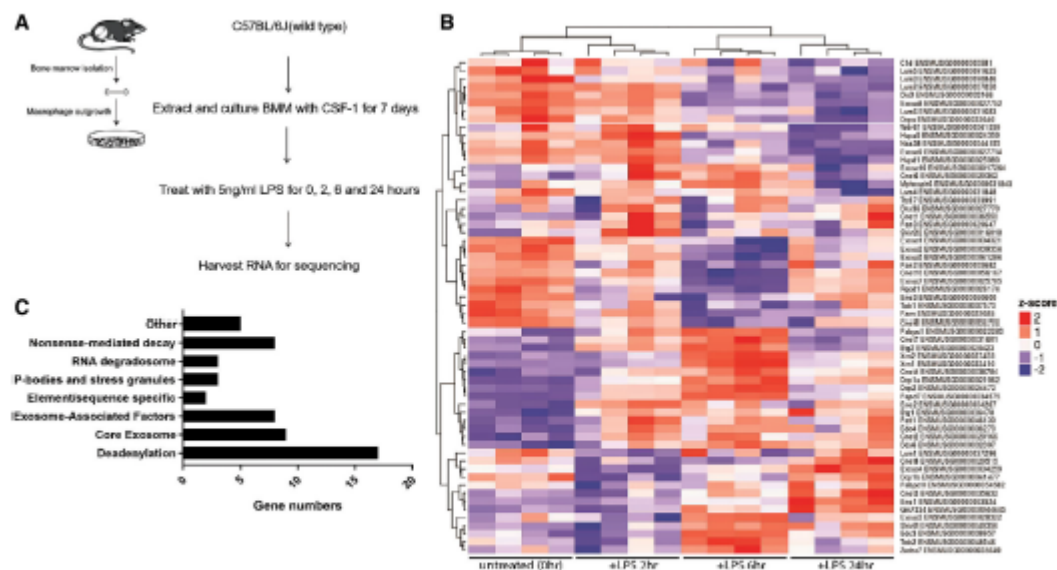
FIGURE 1 RNA sequencing analysis of the LPS response in Mφs. (A) Schematic of the sample production for RNA sequencing. (B) Heat-map was generated from RNA sequencing data and shows RNA decay related genes with regulated over the time-course of the LPS treatment (0, 2, 6, 24 h). Colors indicate the range of each gene's expression in response to LPS treatment, see key on right hand side. (C) Graph indicating the number of genes regulated for each of the major RNA decay pathways

classes were also significantly regulated (Supplementary Fig. S1 and C). Within these gene lists, we noticed a large number of RNA decay genes. To examine this further, we used the Stemformatics platform to examine specifically genes annotated as associated with RNA decay. A heat map showing changes in expression of RNA decay related genes was generated from this data (Fig. 1B). This demonstrated that there were significant alterations of the expression of genes related to RNA decay during an LPS response with 56/60 of the annotated RNA decay genes either up- or down-regulated. The number of genes regulated for each of the RNA decay related pathways is shown in Fig. 1C. These pathways include multiple stages of the RNA decay process deadenylation, core exosome, exosome-associated factors, decapping, P-bodies and stress granules, RNA degradosome, and nonsense mediated decay (NMD). Specific genes shown to be regulated in the heat map (Fig. 1B) have been consolidated in Table 1. Supplementary Fig. S2D shows how these genes are regulated on volcano plots. Similar to the single gene profiles at 2 h, there is less regulation with some significantly up- and down-regulated genes, this is more dramatic at 6 h, with a broader trend toward decreased expression than at 2 h.

3.2 | Validation of gene expression changes by quantitative PCR

A subset RNA decay genes were chosen for validation by quantitative PCR as they represent key regulators of the pathways. The single gene profiles were generated using the Stemformatics platform[16,17] and compared to data from qPCR (Fig. 2 and Supplementary Fig. S3).

The qPCR results confirmed that mRNA for the key catalytic subunit of the nuclear exosome (Dis3) was downregulated but rate limiting components of the decapping pathway Dcp1 and Dcp2a, and 5′ exonuclease XRN1 are induced (Fig. 2A [RNA sequencing data] and B [validation data]). In contrast, components of the exosome (Exosc5 and 7) and a member of the deadenylation complex (Cnot 7) did not show significant regulation in validation samples (Supplementary Fig. S3A [RNA seq data] and B [validation data]). As a positive control, we also validated 2 RNA regulatory proteins known to play an important role in innate immune responses with well-established induction in response to LPS. Tristetraprolin (TTP encoded by Zfp36) is key in regulation via AU-rich elements[23] and Regnase 1 (encoded by Zc3h12a) is a ribonuclease and key negative regulator of TLR responses.[24] The mRNA for both of these was strongly induced in response to LPS (Supplementary Fig. S4A [RNA sequencing data] and S4B [validation data]).

We also examined whether the changes seen at the mRNA level lead to protein level changes for a subset of regulated genes. Western blotting was performed on protein extracts from BMM over a time course in response to LPS treatment (0, 2, 6, 16, 24, 48 h). These results indicated that 5′ exonuclease XRN1 and major decapping enzyme DCP1A are induced during an LPS treatment from 6 h onward. This was expected as mRNA was strongly induced by this timepoint. In contrast to the mRNA data, there were no major changes in Dis3 protein expression during LPS treatment 0–48 h (Fig. 3). This was surprising as the mRNA level was clearly decreased at 6 and 24 h. This indicates that there may be additional layers of regulation of Dis3 expression during the LPS response or that the Dis3 protein is quite stable.
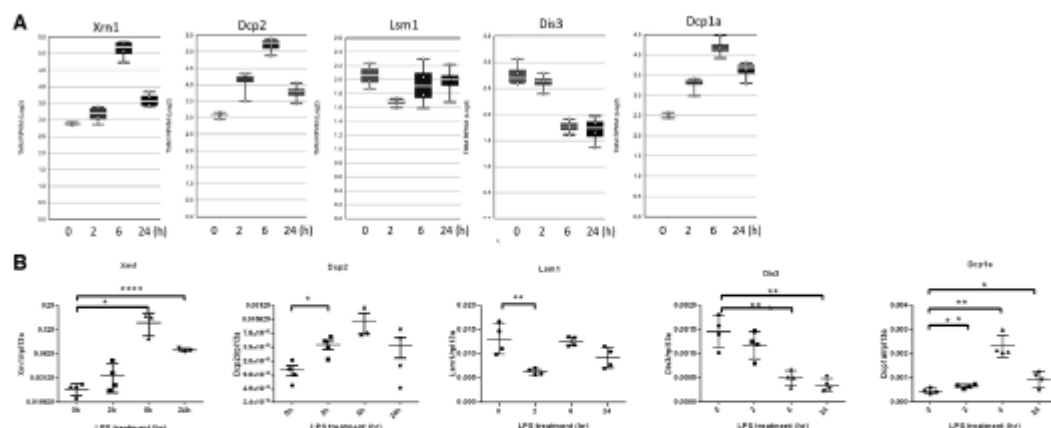
FIGURE 2 Validation of regulation of core RNA decay pathway components in response to LPS. (A) Single gene profiles were generated with the stemformatics platform for genes to be validated. Each graph shows the level of gene expression in a log scale on the y-axis the time course of LPS treatment at 0, 2, 6, and 24 h across the x-axis. For each data group, the white line shows the average expression, the white dots the individual data points for each replicate sample, and the error bars the full range of the independent samples. (B) The expression pattern of a subset of genes was validated by quantitative PCR. The level of each gene was compared to the control gene (rpl 13a) in 3–4 samples from independent mice at 0, 2, 6, and 24 h after LPS treatment. Graphs show the individual values as the symbols and the error bar show the SD. $^*p < 0.05$, $^{**}p < 0.01$, $^{***}p < 0.001$
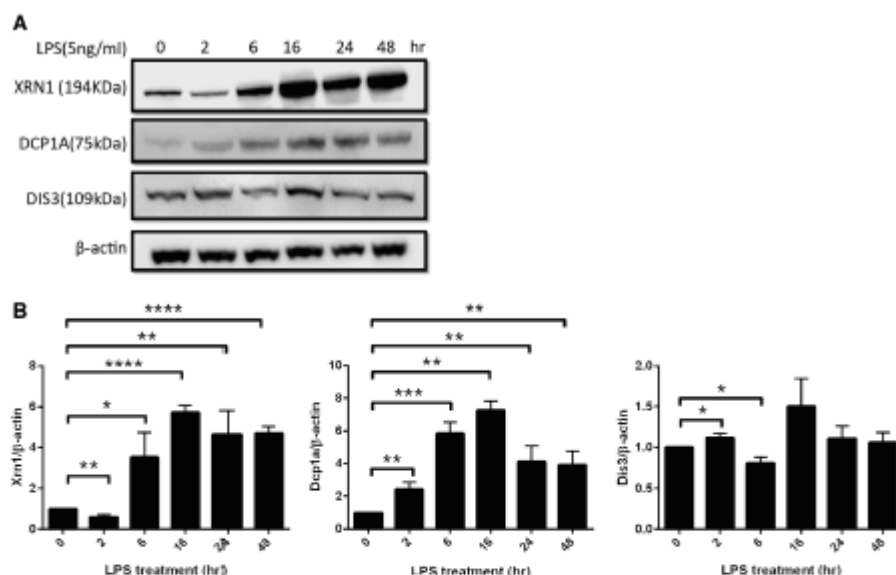
FIGURE 3 Members of the RNA decay pathways are also regulated at the protein level. (A) Representative images of western blots for Xrn1, Dcp1A, Dis3, and β-actin as a loading control. (B) Protein levels were quantified using a Licor Odyssey. The protein level was normalized to β-actin and graphs show data combined from 3 independent animals. Statistical significance was assessed using a t-test in GraphPad Prism. Bars indicate the mean and error bars the SEM. $^*p < 0.05$, $^{**}p < 0.01$, $^{***}p < 0.001$

We also compared our validated genes to data available in the online Macrophage Comparative Expression Gateway (http://macgate.qfab.org/index.htm and ref. 25) as these data were performed at the same timepoints as our analysis but by microarray.

Where available, the online BMM data matched with our data and the profiles across the timecourse in BMM did not differ significantly from human Mφs (example data and p-values for timecourse are available in Supplementary Fig. S5A and B). It should be noted that individual

timepoints for some genes showed a significant difference between mouse and human Mφs but the overall profile was similar. These data indicate that the regulation of RNA decay genes is largely conserved between mouse and human Mφs.

3.3 | Regulation of nonsense-mediated decay pathways during an LPS treatment

We next went on to validate regulation of one of the targeted RNA decay pathways. Nonsense-mediated decay (NMD) is a mechanism that protects cells from the accumulation of aberrant mRNAs with premature termination codon 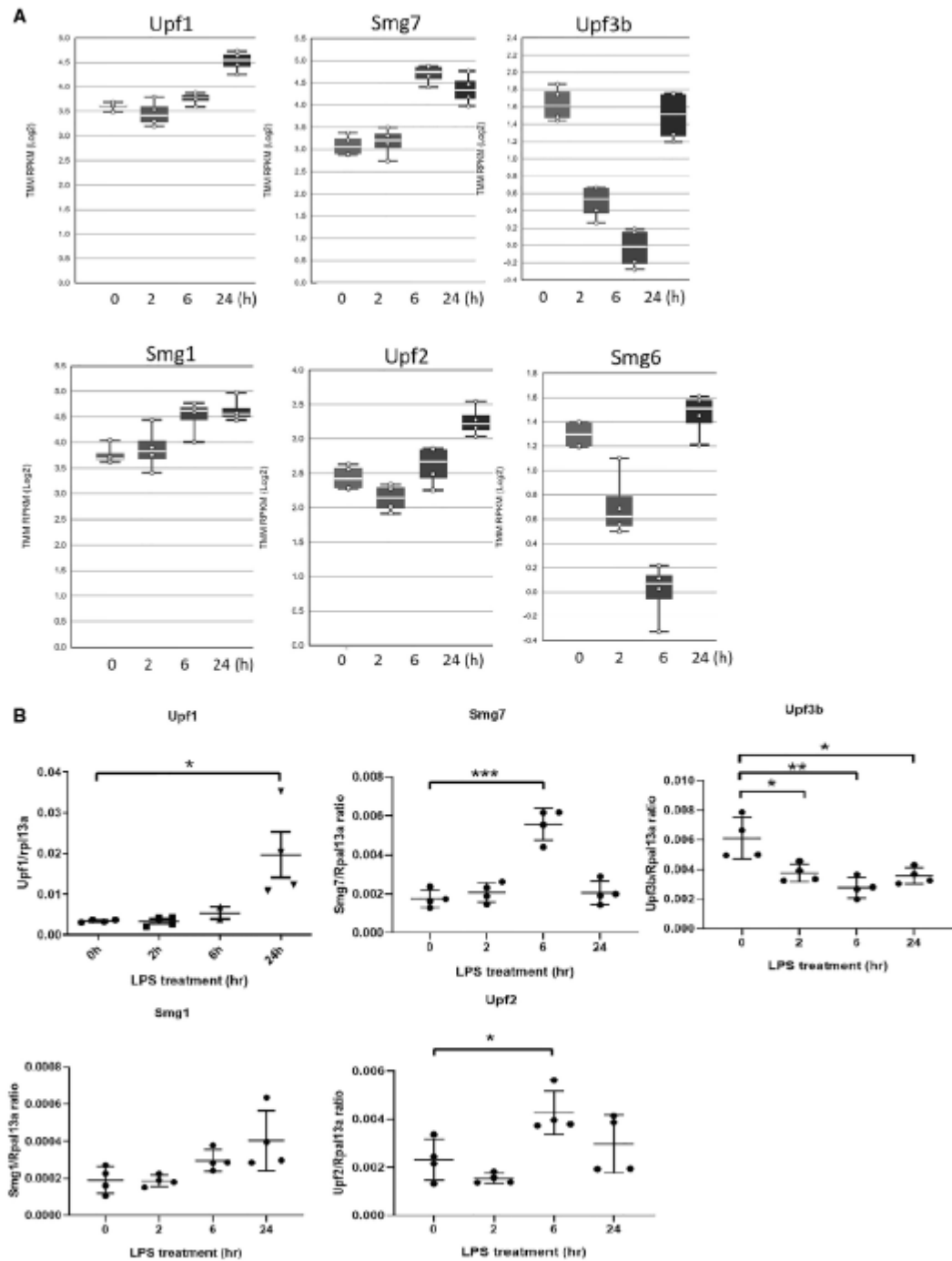(PTC) that may encode for truncated proteins. NMD has also been implicated in regulation of non-PTC containing transcripts (up to 10% of the transcriptome).[26] We chose to examine this pathway as it has been implicated in antiviral responses and is essential for hematopoiesis[27–31] but regulation of NMD during innate immune responses is poorly understood. Briefly, SMG1 phosphorylates UPF1 and phosphorylated-UPF1 recruits SMG-5/SMG-7 and the SMG-6 endonuclease to initiate RNA decay.[32] Single gene stem formatics profiles (Fig. 4A) were compared to the qPCR validation data (Fig. 4B). We validated the changes in expression for key NMD members. The qPCR data confirmed that Upf1 and Smg7 mRNA were strongly induced at 24 and 6 h post-LPS respectively. While Smg1 mRNA trended toward an increase at 6 and 24 h post-LPS, it did not reach statistical significance (Fig. 4A and B). Upf3b appeared to be strongly down-regulated at 2 and 6 h post-LPS in the RNA sequencing data. The qPCR results indicate that this down-regulation, while statistically significant, is of a smaller magnitude than in the sequencing analysis (Fig. 4B). We also examined the protein levels of SMG1, UPF1, and SMG6. We found that SMG1 is induced at 16 h after LPS treatment along with strongly increased UPF1 protein level expression at 16 h onward (Fig. 5A and B). Interestingly Upf1 protein levels appeared to be decreased at 2 h post-LPS. Smg6 levels were induced from 6–48 h post-LPS. This indicates that NMD components are strongly regulated during an LPS response.

SMG1 is a member of the phosphoinositide 3 kinase-like kinase (PIKK) family of proteins,[13] which, unlike classical PI3Ks, phosphorylate proteins at serine/threonine followed by glutamine [(S/T)Q sites]. PIKKs are very large (250–480 kDa) and as such short-term regulation is often by control of their kinase activity rather than control of protein level (as based on average rates transcription and translation of new protein would take over 1 h).[33,34] Upf1 is the key substrate for SMG1 in NMD and SMG1 kinase activity can be measured by the levels of Upf1 phosphorylation.[10] Therefore, we immunoprecipitated Upf1 from the human monocyte cell line THP-1 at 0, 2, and 6 h post-LPS, samples were then analyzed by western blotting for phosphorylated (S/T)Q sites indicating SMG1 mediated phosphorylation of Upf1. Human cells were used here as the available Abs for Upf1 are substantially more effective on the human proteins. Figure 6A (representative image) and B (quantification) shows that UPF1 phosphorylation was increased at 2 h post-LPS but returned to approximate baseline levels by 6 h post-LPS. This suggests that during the early response to LPS SMG1 kinase activity is increased and consequently NMD efficiency is likely also

increased. We therefore measured NMD efficiency in response to LPS. Gas5 is a well-established NMD target and as such its levels decrease when NMD activity increases.[13] Gas5 levels were decreased at all timepoints post-LPS (2–24 h, Fig. 6C) that fits with increased activity of SMG1 and consequent increased Upf1 phosphorylation at early timepoints and increased expression of both SMG1 and Upf1 at later timepoints. This was also the case for the splice variants of Alkbh3 and Luc7l that are NMD targets in BMMs[13] (Fig. 6D). We also examined Gas5 levels in SMG1 heterozygous mice. Complete loss of SMG1 causes early embryonic lethality but SMG1 heterozygous mice are viable with a 50–80% reduction in SMG1 protein level.[13] Basal NMD levels are normal in these animals as described previously,[13] and at the 0 h timepoint, there is no difference in Gas5 levels (Fig. 6C). However, the decrease in Gas5 in response to LPS was not observed in BMM from SMG1 heterozygous animals (Fig. 6C) indicating that SMG1 levels are limiting when there is increased NMD occurring during the LPS response. In THP-1 cells, we saw a decrease in Gas5 expression post-LPS treatment as well but for other known targets of NMD in THP-1 (Atf4, Tbl2, and Tgm2) we saw an initial increase at 2 h post-LPS followed by decreased levels (Supplementary Fig. S5C–E). In response to siRNA knockdown of SMG1, rather than the decrease in Gas5 observed levels were increased (Supplementary Fig. S5D), however it should be noted that knockdown of SMG1 in THP-1 significantly decreases cell growth as we have described for other cells previously.[10] We next treated THP-1 cells with an inhibitor of NMD that acts to disrupt the interaction between Upf1 and Smg7[35] as an independent mechanism of blocking NMD. THP-1 were treated overnight with inhibitor or DMSO alone prior to treatment with LPS, in DMSO treated samples Gas5 levels decreased and this was blunted by the addition of NMD inhibitor but did not reach statistical significance (Supplementary Fig. S5E). Combined these experiments indicate that targets of NMD are decreased in both mouse and human Mφs and that this effect is limited by blocking NMD either by decreasing SMG1 expression or to a lesser degree by chemical inhibition of NMD.

4 | DISCUSSION

Our data show that components of multiple RNA degradation pathways are regulated during the LPS response (summarized in Supplementary Fig. S3). General RNA decay requires deadenylation and decapping. From RNA sequencing data, multiple members of the deadenylation pathway and the exosome were up- or down-regulated at the mRNA level (Fig. 1B and Table 1) though this regulation was not confirmed in independent samples (Supplementary Fig. S3). However, 2 key proteins in the decapping complex, the enzyme Dcp2 and its regulatory subunit Dcp1a were significantly up-regulated in response to LPS as was the endonuclease Xrn1. Regulation of these factors was validated in independent animals and at the protein level for Dcp1a and Xrn1 (Figs. 2 and 3). These are rate limiting factors in RNA decay. Regulation of Dcp1a in response to IL-1α has been described previously.[36] In response to IL-1α Dcp1a is post-translationally modified (phosphorylation and ubiquitylation), and this alters P-body formation and com-

FIGURE 4 The regulation in the mediated by nonsense-mediated decay (NMD) pathway during an LPS treatment. (A) Single gene profiles were generated with the stemformatics platform for genes to be validated. Each graph shows the level of gene expression in a log scale on the

position, and the stability of a set of pro-inflammatory mRNAs. This posttranslational modification occurs early during the IL-1α response (1 h post-treatment).[36] Here, we show that Dcp1a and Dcp2 are also induced in response to LPS with mRNA and protein induced from 2 h post-LPS (Fig. 3) but most dramatically from 6 h post-LPS. Therefore, this later induction may result in reassembly of P-bodies and increased decapping at later timepoints.

Multiple RNA decay pathways will feed transcripts to P-bodies and the associated decapping complex. AU-rich elements and their role in regulating inflammatory mRNA has been well studied and reviewed recently.[3,37] Tristetraprolin (TTP) is induced by LPS (ref. 23 and Supplementary Fig. S4) and it controls multiple feedback pathways in response to LPS. In general, TTP binds to AU-rich elements and targets these mRNAs for decay. However, this function of TTP is also temporally controlled by transient phosphorylation post-LPS. Early in the LPS response TTP is phosphorylated downstream of p38 MAPK and degradation of targeted transcripts is limited. At later timepoints, the phosphorylation is removed and transcripts are targeted to P-bodies. The known increase in TTP expression in response to LPS was also observed in our data (Supplementary Fig. S4). The timing of TTP induction is similar to that for Dcp1a and Dcp2 suggesting this may be a

co-ordinated response to re-induce RNA decay after initial limiting of decay pathways during early inflammatory responses.

Nonsense mediated decay (NMD) is a quality control pathway; as originally described it recognizes the presence of premature termination codons (PTC) in the mRNA and directs these transcripts to be degraded thus preventing the production of truncated proteins. A PTC is recognized as premature if it is located at least 55 nucleotides upstream of an exon-exon junction complex EJC.[38] Detection of a PTC causes the EJC to recruit Upf2 associated with the SURF surveillance complex (SMG-1/Upf1/eRF1/3RF3) leading to SMG1 induced phosphorylation of Upf1. This in turn recruits SMG-5/7, leads to Upf1 dephosphorylation and finally mRNA degradation including endonucleolytic cleavage by SMG6. NMD also regulates transcripts without PTCs; transcriptomics studies suggest that greater than 10% of all transcripts are regulated by NMD[39,40] and that NMD is particularly important for regulating selenoprotein mRNA and alternative splicing.[39] How NMD regulates non-PTC transcripts is not fully understood.

A recent set of articles has implicated NMD in controlling infection.[29-31,41] NMD controlled the expression of genes from potato virus X and turnip crinkle virus.[31] Further turnip mosaic virus and potato

y-axis the time course of LPS treatment at 0, 2, 6, and 24 h across the x-axis. For each data group the white line shows the average expression, the white dots the individual data points for each replicate sample, and the error bars the full range of the independent samples. (B) The expression pattern of a subset of genes was validated by quantitative PCR. The level of each gene was compared to the control gene (rpl13a) in 3–4 samples from independent mice at 0, 2, 6, and 24 h after LPS treatment. Graphs show the individual values as the symbols and the error bar show the standard deviation. $^*p < 0.05$, $^{**}p < 0.01$, $^{***}p < 0.001$
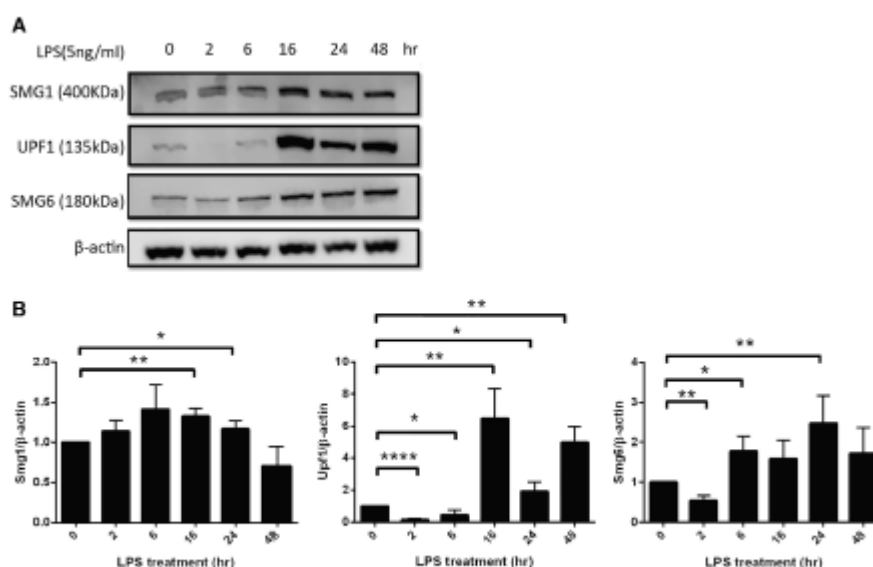
FIGURE 5 Protein level analysis by western blotting for key components of the NMD pathway and quantification. (A) Representative images of western blots for SMG1, UPF1, SMG6, and β-actin as a loading control. (B) Protein levels were quantified using a licor odyssey. The protein level was normalized to β-actin and graphs show data combined from 3 independent animals. Statistical significance was assessed using a t-test in GraphPad Prism. Bars indicate the mean and error bars the SEM. $^*p < 0.05$, $^{**}p < 0.01$, $^{***}p < 0.001$

FIGURE 6 Nonsense medicated decay is regulated during an LPS response. (A) UPF1 was immunopreciptated from THP1 lysates at the indicated time and westerns probed with anti-(S/T)Q Ab to detect SMG1 mediated phosphorylation. UPF1 phosphorylation was increased at 2 h post-LPS but returned to baseline at 6 h post-LPS. (B) Quantification of the ratio of phosphorylated Upf1 to total Upf1 in 2 independent samples. (C) The level of NMD target mRNA, gas5, was measured by qPCR in BMM from wild-type and SMG1 heterozygous mice at indicated times after LPS trea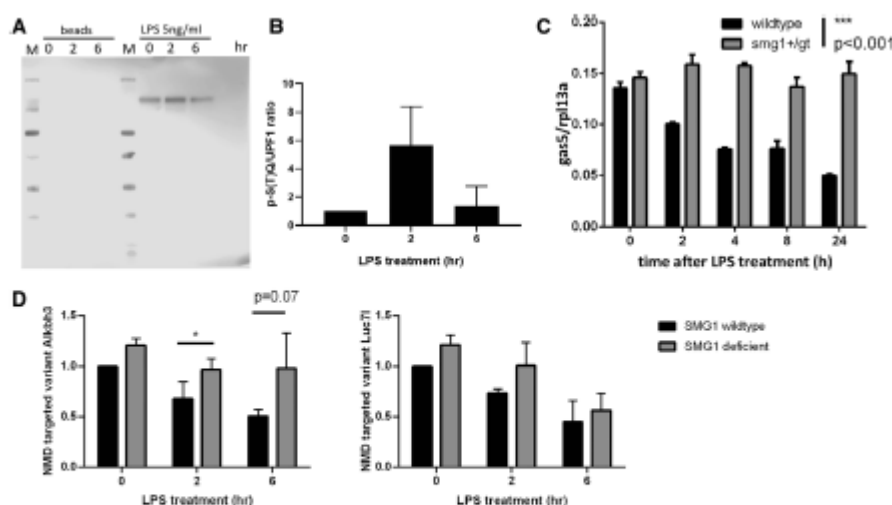tment ($n = 3$). (D) The level of splice variants of Alkbh3 and Luc7l that are known NMD targets. Splice variants were amplified by RT-PCR, separated by polyacrylamide electrophoresis and quantified using a Licor Odyssey system ($n = 3$). Data shown as mean $\pm$ SEM. $^*p < 0.05$

virus X have developed strategies to evade NMD targeting during infection suggesting the NMD targeting adversely affects viral replication and transmission. In a second article, Gloggnitzer et al. showed that bacterial infection reduced NMD efficiency and that plant pathogen recognition receptor expression is controlled by NMD.[29] In a third study, knockdown of key NMD proteins resulted in increased Semliki Forest virus production in HeLa cells.[30] Depletion of SMG1 substrate Upf1 also resulted in greater accumulation of double-stranded RNA in infected cells. Here, we add to these finding by demonstrating that NMD is regulated at multiple levels by TLR4 signaling in mammalian cells. We found that key proteins in NMD were induced at the RNA and protein levels (SMG1, Upf1, Smg7, Smg6, and Upf2) (Figs. 4 and 5). We further demonstrated increased phosphorylation of Upf1 at 2 h post-LPS treatment (Fig. 6A and B). These changes led to increased NMD efficiency as demonstrated by decreased expression of the NMD targets (Fig. 6C and D; Supplementary Fig. S5C–E). The decrease in gas5 expression was clearly dependent on NMD as it was lost in cells from SMG1 heterozygous mice, indicating that SMG1 kinase activity in NMD is rate limiting during an inflammatory response. Further siRNA knockdown of SMG1 or chemical inhibition of NMD blunted the decrease in Gas5 expression in THP-1 in response to LPS. These findings demonstrate NMD activity is initially regulated by posttranscriptional modification and then later by alteration of proteins levels in response to LPS. This process is similar to regulation of decapping and TTP as discussed above and emerges as a pattern of regulation for RNA decay pathways in our data. Given the varied regulation of transcripts in the RNA degradation pathways across the time course feedback mechanisms may be important. One of the most obvious of these is type I IFN; however, only 14 transcripts were up- (bold) or down-(italics) regulated (Table 1) according to the interferome database[42] indicating that type I IFN may contribute to regulation of RNA decay pathways but is not solely responsible. Further work will be required to determine the role/s of other feedback mechanisms in the timing of the regulation of RNA decay pathways.

Given that NMD has the potential to regulate up to 10% of all transcripts including those without PTCs it may have a significant role in sculpting the response to LPS. However, it should be noted that a recent paper has described a separate role for Upf1 (and to a more limited extent SMG1) in regulation of response to LPS and other TLR ligands. Upf1 interacts directly with Regnase-1 to allow direction of a subset of pro-inflammatory mRNAs to degradation.[43] This appears to be only partially dependent on SMG1 phosphorylation of Upf1 at only 1 of sites required for NMD activity so this is likely to represent a role additional to NMD. This pathway was predominantly described in fibroblasts and cell lines, with limited data from myeloid cells included, but it did suggest that this pathway was not as active in either Mφs or dendritic cells but further work will be required to confirm this.

In summary, while separate descriptions of RNA decay regulation in response to inflammation, especially via sequence specific elements, have been described in the literature here we examined broader RNA decay pathways including decapping and deadenylation that form the base of multiple decay pathways. Further this is the first description of the regulation of NMD efficiency during an LPS response. Overall our findings indicate that multiple RNA decay pathways are

regulated during the response to LPS in Mφs (Supplementary Fig. S6 and Table S3) and that each of these acts on different aspects of the response to fine tune RNA levels and subsequent protein expression. As such regulation of RNA decay is an important regulated mechanism during the LPS response in Mφs though future work will be required to establish mechanistic links between individual RNA decay pathways and their impact on the inflammatory response to LPS. Further work will be required to determine if regulation of RNA decay pathways also occurs in other LPS responsive cell types.

ACKNOWLEDGMENTS

AUTHORSHIP

H.L., A.J., J.L., H.Q., U.H., and T.R. performed experiments and analyzed data. T.R., M.L., and P.d.S. designed experiments and conceptualized the study. H.L. and T.R. wrote the manuscript with feedback from all authors.

DISCLOSURE

The authors have declared no conflict of interest.

ORCID

Tara L. Roberts https://orcid.org/0000-0001-9266-0943

REFERENCES

1. Akira S, Takeda K. Toll-like receptor signalling. Nat Rev Immunol. 2004;4(7):499-511.
2. Akira S. TLR signaling. Curr Top Microbiol Immunol. 2006;311:1-16.
3. Carpenter S, Ricci EP, Mercier BC, Moore MJ, Fitzgerald KA. Post-transcriptional regulation of gene expression in innate immunity. Nat Rev Immunol. 2014;14(6):361-376.
4. Medzhitov R, Horng T. Transcriptional control of the inflammatory response. Nat Rev Immunol. 2009;9(10):692-703.
5. Wells CA, Chalk AM, Forrest A, et al. Alternate transcription of the Toll-like receptor signaling cascade. Genome Biol. 2006;7(2):R10.
6. Wang ET, Sandberg R, Luo S, et al. Alternative isoform regulation in human tissue transcriptomes. Nature. 2008;456(7221):470-476.
7. Khabar KS. Post-transcriptional control during chronic inflammation and cancer: a focus on AU-rich elements. Cell Mol Life Sci. 2010;67(17):2937-2955.
8. Stoecklin G, Lu M, Rattenbacher B, Moroni C. A constitutive decay element promotes tumor necrosis factor alpha mRNA degradation via an AU-rich element-independent pathway. Mol Cell Biol. 2003;23(10):3506-3515.
9. Curtale G, Rubino M, Locati M. MicroRNAs as molecular switches in macrophage activation. Front Immunol. 2019;10:799.
10. Brown JA, Roberts TL, Richards R, et al. A novel role for hSMG-1 in stress granule formation. Mol Cell Biol. 2011;31(22):4417-4429.
11. Molleston JM, Cherry S. Attacked from all sides: RNA decay in antiviral defense. Viruses. 2017;9(1):2.
12. Zhang Q, Sharma NR, Zheng ZM, Chen M. Viral regulation of RNA granules in infected cells. Virol Sin. 2019;34(2):175-191.
13. Roberts TL, Ho U, Luff J, et al. Smg1 haploinsufficiency predisposes to tumor formation and inflammation. Proc Natl Acad Sci U S A. 2013;110(4):E285-E294.
14. Roberts TL, Dunn JA, Sweet MJ, Hume DA, Stacey KJ. The immunostimulatory activity of phosphorothioate CpG oligonucleotides is affected by distal sequence changes. Mol Immunol. 2011;48(8):1027-1034.
15. Roberts TL, Idris A, Dunn JA, et al. HIN-200 proteins regulate caspase activation in response to foreign cytoplasmic DNA. Science. 2009;323(5917):1057-1060.
16. Wells CA, Mosbergen R, Korn O, et al. Stemformatics: visualisation and sharing of stem cell gene expression. Stem Cell Res. 2013;10(3):387-395.
17. Choi J, Pacheco CM, Mosbergen R, et al. Stemformatics: visualize and download curated stem cell data. Nucleic Acids Res. 2019;47(D1):D841-D846.
18. Mi H, Muruganujan A, Casagrande JT, Thomas PD. Large-scale gene function analysis with the PANTHER classification system. Nat Protoc. 2013;8(8):1551-1566.
19. Eden E, Navon R, Steinfeld I, Lipson D, Yakhini Z. GOrilla: a tool for discovery and visualization of enriched GO terms in ranked gene lists. BMC Bioinformatics. 2009;10:48.
20. Eden E, Lipson D, Yogev S, Yakhini Z. Discovering motifs in ranked lists of DNA sequences. PLoS Comput Biol. 2007;3(3):e39.
21. Quek H, Luff J, Cheung K, et al. A rat model of ataxia-telangiectasia: evidence for a neurodegenerative phenotype. Hum Mol Genet. 2017;26(1):109-123.
22. Quek H, Luff J, Cheung K, et al. Rats with a missense mutation in Atm display neuroinflammation and neurodegeneration subsequent to accumulation of cytosolic DNA following unrepaired DNA damage. J Leukoc Biol. 2017;101(4):927-947.
23. Tiedje C, Diaz-Munoz MD, Trulley P, et al. The RNA-binding protein TTP is a global post-transcriptional regulator of feedback control in inflammation. Nucleic Acids Res. 2016;44(15):7418-7440.
24. Matsushita K, Takeuchi O, Standley DM, et al. Zc3h12a is an RNase essential for controlling immune responses by regulating mRNA decay. Nature. 2009;458(7242):1185-1190.
25. Schroder K, Irvine KM, Taylor MS, et al. Conservation and divergence in Toll-like receptor 4-regulated gene expression in primary human versus mouse macrophages. Proc Natl Acad Sci U S A. 2012;109(16):E944-E953.
26. Kurosaki T, Popp MW, Maquat LE. Quality and quantity control of gene expression by nonsense-mediated mRNA decay. Nat Rev Mol Cell Biol. 2019.
27. Quek H, Lim YC, Lavin MF, Roberts TL. PIKKing a way to regulate inflammation. Immunol Cell Biol. 2018;96(1):8-20.
28. Weischenfeldt J, Damgaard I, Bryder D, et al. NMD is essential for hematopoietic stem and progenitor cells and for eliminating by-products of programmed DNA rearrangements. Genes Dev. 2008;22(10):1381-1396.

29. Gloggnitzer J, Akimcheva S, Srinivasan A, et al. Nonsense-mediated mRNA decay modulates immune receptor levels to regulate plant antibacterial defense. *Cell Host Microbe*. 2014;16(3): 376-390.

30. Balistreri G, Horvath P, Schweingruber C, et al. The host nonsense-mediated mRNA decay pathway restricts Mammalian RNA virus replication. *Cell Host Microbe*. 2014;16(3):403-411.

31. Garcia D, Garcia S, Voinnet O. Nonsense-mediated decay serves as a general viral restriction mechanism in plants. *Cell Host Microbe*. 2014;16(3):391-402.

32. Yamashita A. Role of SMG-1-mediated Upf1 phosphorylation in mammalian nonsense-mediated mRNA decay. *Genes Cells*. 2013;18(3): 161-175.

33. Stein KC, Frydman J. The stop-and-go traffic regulating protein biogenesis: how translation kinetics controls proteostasis. *J Biol Chem*. 2019;294(6):2076-2084.

34. Singh J, Padgett RA. Rates of in situ transcription and splicing in large human genes. *Nat Struct Mol Biol*. 2009;16(11):1128-1133.

35. Martin L, Grigoryan A, Wang D, et al. Identification and characterization of small molecules that inhibit nonsense-mediated RNA decay and suppress nonsense p53 mutations. *Cancer Res*. 2014;74(11): 3104-3113.

36. Tenekeci U, Poppe M, Beuerle in K, et al. K63-ubiquitylation and TRAF6 pathways regulate mammalian P-body formation and mRNA decapping. *Mol Cell*. 2016;63(3):540.

37. Berget SM, Moore C, Sharp PA. Spliced segments at the 5' terminus of adenovirus 2 late mRNA. *Proc Natl Acad Sci U S A*. 1977;74(8): 3171-3175.

38. Yamashita A, Ohnishi T, Kashima I, Taya Y, Ohno S. Human SMG-1, a novel phosphatidylinositol 3-kinase-related protein kinase, associates with components of the mRNA surveillance complex and is involved in the regulation of nonsense-mediated mRNA decay. *Genes Dev*. 2001;15(17):2215-2228.

39. Huang L, Wilkinson MF. Regulation of nonsense-mediated mRNA decay. *Wiley Interdiscip Rev RNA*. 2012;3(6):807-828.

40. Mendell JT, Sharifi NA, Meyers JL, Martinez-Murillo F, Dietz HC. Nonsense surveillance regulates expression of diverse classes of mammalian transcripts and mutes genomic noise. *Nat Genet*. 2004;36(10):1073-1078.

41. Wachter A, Hartmann L. NMD: nonsense-mediated defense. *Cell Host Microbe*. 2014;16(3):273-275.

42. Rusinova I, Forster S, Yu S, et al. Interferome v2.0: an updated database of annotated interferon-regulated genes. *Nucleic Acids Res*. 2013;41(Database issue):D1040-D1046.

43. Mino T, Iwai N, Endo M, et al. Translation-dependent unwinding of stem-loops by UPF1 licenses Regnase-1 to degrade inflammatory mRNAs. *Nucleic Acids Res*. 2019;47:8838-8859.

SUPPORTING INFORMATION

Additional information may be found online in the Supporting Information section at the end of the article.

Supplementary data
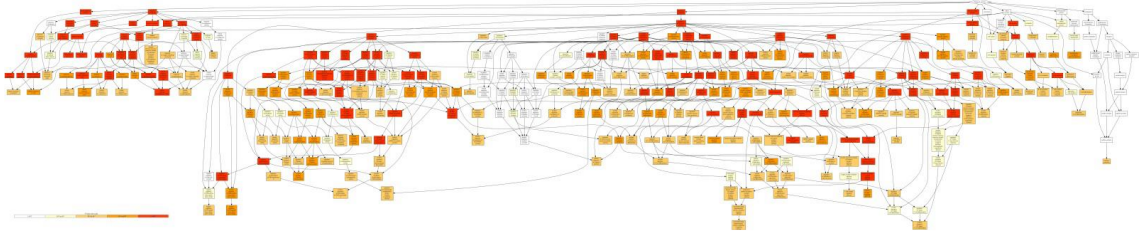
Figure S1: Example of gene ontology analysis using the GOrilla platform. Figure depicts pathways which are enriched for changed gene expression at 2h post-LPS compared to 0h time point. Colours of the boxes indicate the significance of the enrichment, with the brighter the colour indicating greater significance (see key in bottom left hand corner).

Please download this figure from   **https://doi.org/10.1002/JLB.2AB0420-151RR** and then you can enlarge this image from PDF to get the best image resolution.

Figure S2

Figure S2: Validation of regulation of expected proinflammatory cytokines in response to LPS. **A:** Single gene profiles were generated with the stemformatics platform for genes to be validated. Each graph shows the level of gene expression in a log scale on the y-axis the timecourse of LPS treatment at 0, 2 and 6 hours across the x-axis. For each data group the white line shows the average expression, the white dots the individual data points for each replicate sample and the error bars the full range of the independent samples. **B:** The expression pattern of a subset of genes was validated by quantitative PCR. The level of each gene was compared to the control gene (rpl13a) in 4 samples from independent mice at 0, 2, 6 hours after LPS treatment. Bars show the mean and the error bars show the standard error of the mean. $**p<0.01$, $***p<0.001$, $****p<0.0001$. **C:** Statistical results for RNA metabolism pathways as indicated in Figure S1. **D:** Volcano plots of 0 vs 2h samples (left-hand panel) and 2 vs 6h samples (right-hand panel). RNA decay related genes are indicated in green dots.

Figure S3
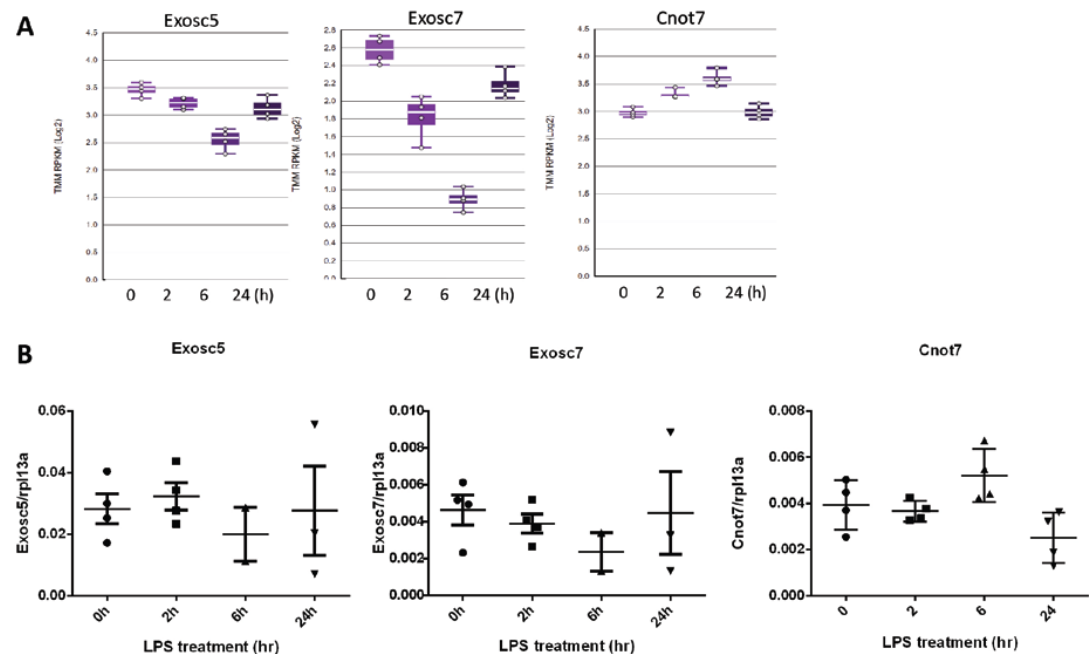
Figure S3: Regulation of components of the exosome (Exosc5 and 7) and a member of the deadenylation complex (Cnot7) did not validate by qPCR. **A:** Single gene profiles were generated with the Stemformatics platform for genes to be validated. Each graph shows the level of gene expression in a log scale on the y-axis the timecourse of LPS treatment at 0, 2, 6 and 24 hours across the x-axis. For each data group the white line shows the average expression, the white dots the individual data points for each replicate sample and the error bars the full range of the independent samples. **B:** The expression pattern of a subset of genes was validated by quantitative PCR. The level of each gene was compared to the control gene (rpl13a) in 3-4 samples from independent mice at 0, 2, 6, 24 hours after LPS treatment. Graphs show the individual values as the symbols and the error bar show the standard deviation.

Figure S4

Figure S4: Tristetraprolin (TTP encoded by Zfp36) and Regnase 1 (encoded by Zc3h12a) are regulated during the LPS response. **A:** Single gene profiles were generated with the Stemformatics platform for genes to be validated. Each graph shows the level of gene expression in a log scale on the y-axis the timecourse of LPS treatment at 0, 2, 6 and 24 hours across the x-axis. For each data group the white line shows the average expression, the white dots the individual data points for each replicate sample and the error bars the full range of the independent samples. **B:** The expression pattern of a subset of genes was validated by quantitative PCR. The level of each gene was compared to the control gene (rpl13a) in 3-4 samples from independent mice at 0, 2, 6, 24 hours after LPS treatment. Graphs show the individual values as the symbols and the error bar show the standard deviation.

Figure S5

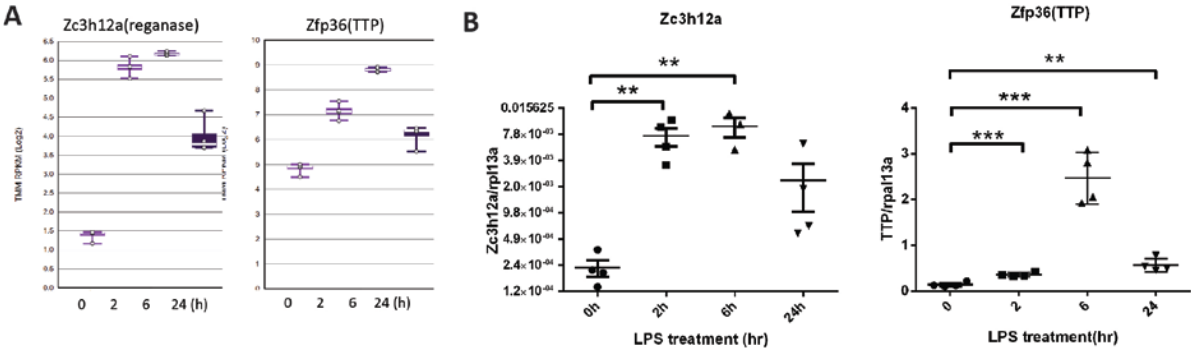| Gene Symbol	Gene Name
DCP1A Links: Ensembl Entrez Gene	mRNA-decapping enzyme 1A (EC 3.-.-.-) (Transcription factor SMIF) (Smad4-interacting transcriptional co-activator) Synonyms: FLJ21691 HSA275986 Nbla00360 SMAD4IP1 SMIF
Dcp1a Links: Ensembl Entrez Gene	mRNA-decapping enzyme 1A (EC 3.-.-.-) (Transcription factor SMIF) (MAD homolog 4-interacting transcription coactivator 1) (Smad4-interacting transcriptional co-activator) Synonyms: 1110066A22Rik 4930568L04Rik AU019772 D14Ertd817e Mitc1 SMIF

HMDM   BMM   TEPM

Gene Symbol	Gene Name
DIS3L Links: Ensembl Entrez Gene RefSeq	DIS3 mitotic control homolog (S. cerevisiae)-like Synonyms: FLJ38088 KIAA1955 MGC4562
Dis3l Links: Ensembl Entrez Gene RefSeq RefSeq	DIS3-like exonuclease 1 (EC 3.1.13.-) Synonyms: AV340375

HMDM   BMM   TEPM

B

Gene	P-value profile
Xrn1	0.43
Dcp1a	0.402
Dcp2	0.765
Dis3	0.965
Exosc7	0.676
Zfp36 (TTP)	0.372
Zc3h12a (Regnase)	0.962

C

D

E

Figure S5: Analysis of RNA decay genes in human samples. A-B: We utilised the MacGate

dataset (http://macgate.qfab.org/index.htm) to look at conservation between human and mouse

macrophages. Panel A shows example data for Dcp1a and Dis3l showing the conservation in gene expression profiles between BMM, human monocyte deribed macrophages (HMDM) and thioglycolate elicited peritoneal macrophages (TEPM). The P-values comparing the HMDM to BMM for available genes are shown in panel B. **C:** The response of NMD targets to LPS treatment were measured in THP-1 cells by quantitative PCR. The level of each gene was compared to the control gene (hprt) in 3 independent samples at 0, 2, 6, 24 hours after LPS treatment. **D:** THP-1 cells were treated with control or anti-SMG1 siRNA for 72h prior to LPS treatment and the impact on Gas5 expression measured by qPCR. Data points show the mean and error bars the range from n=2 samples. **E:** THP-1 cells were treated with NMDI 14 (NMDi) or vehicle control (DMSO) overnight prior to treatment with LPS and the impact on Gas5 expression levels measured by qPCR. Bars show the mean (n=3) and the error bars show the standard error of the mean.

Table S1: Gene list generated from Heat-map and related functions.

Gene	Accession number	Function
C1d	ENSMUSG00000000581	Nuclear exosome cofactor
Lsm5	ENSMUSG00000091625	Member of cytoplasmic Lsm1-7 complex
Lsm3	ENSMUSG00000090846	Member of both Lsm complexes
Lsm2	ENSMUSG00000007050	Member of both Lsm complexes
Dis3	ENSMUSG00000033166	Only catalytic component of the core exosome;3'hydrolytic exonuclease and endonuclease activity
Exosc8	ENSMUSG00000027752	Member of core exosome complex
Lsm6	ENSMUSG00000031683	Member of both Lsm complexes
Dcps	ENSMUSG00000032040	Decapping scavenger enzyme,m7GpppX diphosphatase following the degradation of mRNAs by the 3'->5' exosome-mediated mRNA decay pathway
Wdr61 (Ski8)	ENSMUSG00000061559	A subunit of the human PAF and SKI complexes, which function in transcriptional regulation and are involved in events downstream of RNA synthesis, such as RNA surveillance
Hspa9	ENSMUSG00000024359	Member of the heat shock protein 70 gene family and its function in the regulating of cell proliferation, stress response and maintenance of the mitochondria
Naa38	ENSMUSG00000044155	Auxillary component of the N-terminal acetyltransferase C (NatC) complex which catalyzes acetylation of N-terminal methionine residues
Exosc9	ENSMUSG00000027714	Member of core exosome complex
Hspd1	ENSMUSG00000025980	Member of the chaperonin family and is essential for the folding and assembly of newly imported proteins in the mitochondria.
Exosc10	ENSMUSG00000017264	Nuclear-specific exosome component;3'hydrolytic exonuclease
Cnot6	ENSMUSG00000020362	Member of Ccr4-NOT cytoplasmic deadenylation complex
Mphosph6	ENSMUSG00000031843	A RNA-binding protein that associates with the RNA exosome complex
Lsm4	ENSMUSG00000031848	Member of both Lsm complexes
Ttc37	ENSMUSG00000033991	A Protein Coding gene and may mediate protein-protein interactions and chaperone activity
Dhx36	ENSMUSG00000027770	A member of the DEAH-box family of RNA-dependent NTPases and enhance the deadenylation and decay of mRNAs with 3'-UTR AU-rich elements (ARE-mRNA)
Cnot1	ENSMUSG00000036550	Member of Ccr4-NOT cytoplasmic deadenylation complex
Pan3	ENSMUSG00000029647	A poly(A) specific ribonuclease subunit and its related pathways are gene expression and deadenylation-dependent mRNA decay
Skiv2l2	ENSMUSG00000016018	Helicase,TRAMP complex component,has TRAMP-

		independent functions
Exosc1	ENSMUSG00000034321	Member of core exosome complex
Exosc2	ENSMUSG00000039356	Member of core exosome complex
Exosc5	ENSMUSG00000061286	Member of core exosome complex
Pan2	ENSMUSG00000005686	A poly(A) specific ribonuclease subunit and its related pathways are gene expression and deadenylation-dependent mRNA decay
Cnot10	ENSMUSG00000056167	Member of Ccr4-NOT cytoplasmic deadenylation complex
Exosc7	ENSMUSG00000025785	Member of core exosome complex
Rqcd1 (Cnot9)	ENSMUSG00000026174	Member of the highly conserved RCD1 protein family;a transcriptional cofactor and a core protein of the CCR4-NOT complex
Eno3	ENSMUSG00000060600	Isoenzyme and found in skeletal muscle cells in the adult where it may play a role in muscle development and regeneration
Tob1	ENSMUSG00000037573	Anti-proliferative protein; the function is mediated by association with deadenylase subunits of the CCR4-NOT complex
Pam	ENSMUSG00000022685	Peptidyl-glycine alpha-amidating monooxygenase that catalyzes 2 sequential steps in C-terminal alpha-amidation of peptides
Cnot6l	ENSMUSG00000034724	Member of Ccr4-NOT cytoplasmic deadenylation complex
Pabpc1	ENSMUSG00000022283	Polyadenylate-binding protein; its required for poly(A) shortening which is the first step in mRNA decay
Cnot7	ENSMUSG00000031601	Member of Ccr4-NOT cytoplasmic deadenylation complex
Btg2	ENSMUSG00000020423	Member of the BTG/Tob family; the function is involved in the regulation of the G1/S transition of the cell cycle
Xrn2	ENSMUSG00000027433	5'-3' exonuclease that promotes transcription termination at cotranscriptional cleavage sites
Xrn1	ENSMUSG00000032410	Cytoplasmic 5'exonuclease
Cnot4	ENSMUSG00000038784	Member of Ccr4-NOT cytoplasmic deadenylation complex
Dcp1a	ENSMUSG00000021962	Member of decapping complex with Dcp2
Dcp2	ENSMUSG00000024472	Catalytic pyrophosphatase subunit of decapping complex
Papd7	ENSMUSG00000034575	Catalytic subunit of a TRAMP-like complex which has a poly(A) RNA polymerase activity and is involved in a post-transcriptional quality control mechanism
Eno2	ENSMUSG0000004267	Isoenzyme and found in skeletal muscle cells in the adult where it may play a role in muscle development and regeneration
Btg1	ENSMUSG00000036478	Member of the BTG/Tob family; the function is involved in the regulation of the G1/S transition of the cell cycle
Pat1	ENSMUSG00000046139	DNA topoisomerase 2-associated protein;

		can recruit the hepta-heterodimer Lsm1-Lsm7 complex to P-bodies
Edc4	ENSMUSG00000036270	Enhancer of mRNA-decapping protein 4
Cnot2	ENSMUSG00000020166	Member of Ccr4-NOT cytoplasmic deadenylation complex
Ddx6	ENSMUSG00000032097	RNA helicase; the function is in P-bodies and stress granules, and functions in translation suppression and mRNA degradation
Lsm1	ENSMUSG00000037296	One of member of cytoplasmic Lsm1-7(ring-shaped RNA chaperone) complex
Cnot8	ENSMUSG00000020515	Member of Ccr4-NOT cytoplasmic deadenylation complex
Exosc4	ENSMUSG00000034259	Member of core exosome complex
Dcp1b	ENSMUSG00000041477	core component of the mRNA decapping complex; function in removing the 5' cap from mRNAs, which is a step in regulated mRNA decay
Pabpc1l	ENSMUSG00000054582	Polyadenylate-binding protein; its required for poly(A) shortening which is the first step in mRNA decay
Cnot3	ENSMUSG00000035632	Member of Ccr4-NOT cytoplasmic deadenylation complex
Eno1	ENSMUSG00000063524	Isoenzyme and found in skeletal muscle cells in the adult where it may play a role in muscle development and regeneration
Exosc3	ENSMUSG00000028322	Member of core exosome complex
Skiv2l	ENSMUSG00000040356	RNA Helicase; Component of the SKI complex which is thought to be involved in exosome-mediated RNA decay and associates with transcriptionally active genes in a manner dependent on PAF1 complex (PAF1C)
Edc3	ENSMUSG00000038957	Component of a decapping complex that promotes efficient removal of the monomethylguanosine (m7G) cap from mRNAs, as part of the 5' to 3' mRNA decay pathway
Tob2	ENSMUSG00000048546	Anti-proliferative protein; the function is mediated by association with deadenylase subunits of the CCR4-NOT complex
Zcchc7	ENSMUSG00000035649	TRAMP-like complex RNA-binding factor; the function is related to deadenylation-dependent mRNA

Table S2: Primer sequences are listed below.

* primers designed and validated for this study.

Target Gene	Forward Primer 5'-3'	Reverse Primer 5'-3'	Ref
Rpl13a	GAGGTCGGGTGGAAGTACCA	TGCATCTTGGCCTTTTCCTT	Mogal et al, 2006
IFNβ	CCACAGCCCTCTCCATCAAC	TGAAGTCCGCCCTGTAGGTG	Roberts et al, 2009
TNFα	AGCCCCCAGTCTGTATCCTT	CTCCCTTTGCAGAACTCAGG	*
Upf2	ACTGAGCCGGAGAAGAAACA	CTGGTGGCTTATCTGGCATT	*
Smg7	GCTCCAAGGCAGAACTGAAC	TCCCAATGGGTCCAAAATTA	*
Upf3b	AGGAAACCGGAAAAAGGAGA	ATCATGCGCTCCTGATCTCT	*
Upf1	AACAGAAGGCGCTAGTGGAA	TGCTGCGGTCATAGACAGAC	*
Dcp1a	CCAGCTGAAGCTCCTACCAC	CTGTGGGGTCAACCTGAGTT	*
Lsm1	ACCAGACTGGAGGCAGAGAA	TGGCATCCATGAAAGAATGA	*
TTP	CCCTCTGCAACTCTGGTCTC	TGGCTTTGGCTATTTGCTTT	*
Dis3	GCAAGAGCAGGGAGAGAATG	ACACGTGAAGGCTGGTATCC	*
Cnot7	GTTGGGCTTGTAACCTGGA	GTTGACGTTCCTGGAGGGTA	*
Stau1	GCACAGAGATGCCAAGAACA	GGCCCACTGGAGTTATCAGA	*
Xrn1	CCACTTCAGACTAACAAGCCA	GGGAGGCAGTTTCAACATGAG	*
Dcp2	GACCAGCTTGCTCGCTTGTA	TTGGACTTGGGAGTCATGTCA	*
Zc3h12a	ACGAAGCCTGTCCAAGAATCC	TAGGGGCCTCTTTAGCCACA	*
Exosc5	CGTGCAGACGCCAATTTACTC	GACAGCAGGTTTTGCTCACA	*
Exosc7	CTACATCGTTCATGGAGTGCAG	GCAGACCCACTGGTGTTAGAC	*
Smg1	GACGAGCCTACAATCCATCCT	CAAACTCTGCAACCACCCA	Roberts et al, 2013

Table S3: Summary of RNA decay pathway components and regulation by LPS.

Deadenylation (Multiple complexes)	Exosome	Nonsense Mediated Decay	Element/sequence specific	Decapping	P-bodies and stress granules	Other
CNOT6	Dis3 (nuclear)	Upf1	TTP (AU rich element - ARE)	Dcp1a	Xrn1	Zc3h12a
CNOT6L	Exosc7	Upf2	CELF1 (GU rich elements)	Dcp2	TIA-1	Zcchc6
Nocturnin	Exosc5	Upf3a	Roquin	Xrn2	TIAR	Setx
Angel2	Dis3l (Cytoplasmic)	Upf3b	PTBP1 (poly-pyrimidine tracts)	Xrn1	GW182	Stau1
CNOT7	Dis3l2	Smg6	HNRNPd (AREs)			Stau2
CNOT8	Exosc10	Smg5	ZFP36L2 (AREs)			
Pan3		Smg7	YB1 (stablises ARE)			

Green – downregulated Red – upregulated Blue – unchanged Purple – mixed across timecourse